Coordination Chemistry and Catalytic Applications of 2-Phosphinophosphinines

Robert Newland

Submitted for the degree of Doctor of Philosophy at Heriot-Watt University, on completion of research in the Institute of Chemical Sciences.

June 2018

Abstract

This thesis details research undertaken into investigating the synthesis and coordination chemistry of phosphinophosphinines, as well as the usage of several complexes in a range of catalytic transformations.

The results presented in chapter two are primarily based on the synthesis of new mono- and bis-phosphinophosphinines, as well as some derivatives, including the phosphine-borane and selenide. Crystallographic data are presented for the key compounds, as prior to this research, such data had yet to be reported for underivatised or non-coordinated phosphinophosphinines.

In chapter three, the reactivities of two phosphinophosphinines with group 6 [M(diene)$(CO)_4$] fragments are described, and infrared spectroscopic data are utilised to facilitate comparisons between the donor properties of these ligands as well as more familiar P-donors. To aid in these comparisons, the two phosphinophosphinines (and several hypothetical analogues) were analysed computationally by Dr Natalie Fey at the University of Bristol using the P,P-donor Ligand Knowledge Base. Finally, in collaboration with Sasol UK, results obtained from the use of phosphinophosphinines in the catalytic oligomerisation of ethylene are presented.

Finally, in chapters four and five, the coordination chemistries of a phosphinophosphinine to ruthenium and rhodium (respectively) precursor complexes are discussed. The resulting complexes are analysed in terms of their spectroscopic and structural data, as well as their activity as catalysts for a range of reactions.

Dedication

Without the encouragement and (financial) support that my parents have provided me with over the years, I would not be where I am today.

This thesis is dedicated to them.

Acknowledgements

I am indebted to the work of others who have assisted me during both the course of my research as well as the assembly of this thesis, but most importantly to my supervisor, Dr Mansell. I thank him for allowing me the opportunity to undertake this project, for providing countless, patient answers to my many questions, and for all the help that he has given me with experimental ideas, thesis/paper writing, job hunting, *etc.* Coming from a background of limited crystallography knowledge, I am also very thankful to his hours of assistance in this area, as well as to the extensive work of Dr Mairi Haddow in solving and refining the trickier structures obtained throughout this project.

The work of several academic and industrial collaborators was included in this thesis, and so to Dr Natalie Fey, Dr David Smith, Dr Martin Hanton, Dr Richard Wingad, Dr Mark Wyatt, Dr Jason Lynam, Dr Rebecca How and Prof. Paul Kamer, I must also extend my thanks for the valuable contributions they all made to my research. I was also lucky enough to work alongside two great undergraduate project students, and in particular the contributions of Alana Smith to the synthesis of carbonyl complexes were of great value to this thesis. Whilst the research undertaken by Matthew Delve did not make it into this work, I am hopeful to see it developed further in the Mansell group.

To all the members of the Mansell group, past and present, thank you for everything. In particular, it would be rude not to mention Dr Marta Roselló-Merino and Dr Peter Cleaves, for providing a great deal of experimental assistance.

My appreciation must also be extended to Dr David Ellis, for not only helping me to get to grips with the necessary multinuclear NMR spectroscopy techniques used in characterisation of my products, as well as building the required experiments.

Thanks also to Dr Marcus Drover for his assistance with the calculation and assignment of the coupling constants for complex **4.1**.

Finally, thank you to the groups of Pascal Le Floch, François Mathey and Christian Müller. This project would not have been possible without your work, and the publications, reviews and book chapters you've written made my life so much easier.

Abbreviations

acac	acetylacetonate
app.	apparent
Ar	aryl, a derivative of the phenyl group
ASAP	atmospheric solids analysis probe
bm	broad multiplet
Bn	benzyl, CH_2Ph
^{i}Bu	*iso*-butyl, $CH_2CH(CH_3)_2$
^{n}Bu	*normal*-butyl, $(CH_2)_3CH_3$
^{t}Bu	*tertiary*-butyl, $C(CH_3)_3$
COD	1,5-cyclooctadiene
Cp	cyclopentadienyl
Cp*	pentamethylcyclopentadienyl
CSD	Cambridge Structural Database
Cy	cyclohexyl
d	doublet
DABCO	1,4-diazabicyclo[2.2.2]octane
DCM	dichloromethane, CH_2Cl_2
δ	chemical shift
Δ	heating a chemical reaction
DFT	Density Functional Theory
dme	1,2-dimethoxyethane
dppm	bis(diphenylphosphino)methane
E.I	electron impact
equiv.	equivalents
e.s.d	estimated standard deviation
ESI	electrospray ionisation
Et	ethyl, CH_2CH_3
eV	electron volt
η	hapticity of ligand
HBCat	catecholborane, 1,3,2-benzodioxaborole
HOMO	highest occupied molecular orbital
Hz	Hertz
I.R	infra-red

J	coupling constant
κ	denticity
LUMO	lowest unoccupied molecular orbital
m	multiplet
M	generic metal atom
Me	methyl, CH_3
Mes	mesityl, 2,4,6-$Me_3C_6H_2$
M.S	mass spectrometry
μ	absorption coefficient (in crystallography)
μ	designation for bridging mode
NMR	nuclear magnetic resonance
OAc	acetate, $OC(O)CH_3$
OTf	triflate, OSO_2CF_3
OX	oxidant
Ph	phenyl
ppm	parts per million
^{i}Pr	*iso*-propyl, $CH(CH_3)_2$
^{n}Pr	*normal*-propyl, $(CH_2)_2CH_3$
Py	pyridyl
q	quartet
ρ	density
r.t	room temperature, *ca.* 20°C
t	triplet
T	temperature
TOF	time-of-flight
THF	tetrahydrofuran
TMP	2,2,6,6-tetramethylpiperidine
Tol	toluene
ν	stretching frequency
V	volume
Z	number of molecules in the unit cell
Z′	number of molecules in the asymmetric unit

Key of Compounds

The following structures are new compounds (except for **2.5**) resulting from this research and are discussed throughout this thesis. They are provided here as a point of reference.

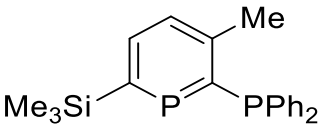

2.1

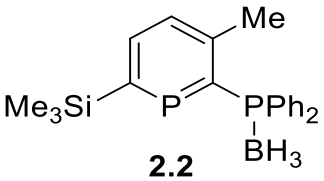

2.2

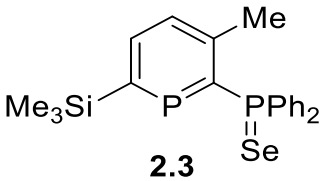

2.3

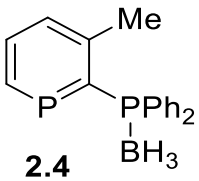

2.4

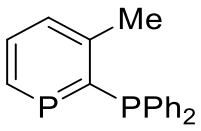

2.5

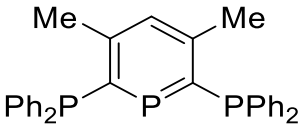

2.6

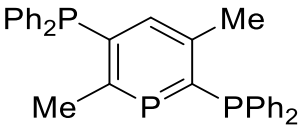

2.7

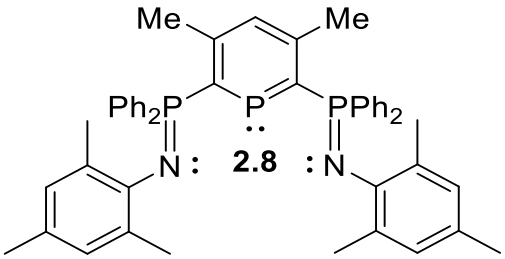

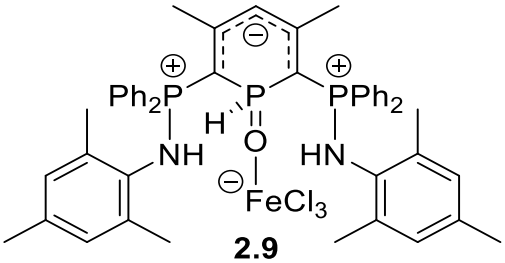

2.9

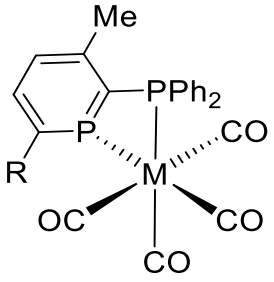

3.1, M = Cr, R = $SiMe_3$
3.2, M = Mo, R = $SiMe_3$
3.3, M = W, R = $SiMe_3$
3.4, M = Cr, R = H
3.5, M = Mo, R = H

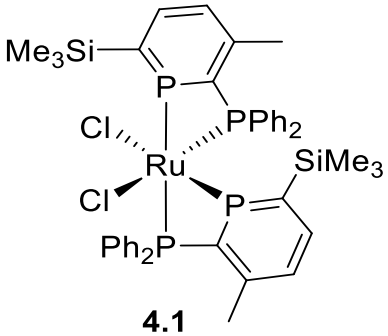

4.1

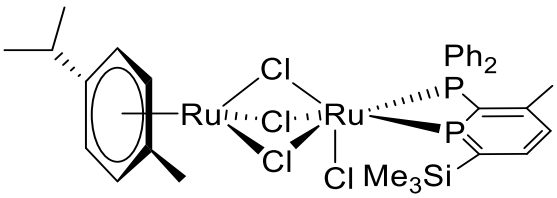

4.2

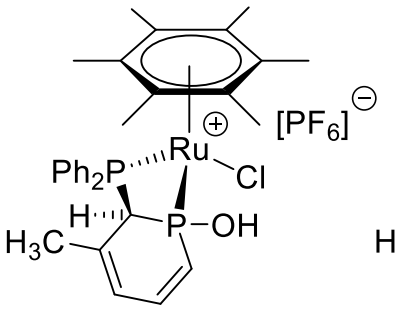
[PF6]
Ru
Ph2P
Cl
H
P
OH
H3C

4.3

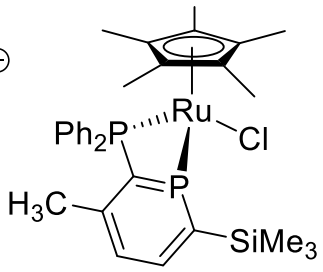
Ru
Ph2P
Cl
P
H3C
SiMe3

4.4

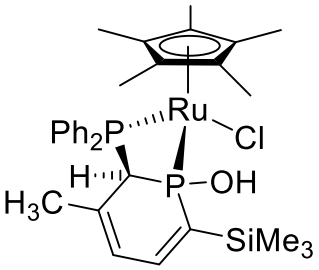
Ru
Ph2P
Cl
H
P
OH
H3C
SiMe3

4.5

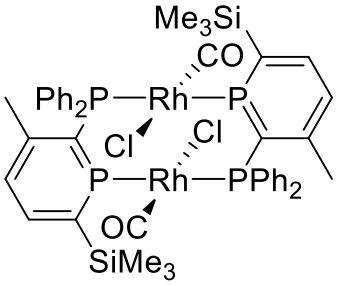
Me3Si
CO
Ph2P
Rh
P
Cl
Cl
P
Rh
PPh2
OC
SiMe3

5.1

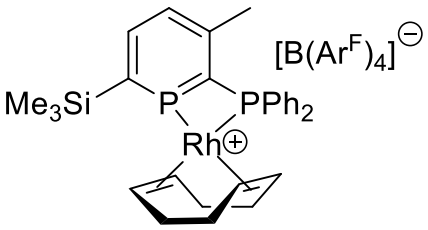
[B(ArF)4]
Me3Si
P
PPh2
Rh

5.2

Table of Contents

1 - Introduction

1.1 Introduction to phosphinines

Whilst synthetic routes to pyridines[1] and the reactivity of these species[2] are well studied, research into the heavier P-analogue of pyridine – phosphinine – is comparatively sparse. Phosphinine and its functionalised derivatives have long been thought of as "chemical curiosities"[3], and were unknown until Märkl's landmark synthesis of 2,4,6-triphenylphosphabenzene (**1.2**) in 1966 from pyrilium salt **1.1** and $P(CH_2OH)_3$ as an air-stable, crystalline solid in 24-30% yield (**Scheme 1-1**).[4] The significance of the synthesis is due to the fact that prior to this publication, the only reported example of a so-called "low-coordinate" phosphorus compound was the parent phosphaalkyne, H-C≡P, for which only spectroscopic evidence was discussed due to its existence as an unstable gas.[5, 6] It is also important to note that the general consensus was that "p-p π-bonding is of little importance in the third and higher period elements"[7] and, therefore, this publication provided incontrovertible proof of the stability of p-block multiple bonding below the second period.[8] The synthesis was later improved – yielding **1.2** in 45% yield – and was adapted to other phenyl/*p*-anisyl-substituted phosphinines by using the appropriate pyrilium iodide and $P(SiMe_3)_3$.[9] Due to the sp^2 (aromatic) phosphorus, **1.2** has a $^{31}P\{^1H\}$ NMR chemical shift of δ = 178.2 ppm, and such a high-frequency resonance is commonplace for phosphinines. The air-stability of **1.2** is important to note, as those familiar with the chemistry of phosphines would assume that similar to small, alkyl phosphines (e.g. PMe_3), **1.2** should react rapidly (and potentially violently) upon exposure to the atmosphere.

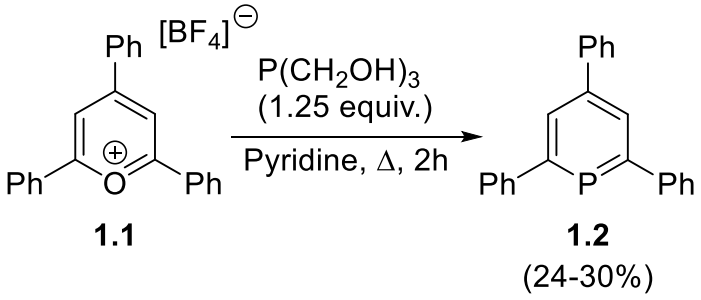

Scheme 1-1.[4] Märkl's 1966 synthesis of 2,4,6-triphenylphosphinine

It was not until 1971 that the parent, unsubstituted, phosphinine (**1.4**) was synthesised by Ashe by reaction of stannacyclohexadiene **1.3** with PBr_3 and an amine base (**Scheme 1-2**). This methodology was also used to prepare the analogous arsabenzene from $AsCl_3$.[10] In comparison to tri-substituted phosphinine **1.1**, **1.4** is an air-sensitive, volatile

oil with a $^{31}P\{^{1}H\}$ NMR chemical shift of $\delta = 206.6$ ppm.[11] From the sensitivity of **1.4**, it can be inferred that the aromatic ring current is not the source of the air-stability of **1.2** (calculations have shown that **1.2** has 88% of the aromaticity of benzene)[12], but more likely a combination of steric protection and electronic effects from the two *ortho* phenyl substituents. As no detailed synthetic procedure was provided by Ashe in the original publication,[10] his route to **1.4** cannot be evaluated in terms of ease of replication or the yield. However, based on a follow-up publication, it was reported that the methodology is not well-suited to the synthesis of *ortho* substituted phosphinines due to the formation of a second product (**1.5**) in varying amounts when attempting to prepare the stannacyclohexadiene using internal alkynes.[13] The *ortho* mono or dimethyl-substituted phosphinines could be prepared in low yields, however, when attempting to prepare 2-phenylphosphinine only the **1.5** isomer was obtained. As **1.5** contains a five-membered ring and an exocyclic alkene, it does not react to form the desired phosphinine.[13] This shows that although this methodology was extremely important in the synthesis of C_5H_5P, it is not useful for preparing more complex derivatives.

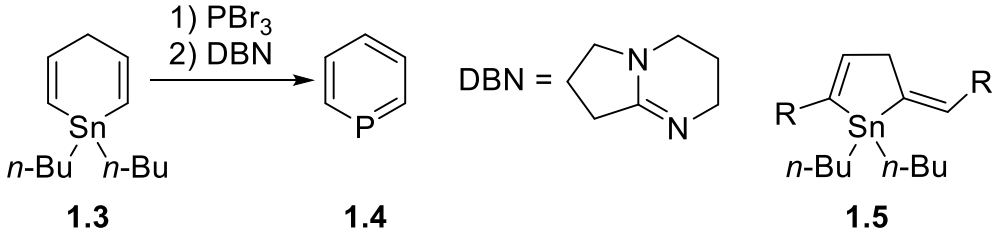

1.3 **1.4** **1.5**

Scheme 1-2.[10, 13] Ashe's 1971 synthesis of phosphinine

1.2 Synthesis of substituted phosphinines

The synthesis of phosphinines has been covered in several reviews,[12, 14-18] and as such only the key methods are covered here. Whilst the work of Märkl[4, 9] and Ashe[10, 13] was vital to the development of this field, many of the key recent milestones in the synthesis of substituted phosphinines have come from the groups of Müller, Le Floch and Mathey.[12] The majority of the phosphinines published by Müller and co-workers have been tri-(hetero)aryl species prepared using the pyrilium salt methodology,[12, 19, 20] as the starting salts can be prepared with a wide range of substituents in only three synthetic steps (**Scheme 1-3**).

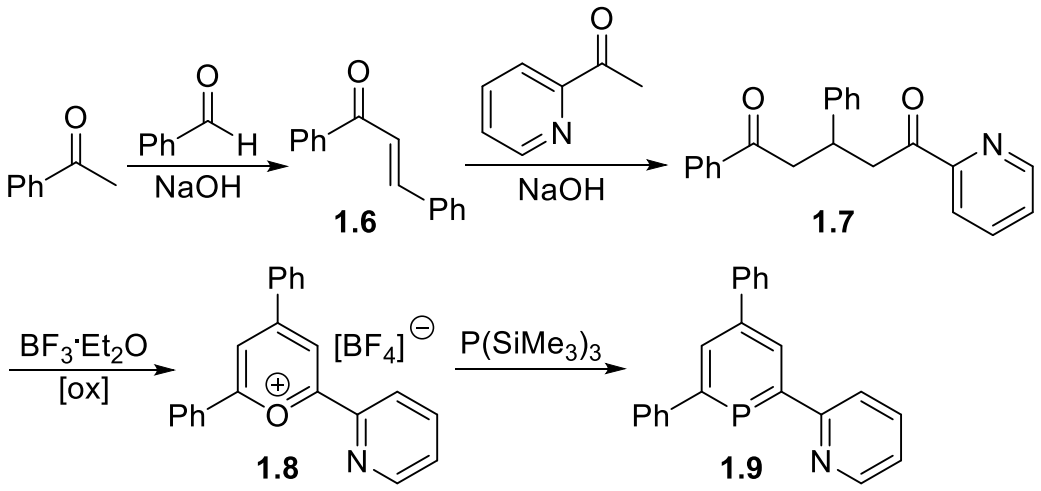

Scheme 1-3.[19] Synthesis of bipyridine analogue **1.9**

After an aldol condensation of acetophenone and benzaldehyde, 2-acetylpyridine undergoes a Michael addition to chalcone (**1.6**) forming the desired 1,5-diketone (**1.7**). Using an excess (8 equivalents) of BF_3-Et_2O in the presence of **1.6** as an oxidant, the diketone is cyclised to the pyrilium salt (**1.8**). As published by Märkl,[9] the phosphinine **1.9** was then isolated after reaction of **1.8** with tris(trimethylsilyl)phosphine. Whilst the synthesis of **1.8** can be achieved using only readily available materials, and two out of three steps require no inert conditions, the pyrilium salts are typically isolated in less than 50% yield, and the resulting phosphinines are commonly obtained in a 10-30% yield.[19] However, an exception to this is the chiral phosphinine **1.11**, which was isolated in an 82% yield from pyrilium salt **1.10** (**Scheme 1-4**).[21] There are only a limited number of examples of other phosphinines derived from chiral pyrilium salts.[22-26] It is also important to note that tris(trimethylsilyl)phosphine is highly pyrophoric, not cheaply available, and is not easy to synthesise.[27]

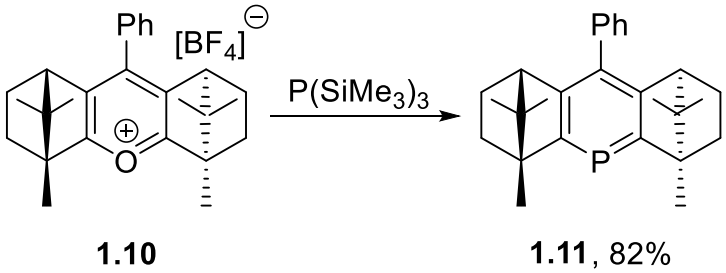

Scheme 1-4. Synthesis of chiral phosphinine **1.11**

Breit and co-workers expanded Märkl's methodology by synthesising 2,6-dialkyl-4-phenylphosphinines (**Scheme 1-5**, **1.12** and **1.13**)[28], using the Balaban-Nenitzescu-Praill reaction.[29] The tetrasubstituted phosphinine **1.15** (**Scheme 1-6**) was prepared

from 1-(2-napthyl)-3-phenylprop-2-enone **(1.14**) by an acid-catalysed tandem rearrangement/electrophilic aromatic substitution reaction.[28] However, this is only a second rare example (after **1.11**) of a substitution pattern outside of the typical 2,4,6 configuration, highlighting another limitation of this synthetic route.

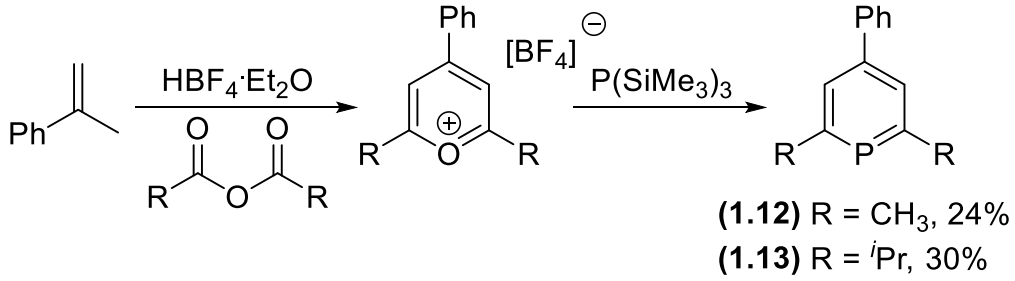

Scheme 1-5.[28] Synthesis of 2,6-dialkyl-4-phenylphosphinines **1.12** and **1.13**

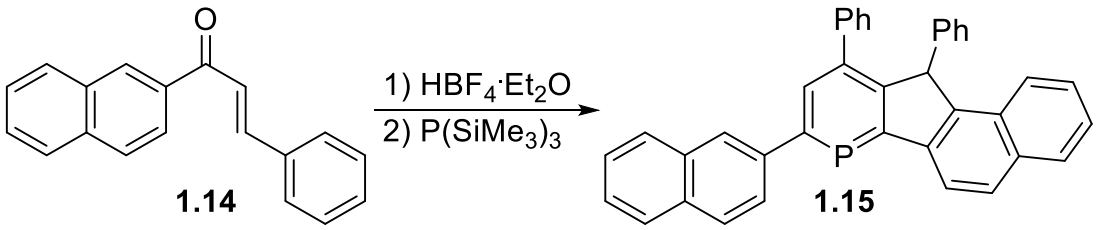

Scheme 1-6.[28] Synthesis of tetrasubstituted, polycyclic aromatic phosphinine **1.15**

Whilst the synthesis of phosphinines through the utilisation of pyrilium salts is commonly observed in the literature, multiple other methods do exist, each with their own limitations. Both Müller[11, 30] and Breit[28] adopted a technique developed by Rösch and Regitz[31] on the decarboxylative [4+2] reaction of phosphaalkynes with 2-pyrones (**Scheme 1-7**). This reaction has been used to prepare phosphinines with low-levels of substitution such as 2-trimethylsilylphosphinine (**1.16**)[11] and chiral oxazoline-substituted phosphinine **1.17**[32] from trimethylsilylphosphaalkyne and *tert*-butylphosphaalkyne respectively. Whilst synthetic routes to the required phosphaalkynes are now well-established,[33, 34] this route still suffers from low yields[20, 32] as well as poor regioselectivity for substituted pyrones.[30] However, Kazunari *et. al.* reported an iron-catalysed [2+2+2] cyclisation of diynes and phosphaalkynes that produces bicyclic phosphinines in yields of up to 87%.[35]

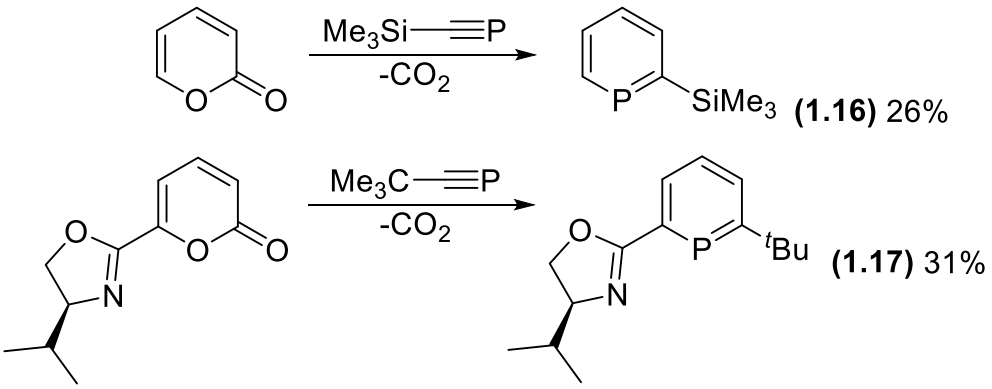

Scheme 1-7.[11, 32] Synthesis of phosphinines **1.16** and **1.17** from pyrones

Whilst the synthesis of phosphinines by the ring-expansion of stannoles with phosphaalkynes was found to be poorly regioselective,[36] Mathey and co-workers have developed several routes to phosphinines by ring-expansion of phospholes.[37-41] It was initially discovered that phospholes (*e.g.* **1.18**, **Scheme 1-8**) reacted with acyl chlorides in the presence of triethylamine to form an acyl phospholium chloride (**1.19**) which, upon hydrolysis, was transformed into a 2-hydroxyphosphacyclohexadiene oxide (**1.20**).[37] By reaction of this species with P_4S_{10}, the dehydroxylated sulfide (**1.21**) was formed, which could then be converted to a single phosphinine (**1.22**) in 46% yield by pyrolysis in the presence of nickel powder.[38]

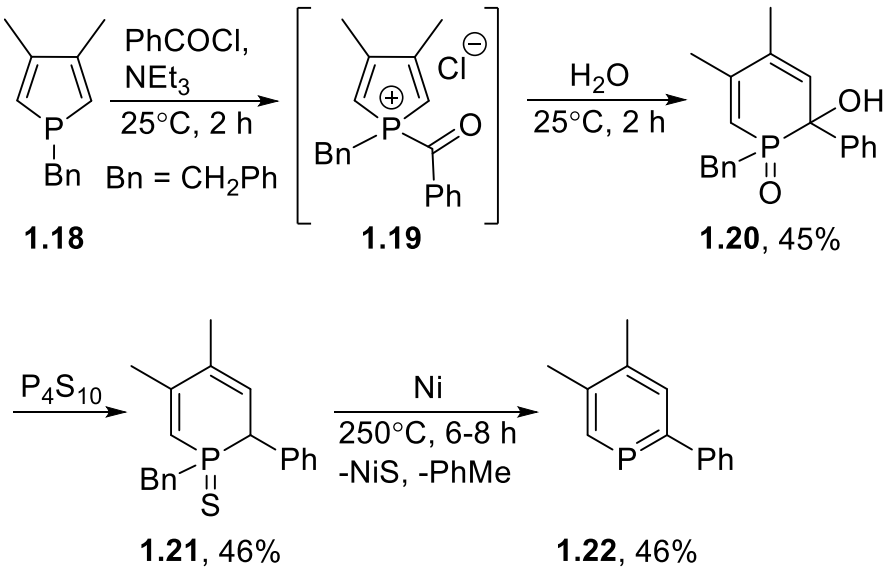

Scheme 1-8.[37, 38] Synthesis of trisubstituted phosphinine **1.22** by ring-expansion of a phosphole with an acyl chloride

Whilst the starting phosphole can be prepared in one synthetic step (although a high pressure vessel is needed),[42] the need for specialist equipment for the pyrolysis as well as a cumulative yield of 9.5% **1.22** from **1.18** limits the practicality of this synthesis.

Further reactivity of phospholes could be enabled by a thermal isomerism-cycloaddition sequence, allowing them to undergo [4+2] cyclisations to form 1-phosphanorbornadienes (**Scheme 1-9**, **1.23**) upon reaction with alkynes.[43] However, as a special case, 1,2,5-triphenylphosphole (**1.24**) could be transformed to 2,3,6-triphenylphosphinine (**1.25**) in 60% yield upon thermolysis in the presence of diphenylacetylene.[43] This work was later expanded to include reactions with 1-phenyl-1-propyne and 1-phenyl-1-butyne.[44]

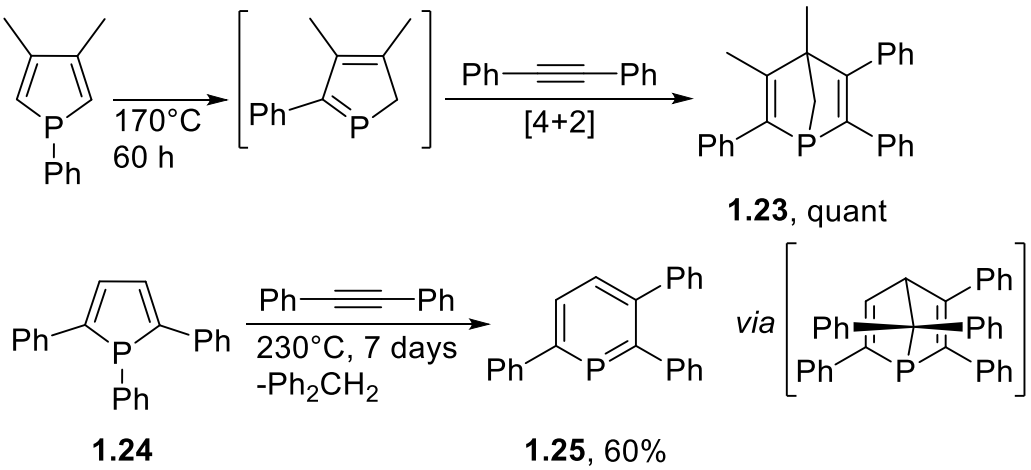

Scheme 1-9.[43] Thermal isomerism of phospholes and their subsequent [4+2] reactions

Following a further three-step sequence, 1-phosphanorbornadienes such as **1.23** were later converted into their respective phosphinines.[41] Mathey and co-workers have also reported two routes to ethyl phosphinine-2-carboxylates *via* the ring expansion of phospholes using ethyldiazoacetate as a carbene source.[40, 45, 46]

A common issue with synthetic routes to phosphinines is that the choice of substituents is often limited to (hetero)aryl or alkyl substituents.[20, 28, 41] However, Le Floch, Mathey and co-workers reported the synthesis of 2-halophosphinines (**Scheme 1-10**, **1.28**, **1.29**) from the reaction of the corresponding (dihalomethyl)dihalophosphine with a diene and excess triethylamine. Upon reaction of the (dihalomethyl)dihalophosphine with base, a transient phosphaalkene (**1.26**) is formed,[47] which then undergoes a [4+2] cyclisation with a diene forming an intermediate 1,2,2-tri(halo)phosphacyclohex-4-ene (**1.27**). By dehydrohalogenation of this intermediate with a further two equivalents of base, the target phosphinine is formed.[47, 48]

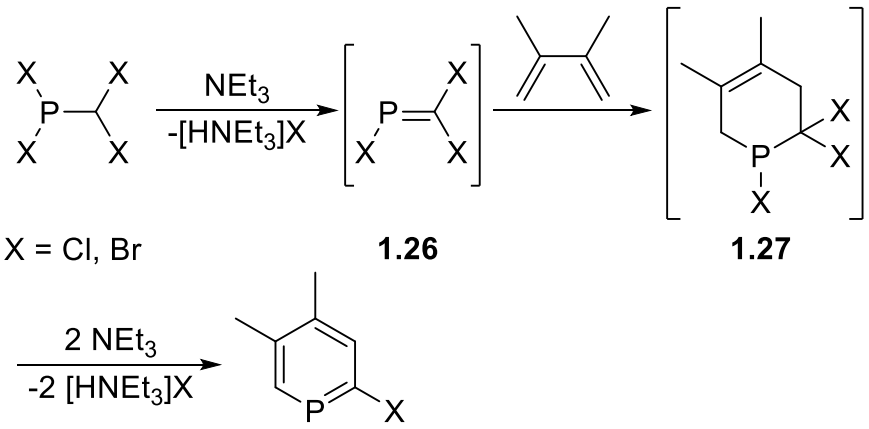

Scheme 1-10.[47, 48] Synthesis of 2-halophosphinines

Extensive studies into the reactivity of these 2-halophosphinines have been reported,[48-53] resulting in early examples of 2-phosphinophosphinines prepared either by trapping the lithiate with $Ph_2P(CN)$[49] or by a palladium-catalysed cross-coupling.[50] Whilst these 2-halophosphinines are synthetically useful, they are also unstable,[49] which limits their practicality. To develop a more general method for the synthesis of polyfunctional phosphinines without relying on unstable intermediates and metal-mediated couplings, Le Floch, Mathey and co-workers expanded on work by Märkl detailing the [4+2] reactions of 1,3-azaphosphinines with alkynes (**Scheme 1-11**, **1.30**).[54, 55]

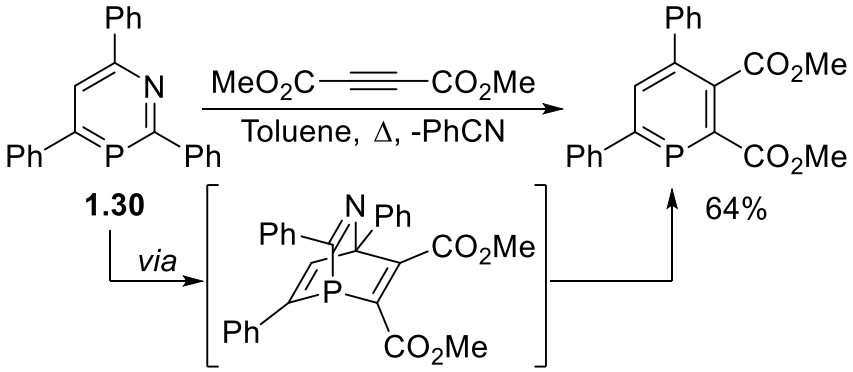

Scheme 1-11.[54] Synthesis of a phosphinines from a 1,3-azaphosphinine

By reaction of this precursor with alkynes, a [4+2] cycloaddition-cycloreversion reaction took place, resulting in the formation of a phosphinine whilst cleanly extruding one equivalent of a nitrile. However, the substitution pattern for the products was determined in part by the chosen 1,3-azaphosphinine (prepared from a 3-azapyrilium salt)[54, 56] and harsh conditions were sometimes required.[55] Therefore, Le Floch, Mathey

and co-workers investigated the reactivity of the 1,3,2-diazaphosphinine (**Scheme 1-12**, **1.31**) as an alternative.[57, 58] As with 1,3-azaphosphinines,[54] the [4+2] reaction of **1.31** with one equivalent of an alkyne produced an equivalent of nitrile, however, the resulting 1,2-azaphosphinine (**1.32**) could then react further. By addition of a second equivalent of a different alkyne, the decreased reactivity of **1.32** allowed for controlled formation of phosphinines containing four different substituents (**1.33**) in the 2,3,5,6 positions.[57, 58]

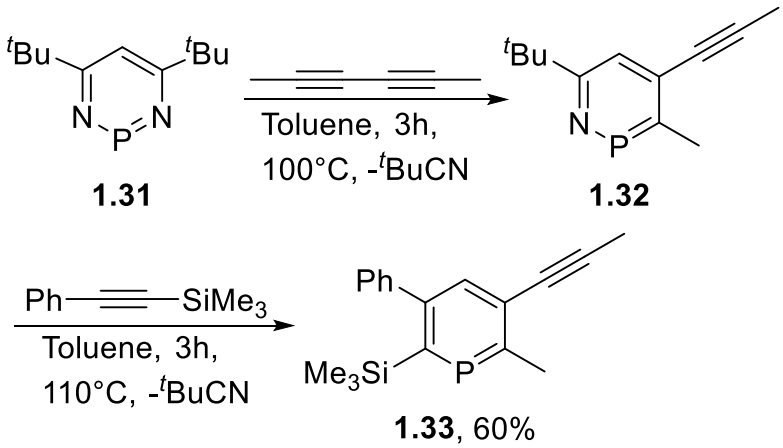

Scheme 1-12. Synthesis of a tetra-substituted phosphinine from a 1,3,2-diazaphosphinine (**1.31**)

1.3 Reactivity of phosphinines

It was first demonstrated by Märkl, shortly after his initial discovery of 2,4,6-triphenylphosphinine,[4] that this product did not react to form the expected salts when treated with the alkylating agents methyl iodide or $[Me_3O][BF_4]$.[59] However, upon treatment with organolithium reagents, strongly coloured ("deep indigo") solutions containing the phosphacyclohexadienide anion (**Scheme 1-13**, **1.34**) were obtained.[59] This also differs from the reactivity of pyridines, which are attacked at the carbons *ortho* to nitrogen.[60] The starting phosphinine is referred to as λ^3, where the number corresponds to the number of bonds to phosphorus, and the structure of phosphacyclohexadienide **1.34** (a λ^4 phosphinine) can be displayed in two other tautomeric forms (**1.35** and **1.36**). Upon addition of an H^+ source to **1.36**, phosphacyclohexadiene **1.37** is obtained exclusively through protonation of an *ortho* carbanion. Trapping anion **1.34** with an alkylating agent (*e.g.* methyl iodide) affords the λ^5 phosphinine **1.38** by alkylation at P.[59] Although **1.38** closely resembles the starting phosphinine **1.2**, it is not aromatic and can be viewed as tautomer **1.39**.[61] Analogous

reactivity to the addition of organolithium reagents is observed with Grignard reagents and alkoxides.[62]

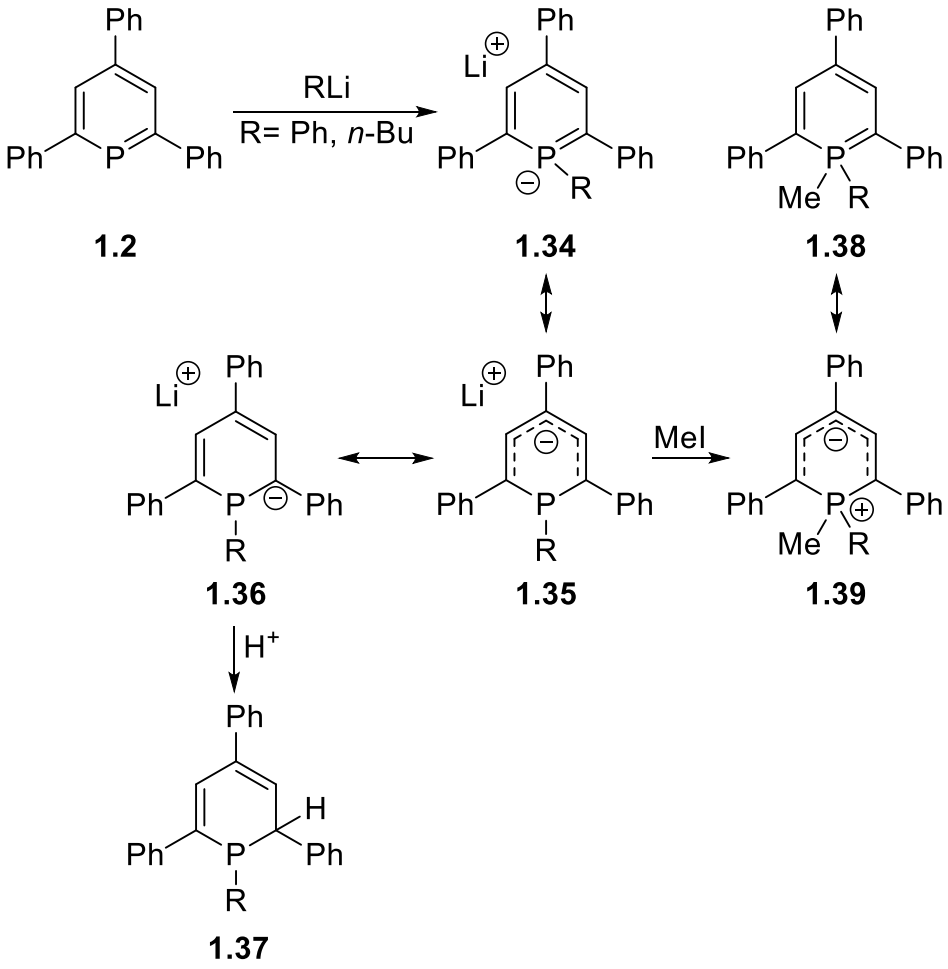

Scheme 1-13.[59, 61] Anion trapping of a λ^4 phosphinine

Whilst λ^5 phosphinine **1.38** is not aromatic, the phosphininium salt **1.41** (**Scheme 1-14**) retains its aromaticity, which is observed by the $^{31}P\{^1H\}$ NMR shift of 160.2 ppm. Calculations revealed that the P-atom in **1.41** is sp^2 hybridised, and so therefore the P-Me bond will involve the phosphorus lone-pair,[63] in a similar fashion to a phosphonium salt.[64]

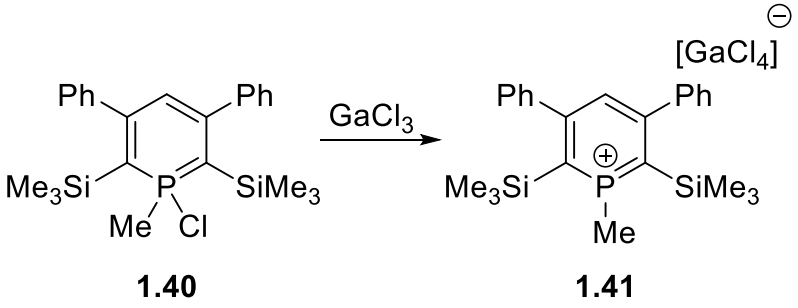

Scheme 1-14.[63] Synthesis of phosphininium salt **1.41**

1.4 Coordination chemistry of phosphinines

1.4.1 Ligand Properties

Phosphinine ligands are of interest due to their unusual properties in comparison to other heterocycles (*e.g.* pyridine) and to common phosphorus ligands (PR_3, where R = aryl, alkyl, OR, NR_2, halide...). However, whilst the coordination chemistry of phosphinines has been thoroughly reviewed,[3, 8, 14, 65] little research has been published on the development of phosphinine ligands for their catalytic utility.

Using DFT, the molecular orbitals of the parent phosphinine were calculated, and its aromaticity shown to be *circa* 88% of that of benzene.[12] The LUMO of phosphinine has a large amount of P-character at phosphorus, and is much lower in energy than pyridine (**Figure 1-1**), and as a result, phosphinines are π-accepting ligands. Whilst phosphinine's lone-pair is higher in energy than the nitrogen lone-pair in pyridine, because the lone-pair is in the HOMO-2 – compared to the HOMO in pyridine – phosphinine is a much poorer σ-donor and is non-nucleophilic.[12]

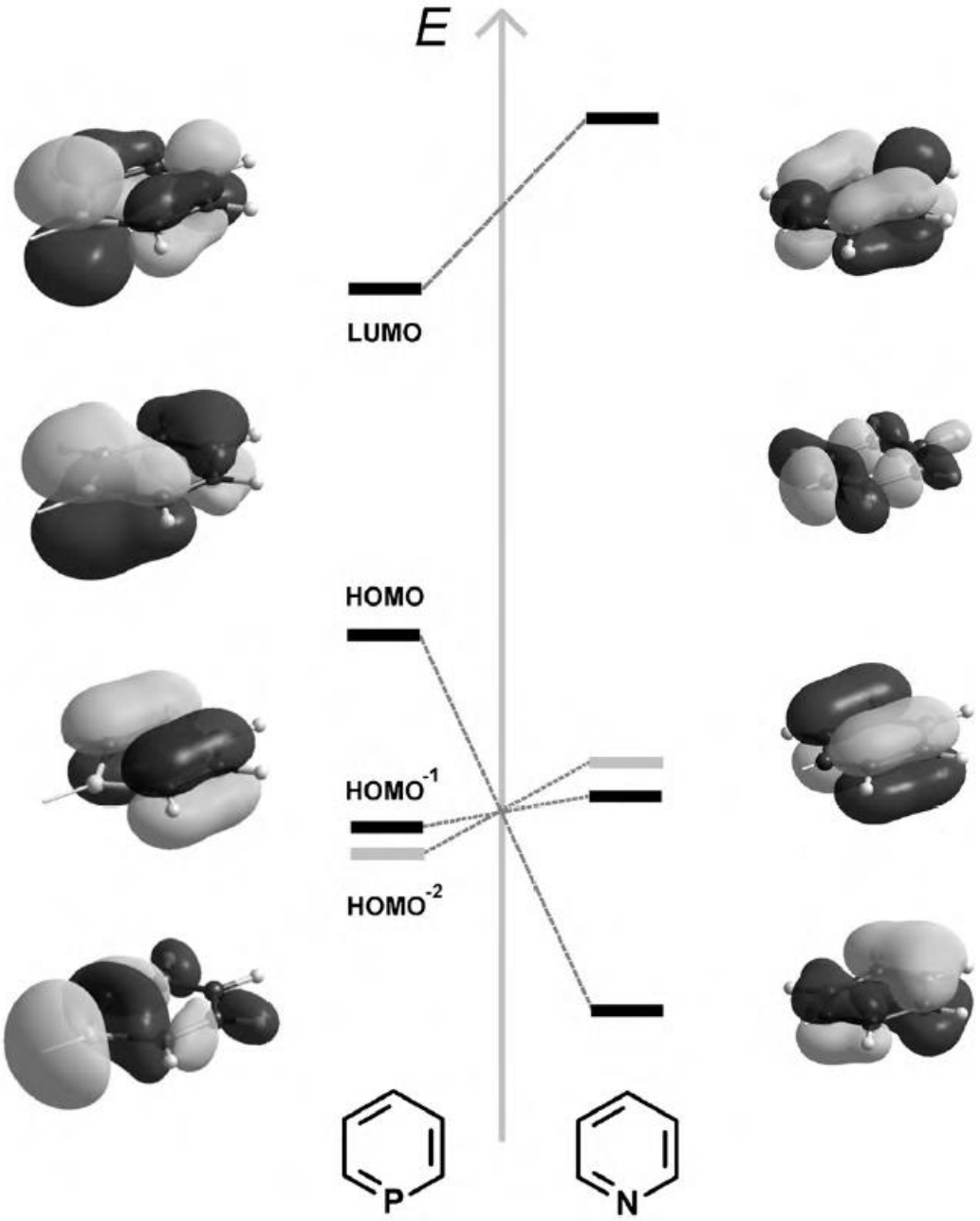

Figure 1-1.[12] The molecular orbitals of phosphinine in comparison to pyridine. Reproduced from: C. Müller, D. Vogt, *C. R. Chimie*, **2010**, 13, 1127-1143.

The donor properties of phosphinines have also been evaluated experimentally, by comparison of the values for ν(CO) obtained from infrared spectra of $[Ni(L)(CO)_3]$ complexes. **Table 1-1** shows that the CO stretching frequency obtained from the complex of 2,4,6-triphenylphosphinine (2079 cm^{-1}) is almost identical to that of trimethylphosphite (2080 cm^{-1}), indicating a high level of π-acceptance.[66]

Table 1-1. Comparison of ν(CO) values for [Ni(L)(CO)$_3$] complexes

	Ligand	ν(CO) (cm^{-1})	Reference
Stronger σ-donors ↓	$P(OMe)_3$	2080[a]	66
	2,4,6-triphenylphosphinine	2079	67
	PPh_3	2069[a]	66
	$P(^tBu)_3$	2056[a]	66

[a]: Values for ν(CO) rounded to the nearest integer

1.4.2 η^1 Coordination of phosphinines

Despite being poor donors and relatively non-nucleophilic,[12] the coordination of monodentate phosphinines has been demonstrated with a wide range of transition metals.[3, 28, 68-71] Whilst, as previously discussed, their synthesis in comparison to phosphine and pyridine ligands (which are often commercially available) is challenging, the π-accepting properties of phosphinines can stabilise complexes that are otherwise unknown with analogous ligands. For example, Elschenbroich and co-workers have demonstrated the synthesis of homoleptic M(0) Cr,[72] Fe,[69] and Ni[68] complexes (**Scheme 1-15**, **1.42**, **1.43**, and **1.44** respectively) of the parent phosphinine. The pyridine analogues of these complexes are unknown, with the exception of [Ni(Py)$_4$],[73, 74] however, attempts to synthesise [Ni(Py)$_4$] by Elschenbroich and co-workers using the same methodology as used to prepare **1.44** resulted only in "decomposition, with deposition of a nickel slurry".[68]

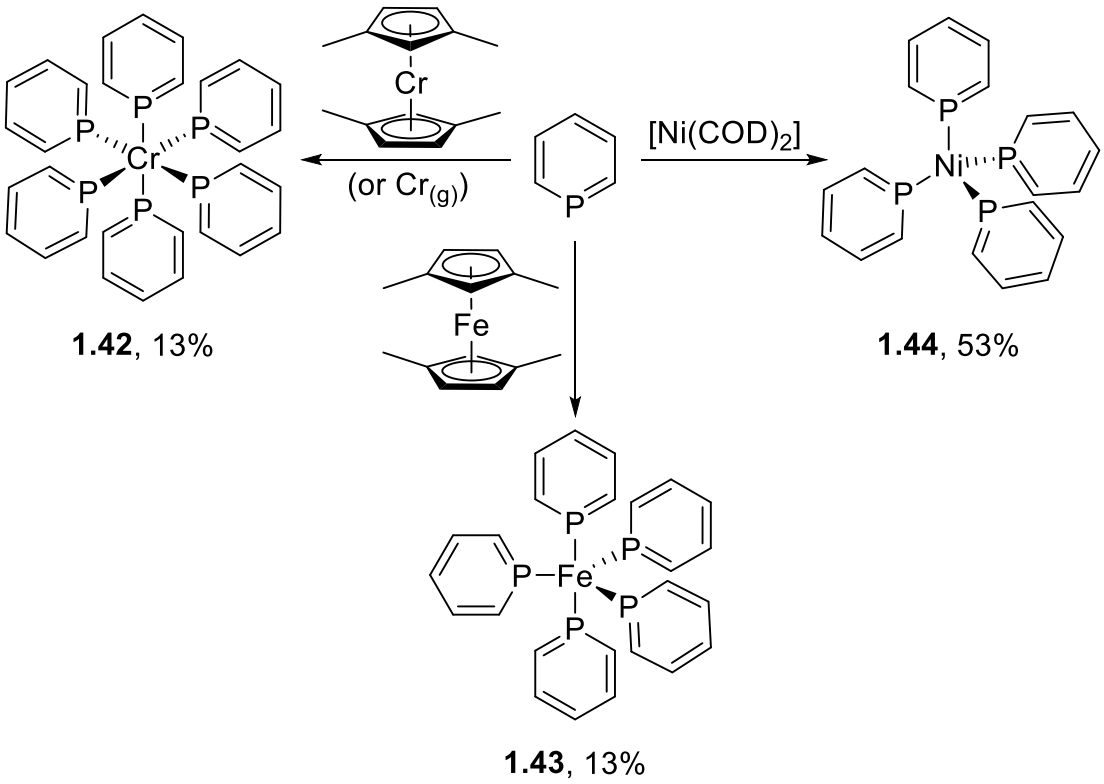

Scheme 1-15.[68, 69, 72] Synthesis of homoleptic M(0) complexes of phosphinine. An excess of phosphinine was used in all reactions

1.4.3 Other coordination modes

Due to the poor σ-donor properties of phosphinines, they will readily bind to metals through the aromatic ring. Of these other binding modes, η^6 coordination is most commonly observed, however, levels of hapticity ranging from η^2 to η^5 are also known.[3] Mathey and co-workers demonstrated that variations in the steric bulk in the *ortho* positions of a phosphinine have an effect on the ligand's tendency to bind η^1 or η^6 (**Scheme 1-16**).[75] By reaction of Ru precursor **1.45** with bromophosphinine **1.46** or bis(trimethylsilyl)phosphinine **1.47** in the presence of silver tetrafluoroborate, the respective η^1 (**1.48**) and η^6 (**1.49**) complexes were formed.

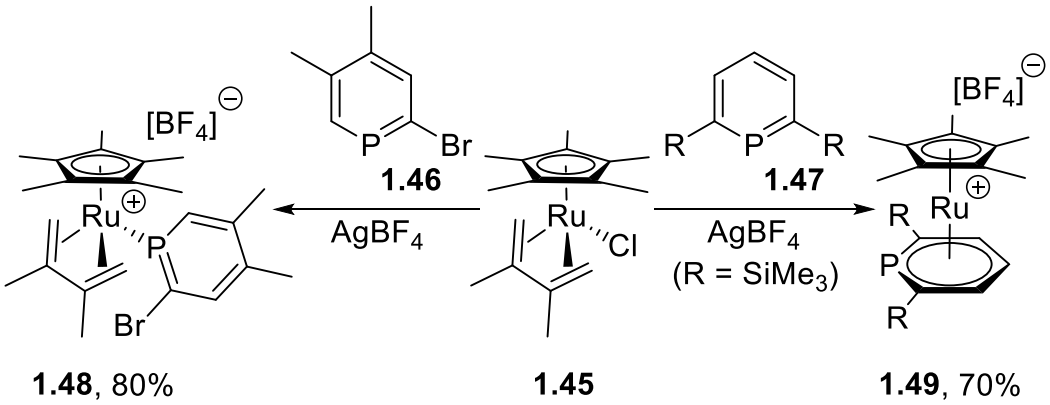

Scheme 1-16.[75] Synthesis of complexes **1.48** and **1.49** through variation of steric bulk in the *ortho* positions

M(0) tricarbonyl complexes of Cr[76] and Mo[77] containing η^6 phosphinines are also known. By the thermal reaction of 2,4,6-triphenylphosphinine with $[Cr(CO)_6]$ and $[Mo(mes)(CO)_3]$ (mes = 1,3,5-trimethylbenzene), complexes **1.50** and **1.51** (**Figure 1-2**) were isolated in 28% and 45% yields respectively. However, photochemical reactions with the homoleptic hexacarbonyls produce the η^1 pentacarbonyl complexes.[78] Thermolysis of the η^1 Mo complex **1.52** in boiling Bu_2O for 30 minutes then produced **1.51** in 90% yield,[77] demonstrating the relative ease of interconversion between coordination modes.

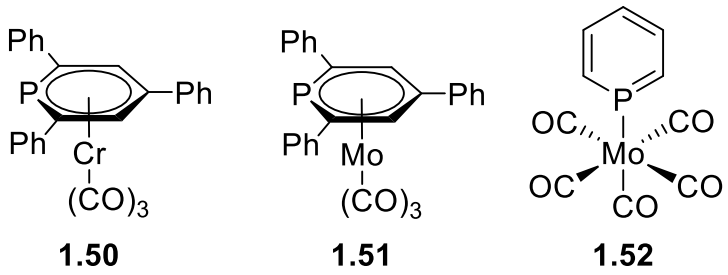

Figure 1-2. Metal carbonyl complexes of 2,4,6-triphenylphosphinine

1.5 Donor-functionalised phosphinines

1.5.1 Background

The synthesis and coordination chemistry of donor-functionalised phosphinines has been covered in several reviews.[3, 12, 14-16, 18] As with more common systems, such as pyridines,[79-81] phosphines,[82, 83] and N-heterocyclic carbenes,[84-86] incorporation of one or more donors to a phosphinine ligand can be beneficial when studying their coordination chemistry and/or their uses in catalysis. Due to phosphinines being relatively non-nucleophilic and poor σ-donors,[3] incorporating them into multidentate ligands can enable more facile coordination. By first allowing for coordination of the second, stronger donor (**Scheme 1-17**, denoted as "L"), coordination of the phosphinine is more favourable due to the chelate effect.[87] Incorporation of a second donor also allows for adjustment of the ligand bite angle, which can enable the ligand to be "tuned" to a specific coordination environment, as well as altering the rates of key catalytic steps, such as oxidative addition or reductive elimination.[82] The bite angle of a ligand is also key to the success of catalysts for industrially important reactions including hydroformylation[88] and ethylene oligomerisation,[89] which benefit from large and small bite angles respectively.

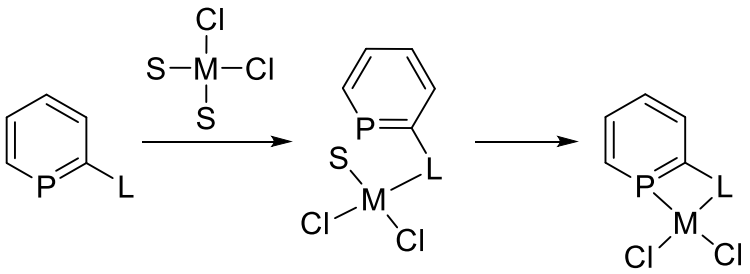

Scheme 1-17. Chelation-assisted coordination of a phosphinine in a bidentate system. S = solvent or labile ligand

1.5.2 Diphosphinines

Analogous to 2,2′-bipyridine, 2,2′-biphosphinines are a known family of ligands,[90-96] although they have seen comparatively little use due to difficulties in their synthesis. The first biphosphinine was reported by Le Floch, Mathey and co-workers, starting from 2-bromo-4,5-dimethylphosphinine **1.29**.[97] Direct coupling of two units of **1.29** using Ni(0) was not successful due to the formation of nickel complexes, without oxidative addition into the C-Br bonds. Therefore, to "activate" the bond, they dearomatised **1.29** by a [4+2] hetero-Diels-Alder reaction with 2,3-dimethylbutadiene in the presence of sulfur and a catalytic amount of pyridine (**Scheme 1-18**), following their

previously reported procedure.[49, 97] Lithiation of **1.53** and addition of sub-stoichiometric Ni(II) afforded the coupled product **1.54** (~35%) as well as two dehalogenated side-products ~45% total, not shown). After a one-pot desulfurisation and thermal retro-Diels-Alder reaction, biphosphinine **1.55** was obtained as the minor product (~22% from **1.29**, as well as ~32% 3,4-dimethylphosphinine).[97]

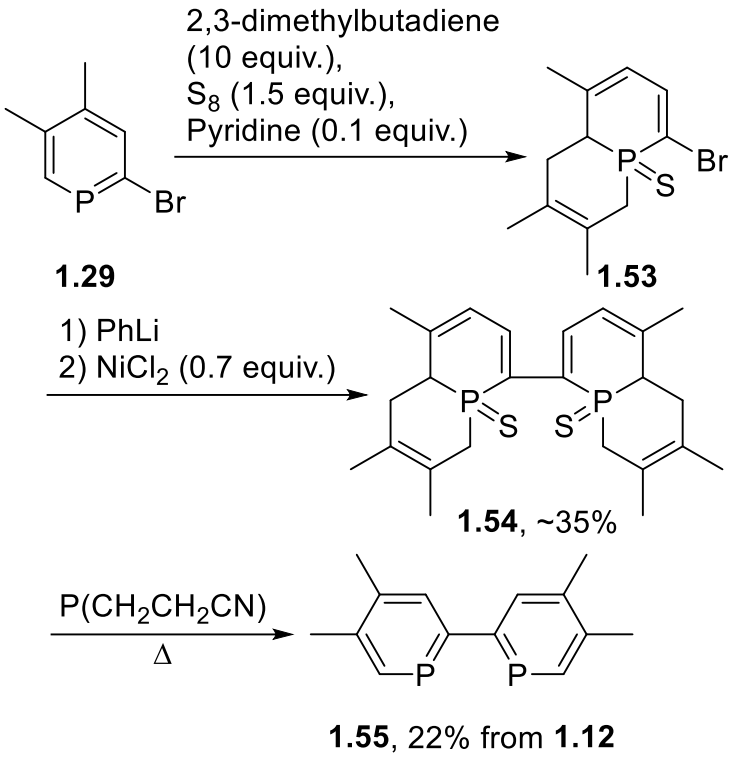

Scheme 1-18.[97] Synthesis of biphosphinine **1.55** from bromophosphinine **1.29**

After this initial publication, simpler methods have been reported, including the homocoupling of phosphininyl zirconocenes,[51, 94] the homocoupling of 2-bromophosphinines using LiTMP (TMP = 2,2,6,6-tetramethylpiperidyl),[90, 98] and the Stille coupling of 2-bromo and 2-stannyl phosphinines.[52] However, each of these routes requires starting from a 2-halophosphinine and affords the biphosphinine in low yields.

Biphosphinines have been coordinated to a range of transition metals,[18] including chromium,[52, 90] molybdenum,[52, 90] tungsten,[52, 90] manganese,[90] rhenium,[90] iron,[96] ruthenium,[92, 96, 99] osmium,[100] cobalt,[95] rhodium,[95] and nickel[52, 101] by Le Floch, Mathey and coworkers. However, it is most notable that they have been used to stabilise unusual oxidation states, including Co(-1),[95] Rh(-1),[95] Fe(-2),[96] and Ru(-2).[96] Other π-accepting ligands such as PF_3,[102] isocyanides,[103] and alkenes[104, 105] have previously been demonstrated to stabilise negative oxidation states, but biphosphinines provide a

measure of convenience as they can be doubly reduced prior to coordination.[92] To synthesise the Ru(-2) complex **1.57**, after reaction of **1.55** with two equivalents of lithium in THF (**Scheme 1-19**), the diamagnetic dianion **1.56** was then simply added to 0.5 equivalents of [Ru(COD)(acac)$_2$] (acac = acetylacetonate), affording the dilithium salt.[96]

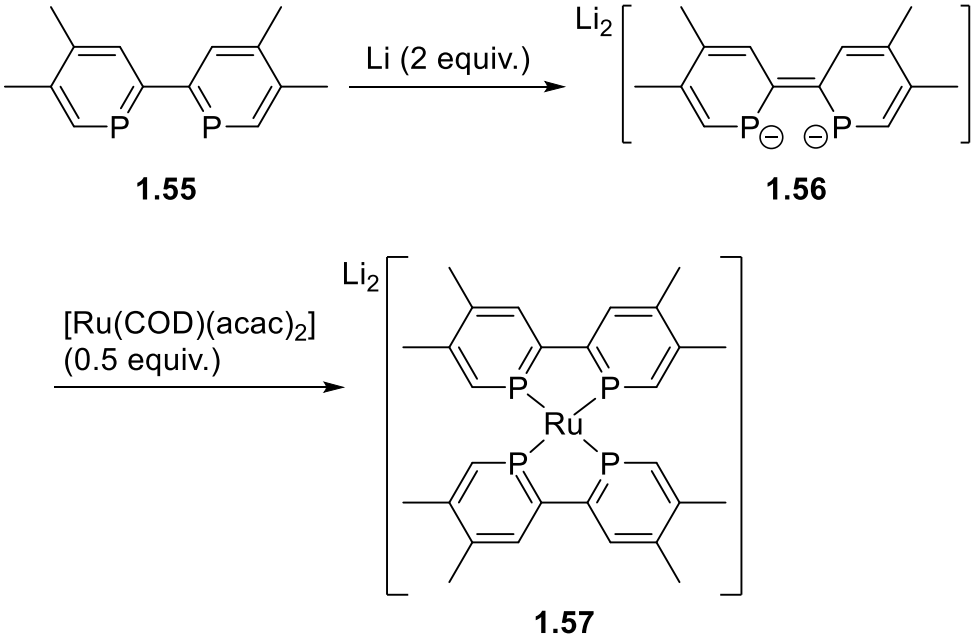

1.55 **1.56** **1.57**

Scheme 1-19.[96] Synthesis of Ru(-2) complex **1.57**

As shown in **Scheme 1-12**, biphosphinines cannot be prepared from the reaction of diazaphosphinine **1.31** with diynes due to the regiochemistry of the product obtained.[58] However, Le Floch, Mathey and co-workers published the synthesis of three diphosphinines **1.60**, **1.61**, and **1.63** (**Scheme 1-20**) from **1.31** by exploiting the tendency of silyl and phosphino[106] alkynes to regioselectively deliver the *ortho*-Si or –P substituted products in reactions with diazaphosphinines.[58,107] The coordination chemistry of these three species has not been reported in the literature, however, the one-electron reduction of **1.61** has been published.[108]

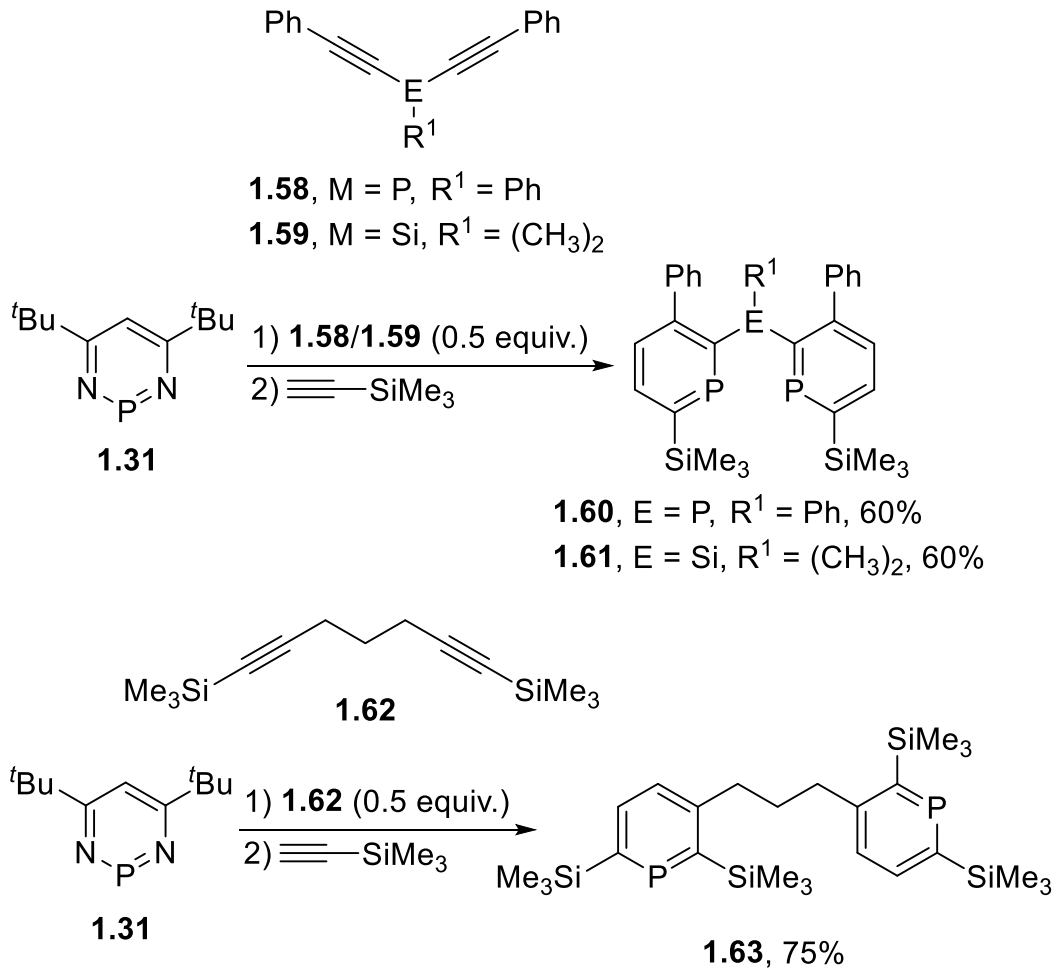

Scheme 1-20.[58] Synthesis of diphosphinines from the reaction of a diazaphosphinine with diynes

1.5.3 Triphosphinines

Due to their ease of synthesis and commercial availability, terpyridines (**Figure 1-3**, **1.64**) (derivatives of 2,6-di(2-pyridyl)pyridine) have been used extensively in coordination chemistry and catalysis.[109] However, unlike biphosphinines, a direct P-analogue of terpyridine (**1.65**) has yet to be reported in the literature. Whilst 2,6-dibromophosphinines are known,[50, 52] transition-metal mediated coupling of these species (analogous to the synthesis of biphosphinines)[90] has not been extended to a terphosphinine, although it is known that they cannot be prepared using LiTMP.[98, 110]

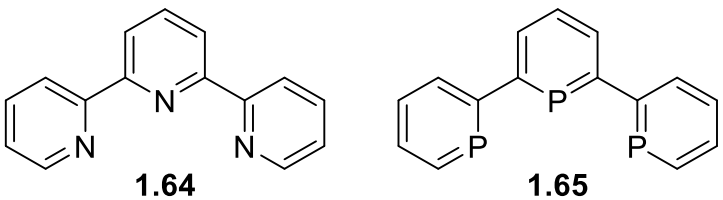

Figure 1-3. Terpyridine and the hypothetical P-analogue

The closest triphosphinine to **1.65** in the literature (**Scheme 1-21**, **1.69**) is derived from a bis(alkynyl)silane (**1.66**) and 1,3,2-diazaphosphinine (**1.31**).[58] By reaction of **1.31** with four equivalents of **1.66** to suppress polymerisation, phosphinine **1.67** was isolated in 70% yield. Heating a mixture of **1.67** with two equivalents of **1.31** under reflux and then addition of an excess of trimethylsilylacetylene afforded triphosphinine **1.69** in 60% yield.[58]

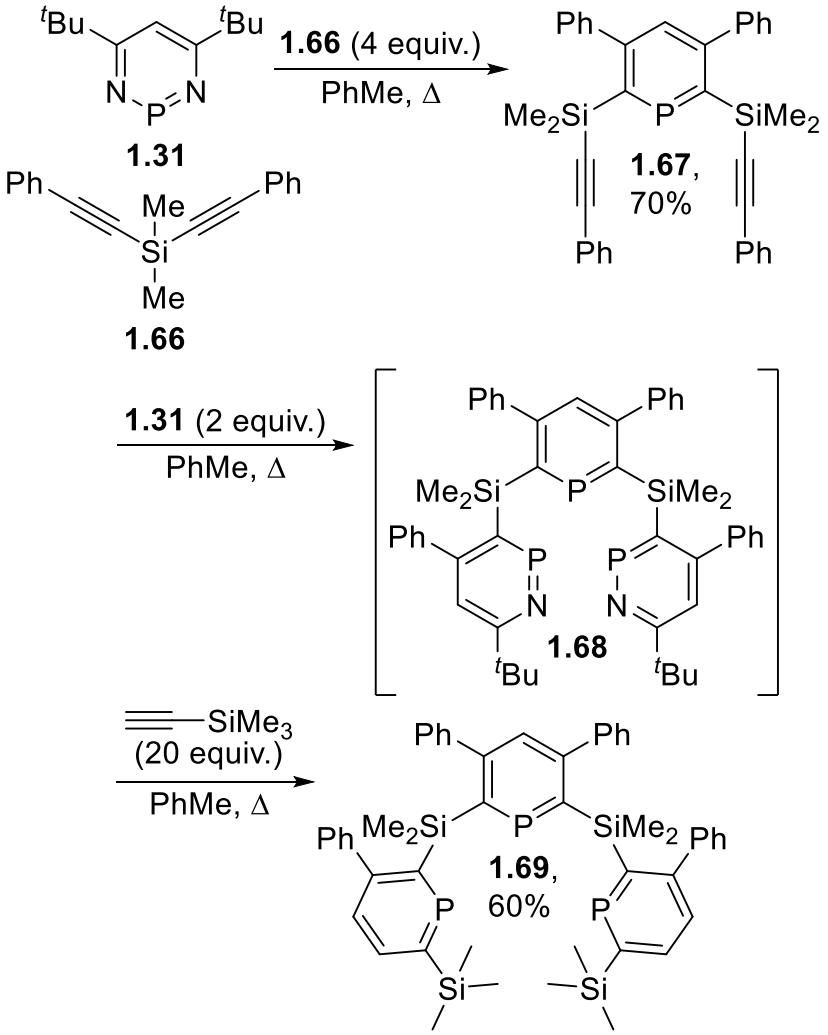

Scheme 1-21.[58] Synthesis of triphosphinine **1.69**

Triphosphinine **1.69** has been coordinated to Rh and Ir, with the chloro and cationic acetonitrile complexes published for both metals as well as the rhodium carbonyl complex **1.70** (**Scheme 1-22**).[18, 111] The carbonyl ligand in complex **1.70** has a single stretching frequency of ν(CO) = 2035 cm^{-1}, which is notably higher than for the terpyridine complex **1.71** (**Figure 1-4**, 1990 cm^{-1})[112], indicative of the three strongly π-accepting phosphinine donors.

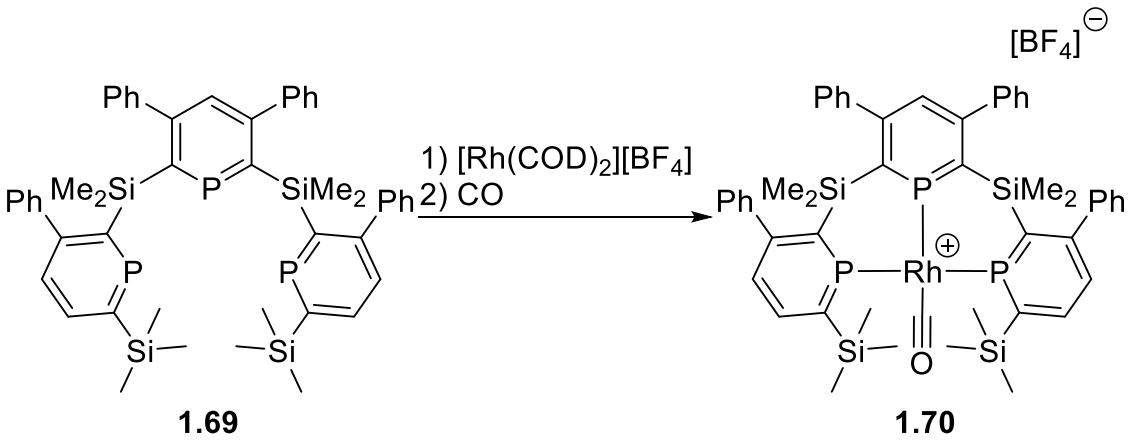

1.69 **1.70**

Scheme 1-22.[18, 111] Synthesis of Rh complex **1.70** (no yield reported)

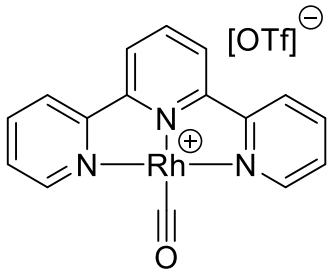

1.71

Figure 1-4.[112] Rh terpyridine complex **1.71**. OTf = trifluoromethanesulfonate

The diazaphosphinine methodology was then applied to the synthesis of "tripodal" ligands in a tetrahedral geometry based on a central silicon or carbon. By reaction of excess **1.31** with tris(alkynyl)silane **1.72** (**Scheme 1-23**) and subsequent completion of the phosphinine with excess trimethylsilylacetylene or 4-octyne, tripodal ligands **1.73** and **1.74** were isolated in 70% and 76% yields (based on **1.72**) respectively. Attempts to prepare the analogous (phenyl-substituted) product to **1.73** using tris(2-phenylethynyl)phenylsilane were unsuccessful due to the isolation of an inseparable mixture of bis and tris(phosphinine).[18, 113]

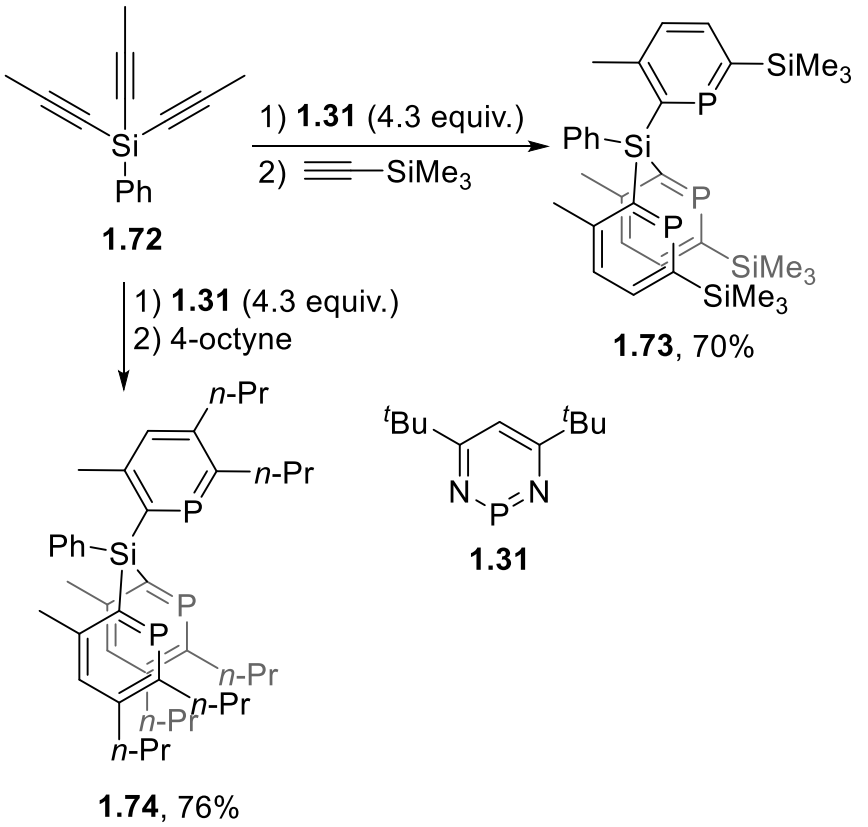

Scheme 1-23.[18, 113] Synthesis of tripodal phosphinine ligands **1.73** and **1.74**

Attempts to prepare the group 6 M(0) tricarbonyl complexes of **1.73** were met without success due to the steric bulk of the trimethylsilyl groups over the "open" face of the ligand. However, the tungsten tricarbonyl complex of **1.74** was obtained in a 56% yield by heating a toluene solution of the ligand and $[W(CO)_5(THF)]$ under reflux for twenty hours. The reaction of **1.31** with non-polar alkynes is sluggish, and the synthesis of **1.74** required heating to 120°C for one week. As a result, the synthesis of the larger tripodal ligand **1.75** (**Figure 1-5**) was reported, using the same methodology as in **Scheme 1-23**. The issue of steric bulk still prevented coordination of this ligand, however, the hexapropyl analogue **1.76** once again was coordinated to a tungsten tricarbonyl fragment.[113]

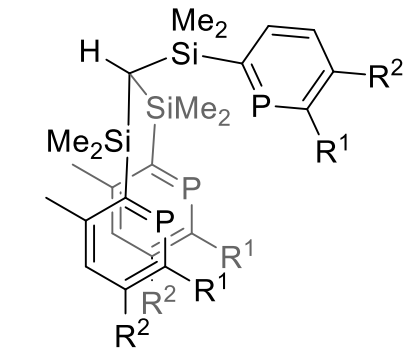

1.75, $R^1 = SiMe_3$, $R^2 = H$, 75%
1.76, $R^1 = R^2 = n$-Pr, 35%

Figure 1-5.[113] Expanded tripodal ligands **1.75** and **1.76**

Using a modification of the reaction between phosphaalkynes and 2-pyrone (**Scheme 1-7**), Grützmacher and co-workers prepared sodium 2-phosphaphenolate (**1.77**, **Scheme 1-24**) by combination of the readily available sodium phosphaethynolate salt[114] and 2-pyrone in hot dimethoxyethane.[115] The product **1.77** is an air and moisture stable microcrystalline solid that can be dissolved in water without hydrolysis and allows easy access to triphosphinine ligand **1.78** containing a central phosphite as a fourth donor through reaction with PCl_3. Phosphonitophosphinine **1.79** and ethyldiphosphininophosphite **1.80** have also been synthesised and their coordination chemistry investigated. Upon reaction of **1.78** with [{Rh(COD)(μ-Cl)}$_2$] and triphenylphosphine, the pentacoordinate, cationic Rh complex **1.81** was isolated (**Scheme 1-25**).[116]

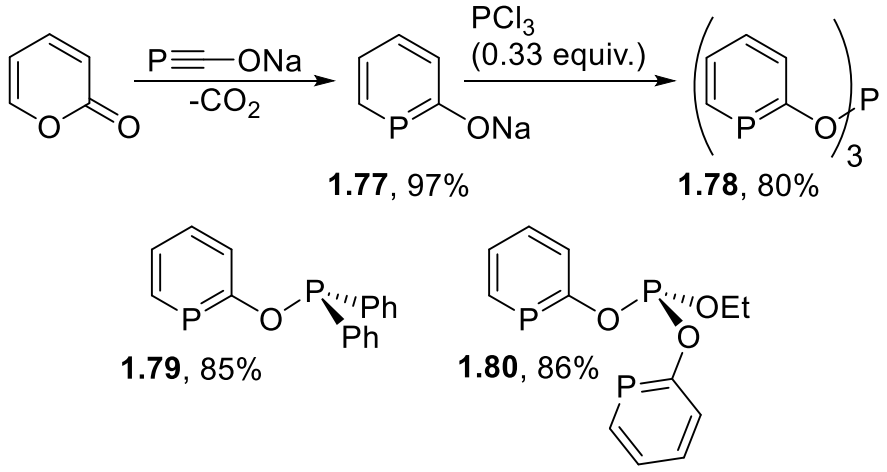

Scheme 1-24.[115-117] Synthesis of 2-phosphaphenolate and its P(III) derivatives

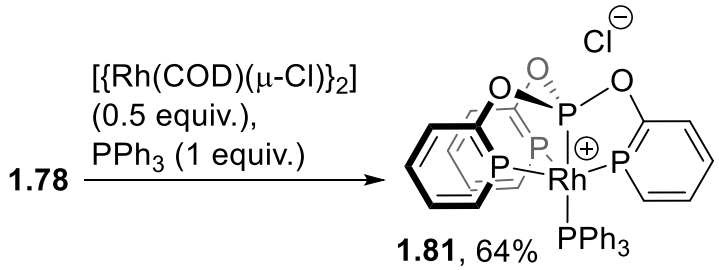

Scheme 1-25.[116] Synthesis of Rh complex **1.81**

1.5.4 Macrocyclic phosphinines

Macrocyclic ligands including calixarenes,[118, 119] phthalocyanines,[120, 121] and porphyrins[122-125] have been used extensively in a range of catalytic reactions. As triphosphinine ligands such as **1.69** (**Scheme 1-21**) had already been reported,[58] Le Floch, Mathey and co-workers investigated the final necessary steps to a series of phosphinine macrocycles (**Scheme 1-26**).[126-129] By reaction of bis(azaphosphinine) **1.68** with a further equivalent of bis(alkynyl)silane **1.66** under high dilution, tris(phosphinine) macrocycle **1.82** was isolated in 20% yield. Alternatively, addition of **1.67** (under high dilution) afforded tetraphosphinine macrocycle **1.83** in 20% yield. Low yields were obtained for both macrocycles due to the formation of polyphosphinines.[126, 128]

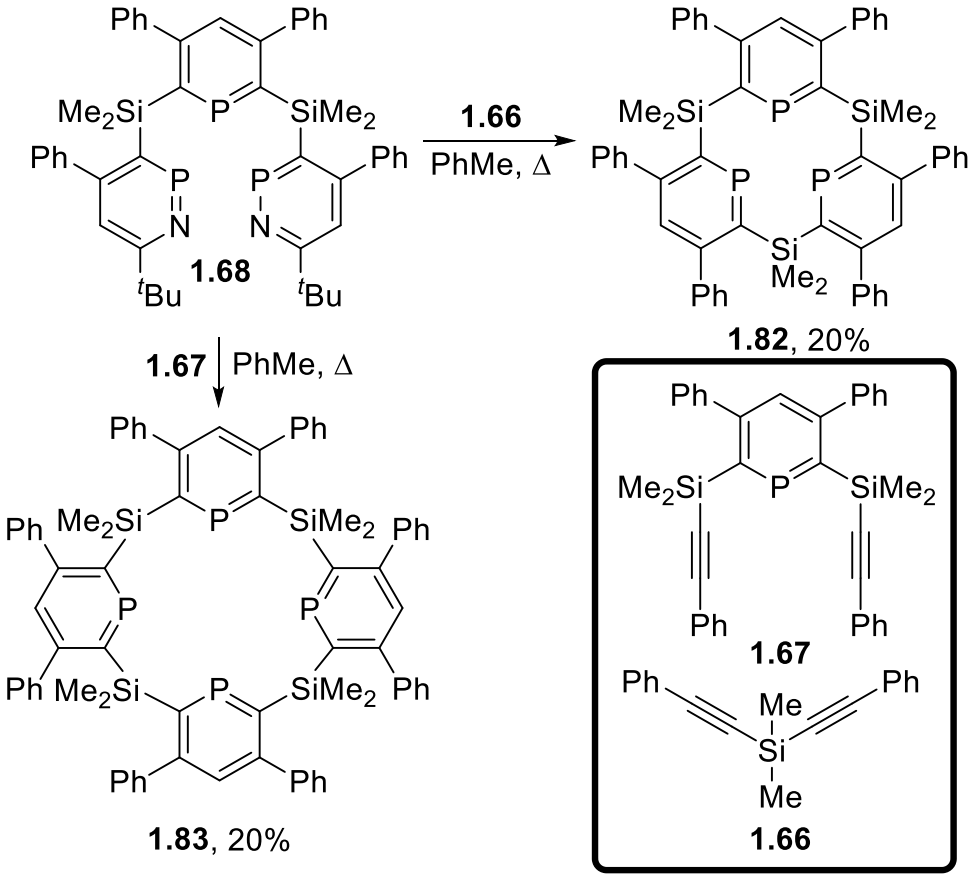

Scheme 1-26.[126, 128] Synthesis of phosphinine macrocycles **1.82** and **1.83**

Whilst the smallest macrocycle **1.82** has only been coordinated to a $W(CO)_3$ fragment, Rh(I) and Ir(I) complexes of **1.83** have been reported.[18, 126] However, it was also demonstrated that one-electron reduction of an Au(I) complex (**1.84**, **Scheme 1-27**) could be performed, affording an Au(0) complex that was stable below -43°C.[18, 130] The instability of Au(0) complexes is known, with only carbonyl complexes reported (but not isolated).[131] Therefore, the quasi-stability of **1.85** is most likely a result of the π-accepting nature of phosphinines,[130] and it has been demonstrated that they are able to stabilise unusual complexes and oxidation states elsewhere.[68, 72, 95, 96, 101 69]

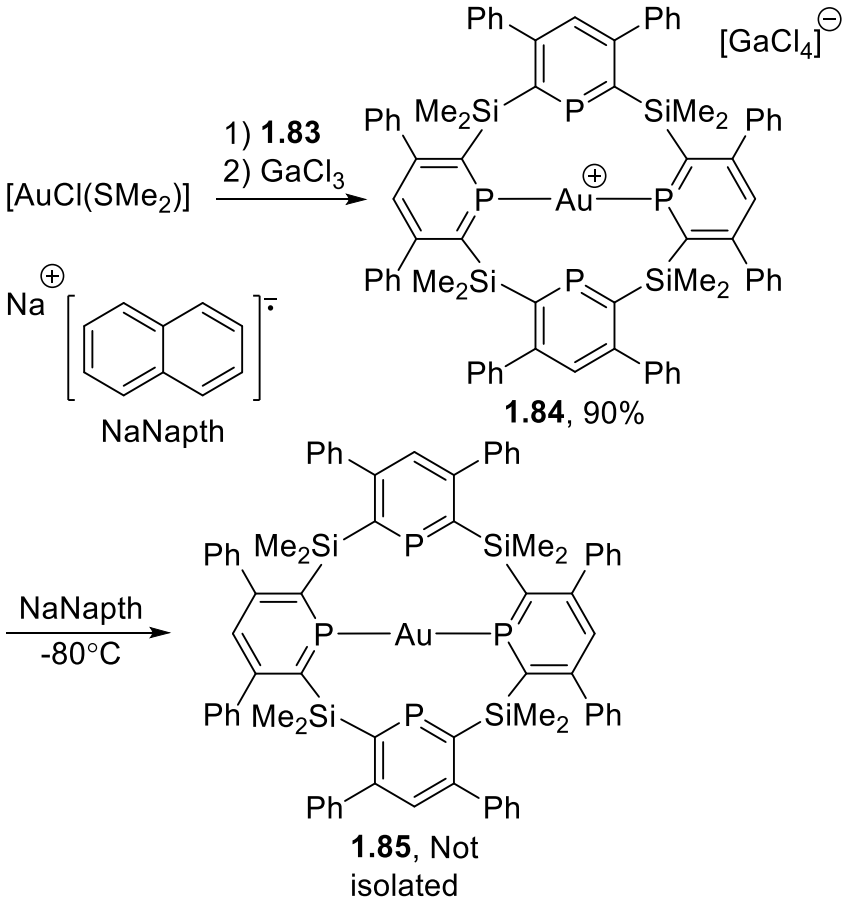

Scheme 1-27.[18, 130] Synthesis of Au macrocyclic complexes.

Starting from the bis(alkynylsilyl)furan/thiophene precursors **1.86** and **1.87**, addition of two equivalents of diazaphosphinine **1.31** and subsequent reaction with a second equivalent of bis(alkyne) under high dilution afforded the diphosphinine macrocycles **1.88** and **1.89**, both in 20% yield (**Scheme 1-28**).[128] An analogous Au(I) complex was prepared in 91% yield from **1.88**, however, attempts to reduce it indicated that the desired Au(0) product was not stable enough for spectroscopic characterisation.[18, 130]

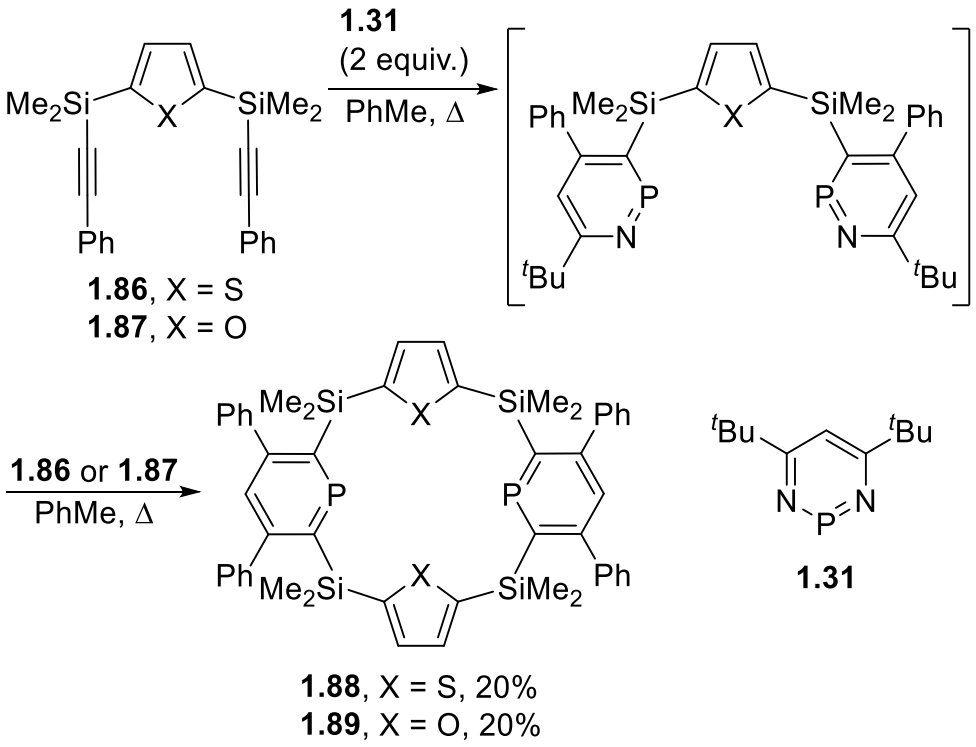

Scheme 1-28.[128] Synthesis of furan/thiophene-containing diphosphinine macrocycles

Four final examples of phosphinine macrocycles containing Si-O-$(CR_2)_n$-$(O)_x$-Si (n = 0, 2, 3; x = 0, 1) linkages were prepared from dialkynes **1.90** to **1.92** (**Figure 1-6**) and diazaphosphinine **1.31**.[127, 129] Condensation of two equivalents of **1.31** with a dialkyne and subsequent completion of the macrocycle with a second equivalent of dialkyne afforded bis(phosphinine) macrocycles **1.93** to **1.95** (**Figure 1-7**).[127, 129] To allow for the inclusion of a third phosphinine unit, **1.31** was reacted with an excess of the dialkyne containing only an Si-O-Si linkage (**1.90**), affording bis(alkynyl)phosphinine **1.96**. Analogously to **Scheme 1-26**, addition of two equivalents of **1.31** and cyclisation with a final equivalent of **1.90** produced triphosphinine **1.97** (**Scheme 1-29**).[129] The coordination chemistry of **1.93** to **1.95** is not known in the literature, however, the di(reduction) of **1.93** has been reported.[132] Macrocycle **1.97** has been coordinated to group 11 (+1) salts.[129]

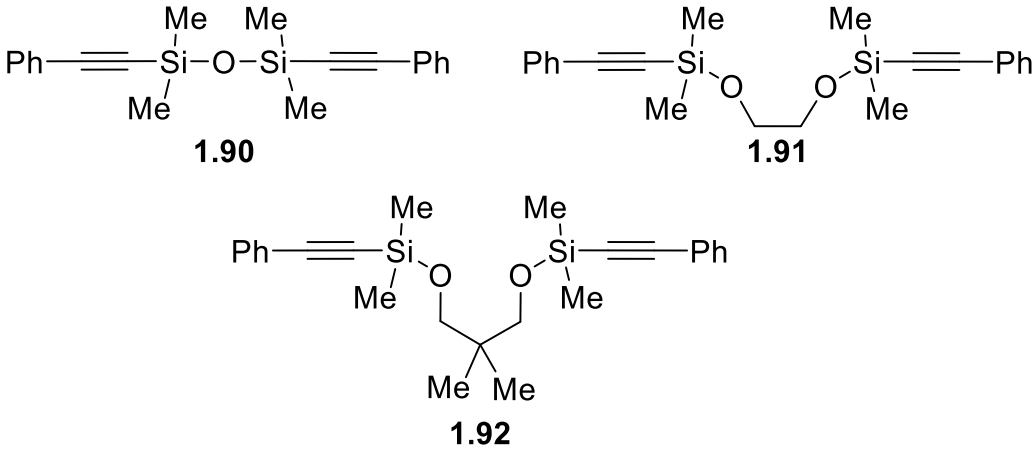

Figure 1-6.[127, 129] Silyloxy dialkynes

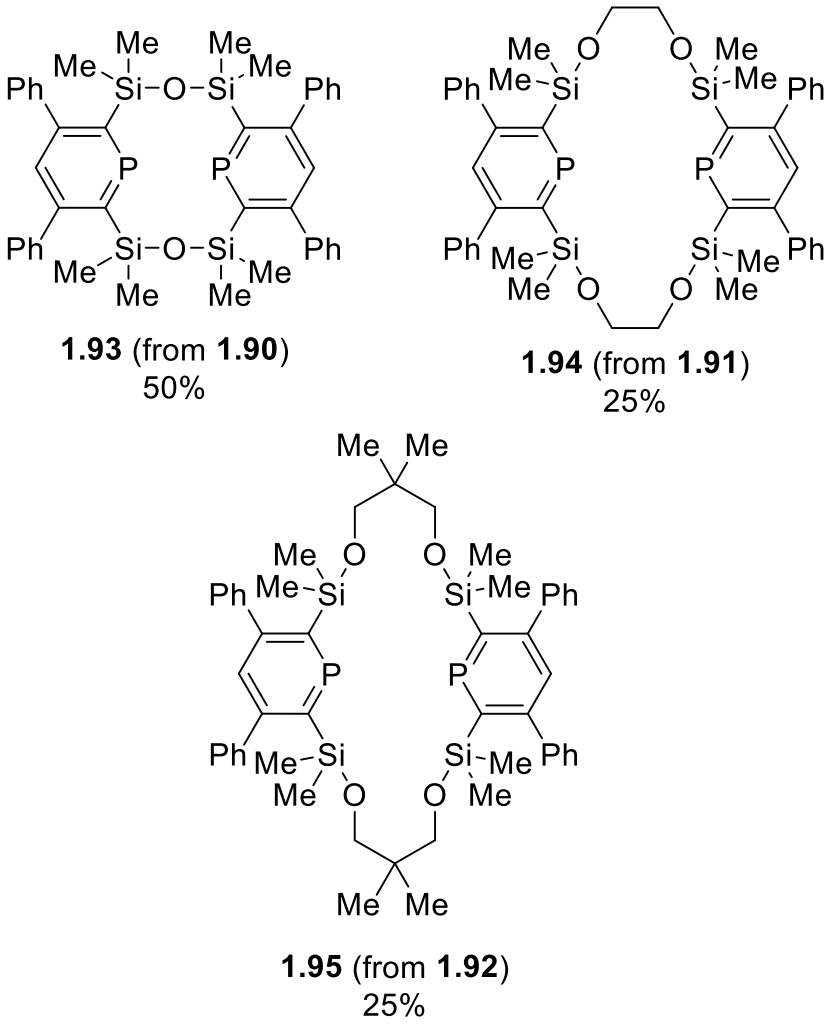

Figure 1-7.[127, 129] Bis(phosphinine) macrocycles derived from **1.90** to **1.91**

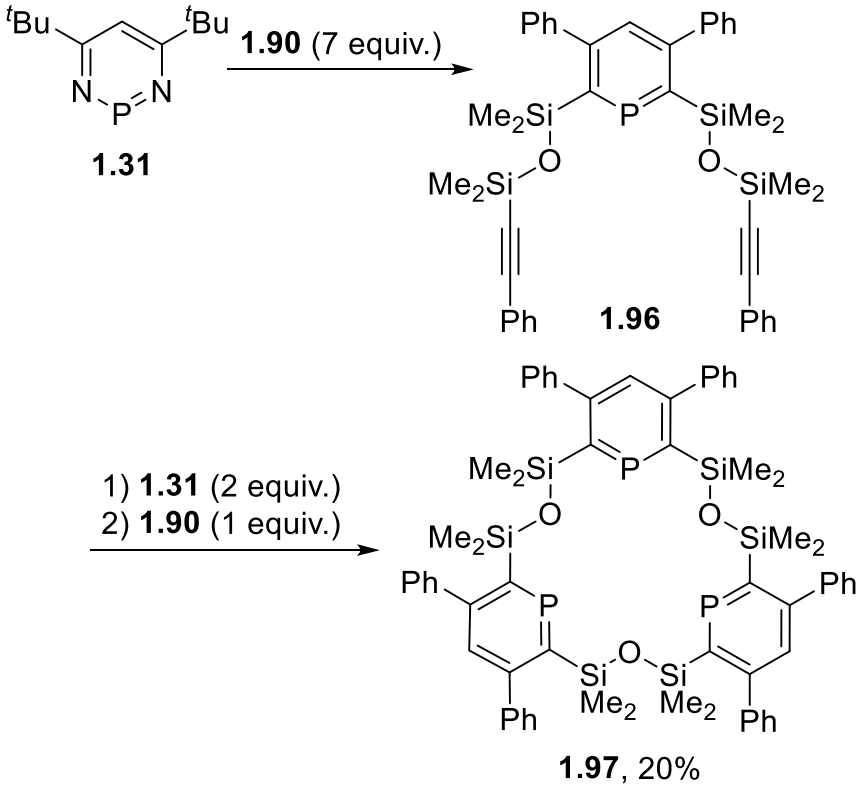

Scheme 1-29.[129] Synthesis of tris(phosphinine) macrocycle **1.97**

1.5.5 Phosphinophosphinines

The first synthesis of a phosphine-functionalised phosphinine was reported in 1988 by Holah *et. al.*,[133] who adapted the methodology of Mathey and co-workers (**Scheme 1-9**) in the synthesis of phosphinines by the thermal rearrangement and expansion of 1,2,5-triphenylphosphole (**1.24**).[43, 44] Whilst this reaction fails when bis(trimethylsilyl)acetylene is added as the necessary alkyne,[44] Holah *et. al.* demonstrated that after extended thermolysis (220°C for five days), phosphinine **1.98** could be isolated (17.5%) from a mixture of **1.24** and bis(diphenylphosphino)acetylene (**Scheme 1-30**).[133]

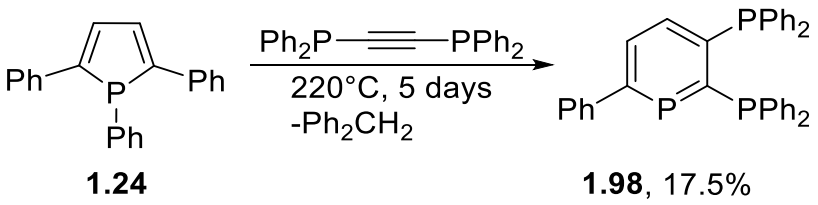

Scheme 1-30. Synthesis of 2,3-bis(diphenylphosphino)-6-phenylphosphinine **1.98**

The synthesis of **1.98** requires only a single step from a readily available precursor (**1.24**).[134] However, the thermolysis requires not only high temperatures, but a very high vacuum (10^{-7} torr) and the appropriate glassware, which limits the practicality of

this synthesis.[133] It was also observed that when attempts were made to coordinate **1.98** to Ni and Pt (**Scheme 1-31**, **1.99** and **1.100** respectively), binding occurred exclusively through the two phosphines, likely due to their stronger donating ability.[133] The wider bite angle resulting from a five-membered chelate is also more stable for a four-coordinate complex.[82]

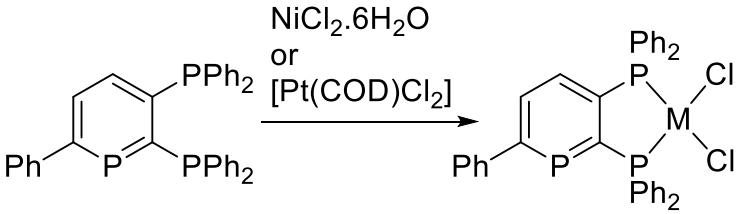

1.98 **1.99**, M = Ni, 100%
1.100, M = Pt, 67%

Scheme 1-31.[133] Synthesis of two complexes of **1.98**

Whilst the two complexes were not structurally characterised, their $^{31}P\{^{1}H\}$ NMR spectra (**Figure 1-8**, **Table 1-2**) confirm the coordination mode. Negligible changes were recorded in the shifts for P(1) in **1.99** and **1.100**, whereas the values for P(2) and P(3) are substantially different.

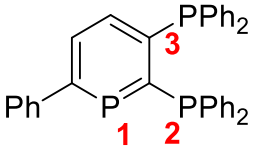

1.98

Figure 1-8. Numbering of the $^{31}P\{^{1}H\}$ NMR signals for **1.98**

Table 1-2. $^{31}P\{^{1}H\}$ NMR shifts (in ppm) for **1.98**, **1.99** and **1.100**

	1.98	**1.99**	**1.100**
P(1)	228.20	228.00	229.00
P(2)	-6.98	64.86	50.97
P(3)	-8.34	72.87	54.80

The next examples of phosphinophosphinines were reported by Märkl and co-workers, by reaction of 1,3-azaphosphinines with 1-(diphenylphosphino)alkynes (**Scheme 1-11**). They successfully synthesised a range of both 2- and 3-phosphinophosphinines (**1.101** to **1.108**, **Scheme 1-32**) by varying the phosphinoalkyne as well as the aromatic substituents on the 1,3-azaphosphinine, demonstrating that the regioselectivity of the cycloaddition-cycloreversion reaction could be altered by changing the electronics of

the alkyne C≡C triple bond.[55] There are substantial limits to the practicality of this synthesis, however, as the synthesis of the 1,3-azaphosphinine requires the reaction of an azapyrilium salt (for which limited synthetic details are available)[135] with $P(SiMe_3)_3$,[54] and the majority of the phosphinophosphinines were obtained in low yields under forcing conditions.[55] The synthesis of a chelating tungsten tetracarbonyl complex of **1.107** was briefly discussed in the literature, however only the yield, appearance, melting point and the observation of the molecular ion were reported.[55]

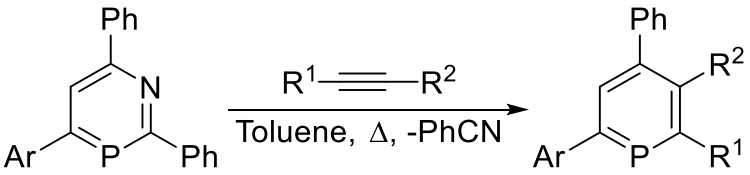

1.101, Ar = Ph, R^1 = H, R^2 = PPh_2, 8.2%
1.102, Ar = 4-Tol, R^1 = H, R^2 = PPh_2, 25%
1.103, Ar = Ph, R^1 = PPh_2, R^2 = PPh_2, 27%
1.104, Ar = 4-Tol, R^1 = PPh_2, R^2 = PPh_2, 34%
1.105, Ar = Ph, R^1 = PPh_2, R^2 = CH_3, 36%
1.106, Ar =4-Tol, R^1 = PPh_2, R^2 = CH_3, 35%
1.107, Ar = Ph, R^1 = PPh_2, R^2 = Ph, 60%
1.108, Ar = 4-Tol, R^1 = PPh_2, R^2 = Ph, 33%

Scheme 1-32. Synthesis of mono/bis(diphenylphosphino)phosphinines from 1,3-azaphosphinines and phosphinoalkynes. 4-Tol = 4-methylphenyl

Le Floch, Mathey and co-workers then published a series of papers, detailing the synthesis of functionalised phosphinines (including phosphinophosphinines) starting from bromophosphinines, either by lithiation,[49] a palladium cross-coupling,[50, 52] or direct reaction with PBr_3.[136] In two subsequent publications, they then investigated the coordination chemistry of a range of 2-phosphinophosphinines with Mn, Mo, Fe, Ni and Cu precursors.[137, 138] The coordination chemistry of several phosphino-, phosphonito- and phospholyl phosphinines was investigated, however **1.109** was the only ligand to be both reacted with each metal precursor and incorporated into a structurally characterised complex.[138] Whilst these initial synthetic routes published by Le Floch, Mathey and co-workers required extra steps to install a phosphine functionality,[49, 50, 52, 136] the later-developed diazaphosphinine (**1.31**) precursor allowed for the regioselective incorporation of 2-phosphino substituents.[57, 58]

Upon reaction of phosphonitophosphinine **1.109** (prepared from a (dibromophosphino)phosphinine and ethanol)[136] with $[\{Mn(Cp)(CO)_2\}_2]$ in THF,

dinuclear tetracarbonyl complex **1.110** was obtained in 75% yield (**Scheme 1-33**). It was then demonstrated that upon thermolysis in boiling xylenes, **1.110** lost two equivalents of carbon monoxide, affording **1.111** – containing a Mo≡Mo triple bond – in 55% yield.[138]

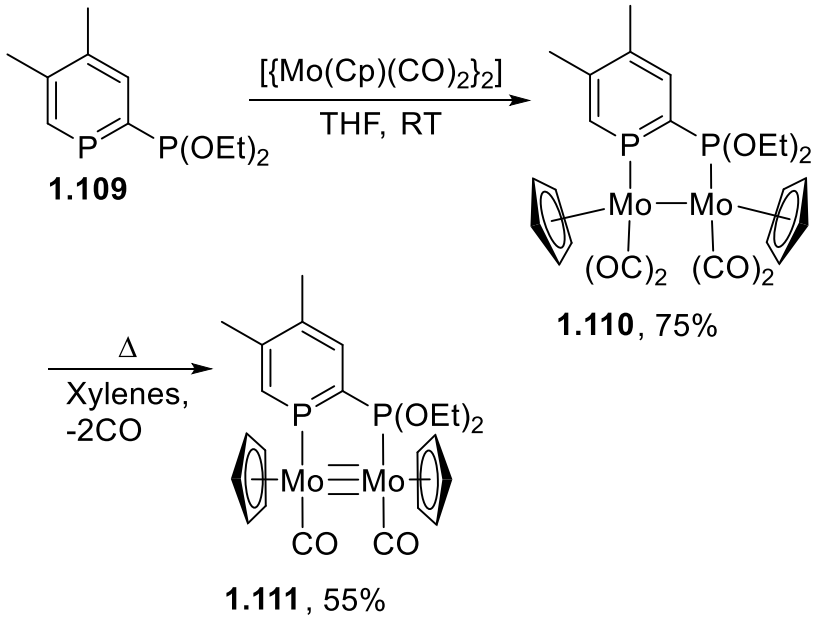

Scheme 1-33. Synthesis of two bridging Mo_2 complexes of **1.109**

The analogous reaction with [{Fe(Cp)(CO)$_2$}$_2$] (although UV irradiation at -80°C was required) afforded diiron dicarbonyl complex **1.112** in 60% yield (**Scheme 1-34**). Dimanganese octacarbonyl complex **1.113** was isolated in 50% yield by heating a mixture of **1.109** and [$Mn_2(CO)_{10}$] under reflux in xylenes.[138]

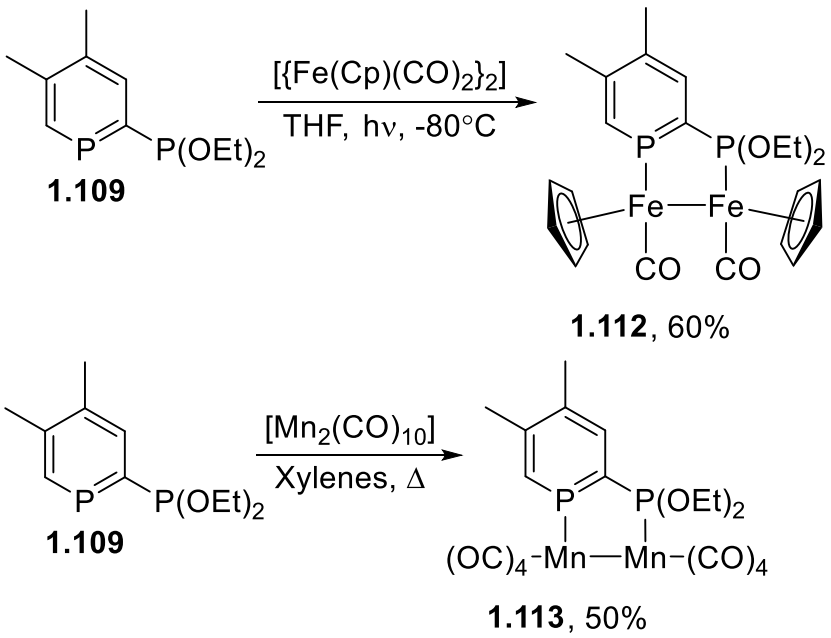

Scheme 1-34.[138] Synthesis of carbonyl complexes **1.112** and **1.113**

The coordination chemistry of phosphinophosphinine **1.114** (**Scheme 1-35**) was then demonstrated by testing its reactivity with sources of Ni(0) ([Ni(COD)$_2$] or *in-situ* reduction of [NiBr$_2$(dme)] with Zn) followed by admission of CO, or with CuI, affording complexes **1.115** and **1.116** respectively.[137]

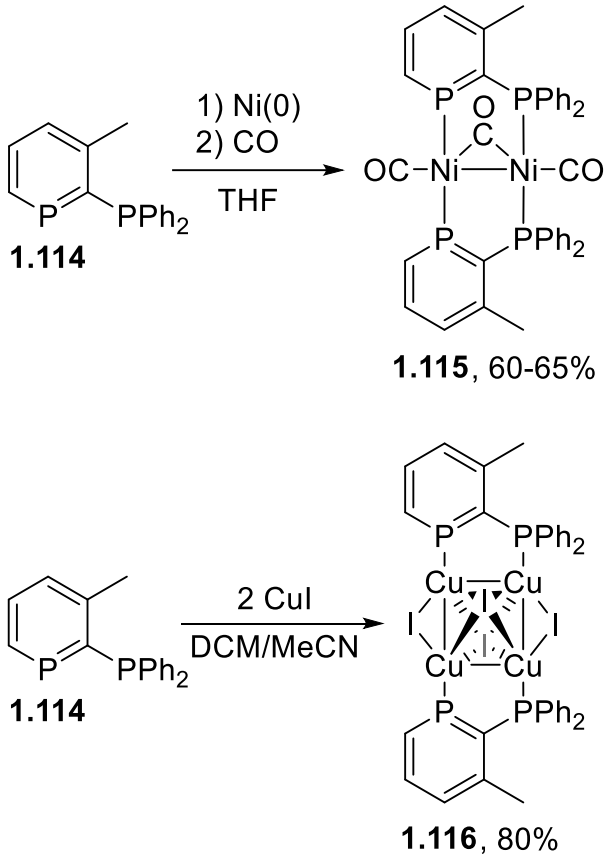

Scheme 1-35.[137] Synthesis of complexes **1.115** and **1.116** from phosphinophosphinine **1.114**

Grützmacher and co-workers used the 2-phosphaphenolate **1.77** precursor to prepare 2-(diphenylphosphinito)phosphinine **1.79** (**Scheme 1-24**) by its reaction with Ph$_2$PCl.[115, 117, 139] Their initial studies into the coordination chemistry of **1.79** involved reactions with one equivalent of CuX (X = Cl, Br, I), affording the three complexes **1.117** to **1.119** (**Scheme 1-36**). The resulting dinuclear complexes contain two tetrahedral CuX units complexed by two equivalents of **1.79**, and unusually both phosphinine donors are bridging between the two Cu(I) centres (**Figure 1-9**).[117]

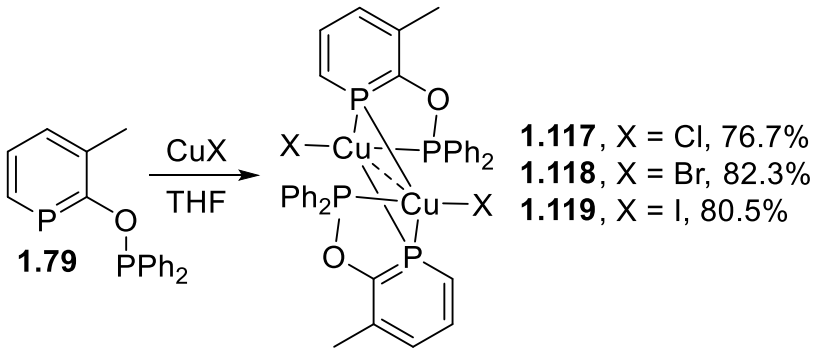

Scheme 1-36.[117] Synthesis of Cu complexes **1.117** to **1.119**

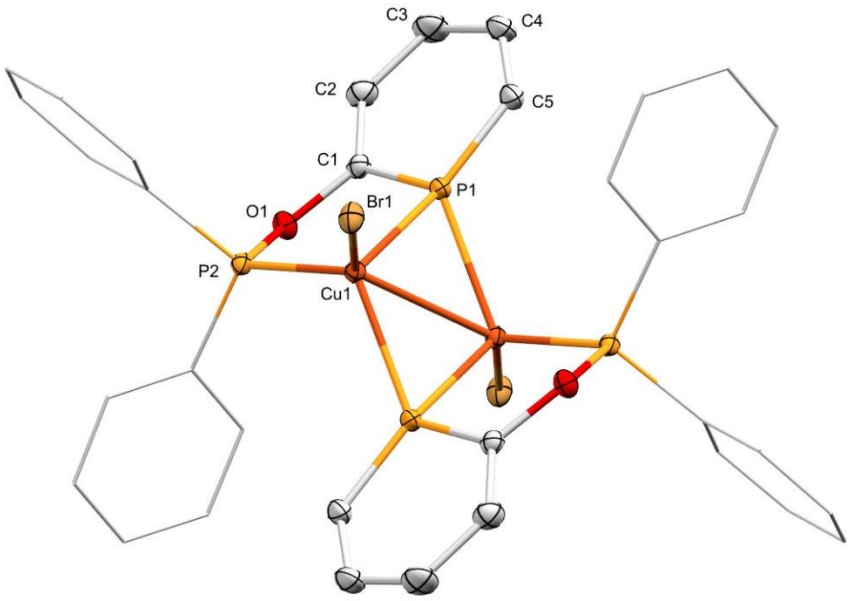

Figure 1-9.[117, 140] Molecular structure of **1.118**. Thermal ellipsoids at 50% probability, Ph rings set to wireframe for clarity

Upon reaction of **1.79** with $[Pd(PhCN)_2Cl_2]$, the expected square-planar complex **1.120** was isolated in 94% yield (**Scheme 1-37**). Upon addition of excess water to a THF solution of **1.120**, the unsubstituted P=C double bond underwent a *syn*-addition of water, forming P-hydroxy complex **1.121**. This was not only demonstrated by X-ray crystallography but by $^{31}P\{^{1}H\}$ NMR spectroscopy as well, with a change in chemical shift from δ = 165.9 ppm to 100.9 ppm.[139]

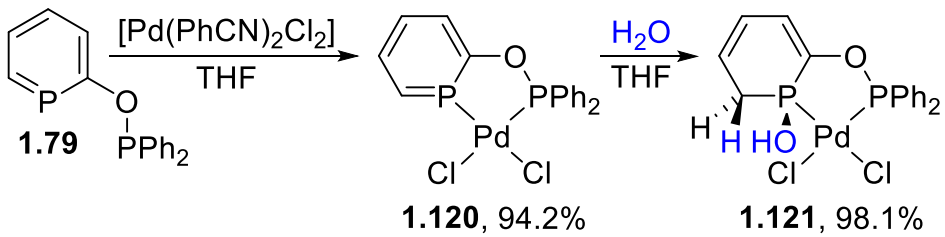

Scheme 1-37.[139] Synthesis of Pd complexes **1.120** and **1.121**

Whilst the hydrolysis of P=C double bonds in coordinated phosphinines has also been reported previously for non-phosphine functionalised phosphinines,[49, 141-144] coordinated complexes of phosphinophosphinines (and their P(V) derivatives, such as **1.122**) are increasingly susceptible to attack by anionic nucleophiles.[145] Free phosphinines readily react with alkoxides, organolithiums and Grignard reagents,[59, 62, 146] and Le Floch and coworkers demonstrated that the tridentate "SPS" ligand **1.122** reacted with [Pd(COD)Cl_2] to form neutral complex **1.123** containing a λ^5 phosphinine (**Scheme 1-38**) instead of the expected, ionic product **1.124**.[145]

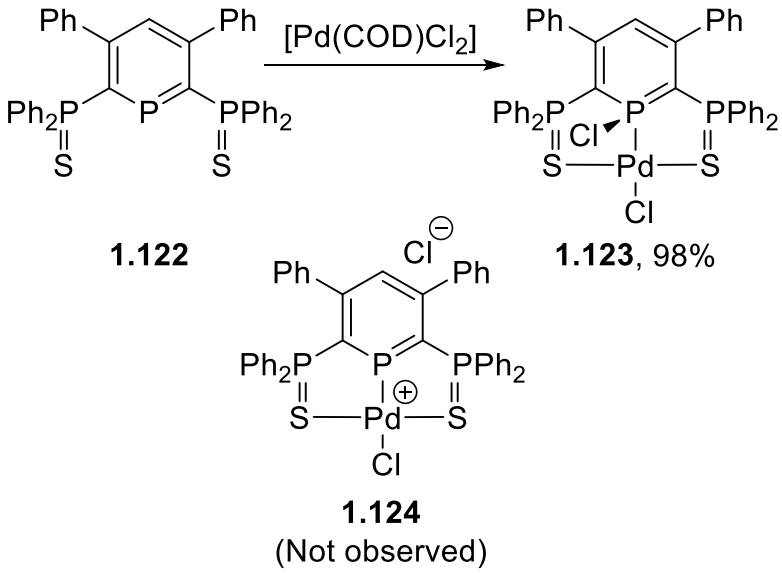

Scheme 1-38.[145] Synthesis of λ^5 phosphinine complex **1.123**

The reactivity in **Scheme 1-38** is specific to phosphinines containing π-accepting functional groups (such as phosphines) in the *ortho* positions, as there are known examples of complexes of phosphinines containing nucleophilic anions such as chloride that do not exhibit this behaviour.[143] According to calculations by Le Floch and co-workers, the presence of these π-accepting substituents increases the partial positive charge at the phosphinine P to a level at which it "becomes highly sensitive to nucleophilic attacks".[145] The benefit of this non-innocent behaviour is that coordinated (phosphino)phosphinine ligands have the potential to undergo "cooperative"[147] reactivity during a catalytic cycle, or could undergo attack by nucleophiles, resulting in ligand dearomatisation (**Scheme 1-39**). Whilst this behaviour is an opportunity to develop new pathways for catalyst activation or for catalytic cycles, alternatively, this reactivity could promote catalyst deactivation.

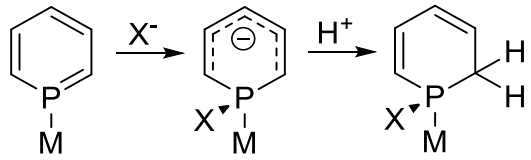

Scheme 1-39. Dearomatisation of a coordinated phosphinine by nucleophilic attack and subsequent protonation

1.5.6 Heterocycle-substituted phosphinines

Whilst a variety of heteroaryl-substituted phosphinines have been reported in the literature by the groups of Le Floch, Mathey and Müller,[12, 20, 39, 148] only three of these – containing pyridyl substituents – have been coordinated to (transition) metals, **1.125**[141] (NIPHOS), **1.9**[19] (**Scheme 1-3**), and **1.126**[148] (**Figure 1-10**).

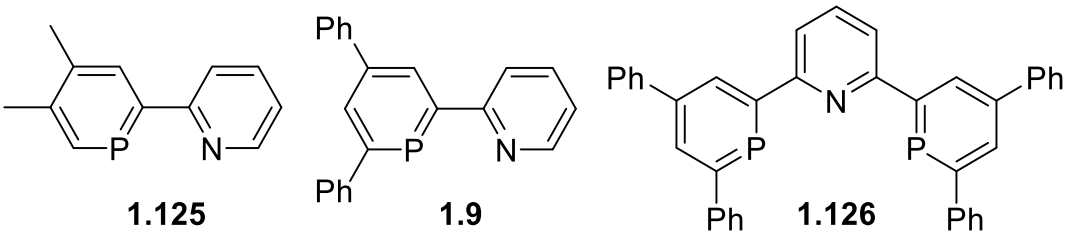

Figure 1-10. The structures of known pyridyl phosphinine ligands

Pyridyl phosphinine **1.125** was reported by Mathey and co-workers in 1982, following an adaptation of the methodology detailed in **Scheme 1-8**. However, its use in coordination chemistry has been entirely within the groups of Le Floch and Mathey,[141, 149, 150] due to difficulties in its synthesis and handling.[3] Their initial investigation into the coordination chemistry of **1.125** involved the synthesis of the three group six tetracarbonyl complexes from suitable precursors. The room-temperature reaction with $[Cr(CO)_5(THF)]$ and $[W(CO)_5(THF)]$ afforded their respective complexes, **1.127** and **1.129**, in 85% and 45% yields (**Scheme 1-40**). To prepare the Mo complex, neat **1.125** and $[Mo(CO)_6]$ were heated to 155°C in a sealed tube, allowing the isolation of **1.128** in 85% yield. The coordination of **1.125** to Rh,[150] Ir,[150] Pt,[141] and Pd[150] has also been investigated.

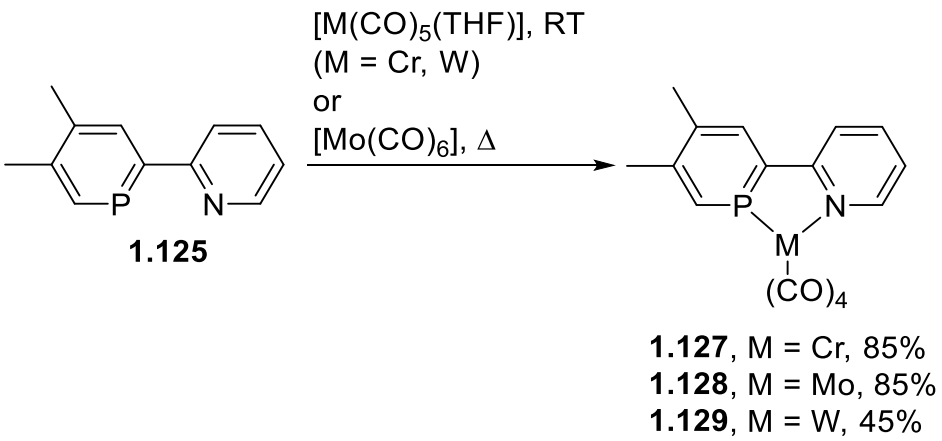

Scheme 1-40.[149] Synthesis of the group six tetracarbonyl complexes of **1.125**

Pyridyl phosphinines **1.9** and **1.126** were prepared using the pyrilium salt route (**Scheme 1-3**), and Müller and co-workers have investigated their coordination chemistry.[20, 148] Similarly to **1.125**, bidentate ligand **1.9** has been coordinated to all three group six metals,[151] and a range of the "platinum group" metals, including Rh,[142, 143, 152] Ir,[142, 143] Pt,[153] and Pd.[153] A representative reaction of the synthesis of **1.130** (66% yield) by reaction of **1.9** with $[Rh(COD)_2][BF_4]$ is shown (**Scheme 1-41**).[152] The structure and infrared spectroscopy data for [Re(**1.9**)$(CO)_3$Br] has also been included in a review,[3] however, no experimental details, NMR spectra or a CIF file have been published.

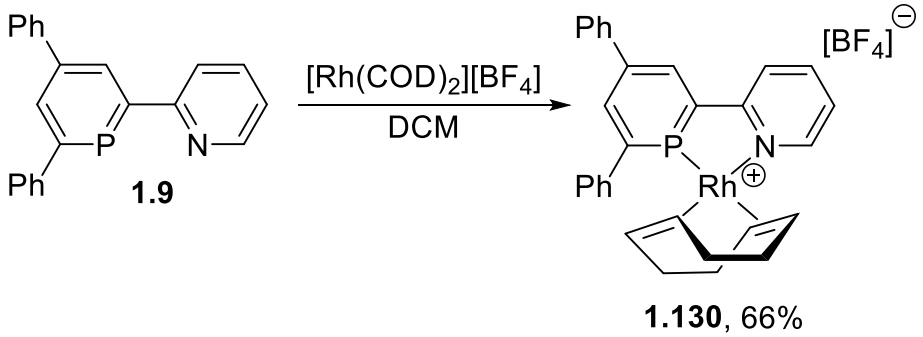

Scheme 1-41.[152] Synthesis of cationic Rh(I) complex **1.130**

Only one complex of the tridentate ligand **1.126** has been published – from its reaction with $[CuBr(SMe_2)]$ – (**Scheme 1-42**), with the tetrahedral complex **1.131** isolated in a 51% yield.

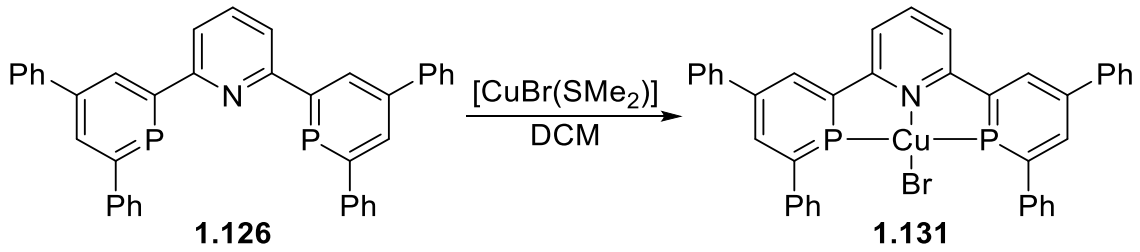

Scheme 1-42.[148] Synthesis of Cu complex **1.131**

1.6 Phosphinines in catalysis

The use of phosphinine ligands in catalysis has been covered in several book chapters and reviews,[14-16, 154] and covers areas as diverse as asymmetric hydrogenation[26] and the electrocatalytic oxidation of water.[144] As such, only a selection of key examples are discussed here. The first report of a catalytically active phosphinine complex was by Knoch *et. al.*, in collaboration with Le Floch and Mathey. Together, they demonstrated that the Fe complex **1.132** (**Scheme 1-43**), containing an η^6 phosphinine ligand, cyclotrimerised a combination of butyronitrile and propargyl methyl ether, yielding a mixture of two pyridines and two derivatised benzenes (**1.133** to **1.136**). However, the reaction was poorly chemoselective, and favoured formation of benzenes **1.135** and **1.136** (exact ratios of **1.135** : **1.136** not given) over the two pyridines.[155] Analogous complexes with varied 1,4-diaza-1,3-butadiene (bis(imino)ethane) ligands instead of COD have also been used for the cyclodimerisation of 1,3-butadiene.[156]

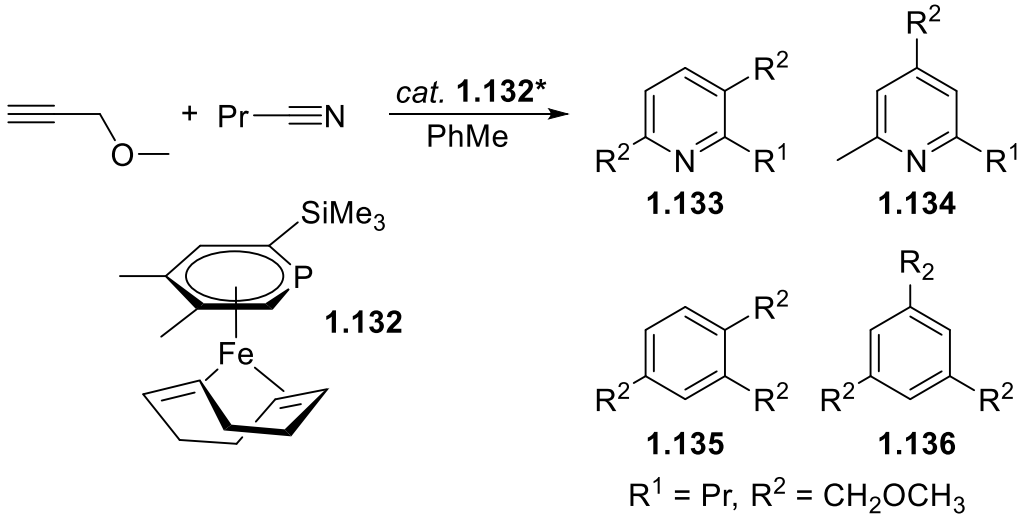

Scheme 1-43. Cyclotrimerisation of propargyl methyl ether and butyronitrile catalysed by **1.132**. *****catalyst loading at various values between 0.00025 and 0.0016 mol%

DiMauro and Kozlowski reported the use of phosphinine ligands in the Ni(0) catalysed cycloaddition of dienyne **1.137** (**Scheme 1-44**). Their results indicated that triphenylphosphinine **1.2** produced the most active catalyst (comparable to a bulky tri(biphenyl)phosphite), and that as the *ortho* phenyl substituents were successively replaced with methyl groups, the yield of **1.138** decreased. Using tri(*tert*-butyl)phosphinine **1.140** produced a poor catalytic system, which indicates that the reduction in yield observed when using ligands **1.139** or **1.12** instead of **1.2** is not necessarily to do with the "bulkiness" of the phosphinine ligand.[157] Müller and coworkers also investigated the use of gold phosphinine complexes in catalytic cycloaddition reactions, and found them to be competitive with or superior to catalysts containing phosphine, phosphite, or non-classical N-heterocyclic carbene ligands.[158]

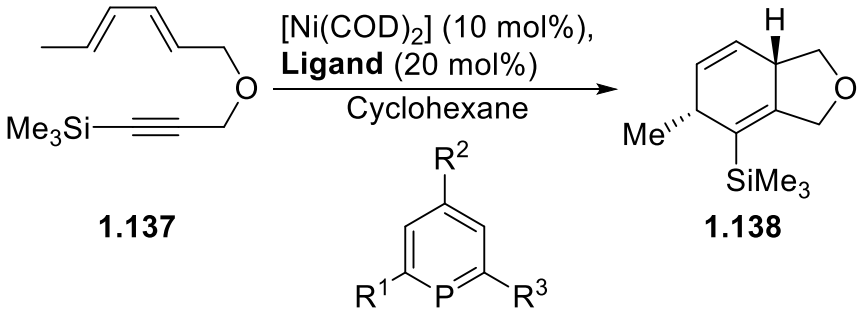

1.2, R^1, R^2, R^3 = Ph, 92%
1.139, R^1 = Me, R^2, R^3 = Ph, 81%
1.12, R^1 = Me, R^2 = Ph, R^3 = Me, 66%
1.140, R^1, R^2, R^3 = ^{t}Bu, 31%

Scheme 1-44. Ni(0)/phosphinine catalysed cycloaddition of dienyne **1.137**

The most significant catalytic results obtained from using phosphinine ligands have been from hydroformylation, an industrially important reaction that often makes use of π-accepting ligands such as CO and phosphites.[159] Breit and co-workers published a series of papers detailing their investigations into the use of mono/bi/multidentate phosphinine ligands, and their results indicated that a high level of alkene conversion with excellent selectivity could be obtained by using the appropriate phosphinine ligand.[28, 32, 160, 161] Their initial results demonstrated that 80% conversion of styrene was observed with a selectivity of 26.6 : 1 branched : linear (**1.141** : **1.142**) when ligand **1.139** was used, a far superior result to that obtained from triphenylphosphine (**Scheme 1-45**, **Figure 1-11**, **Table 1-3**) or dicyclohexylphosphinine **1.143**. Expanding the ligand scope to include **1.144** – **1.146** increased the styrene conversion to 98% when **1.146** was used (24.8 : 1 branched : linear selectivity).[160]

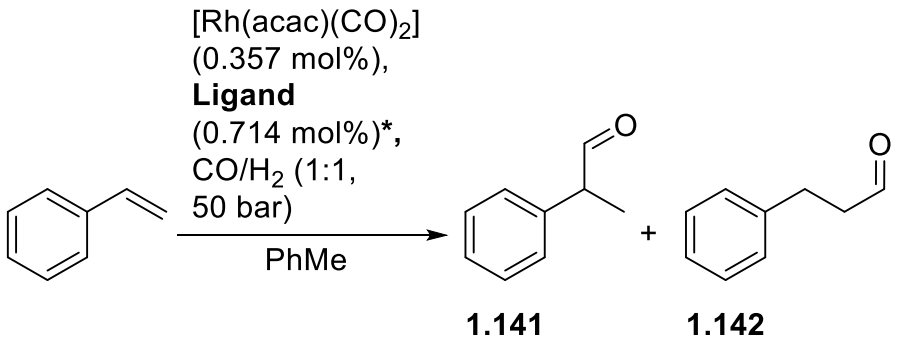

Scheme 1-45.[160] Hydroformylation of styrene. * 7.14 mol% PPh_3/**1.143** was used

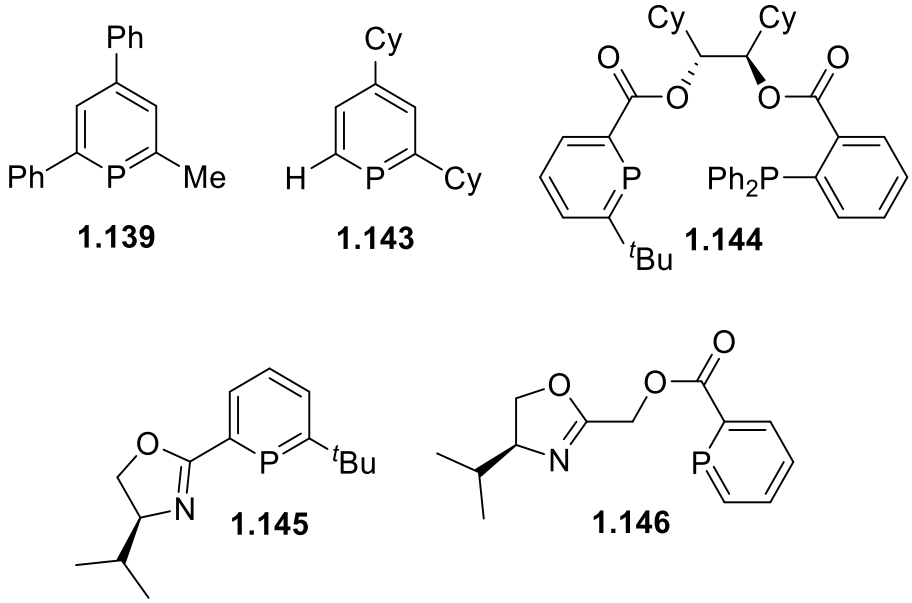

Figure 1-11.[160] Phosphinine ligands used in the hydroformylation study. Cy = cyclohexyl

Table 1-3.[160] Conversion (%) and selectivity data for the hydroformylation of styrene using phosphinine-based ligands

Ligand	Conversion (%)	1.141 : 1.142 Ratio
PPh_3[a]	31	25.8 : 1
1.139	80	26.6 : 1
1.143[a]	0	-
1.144	42	21.4 : 1
1.145	5	100 : 0
1.146	98	24.8 : 1

[a]: 7.14 mol% ligand used (20 equiv. relative to Rh)

The results in **Table 1-3** indicate that ligands **1.139** and **1.146** are by far the superior ligands tested in this study (other families of ligands were also tested but were inferior to PPh_3).[160] The activity of a catalytic system for hydroformylation can be related to the size of the bite angle (with wide bite-angle ligands often preferred),[88] so it is logical that

the results obtained from **1.146** were superior to **1.145**. Whilst **1.144** could potentially contain the largest bite angle, the non-competitive conversion (compared to **1.139** and **1.146**) observed indicates that it is likely that it cannot chelate effectively. Ligands **1.144** to **1.146** were all employed in an enantiomerically pure state, however, no enantiomeric excess was observed.[160] Further uses of ligand **1.145** in catalysis (as well as derivatives with different oxazoline substituents) were investigated, however, only poor to moderate enantioselectivities were observed.[162]

Other studies on the uses of phosphinines in hydroformylation have been published,[24, 28, 32, 161] in particular, Reetz and Li demonstrated that by using combinations of phosphinines with triphenylphosphine, highly regioselective systems were obtained for the hydroformylation of *tert*-butyl methacrylate.[163] A comprehensive theoretical investigation into the reasons behind the utility of phosphinines in hydroformylation has also been published by Müller, Hirst, Carbó and co-workers.[164]

1.7 Project aims

The aims for this research were to:

- Synthesise a 2-phosphinophosphinine ligand
- Investigate its coordination to group 6 metal tetracarbonyl fragments to facilitate analysis of the donor properties
- Investigate its use in the Cr-catalysed oligomerisation of ethylene
- Investigate its coordination to Ru fragments and prepare a catalyst for the transfer hydrogenation of aryl ketones as well as for the "upgrading" of ethanol and methanol to isobutanol
- To prepare a Rh complex containing a labile diene ligand that would be suitable for investigating a variety of catalytic reactions

2 - Ligand synthesis

2.1 Synthesis of 2-(diphenylphosphino)phosphinines

The synthesis of small bite-angle R_2P-E-PR_2 diphosphines (E = C, N) is well developed, their donor-properties are understood and their popularity in catalysis is increasing.[82] However, whilst the synthesis of 2-phosphinophosphinines (which can be viewed as analogues of dppm with one carbon atom separating the P atoms) has become achievable due to work by the group of Le Floch and Mathey,[50, 57, 58] research into their coordination chemistry has been primarily limited to bridging derivatives.[137, 138] A chelating tungsten carbonyl complex was reported, although experimental conditions were not provided (only a yield, melting point and the m/z for the molecular ion were reported).[55] Therefore, the initial goal for this project was to develop the synthesis of a simple 2-phosphinophosphinine proligand that could be reacted with a range of transition metal complexes in order to facilitate the evaluation of its donor properties, determine the stability of its complexes and their uses in catalysis.

2.1.1 Synthesis from a 1,3,2-diazaphosphinine

Whilst multiple routes to phosphinines are available in the literature, none of them are synthetically simple, generally requiring multiple steps and non-commercially available precursors. As such, it was decided to follow the 1,3,2-diazaphosphinine methodology developed by Le Floch, Mathey and co-workers[58] because they reported high yields and excellent regioselectivity as well as wide functional-group tolerance. The chosen synthetic route involved reaction of the diazaphosphinine precursor with a phosphinoalkyne and subsequent formation of the phosphinine heterocycle with trimethylsilylacetylene (HC≡C-$SiMe_3$, **Scheme 2-1**). As DFT calculations have provided evidence that phosphinines are π-accepting ligands that are poorly nucleophilic due to the low-lying molecular-orbital corresponding to the lone pair,[12] installation of the 2-diphenylphosphine substituent was selected to enable more facile coordination to transition metals whilst providing greater stability to oxidation than more strongly σ-donating alkyl phosphines. The 6-trimethylsilyl substituent was incorporated as calculations have shown that *ortho*-trimethylsilyl phosphinines possess better σ-donor and π-acceptor properties.[165] Previously, a phosphinophosphinine similar in structure to the target **2.1** was reported with a second diphenylphosphine moiety in the 3-position by reaction of the diazaphosphinine precursor with bis(diphenylphosphino)acetylene (Ph_2P-C≡C-PPh_2).[58] However, prior work has shown

that 2,3-bis(diphenylphosphino)phosphinines preferentially coordinate through the two phosphines and not the phosphinine.[133]

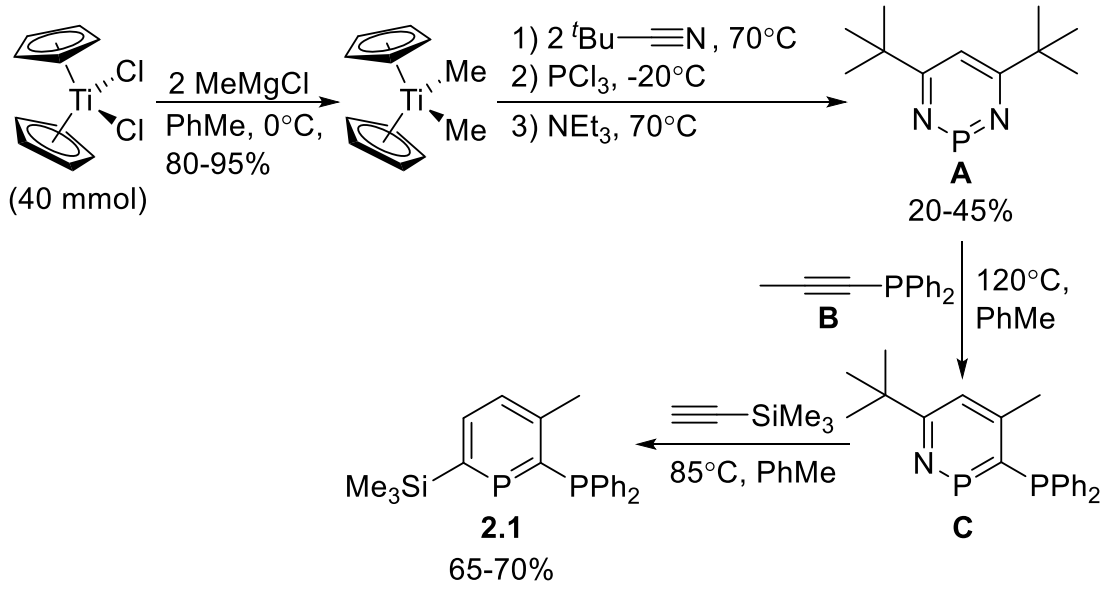

Scheme 2-1. Synthesis of **2.1**

By following the literature protocol for the synthesis of diphenyl(1-prop-1-ynyl)phosphine (H_3C-C≡C-PPh_2, **Scheme 2-1**, **B**),[166] it was isolated in good yield and high purity as an air-stable oil. Upon reaction with the diazaphosphinine precursor in toluene at 120°C in a sealed flask, clean formation of the azaphosphinine (**Scheme 2-1**, **C**) intermediate was observed by $^{31}P\{^{1}H\}$ NMR spectroscopy (δ = 283.6 (d), -18.7 (d) ppm). The high regioselectivity of the [4+2] cycloaddition-reversion reaction between the diazaphosphinine and the phosphinoalkyne (**Scheme 2-2**) is a consequence of both the P2-C5 dipole and the dipole of the carbon-carbon triple bond. Due to the significant positive and negative charges at P2 and C5 respectively in the diazaphosphinine, as well as significant polarisation of the triple bond in the phosphinoalkyne, the most-shielded (with δ^- partial charge) sp carbon regioselectively reacts with the phosphorus.[57]

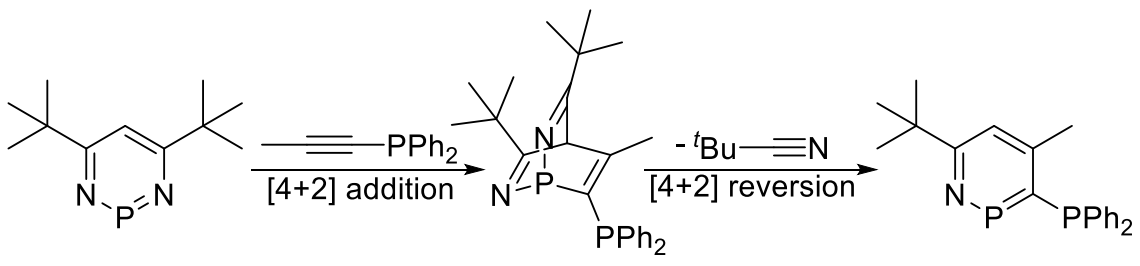

Scheme 2-2. [4+2] cycloaddition-reversion reaction

The conversion of the intermediate azaphosphinine to **2.1** with HC≡C-$SiMe_3$ did not proceed as cleanly as the reaction with the phosphinoalkyne – multiple unidentified minor side-products were commonly observed by ^{31}P NMR spectroscopy – although these were minimised by conducting this step at a lower temperature. When the reaction was run at a temperature higher than 85°C, signals corresponding to 2,6-bis(trimethylsilyl)phosphinine (δ = 254.6 ppm)[57] and the phosphinoalkyne (δ = -32.0 ppm)[167] were increasingly observed by $^{31}P\{^1H\}$ NMR. No reaction was observed after heating pure **2.1** with excess HC≡C-$SiMe_3$ at 100°C in C_6D_6 overnight, implying that the formation of the bis(silyl)phosphinine was due to displacement of the phosphinoalkyne from the intermediate azaphosphinine by the silyl acetylene, or potentially by pivalonitrile (first reforming the diazaphosphinine).

Once the reaction conditions were optimised, with a single major product observed by $^{31}P\{^1H\}$ NMR spectroscopy (δ = 249.8 (d) and -7.5 ppm (d)) in the crude product, the isolation of the pure product from minor side-products and Cp_2TiCl_2 impurities was investigated. Repeated extraction and filtration of the crude material with portions of anhydrous 40-60 petroleum ether removed the majority of impurities, however extended storage of concentrated solutions at -25°C failed to provide any crystalline material. A previous study demonstrated that reaction of phosphinophosphinines with borane-dimethylsulfide proceeded without involvement of the heterocycle and that this reaction allowed for the isolation of oily, air-sensitive phosphinophosphinines as air-stable, solid borane complexes.[136] As such, the reaction of **2.1** with BH_3-SMe_2 was investigated to prepare **2.2** (**Scheme 2-3**).

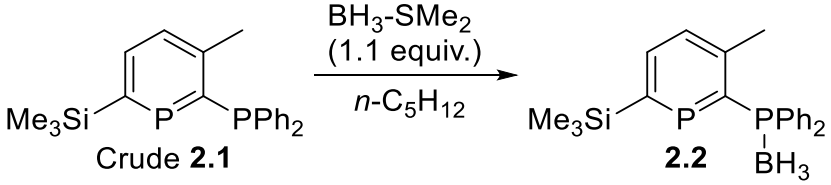

Scheme 2-3. Synthesis of **2.2**

Upon addition of a slight excess of borane-dimethylsulfide complex to an *n*-pentane solution of crude **2.1**, a rapid reaction occurred, producing **2.2** as an air-stable, colourless precipitate (69% from the diazaphosphinine precursor). Single crystal X-ray diffraction analysis of **2.2** confirmed the anticipated molecular structure (**Figure 2-1**) containing a planar, aromatic phosphinine ring substituted in the *ortho*-positions with diphenylphosphine and trimethylsilyl groups. The carbon-carbon bond lengths around the ring (**Table 2-1**) range from 1.385(2) to 1.407(2) Å and are consistent with those in

benzene (1.391(1) Å),[168, 169] *i.e.* longer than a C=C double bond but shorter than a C-C single bond,[170] indicating aromatic delocalisation.

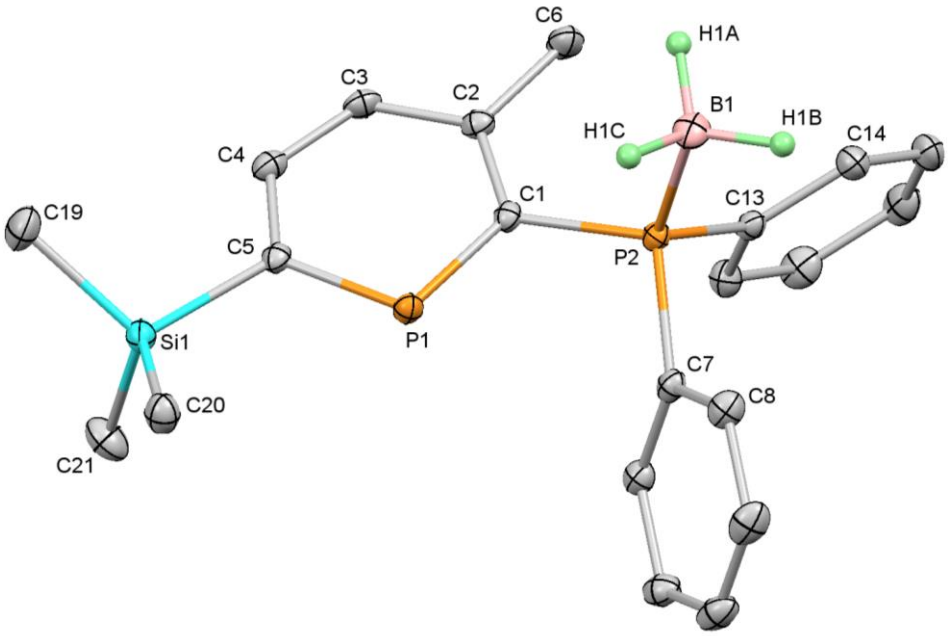

Figure 2-1. Molecular structure of **2.2** (thermal ellipsoids at 50% probability). All H-atoms except for those attached to B have been omitted for clarity

Table 2-1. Key bond lengths and angles for **2.2**

Bond Lengths (Å)		**Bond Angles (°)**	
P(1)-C(1)	1.754(1)	P(1)-C(1)-C(2)	124.2(1)
C(1)-C(2)	1.407(2)	C(1)-C(2)-C(3)	120.5(1)
C(2)-C(3)	1.405(2)	C(2)-C(3)-C(4)	125.1(1)
C(3)-C(4)	1.385(2)	C(3)-C(4)-C(5)	124.2(1)
C(4)-C(5)	1.399(2)	C(4)-C(5)-P(1)	121.2(1)
C(5)-P(1)	1.734(1)	C(5)-P(1)-C(1)	103.7(1)
C(1)-P(2)	1.827(1)	P(1)-C(1)-P(2)	114.5(1)
P(2)-B(1)	1.928(2)		

As expected, the cyclic phosphorus-carbon bonds were significantly elongated compared to the carbon-carbon bonds due to the larger atomic radius of phosphorus. These bonds are also part-way between a P=C double bond (*ca.* 1.70 Å for $HP{=}CH_2$)[171] and a P-C single bond (1.827(1) Å for C(1)-P(2)). There are substantial variations in the bond angles around the ring, distorting the ring from the regular hexagonal structure of benzene with six internal angles of 120°, although this can be explained by the significant variations in the cyclic bond lengths. After filtration and washing with petroleum ether, crystalline **2.2** was pure enough for use in subsequent deboronation reactions to allow isolation of **2.1**. However, optimisation of this procedure initially

proved to be troublesome. Using reagents that were to-hand, stirring **2.2** in anhydrous triethylamine heated to 100°C was initially investigated, but the reaction proceeded extremely slowly. A method reported by Pringle and co-workers for use with phosphine-boranes[172] involving addition of aqueous diethylamine to a toluene solution of **2.2** was also unsuitable as a strongly coloured solution was obtained, implying formation of a λ^4 or λ^5 phosphinine.[173] With little progress made from these initial reactions, the classical method of deprotection involving addition of one or more equivalents of DABCO (1,4-diazabicyclo[2.2.2]octane, **Scheme 2-4**, **A**) in toluene was tested.[174] Due to its bicyclic structure, DABCO is highly nucleophilic as the nitrogen lone-pairs are sterically unhindered,[175] allowing for facile deprotection of phosphine-borane complexes.[176] Following a slight adaptation of literature conditions,[174] one equivalent of DABCO was stirred with **2.2** in toluene overnight at 20°C. $^{31}P\{^1H\}$ NMR spectroscopic analysis of the crude reaction mixture revealed clean formation of **2.1**, however, after working up the reaction by elution through a plug of neutral alumina to remove the [DABCO.BH_3] side-product, a poor yield of a product contaminated with borane side-product was obtained. Yields over 50% could not be obtained, and removal of the residual [DABCO.BH_3] proved challenging. An acceptable yield of **2.1** from reaction of **2.2** with DABCO was finally achieved by using only 0.5 equivalents of DABCO, leading to the formation of the poorly-soluble by-product [DABCO.$(BH_3)_2$] (**Scheme 2-4**, **B**).

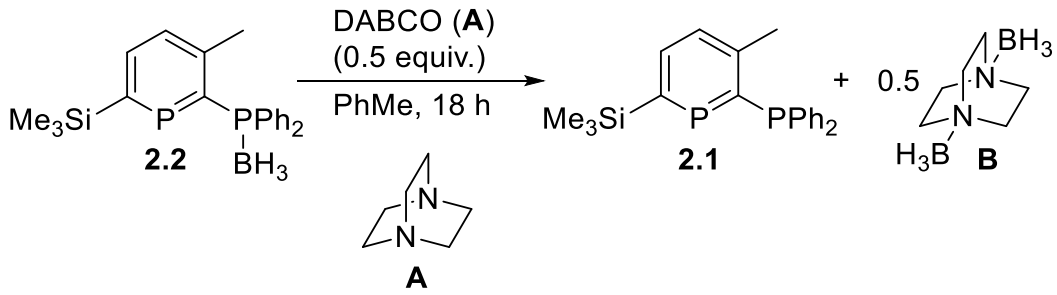

Scheme 2-4. Deprotection of **2.2** with DABCO

The reaction proceeded as predicted, with a suspension of [DABCO.$(BH_3)_2$] visible in the reaction flask after stirring at 20°C for 18 hours. The bis(borane) side-product proved to be partially soluble in toluene, so removal of the reaction solvent *in vacuo* and extraction of the residue with pentane, was required to isolate pure **2.1** as a pale yellow solid (97% from **2.2**). **2.1** proved to be relatively air stable; although samples stored under air for extended periods (weeks to months) showed a slight red discolouration, no obvious impurities were visible by ^1H or $^{31}P\{^1H\}$ NMR spectroscopy. Once the air

stability of **2.1** was realised, direct purification of crude **2.1** from the diazaphosphinine was investigated to reduce the number of steps in the synthesis. Thin-layer chromatographic analysis of the crude reaction mixture revealed that side products formed during the reaction of the azaphosphinine (**Scheme 2-1**, **C**) readily eluted in neat petroleum ether, along with the non-polar side-product 2,6-bis(trimethylsilyl)phosphinine that was commonly observed in small amounts. **2.1** was then eluted by addition of 5% ethyl acetate. Chromatographic purification of the crude reaction mixture proved to be facile, with a notable yellow band containing **2.1** eluting rapidly upon addition of ethyl acetate to the solvent mixture. Removal of solvent from the combined fractions gave a thick yellow oil that solidified on standing at 20°C. Minor side-products observed in the $^{31}P\{^{1}H\}$ NMR spectrum of this solid were removed by recrystallisation from pentane at -25°C overnight, providing analytically pure **2.1**, in comparable yields (60-70%) to those obtained from deboronation of **2.2**, after concentration of the filtrate and isolation of a second crop. Crystallisation of **2.1** from *n*-hexane at -25°C provided single crystals suitable for X-ray diffraction (**Figure 2-2**). The synthesis of **2.1** and **2.2** has been published.[177]

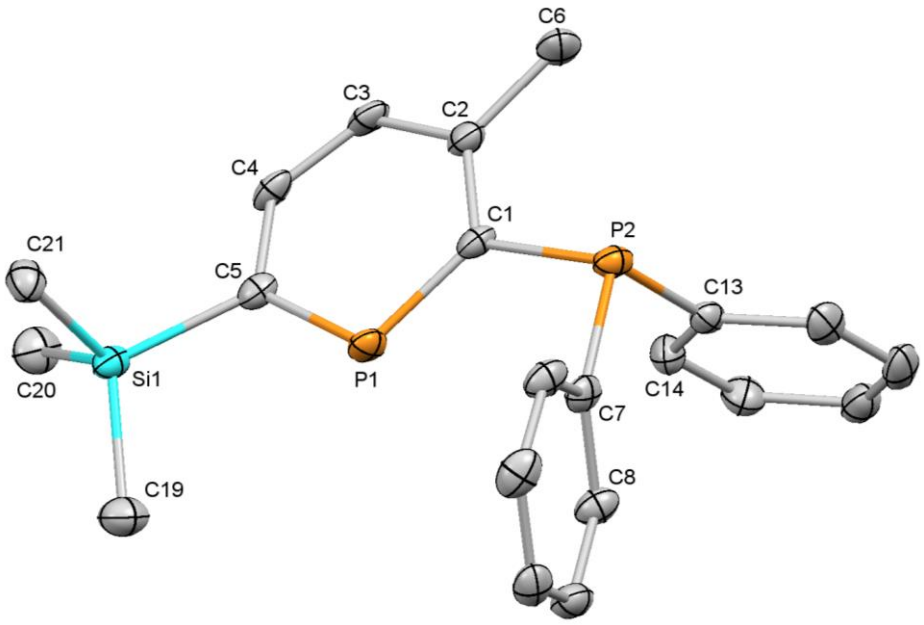

Figure 2-2. Molecular structure of **2.1** (thermal ellipsoids at 50% probability). All H-atoms have been removed for clarity

Table 2-2. Key bond lengths and angles for **2.1**

Bond Lengths (Å)		Bond Angles (°)	
P(1)-C(1)	1.754(3)	P(1)-C(1)-C(2)	124.0(2)
C(1)-C(2)	1.423(4)	C(1)-C(2)-C(3)	120.6(3)
C(2)-C(3)	1.404(4)	C(2)-C(3)-C(4)	124.9(2)
C(3)-C(4)	1.393(4)	C(3)-C(4)-C(5)	125.5(2)
C(4)-C(5)	1.396(4)	C(4)-C(5)-P(1)	121.0(2)
C(5)-P(1)	1.749(3)	C(5)-P(1)-C(1)	103.6(1)
C(1)-P(2)	1.847(3)	P(1)-C(1)-P(2)	119.9(1)

Only minor differences between **2.1** and **2.2** are obvious by comparison of the ring bond lengths and angles, as would be expected due to their similar structures. The C(1)-C(2) bond is slightly elongated in **2.1** (1.423(4) versus 1.407(2) Å), likely due to a mesomeric effect from the phosphine moiety (**Scheme 2-5**). However, a notable increase in the free P(1)-C(1)-P(2) angle can be observed (119.9(1) versus 114.5(1)° in **2.2**) as well as a different conformation as shown by the C2-C1-P2-C13 torsion angle (-81.5(2) for **2.1** versus -48.4(1)° for **2.2**). Structural data on phosphinophosphinines in the CSD is limited, however, comparison to the acyclic unsaturated diphosphine vdpp (1,1-bis(diphenylphosphino)ethylene), shows that the P(1)-C(1)-P(2) angles are almost identical (119.0(3) for vdpp,[178] 119.9(1) for **2.1**).

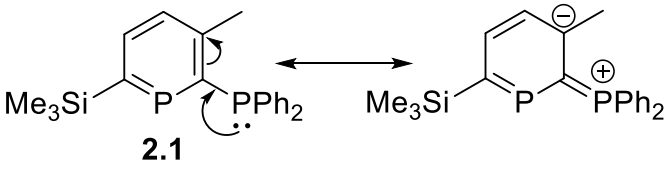

Scheme 2-5. Tautomerisation of **2.1**

2.1.2 Synthesis of the selenide of **2.1**

As with the other chalcogens, reacting phosphines with elemental selenium yields the P(V)-selenide. The utility of phosphine selenides stems from the NMR active (spin ½) isotope ^{77}Se because the size of the $^{1}J_{P\text{-}Se}$ coupling constant observed by $^{31}P\{^{1}H\}$ NMR spectroscopy is directly correlated to the degree of s-character in the P lone-pair.[179] Due to the ease of synthesis of phosphine selenides, $^{1}J_{P\text{-}Se}$ coupling constants have been widely reported in the literature, and as such derivatisation of **2.1** to **2.3** allowed for the facile (transition metal-free) assessment of the donor properties of **2.1** by comparison to available literature data (**Table 2-3**). Due to the relatively non-nucleophilic character of phosphinines,[12] reaction of **2.1** with excess selenium under forcing conditions (**Scheme**

2-6) selectively produced **2.3** (60% from **2.1**). Whilst phosphinine sulfides are known,[180] a phosphinine selenide has yet to be unambiguously characterised.[181] Attempts to apply a methodology used for the synthesis of a phosphinine sulfide (five equivalents of selenium, 100°C for one week in C_6D_6)[182] to the synthesis of a phosphinine selenide led only to the production of **2.3**.

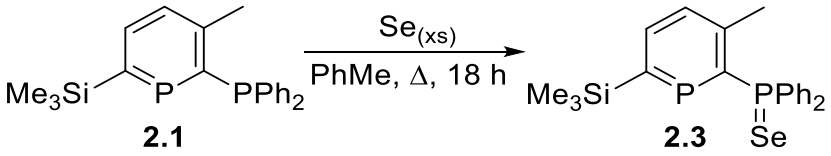

Scheme 2-6. Synthesis of **2.3**

Table 2-3. $^1J_{P\text{-}Se}$ coupling constants of some heterocyclic/heteroatom-substituted diphenylphosphines[179, 183, 184]

R_3P=Se	$^1J_{P\text{-}Se}$ (Hz)
PPh_3	732
PPh_2(2-Thienyl)	743
$PPh_2(NEt_2)$	748
PPh_2(2-Pyr)	749
2.3	749
PPh_2(2-Furanyl)	754
PPh_2(OEt)	796

As can be seen, the coupling constant for **2.3** is identical to that for $SePPh_2$(2-Pyr), and similar to $SePPh_3$. The 20 Hz difference relative to $SePPh_3$ indicates a slight increase of π-accepting ability for the phosphine donor, but much less than for better π-acceptors such as ethyl diphenylphosphinite ($^1J_{P\text{-}Se}$ = 796 Hz)[183] or triethylphosphite ($^1J_{P\text{-}Se}$ = 949 Hz).[185]

2.1.3 Desilylation of **2.1** and **2.2**

Calculations have shown that incorporation of an *ortho*-trimethylsilyl substituent increases the σ-donating and π-accepting properties of a phosphinine ligand,[165] however, this has been contradicted by a recent paper by Müller *et. al*. Their work showed (by DFT calculations) that -$SiMe_3$ substitution of the parent phosphinine had little effect on the π-accepting properties.[11] In order to obtain experimental data, a synthetic route to the desilylated analogue of **2.1** was investigated. This compound had already been reported in the literature by the group of Le Floch and Mathey,[50] however, there were drawbacks to their synthesis including the need for large amounts of an expensive diene[186] and a palladium-catalysed cross-coupling was required to install the

phosphine.[50] Preparation of the desilylated product directly using the diazaphosphinine precursor would require the use of anhydrous acetylene gas, but Le Floch and coworkers have also published a mild, fluoride-free methodology for the cleavage of *ortho*-trimethylsilyl groups from phosphinines that requires only an ethereal solution of HCl.[187] Their publication reported clean and rapid desilylation (30 minutes) of *meta*-alkyl or phenyl-subsituted *ortho*-trimethylsilylphosphinines. Müller and co-workers have also adapted this methodology for the synthesis of phosphinine from 2-trimethylsilylphosphinine.[11] In order to make use of this methodology, initial tests investigated the reaction of borane-protected **2.2** with ethereal HCl (**Scheme 2-7**) because the acid-sensitivity of **2.1** was not known.

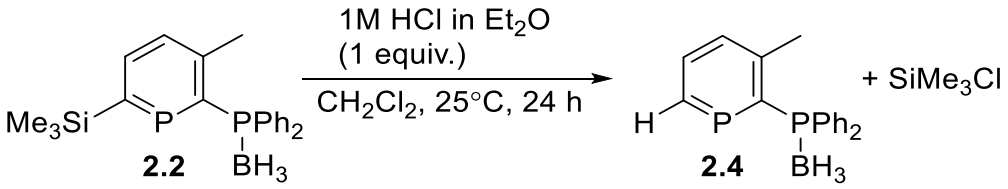

Scheme 2-7. Desilylation of **2.2**

Reaction of **2.2** with HCl in ether cleanly generated **2.4**, which was observed spectroscopically by considerable shifts in the $^{31}P\{^{1}H\}$ NMR resonances (229.7 (d), 23.0 (s) ppm), as well as a new ^{1}H resonance for the 6-H atom (8.59 ppm). The reaction proceeded more slowly than reported by Le Floch and coworkers (they reported 30 minutes for full conversion),[187] initially this was assigned to additional steric hindrance, however, the Müller group's synthesis of phosphinine suffered from the same issue.[11] The resulting desilylated product **2.4** displayed reduced solubility compared to **2.2**, however, this was exploited by dissolution in a minimum of boiling toluene and subsequent storage at -25°C to obtain colourless single crystals of **2.4** suitable for X-ray diffraction in 53% yield.

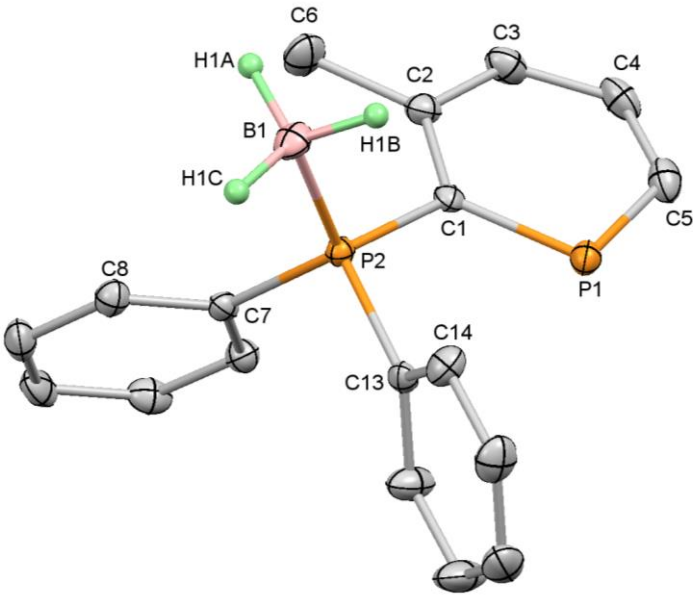

Figure 2-3. Molecular structure of **2.4** (thermal ellipsoids at 50% probability). All H-atoms except those attached to B have been removed for clarity

Table 2-4. Key bond lengths and angles for **2.4**

Bond Lengths (Å)		**Bond Angles (°)**	
P(1)-C(1)	1.746(2)	P(1)-C(1)-C(2)	124.7(2)
C(1)-C(2)	1.410(3)	C(1)-C(2)-C(3)	121.0(2)
C(2)-C(3)	1.403(3)	C(2)-C(3)-C(4)	124.5(2)
C(3)-C(4)	1.382(3)	C(3)-C(4)-C(5)	123.3(2)
C(4)-C(5)	1.380(3)	C(4)-C(5)-P(1)	124.9(2)
C(5)-P(1)	1.721(2)	C(5)-P(1)-C(1)	101.4(1)
C(1)-P(2)	1.822(2)	P(1)-C(1)-P(2)	114.9(1)
P(2)-B(1)	1.934(3)		

Comparison of the key bond lengths and angles in **2.4** to those in the silylated borane complex **2.2** reveals remarkably few differences between the two structures. The most significant structural changes are the wider C(4)-C(5)-P(1) bond angle (124.9(2) versus 121.2(1)° in **2.2**) and the more acute C(5)-P(1)-C(1) bond angle (101.4(1) versus 103.7(1)° in **2.2**).

Whilst the desilylation of borane complex **2.2** provided a precursor to the desired phosphinine **2.5**, removal of the borane was not as facile as desired. A major issue was complete removal of the [DABCO.$(BH_3)_2$] by-product, which was difficult to achieve due to the decreased difference in solubility between **2.4** and [DABCO.$(BH_3)_2$]. In order to isolate analytically pure material the desilylation of the free phosphinophosphinine **2.1** was subsequently investigated (**Scheme 2-8**).

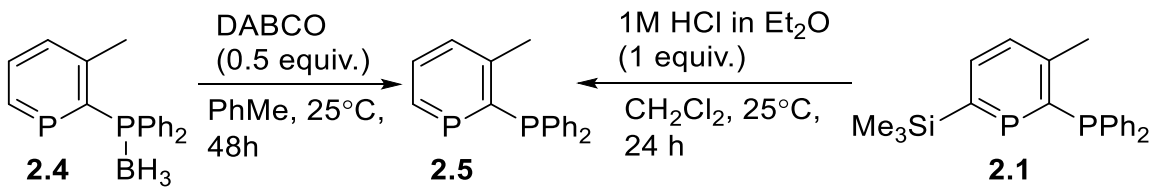

Scheme 2-8. Synthetic routes to **2.5**

Reaction of **2.1** with ethereal HCl proceeded without undesired protonation of the phosphine moiety – likely due to its weak basicity – producing **2.5** (δ = 224.9 (d), -7.6 (d) ppm – data matches literature values)[50] with only volatile $SiMe_3Cl$ as a side-product. After recrystallisation of the product from petroleum ether at -25°C, analytically pure **2.5** was obtained as a colourless microcrystalline powder (77% from **2.1**). Repeated attempts to produce single crystals of **2.5** gave the same result. This synthesis of **2.5** has recently been published.[188]

2.2 Synthesis of bis(diphenylphosphino)phosphinines

2.2.1 Attempted preparation of a bis(phosphinomethyl)phosphinine

The use of tridentate bis(phosphinomethyl)pyridine pincer ligands (**Figure 2-4**, **A**) in cooperative catalysis has been pioneered by Milstein and others.[79] Due to the increased acidity of the methylenic protons,[189] reaction of the corresponding metal complexes with a strong base allowed for isolation of the dearomatised complexes which readily react with E-H (E = N, O, S) bonds as part of a catalytic cycle in order to regain aromaticity.[81, 190] By preparation of analogous phosphinine pincer ligands (**Figure 2-4**, **B**), we hoped to investigate any differences in reactivity, particularly in respect to the energy differences associated with aromaticity.

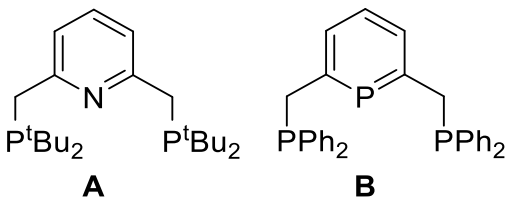

Figure 2-4. Heterocyclic pincer ligands

The synthetic methodology used to investigate the synthesis of the tridentate ligand involved the reaction of two equivalents of the propargyl phosphine (**Scheme 2-9**, **A**) with the diazaphosphinine. Preparation of the propargyl phosphine proved difficult because it tended to isomerise to the internal alkyne (H_3C-C≡C-PPh_2), especially during

attempts at purification by high-vacuum distillation. To circumvent this issue, the crude phosphine (calculated to be greater than 95% purity by inverse-gated $^{31}P\{^{1}H\}$ NMR spectroscopy) was used and reacted with the diazaphosphinine precursor as a toluene solution. However, the reaction was not regioselective, as had been previously observed by Le Floch and co-workers with the reaction of Ph-C≡C-CH_2-PPh_2.[191]

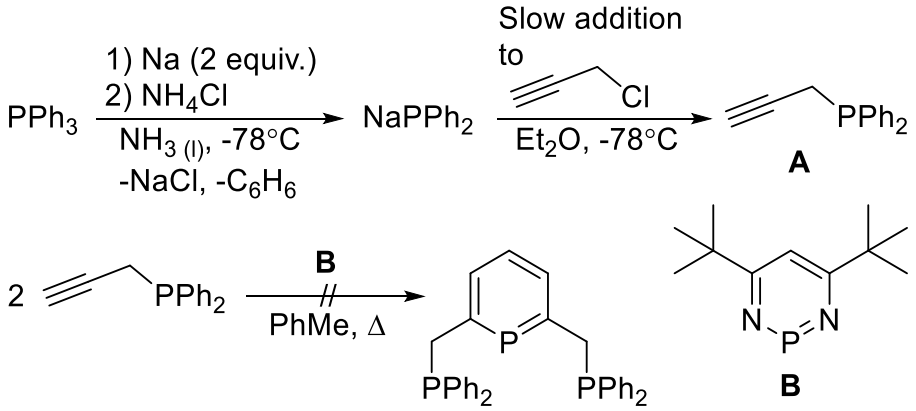

Scheme 2-9. Attempted synthesis of 2,6-bis(diphenylphosphinomethyl)phosphinine

After extended heating of a 2:1 mixture of the propargyl phosphine **A** with diazaphosphinine **B** at 120°C, a complex mixture of products was observed by $^{31}P\{^{1}H\}$ NMR spectroscopy. As the group of Le Floch and Mathey reported difficulties in separation of isomeric phosphinines by column chromatography,[57] the reaction was not investigated further.

2.2.2 Synthesis of two isomeric bis(diphenylphosphino)phosphinines

The reaction with two equivalents of H_3C-C≡C-PPh_2 was also investigated (**Scheme 2-10**). Whilst it was anticipated that the desired product would not act as a tridentate ligand due to the narrow bite-angles, the group of Le Floch and Mathey had reported a 2,6-bis(diphenylphosphino)phosphinine[57, 58] and the subsequent preparation of the disulphide derivative,[145] which has been used extensively as a ligand (exclusively as the λ^5-phosphinine derivative).[192-196] A λ^5 derivative has also been used in the palladium-catalysed borylation of aryl iodides.[146]

As for the synthesis of the mono(phosphino)phosphinine **2.1**, reaction of H_3C-C≡C-PPh_2 with the diazaphosphinine precursor regioselectively formed an azaphosphinine containing an *ortho*-phosphine substituent within two hours in toluene at 120°C. However, incorporation of a second equivalent proceeded considerably more slowly, requiring two weeks at 120°C for complete consumption of the azaphosphinine

(**Scheme 2-10**). Whilst only the desired 2,6-bis(phosphino) isomer was reported in the literature for the reaction of two equivalents of Ph-C≡C-PPh_2,[57] it was observed by $^{31}P\{^1H\}$ NMR spectroscopy that two isomeric phosphinines, **2.6** and **2.7**, were produced in a 60:40 ratio (respectively) with H_3C-C≡C-PPh_2.

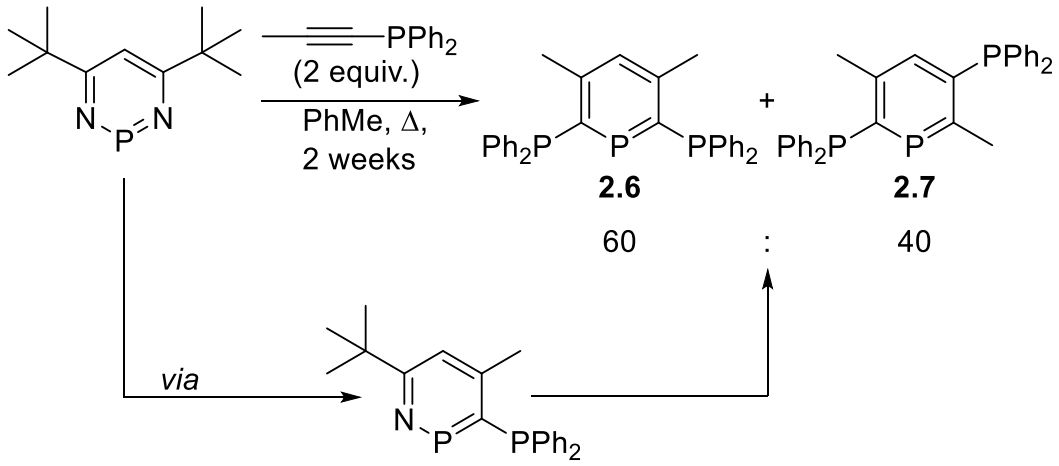

Scheme 2-10. Synthesis of isomeric bis(phosphino)phosphinines **2.6** and **2.7**

Separation of the two regioisomers was readily achieved without the need for chromatographic purification due to their different solubilities. **2.6** is sparingly soluble in aliphatic solvents and as such was extracted using large volumes of petroleum ether. After crystallisation from toluene at -25°C, analytically pure **2.6** was obtained (51%, δ = 244.8 (t, 1P), 8.1 (d, 2P) ppm) as a colourless powder that is air-stable in the solid state but decomposes under air within hours in solution. By recrystallisation from 10:1 THF:petroleum ether at -25°C, single crystals of **2.6** suitable for X-ray diffraction were obtained.

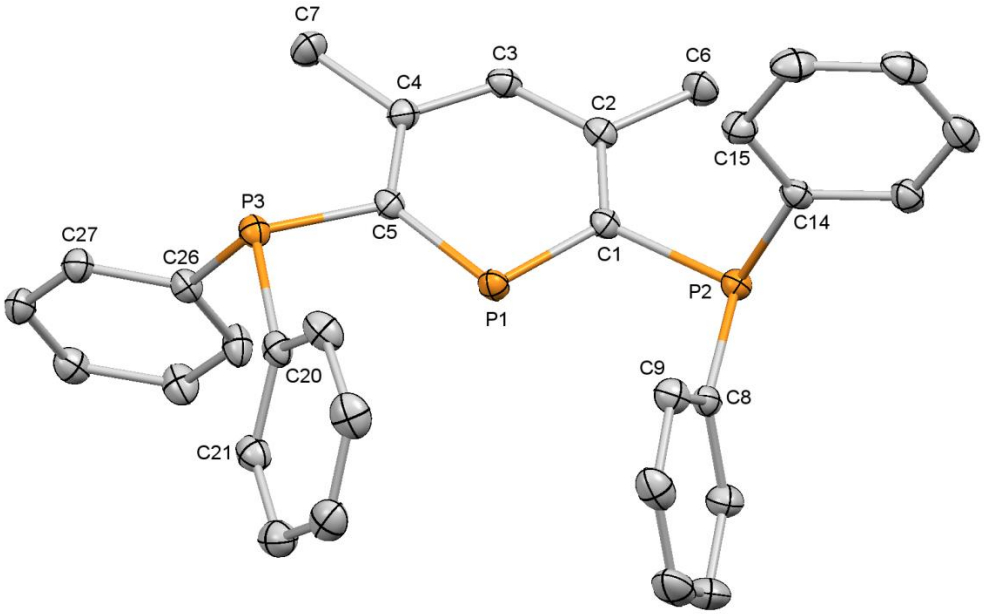

Figure 2-5. Molecular structure of **2.6** (thermal ellipsoids at 50% probability). All H-atoms have been removed for clarity

Table 2-5. Key bond lengths and angles for **2.6**

Bond Lengths (Å)		Bond Angles (°)	
P(1)-C(1)	1.741(1)	P(1)-C(1)-C(2)	124.01(9)
C(1)-C(2)	1.409(1)	C(1)-C(2)-C(3)	121.5(1)
C(2)-C(3)	1.394(2)	C(2)-C(3)-C(4)	126.1(1)
C(3)-C(4)	1.399(2)	C(3)-C(4)-C(5)	121.8(1)
C(4)-C(5)	1.406(2)	C(4)-C(5)-P(1)	123.73(9)
C(5)-P(1)	1.742(1)	C(5)-P(1)-C(1)	102.76(5)
C(1)-P(2)	1.836(1)	P(1)-C(1)-P(2)	118.52(6)
C(5)-P(3)	1.844(1)	P(1)-C(5)-P(3)	118.31(6)

The solid-state structure of **2.6** shows that the C_2-symmetric structure packs with the phosphines rotated *anti* to each other, likely to minimise steric clashes. Analysis of the ring bond lengths and angles confirmed that the ring is, as expected, symmetric. The P(1)-C(1)/P(1)-C(5) bond lengths are slightly contracted with respect to the P(1)-C(1) bond length of **2.1** (1.741(1) versus 1.754(3) Å for **2.1**).

Surprisingly, **2.7** displayed poor solubility in every common laboratory solvent tested. However, isolation from the crude product mixture (after separation of **2.6**) was achieved by Soxhlet extraction under air using *n*-hexane over seven days. Filtration and recrystallisation from boiling toluene yielded **2.7** as a colourless solid (22%, δ = 220.8 (dd), -9.1 (dd), -10.4 (d) ppm). Single crystals were obtained by dissolution in boiling THF then layering the cooled solution with ether, however, the molecular structure obtained was disordered, with two molecules superimposed on each other. This led to

the two positions for P1 and C1-C5 being located very close to each other and this makes further discussion of bond lengths and angles for the phosphinine unreliable.

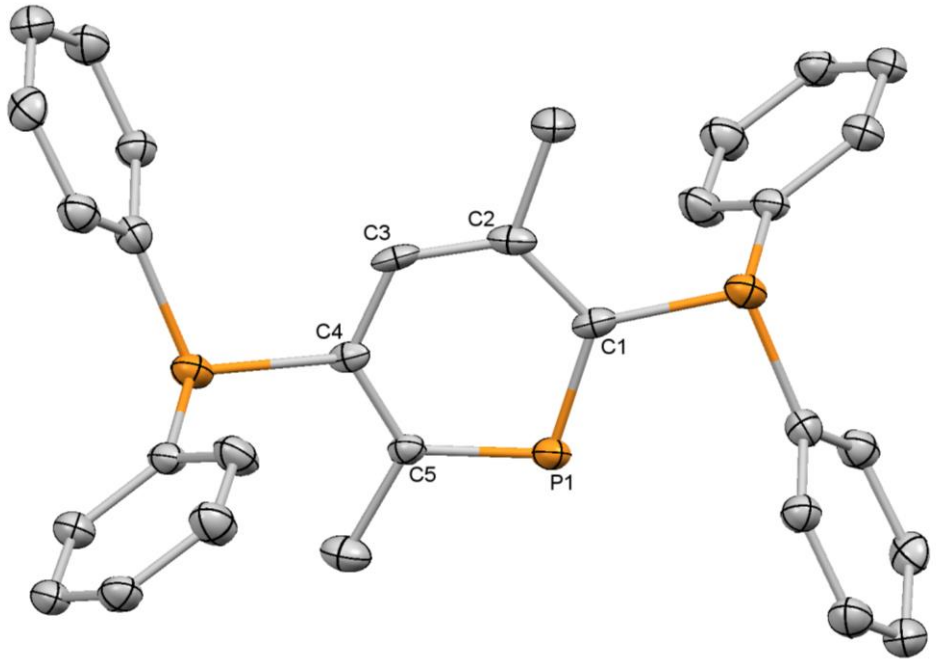

Figure 2-6. Molecular structure of **2.7** (thermal ellipsoids at 50% probability). All H-atoms have been removed for clarity, along with the positions of the disordered phosphinine ring

2.2.3 Synthesis of a bis(iminophosphorano)phosphinine

The group of Le Floch and Mathey have demonstrated the rich coordination chemistry of bis(diphenylphosphine-sulfide)phosphinines, so the synthesis of a bis(iminophosphorano)phosphinine was targeted. Iminophosphoranes take the form of $R_3P{=}NR$, and are strongly σ-donating, hard donors with minimal π-accepting ability.[197] This ligand would also structurally resemble the very successful ligand class of bis(imino)pyridines,[198] although with very different donor properties for all three donor sites. Classically, there are two common routes to iminophosphoranes, the Kirsanov reaction (**Scheme 2-11**, **Route A**)[199] and the Staudinger reaction (**Scheme 2-11**, **Route B**):[199, 200]

Route A:

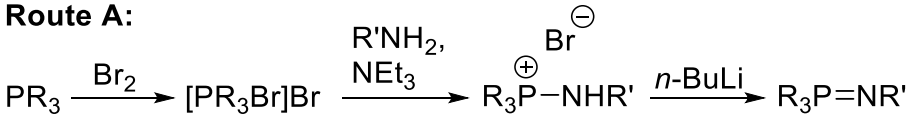

Route B:

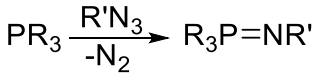

Scheme 2-11. Synthetic routes to iminophosphoranes

Whilst both routes are commonly used in the literature, there are disadvantages to both because the Kirsanov reaction requires elemental bromine as well as butyl/methyllithium and involves multiple steps, whereas the Staudinger reaction requires the use of azides. However, the phosphinine centre in **2.6** could react with bromine,[136] as well as alkyllithium reagents,[146] which left the Staudinger reaction as the only practical option. As alkyl/aryl azides can present a significant safety risk during production and subsequent reactions, the general rule is that hydrocarbyl azides containing (nC + nO)/nN ≥ 3 are considered safe to handle (at room temperature) with minimal precautions required.[201] As the purchase of azido compounds often involves considerable expense, a suitable, stable azide that could be prepared on a practical scale with minimal safety concerns was required. Mesityl (2,4,6-trimethylphenyl) azide has a (C + O)/N value of 3 and was readily prepared on a 0.1 mole scale before purification using column chromatography instead of distillation. By heating a suspension of **2.6** in hexamethyldisiloxane (HMDSO - $(Me_3Si)_2O$) with a slight excess of mesityl azide under reflux overnight (**Scheme 2-12**), the desired bis(iminophosphorane) product **2.8** was isolated as a bright yellow powder (85%, δ = 246.9 (t), -9.4 (d, 2P) ppm). The product was extremely sensitive to moisture and stringent drying of solvents as well as the use of freshly recrystallised **2.6** was key to isolation of pure material, otherwise an orange or brown powder containing multiple decomposition products was isolated. Despite repeated attempts, single crystals of **2.8** could not be obtained, however, the structure was confirmed by high-resolution mass spectrometry, elemental analysis, and $^{1}H/^{13}C/^{31}P\{^{1}H\}$ NMR spectroscopy.

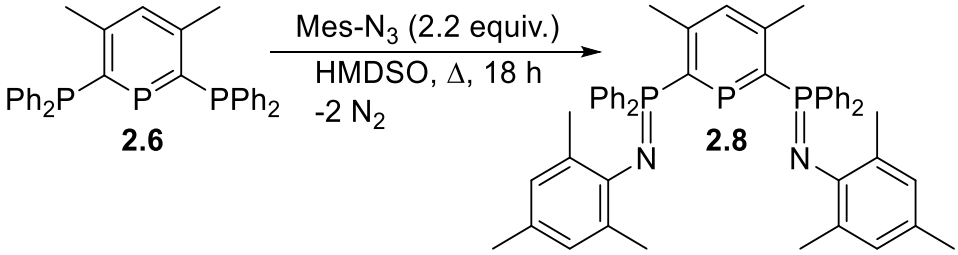

Scheme 2-12. Synthesis of **2.8**

Coordination of **2.8** would facilitate structural characterisation of this new ligand, however, despite multiple attempts at coordination to various transition metals little success was achieved. As such, the results of these reactions are briefly described here.

Initial efforts at coordinating **2.8** involved the reaction with anhydrous $FeCl_2$. By heating a solution of **2.8** in THF with $FeCl_2$ (**Scheme 2-13**), the formation of signals corresponding to a new product (δ = 32.3 (d, 2P), 28.4 (t) ppm) were observed by $^{31}P\{^1H\}$ NMR spectroscopy, however, the chemical shifts of the new resonances indicated that the phosphinine ring had changed, likely forming λ^5 phosphinine. Recrystallisation of the crude reaction mixture by slow diffusion of petroleum ether into a dichloromethane solution yielded yellow needles of the unexpected product **2.9**. Analysis of these by $^{31}P\{^1H\}$ NMR spectroscopy revealed a single new resonance (δ = 18.4 ppm (bs)). Despite maintaining strictly anhydrous conditions, repetition of the reaction produced an identical product. The obtained structure showed that, upon reaction with water, both iminophosphorane substituents had been protonated whilst the phosphorus in the ring had been oxidised. The iron centre was also observed to have gained an extra chloride ligand. Several Lewis structures can be drawn for **2.9**, and the most relevant canonical forms shown are based upon comparison of bond lengths and angles (**Table 2-6**) to those of **2.6**. The position of the protons on the P and N atoms were confirmed by crystallography, along with the P=O double bond.

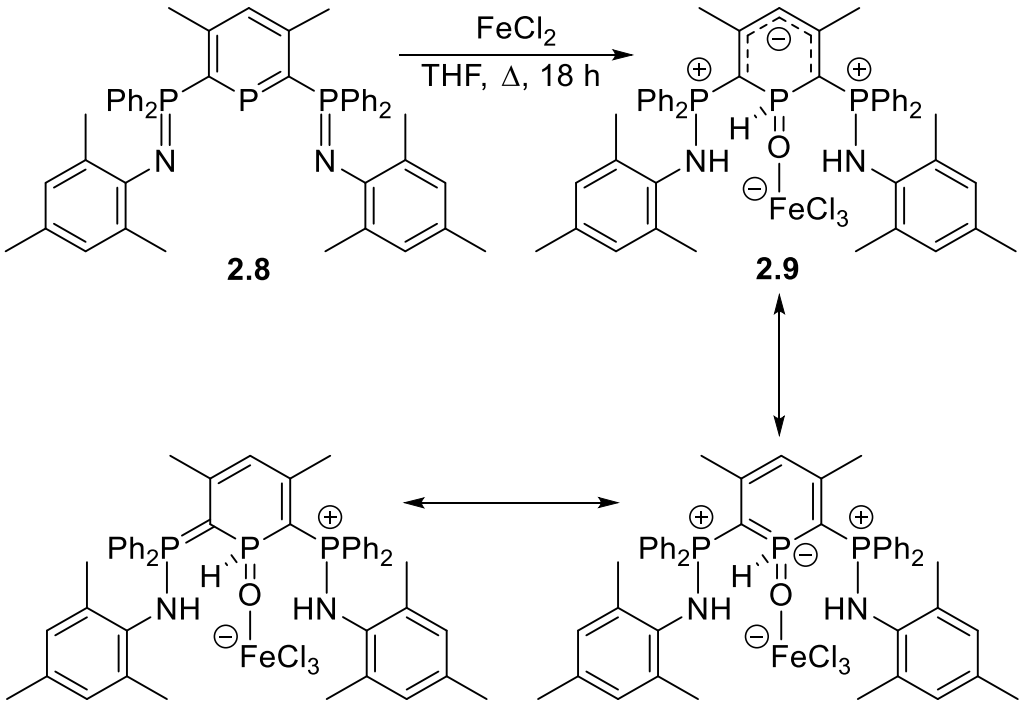

Scheme 2-13. Synthesis and possible resonance structures of **2.9**

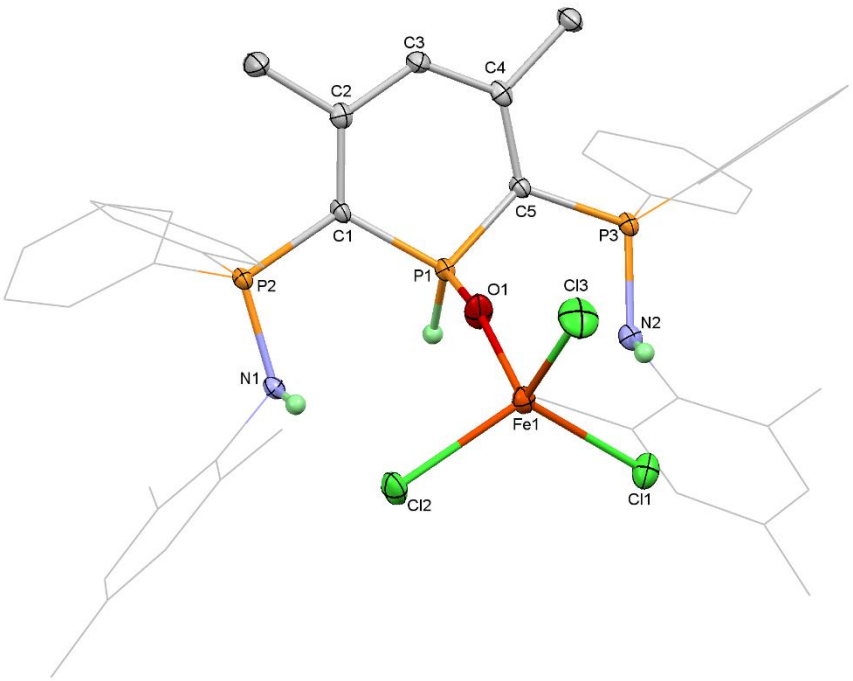

Figure 2-7. Molecular structure of **2.9** (thermal ellipsoids at 50% probability). Phenyl and mesityl rings are represented in wireframe, and all H-atoms (apart from those connected to N or P that were located in the electron density map and refined) and solvating dichloromethane molecules have been omitted for clarity

Table 2-6. Key bond lengths and angles for **2.9**

Bond Lengths (Å)		Bond Angles (°)	
P(1)-C(1)	1.756(2)	P(1)-C(1)-C(2)	118.9(2)
C(1)-C(2)	1.405(4)	C(1)-C(2)-C(3)	122.9(2)
C(2)-C(3)	1.394(3)	C(2)-C(3)-C(4)	126.1(2)
C(3)-C(4)	1.397(4)	C(3)-C(4)-C(5)	122.7(2)
C(4)-C(5)	1.410(4)	C(4)-C(5)-P(1)	119.1(2)
C(5)-P(1)	1.755(3)	C(5)-P(1)-C(1)	104.6(1)
C(1)-P(2)	1.762(2)	P(1)-C(1)-P(2)	117.0(1)
C(5)-P(3)	1.765(3)	P(1)-C(5)-P(3)	117.8(1)
P(2)-N(1)	1.657(2)	C(1)-P(2)-N(1)	107.4(1)
P(3)-N(2)	1.651(2)	C(5)-P(3)-N(2)	107.9(1)
P(1)-O(1)	1.509(3)		
O(1)-Fe(1)	1.997(3)		
Fe(1)-Cl(1)	2.3078(9)		

Comparison of the bond lengths and angles for **2.9** to those for **2.6** revealed that the C-C distances are almost identical around the ring. The P(1)-C(1)/C(2) bond lengths are slightly elongated (1.756(2) versus 1.741(1) Å for **2.6**), however, and the bonds to the exocyclic phosphorus atoms have contracted (for C(1)-P(2): 1.762(2) versus 1.836(1) Å for **2.6**). There are also notable differences in the P(1)-C(1)-C(2) (118.9(2)° versus 124.01(9)° for **2.6**) and C(4)-C(5)-P(1) (119.1(2)° versus 123.73(9)° for **2.6**) bond angles.

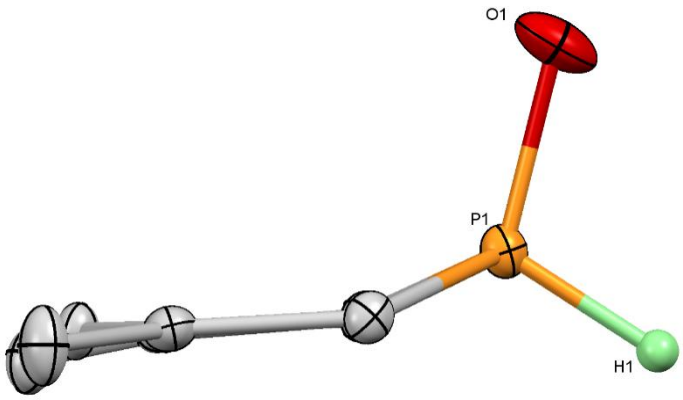

Figure 2-8. Side-on view of **2.9** (ring only, the rest of the structure is hidden for clarity) showing non-planar distortion of the heterocyclic phosphacyclohexadienyl ring

The P(1)-O(1) bond length (1.509(3) Å) indicated a P=O double bond, and comparison of the O(1)-Fe(1) bond (1.997(3) Å) to a known iron phosphine oxide complex (O(1)-Fe(1) = 1.998(4) Å)[202] confirmed an interaction with the Fe atom. Whilst the structure was not desired, **2.9** represents the first example of a 1-phosphinine oxide complex. As strictly anhydrous conditions were maintained during both repetitions of this synthesis

and subsequent crystallisation, the source of water is unknown, but could be a result of low-quality anhydrous $FeCl_2$.

Further efforts to prepare a transition metal complex of **2.8** proved troublesome, with a range of precursors either failing to react at all including $[Rh(PPh_3)_3Cl]$ and $[\{Rh(COD)Cl\}_2]$, or producing multiple products ($[Pt(COD)Cl_2]$, $[\{Rh(CO)_2Cl\}_2]$, *cis*-$[Ru(dmso)_4Cl_2]$). For those metal precursors that produced multiple products, the formation of λ^5 phosphinines was commonly observed by $^{31}P\{^1H\}$ NMR, presumably due to the migration of chlorides to the phosphinine centre. Attempts to circumvent this by addition of $AgBF_4$ (as a source of a non-coordinating anion) to the reaction mixture only served to complicate matters. This echoed the results observed by the group of Le Floch and Mathey who found that addition of $AgBF_4$ to a Pd(II) complex containing the λ^5 bis(diphenylphosphine-sulfide) derivative formed a complex mixture of inseparable products.[145]

The reason why **2.8** proved to be such a poor ligand for transition metals is unknown, but it is unlikely to be due to steric clashes with the mesityl groups as bulky aryl substituents have been essential to the success of the bis(imino)pyridine ligand class.[198] The most logical reason remaining is that the combination of two types of polar-opposite donors (a soft, π-accepting phosphinine with two hard, σ-donating iminophosphoranes) resulted in a "mismatched" ligand with no distinct preference to coordinate to hard or soft metals. A paper including the synthesis of **2.6** to **2.9** is in preparation.

2.3 Conclusions.

Using the diazaphosphinine precursor developed by Le Floch, Mathey and co-workers,[57, 58] three previously unknown phosphinophosphinines were synthesised. They were characterised using multinuclear NMR spectroscopy, elemental analysis and by X-ray diffraction to obtain their molecular structures. The structural data obtained for **2.1** was the first reported for a free, underivatised 2-phosphinophosphinine, and allowed comparison between the P(1)-C(1)-P(2) angle of **2.1** and vdpp[178] (1,1-bis(diphenylphosphino)ethylene) as a structural analogue with limited coordination chemistry.[203-206] Derivatives of **2.1** were also prepared, including the borane adduct **2.2** and the selenide **2.3**, the $^{31}P\{^1H\}$ NMR spectrum of which facilitated evaluation of the donor properties of the phosphine by comparison of the $^1J_{P\text{-}Se}$ coupling constant value to other heterocyclic diphenylphosphines and triphenylphosphine. The observed coupling constant (749 Hz) for **2.3** indicated that the phosphine donor in **2.1** is more π-accepting

than PPh_3 (732 Hz), however, an identical coupling constant was reported for 2-(diphenylphosphino)pyridine.[184]

By adaptation of a literature procedure,[187] the trimethylsilyl substituent on **2.1** was cleaved, cleanly producing the known phosphinophosphinine **2.5** in good yield without need for a Pd(0) catalysed cross-coupling reaction[50] and without need for protection of the free phosphine.

Reaction of the diazaphosphinine precursor with two equivalents of 1-(diphenylphosphino)-1-propyne produced an isomeric, 1.5 : 1, mixture of the two bis(phosphino)phosphinines **2.6** and **2.7**, which were readily separated without chromatography due to their differing solubilities. The mixture of two products was not anticipated because 2,6-diphenylphosphino-3,5-diphenylphosphinine was reported to be selectively formed by Le Floch, Mathey and co-workers without the formation of a 2,5-isomer.

Compound **2.6** was reacted with two equivalents of mesityl azide, affording the highly moisture-sensitive bis(iminophosphorane) **2.8** *via* the Staudinger reaction. Attempts were made to coordinate **2.8** to a range of transition metals, however, in all-but-one reaction either no reaction or an inseparable mix of products was observed. By reaction with $FeCl_2$, phosphinine oxide complex **2.9** was obtained due to the presence of water. The reaction was repeated multiple times with thorough exclusion of moisture, however, **2.9** was the sole product that could be characerised.

3 - Group 6 complexes of 2-phosphinophosphinines

3.1 Introduction

Homoleptic transition metal carbonyl complexes have uses as stoichiometric reagents[207] and catalysts,[208] however, addition of phosphine ligands can alter their properties giving higher yields and/or improved selectivity.[208, 209] Aside from their use in chemical transformations, metal carbonyl complexes are commonly used in order to quantify the donor properties of bound ligands using the distinct stretching frequencies for the C≡O triple bond observed *via* infrared spectroscopy. Historically, monodentate phosphine ligands were coordinated to the nickel carbonyl fragment, which provided the Tolman electronic parameter from the resultant [Ni(L)(CO)$_3$] complexes.[66] However, due to the high toxicity of [Ni(CO)$_4$], safer alternatives were required. The rhodium complex [{Rh(CO)$_2$(μ-Cl)}$_2$] has also been used to form *trans*-[Rh(L)$_2$(CO)Cl] complexes,[210] although the widespread application of this method is limited due to the high cost of rhodium and that (like Tolman's method)[66] it is also exclusive to monodentate ligands. Anton and Crabtree reported that the highest carbonyl stretching frequency (the A$_1$ symmetric stretch) observed in the infrared spectrum for *cis*-[Mo(L)$_2$(CO)$_4$] complexes could be directly correlated to the Tolman electronic parameter obtained from [Ni(L)(CO)$_3$] complexes (with a correlation coefficient of 0.996).[211] It was therefore anticipated that by coordination of 2-phosphinophosphinines **2.1** and **2.5** to a molybdenum tetracarbonyl fragment, their donor properties could be assessed and that the effect of the presence of an *ortho*-trimethylsilyl substituent on a phosphinine ligand could be evaluated experimentally for the first time. The results in this chapter have been recently published.[188]

3.2 Group 6 tetracarbonyl complexes

3.2.1 Synthesis

Although one tungsten tetracarbonyl complex of an *ortho*-phosphinophosphinine (2-diphenylphosphino-3,4,6-triphenylphosphinine) was reported by Märkl and co-workers in 1990,[55] the complex was only partially characterised and no synthetic conditions were provided, other than that the proligand was reacted directly with [W(CO)$_6$]. Also, only the yield (41%) and observation of a molecular ion peak by mass spectrometry was described.[55] The complete characterisation of group 6 carbonyl complexes of ligands **2.1** and **2.5** was therefore sought after, including their molecular structures and carbonyl stretching frequencies. Due to the low yield reported for the direct reaction of the 2-

phosphinophosphinine with $[W(CO)_6]$,[55] it was expected that by substituting the homoleptic carbonyl complexes for $[M(diene)(CO)_4]$ precursors, a more practical and convenient route to these complexes could be developed. In collaboration with an undergraduate research student, Alana Smith (who prepared **3.1** to **3.3**), five new M(0) tetracarbonyl complexes were prepared (**Scheme 3-1**, **Table 3-1**).[188]

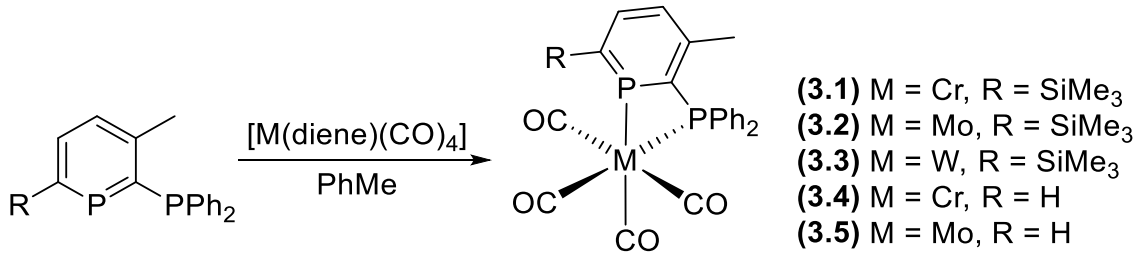

Scheme 3-1. Synthesis of metal tetracarbonyl complexes

Table 3-1. Experimental conditions and ^{31}P NMR spectroscopy data

	3.1	**3.2**	**3.3**	**3.4**	**3.5**
M	Cr	Mo	W	Cr	Mo
R	$SiMe_3$	$SiMe_3$	$SiMe_3$	H	H
Diene[a]	NBD	NBD	COD	NBD	NBD
Temp (°C)	60	20	75	60	20
Time (h)	24	2	96	24	2
Yield (%)[b]	75	30	69	32	60
^{31}P δ (ppm)	273.6, 40.5	244.8, 18.9	209.6, -0.1	250.3, 41.8	222.7, 20.0
$^{3}J_{P\text{-}P}$ (Hz)	38.2	72.8	78.0	33.8	71.1

[a]: NBD = norbornadiene, COD = 1,5-cyclooctadiene. [b]: Isolated yields of analytically pure material.

As is shown in **Table 3-1**, complexes **3.1** to **3.5** were isolated as crystalline, pure materials in low to good yields (30 to 75%), and were fully characterised by multinuclear NMR spectroscopy, elemental analysis, high-resolution mass-spectrometry, infrared spectroscopy and X-ray crystallography (except **3.5** where single crystals were not achieved). Out of the three $[M(diene)(CO)_4]$ precursors used, the molybdenum norbornadiene complex was the most reactive, with clean production of a single complex within two hours at 20°C. The Cr and W precursors were less reactive, requiring extended reaction times and elevated temperatures (*e.g.* 4 days at 75°C for **3.3**), and it was also observed that various side-products were produced during these reactions. The synthesis of Cr complex **3.4** proved to be the most challenging, with the

product proving to be temperature sensitive in solution, as well as over extended periods in the solid state, resulting in a low isolated yield.

3.2.2 Infrared spectroscopy of metal tetracarbonyl complexes

Previous DFT calculations by Ferro *et. al.* suggested that incorporation of two trimethylsilyl substituents on a phosphinine ring would increase the σ-donor properties of the P-atom due to an increase in energy in the lone pair (their calculations showed that the lone pair would become the HOMO-1 instead of the HOMO-2).[165] This result was echoed in a recent publication by Müller and co-workers, who used theoretical calculations to investigate the donor properties of 2-trimethylsilylphosphinine in comparison to those of the parent phosphinine.[11] However, their results did not agree with the assertion in the Ferro publication that *ortho*-$SiMe_3$ substitution would also increase the π-acceptor properties of the phosphinine, with the Müller group's calculations implying that the presence of such a substituent would only engender a minor change in the energy of the LUMO.[11, 165] In order to make effective comparisons between the donor properties of **2.1** and **2.5**, and confirm or disprove the hypothesis of increased π-acceptance, infrared spectra of complexes **3.1** to **3.5** were recorded (**Table 3-2**) using crystalline material in the solid state due to the air-sensitivity of the complexes in solution phase. Whilst the infrared spectroscopy data obtained from complexes of ligands **2.1** and **2.5,** as well as dppm, PPh_3 and $P(OMe)_3$, in **Table 3-2** is discussed in terms of the π-accepting abilities of these ligands, it is important to remember that M-CO bonding consists of both σ-donation and π-back-bonding. As both bonding components are synergic, their influence on the nature of the M-CO bonds in the metal carbonyl species are not easily separated.

Table 3-2. Infrared spectroscopy data for group 6 tetracarbonyl complexes

Complex	Metal	Ligand	ν(CO) (cm^{-1})	Reference
3.1	Cr	**2.1**	1895, 1906, 2013	188
3.2	Mo	**2.1**	1888, 1926, 2026	188
3.3	W	**2.1**	1883, 1914, 2021	188
3.4	Cr	**2.5**	1864, 1898, 2003	188
3.5	Mo	**2.5**	1867, 1910, 2017	188
–	Cr	dppm[a]	1891, 1903, 1922, 2012	212
–	Mo	dppm[a]	1897, 1917, 1929, 2020	212
–	W	dppm[a]	1980, 1907, 1935, 2015	212
-	Mo	2 PPh_3	1897, 1908, 1927, 2023	213
-	Mo	2 $P(OMe)_3$	1922, 1944, 1952, 2034	214

[a]: dppm = bis(diphenylphosphino)methane

According to the Dewar-Chatt-Duncanson synergic bonding model for metal carbonyls,[215, 216] if **2.5** was confirmed to be a poorer π-acceptor ligand than **2.1**, it would be anticipated that the observed ν(CO) value for its complexes would be observed at a lower wavenumber than for those of **2.1**. As is known, this is due to an increased level of M→CO π* back-bonding. The lower stretching frequencies recorded for complexes **3.4** and **3.5** (by *ca.* 10 cm^{-1}) over the silylated analogues agrees with the theoretical results reported by Ferro *et. al.*,[165] and confirms that **2.5** is more weakly π-accepting. The A_1 symmetric stretches for complexes of **2.1** were also observed at a higher stretching frequency than for the analogous complexes of dppm, indicating that, as hypothesised, **2.1** is more π-accepting. The stretching frequency for **3.2** (2026 cm^{-1}) is also higher than for the triphenylphosphine complex *cis*-$[Mo(PPh_3)_2(CO)_4]$ (2023 cm^{-1})[213], but lower than for the phosphite complex *cis*-$[Mo(P\{OMe\}_3)_2(CO)_4]$ (2034 cm^{-1})[214], which implies that **2.1** is electronically more similar to an aryl phosphine than a strongly π-accepting phosphite. However, it was noted that the complexes of **2.5** had smaller values of ν(CO) than the analogous dppm complexes; this was not anticipated as it implies that (as an average over both donors) **2.5** is less π-accepting than dppm.

3.2.3 X-ray crystallography

Complexes **3.1** to **3.4** were characterised by X-ray diffraction (**Figure 3-1**, **Figure 3-2**, **Table 3-3**, **Table 3-4**), and **3.1** – **3.3** were observed to be isostructural.

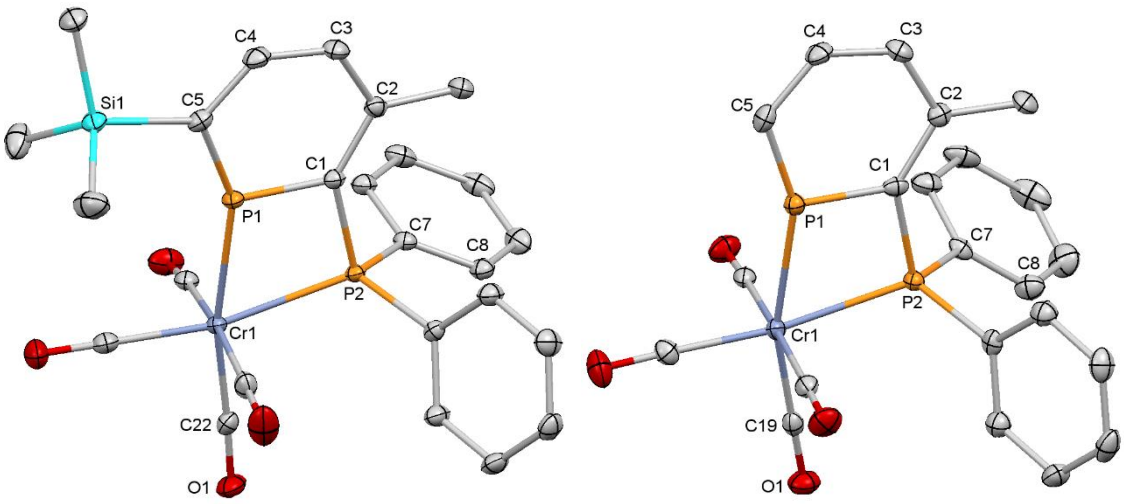

Figure 3-1. Molecular structure of Cr complexes **3.1** and **3.4**‡
‡ = Thermal ellipsoids at 50% probability, all H-atoms have been omitted for clarity

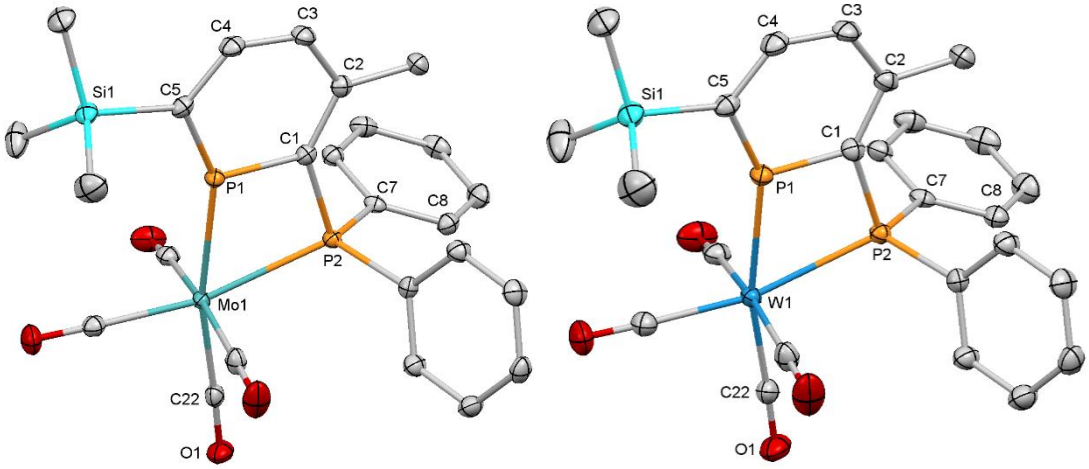

Figure 3-2. Molecular structure of Mo (**3.2**) and W (**3.3**) complexes‡

Table 3-3. Key bond lengths for complexes **3.1** to **3.4**

Distances (Å)	**3.1**	**3.4**	**3.2**	**3.3**
M(1)-P(1)	2.3752(5)	2.3464(11)	2.5028(4)	2.4866(6)
M(1)-P(2)	2.4340(5)	2.4030(13)	2.5599(4)	2.5462(6)
P(1)-C(1)	1.736(2)	1.720(4)	1.726(2)	1.721(2)
P(1)-C(5)	1.735(2)	1.705(4)	1.721(2)	1.723(2)
P(2)-C(1)	1.840(2)	1.819(4)	1.830(2)	1.828(2)
C(1)-C(2)	1.401(2)	1.402(6)	1.397(2)	1.390(3)
C(2)-C(3)	1.414(2)	1.412(6)	1.403(2)	1.405(3)
C(3)-C(4)	1.407(2)	1.392(6)	1.391(2)	1.397(3)
C(4)-C(5)	1.412(2)	1.394(6)	1.405(2)	1.396(3)
M(1)-C(22)	1.864(2)	C19: 1.849(4)	1.978(2)	1.974(2)
M(1)-C(23)	1.876(2)	C20: 1.867(5)	1.996(2)	1.986(2)
M(1)-C(24)	1.910(2)	C21: 1.892(5)	2.047(2)	2.034(3)
M(1)-C(25)	1.911(2)	C22: 1.890(5)	2.043(2)	2.027(2)
C(22)-O(1)	1.167(2)	C19: 1.159(4)	1.151(2)	1.152(3)
C(23)-O(2)	1.161(2)	C20: 1.159(6)	1.146(2)	1.153(3)
C(24)-O(3)	1.151(2)	C21: 1.155(6)	1.137(2)	1.139(3)
C(25)-O(4)	1.154(2)	C22: 1.156(5)	1.142(2)	1.145(3)

Table 3-4. Key bond angles for **3.1** to **3.4**

Angles (º)	**3.1**	**3.4**	**3.2**	**3.3**
P(1)-C(1)-C(2)	125.3(1)	126.4(3)	124.8(1)	124.9(2)
C(1)-C(2)-C(3)	118.2(2)	118.0(4)	118.2(1)	118.1(2)
C(2)-C(3)-C(4)	125.3(2)	124.9(4)	125.9(1)	125.7(2)
C(3)-C(4)-C(5)	127.7(2)	126.3(4)	127.2(1)	127.4(2)
C(4)-C(5)-P(1)	116.6(1)	119.8(3)	116.9(1)	116.5(2)
P(1)-M(1)-P(2)	67.99(2)	68.29(4)	65.09(1)	65.07(2)
P(1)-C(1)-P(2)	97.50(8)	97.7(2)	99.98(7)	99.40(11)
C(1)-P(1)-C(5)	106.5(1)	104.5(2)	106.69(7)	106.9(1)

The molecular structures of all four complexes show either **2.1** or **2.5** chelating to the corresponding $M(CO)_4$ fragment in a distorted octahedral geometry. The majority of the bond lengths and angles around the phosphinine ring for each compound are very similar, indicating that both removal of the trimethylsilyl substituent and the choice of group six metal coordinated to the ligand has little effect on the geometry of the ring. The exception to this is the C(4)-C(5)-P(1) bond angle in the desilylated chromium complex **3.4**, which is 119.8(3)° compared to 116.6(1)° in complex **3.1**. The P(1)-M(1)-P(2) bite angle for all four complexes are notably smaller than their analogous $[M(dppm)(CO)_4]$ complexes. For example, in $[Cr(dppm)(CO)_4]$ this value is 70.19(2)°,[217] compared to 67.99(2)° and 68.29(4)° for **3.1** and **3.4** respectively. Whilst the removal of the trimethylsilyl substituent doesn't have a significant effect on the geometry of the phosphinine ring, complex **3.4** possesses a notably more distorted octahedral geometry based on the C(22)/C(19)-Cr(1)-P(1) bond angles of 167.9(1)° and 163.4(1)° for **3.1** and **3.4** respectively.

3.2.4 Stability of **3.4**

Whilst all five complexes were air-sensitive to some degree, the chromium complexes **3.1** and **3.4** were particularly sensitive to temperature as well, with multiple side-products observed by $^{31}P\{^1H\}$ NMR spectroscopy in the crude reaction mixture. As a result, it was noted that during the first attempt to recrystallise desilylated complex **3.4** by the slow diffusion of petroleum ether into a dichloromethane solution of the crude material at 20°C, the solution changed from a clear, bright orange colour into a green/grey solution with a large amount of fine precipitate observed. A small crop of orange crystals were observed at the bottom of the flask, which allowed for analysis of this material by X-ray diffraction (**Figure 3-3**). The obtained structure indicates that the formation of **3.6** proceeded *via* an initial [4+2] cyclisation (**Scheme 3-2**) between two coordinated phosphinine rings and that the resulting (non-aromatic) P=C double bonds then reacted with any trace moisture present in solution, forming the P-O-P linkage. The decreased stability of complex **3.4**, due to the removal of the trimethylsilyl substituent, is likely a result of reduced steric protection of the sp^2 phosphorus. This suggests that for future investigations into ligand design, the impact of steric bulk in the *ortho* position is an important consideration, not only due to the implications on coordination mode,[75] but also on ligand stability.

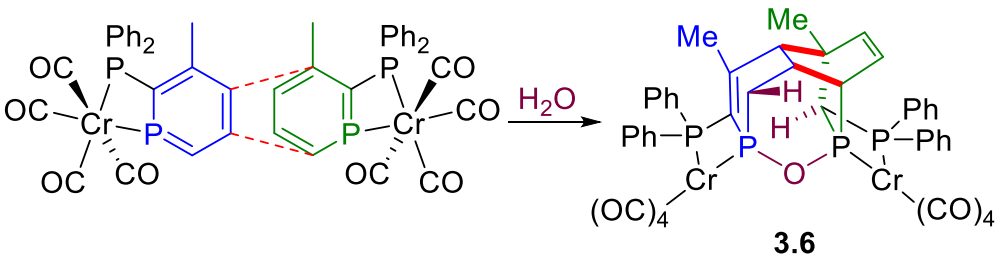

Scheme 3-2. Formation of **3.6**

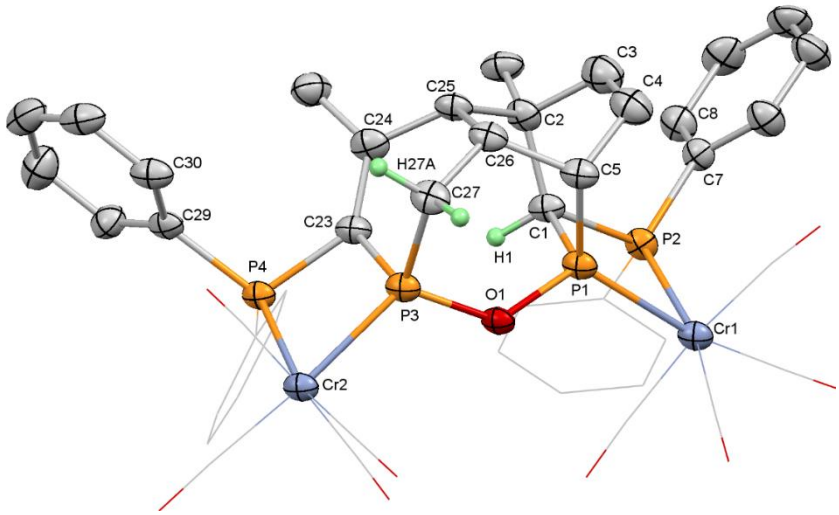

Figure 3-3. Molecular structure of **3.6** (thermal ellipsoids at 50% probability). All H-atoms apart from those on non-methyl sp^3 carbons have been omitted, and all carbonyl ligands and two phenyl rings are displayed in wireframe for clarity.

Table 3-5. Key bond lengths and angles in **3.6**

Bond Lengths (Å)		Bond Angles (°)	
P(1)-C(1)	1.836(4)	P(1)-C(1)-C(2)	114.5(3)
C(1)-C(2)	1.526(6)	C(1)-C(2)-C(3)	105.7(4)
C(2)-C(3)	1.534(8)	C(2)-C(3)-C(4)	118.0(5)
C(3)-C(4)	1.345(8)	C(3)-C(4)-C(5)	117.1(5)
C(4)-C(5)	1.482(6)	C(4)-C(5)-P(1)	107.1(3)
C(5)-P(1)	1.839(5)	C(5)-P(1)-C(1)	97.3(2)
C(1)-P(2)	1.877(4)	P(1)-C(1)-P(2)	93.2(2)
P(1)-Cr(1)	2.293(1)	P(3)-C(23)-C(24)	122.0(4)
P(2)-Cr(1)	2.371(1)	C(23)-C(24)-C(25)	119.9(4)
P(3)-C(23)	1.805(5)	C(24)-C(25)-C(26)	115.9(3)
C(23)-C(24)	1.382(6)	C(25)-C(26)-C(27)	115.3(4)
C(24)-C(25)	1.516(7)	C(26)-C(27)-P(3)	110.3(3)
C(25)-C(26)	1.591(6)	C(27)-P(3)-C(23)	98.0(2)
C(26)-C(27)	1.528(7)	P(3)-C(23)-P(4)	97.1(2)
C(27)-P(3)	1.813(5)	C(2)-C(25)-C(26)	111.3(3)
C(23)-P(4)	1.823(5)	C(25)-C(26)-C(5)	111.6(4)
P(3)-Cr(2)	2.273(1)	C(26)-C(5)-C(4)	105.6(4)
P(4)-Cr(2)	2.391(1)	C(3)-C(2)-C(25)	104.3(4)
P(1)-O(1)	1.645(3)	P(1)-O(1)-P(3)	128.7(2)
P(3)-O(1)	1.651(3)	P(1)-Cr(1)-P(2)	70.70(4)
		P(3)-Cr(2)-P(4)	71.31(4)

There is substantial variation in the bond lengths and angles within the molecular structure due to the large number of unique environments. The cyclic P-C bonds within each former-phosphinine unit are similar to each other (P(1)-C(1) is 1.836(4) Å and C(5)-P(1) is 1.839(5) Å, P(3)-C(23) is 1.805(5) Å and C(27)-P(3) is 1.813(5) Å) despite the different carbon environments (for example, C(23) is sp^2 whereas C(27) is sp^3). As a result of the [4+2] cyclisation, the P(1)-C(5) ring exists in a bicyclic structure (with C(25) and C(26) as the bridgehead), and consequently the C(1)-C(2)-C(3) and C(4)-C(5)-P(1) angles are notably more acute (105.7(4)° and 107.1(3)° respectively) than the other angles in rings P(1)-C(5) or P(3)-C(27), with the exception of the C-P-C angles. The two remaining C=C double bonds are C(3)-C(4) and C(23)-C(24) (1.345(8) Å and 1.382(6)Å, respectively).

Phosphinines are known to undergo reactions with anionic nucleophiles, such as alkyllithium reagents,[173, 218, 219] forming the corresponding P-alkylated λ^4 phosphinine anions. This reactivity has also been demonstrated with diethylaluminium ethoxide (Et_2AlOEt) in combination with [$Ni(acac)_2$] (acac = acetylacetonate), forming a dinickel complex containing two P-ethylated λ^4 phosphinine ligands.[220] With intentions to investigate the catalytic oligomerisation of ethylene (*vide infra*) in the presence of

excess MMAO (modified methylaluminoxane), it was necessary to investigate the reactivity of both **2.1** and chromium complex **3.1** with MMAO, to assess whether P-alkylation would occur in solution. Therefore, excess (30 equivalents) of MMAO-12 was added to solutions of **2.1** and **3.1** in C_6D_6. As λ^4/λ^5 phosphinines are strongly coloured,[20] and do not contain a resonance at high chemical shift in their ^{31}P NMR spectra, any P-alkylated species would have been easily identifiable. For both free phosphinophosphinine **2.1** and complex **3.1**, no change in chemical shift was observed by $^{31}P\{^1H\}$ NMR spectroscopy, nor any colour change after twenty four hours (**Figure 3-4**). However, the formation of a poorly-soluble, gel-like material was observed in both reactions (**Figure 3-5**).

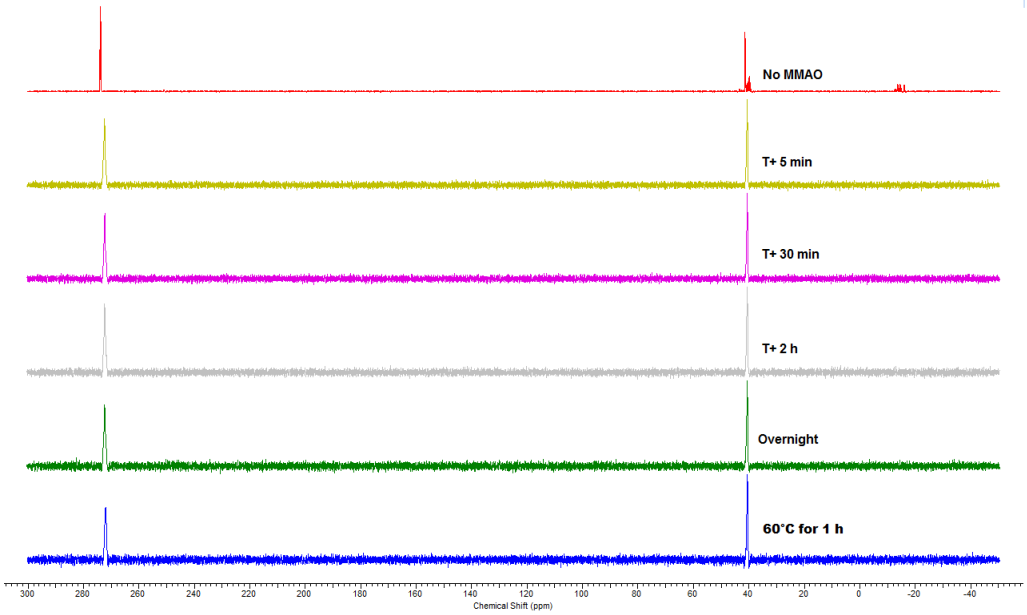

Figure 3-4. $^{31}P\{^1H\}$ NMR spectra obtained from reaction of **3.1** with excess MMAO-12.

Figure 3-5. Insoluble material observed after reaction of **3.1** with excess MMAO-12.

3.3 Catalytic ethylene oligomerisation

3.3.1 Introduction

Ethylene is a highly important chemical building block, in part because it is cheap and is produced on a very large scale from ethane (although efforts to synthesise it from renewable sources are ongoing).[221] It can also be used as a precursor to multiple value-added products[222] including linear alpha-olefins (LAO).[223, 224] LAO (in particular 1-hexene and 1-octene) are important co-monomers in the production of low-density polyethylene.[225] Traditional catalysts used to prepare LAO, such as in the SHOP process,[226] have suffered from issues such as poor selectivity. However, a step-change in performance originating from a metallacyclic mechanism (**Figure 3-6**) has resulted from the development of ligands that produce highly selective catalysts.[89, 227] As such, a great deal of research on the selective synthesis of these two LAOs has been published.[228-232] Currently, the two bis(phosphino)amine (PNP) ligands **A** and **B** (**Figure 3-7**, **Table 3-6**) are the most selective for production of 1-hexene (although this has not been commercialised)[229, 233] and 1-octene[230, 231] respectively, when coordinated to the catalytically active chromium centre. The steric-bulk of ligand and potentially hemilability of **A** results in the selective production of 1-hexene because the four *ortho*-methoxy groups on the phosphines hinder the growth of the metallacycle past six carbon atoms.[89] Conversely, the less bulky **B** allows for growth of the metallacycle to eight carbon atoms, resulting in production of 1-octene.

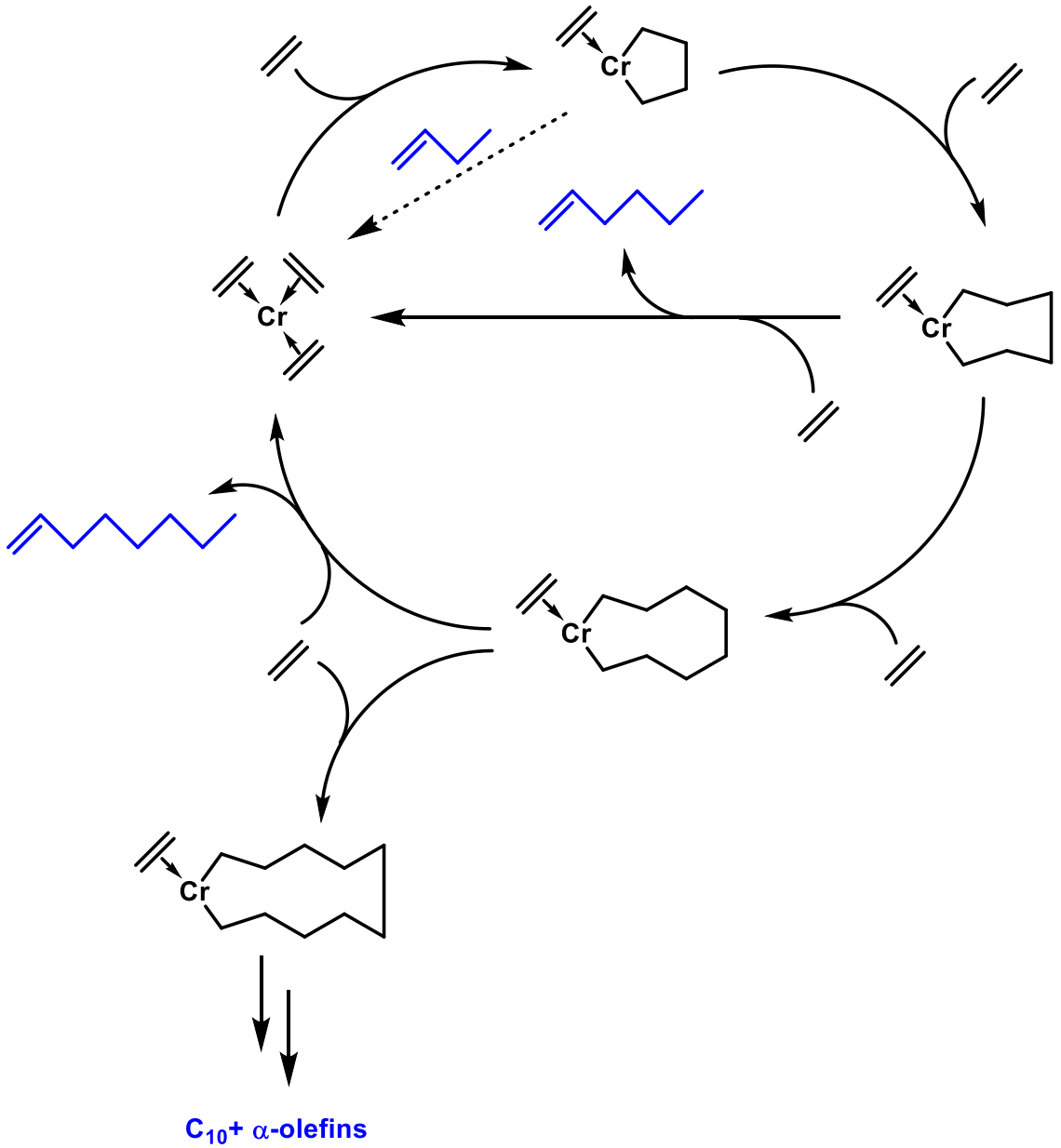

Figure 3-6 -The metallacyclic mechanism implicated in the production of 1-hexene and 1-octene

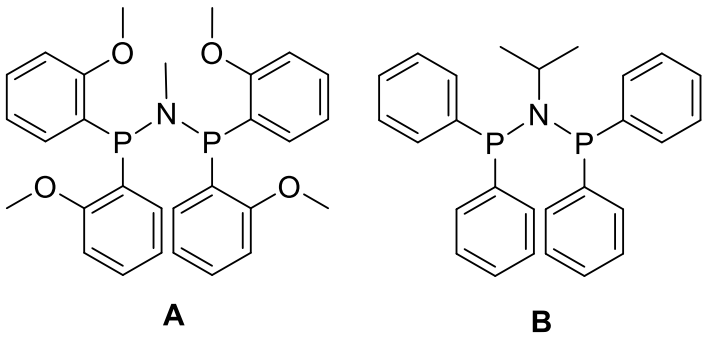

Figure 3-7. Chemical structures of bis(phosphino)amine ligands **A** and **B**

3.3.2 Computational mapping of ligands

Small bite-angle ligands such as **A** and **B** create highly active catalysts in ethylene oligomerisation,[229-231, 233] however, an important stipulation in ligand choice is the lack of any acidic α-protons between the two phosphorus donors. For example, dppm is not a selective ligand, and produces a Schulz-Flory distribution of oligomers (likely due to deprotonation of the methylene bridge).[234] However, the use of methyl-substituted dppm (1,1-bis(diphenylphosphino)ethane) provided increased catalytic activity as well as some selectivity to the production of 1-hexene and 1-octene (although it also produced 53.7 weight % polymer).[235] Small bite-angle phosphinophosphinine ligands **2.1** and **2.5** possess no α-protons, and investigation into their utility as a potential new class of ligands for the oligomerisation of ethylene was therefore appealing. However, a comparison of the properties of these compounds to other known P,P-bidentate ligands was desirable before any catalytic data was collected.

As can be seen in **Table 3-6**, the chromium tetracarbonyl complexes of ligands **A, B** and **2.1** have a similar P-Cr-P bite angle, whilst the values for the highest carbonyl stretching frequency are notably different. Ligand **2.5**, however, possesses more comparable electronic properties to **A** and **B** but the P-Cr-P bite angle is more acute. Therefore, a comprehensive method to allow comparisons between the properties of phosphinophosphinines **2.1** and **2.5** to the two PNP ligands (and others) was required to fully understand their properties. In collaboration with Dr Natalie Fey at the University of Bristol, a series of structures (**Figure 3-8**) were entered into the existing P,P-donor ligand knowledge base (LKB).[236] Not only were the structures of known compounds **2.1** and **2.5** entered, but eleven structural variants (**N3** to **N13**) were also added in order to assist with future ligand design.[188]

Table 3-6. P-Cr-P bite angles and the carbonyl stretching frequencies of $[Cr(L)(CO)_4]$ complexes of ligands **A**, **B**, **2.1** and **2.5**

Ligand	ν(CO) (cm^{-1})	P-Cr-P angle (°)	Reference
A	1869, 1888, 1907, 2002	68.44(3)	237
B	1889, 1919, 2006	67.82(4)	237
2.1	1895, 1906, 2013	67.99(2)	188
2.5	1864, 1898, 2003	65.07(2)	188

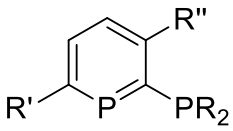

N1, **2.1**, R = Ph, R' = $SiMe_3$, R'' = Me
N2, **2.5**, R = Ph, R' = H, R'' = Me
N3, R = Ph, R' = $SiMe_3$, R'' = H
N4, R = Ph, R' = H, R'' = H
N5, R = Ph, R' = Si^iPr_3, R'' = Me
N6, R = Me, R' = $SiMe_3$, R'' = Me
N7, R = ^{n}Bu, R' = $SiMe_3$, R'' = Me
N8, R = ^{i}Pr, R' = $SiMe_3$, R'' = Me
N9, R = ^{t}Bu, R' = $SiMe_3$, R'' = Me
N10, R = Me, R' = H, R'' = Me
N11, R = ^{n}Bu, R' = H, R'' = Me
N12, R = ^{i}Pr, R' = H, R'' = Me
N13, R = ^{t}Bu, R' = H, R'' = Me

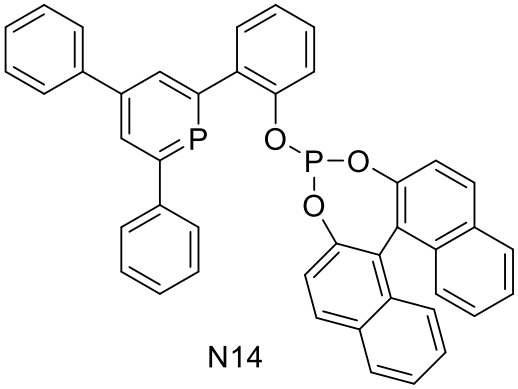

N14

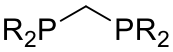

3, R = ^{t}Bu
5, **C**, R = Ph
7, R = *o*-tolyl
8, R = *o*-OMe-C_6H_4

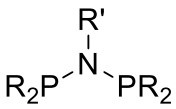

16, R = Ph, R' = H
21, R = Ph, R' = Me
22, R = *o*-tolyl, R' = Me
24, **A**, R = *o*-OMe-C_6H_4, R' = Me
31, **B**, R = Ph, R' = ^{i}Pr
35, R, R' = Ph

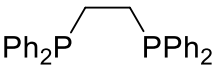

52, **F**

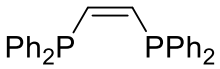

71, **G**

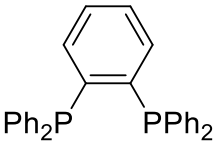

77, **H**

Figure 3-8. Structures in the P,P-donor LKB relevant to this work.[188]

By calculating a set of twenty-eight parameters relating to the ligand properties, and combining these into four principal components (PC, specific details on the calculations are explained in the literature),[188] maps of the ligand properties were obtained by plotting one PC against a second. Deconvolution of the four principal components into exact chemical properties (such as ligand bite-angle, or electronics) cannot readily be achieved (although PC1 and PC2 have large steric and electronic components,[238] respectively), in part due to the combination of the twenty-eight parameters used, and because this is also not the end goal of the LKB. However, the data obtained by mapping one PC against another allows for spatial comparison of ligands; if two ligands are close to one another in a map, then they are likely to have some measure of similarity in their reactivity. By entering the structures of hypothetical ligands into the database, this can therefore allow for a targeted approach to ligand development, instead

of attempts based on trial-and-error.[239] Analysis of **Figure 3-9** shows that the phosphinine ligands (orange dots) detailed in **Figure 3-8** are close in space to the phosphites (red diamonds) and aryl phosphines (blue dots) as would be expected.

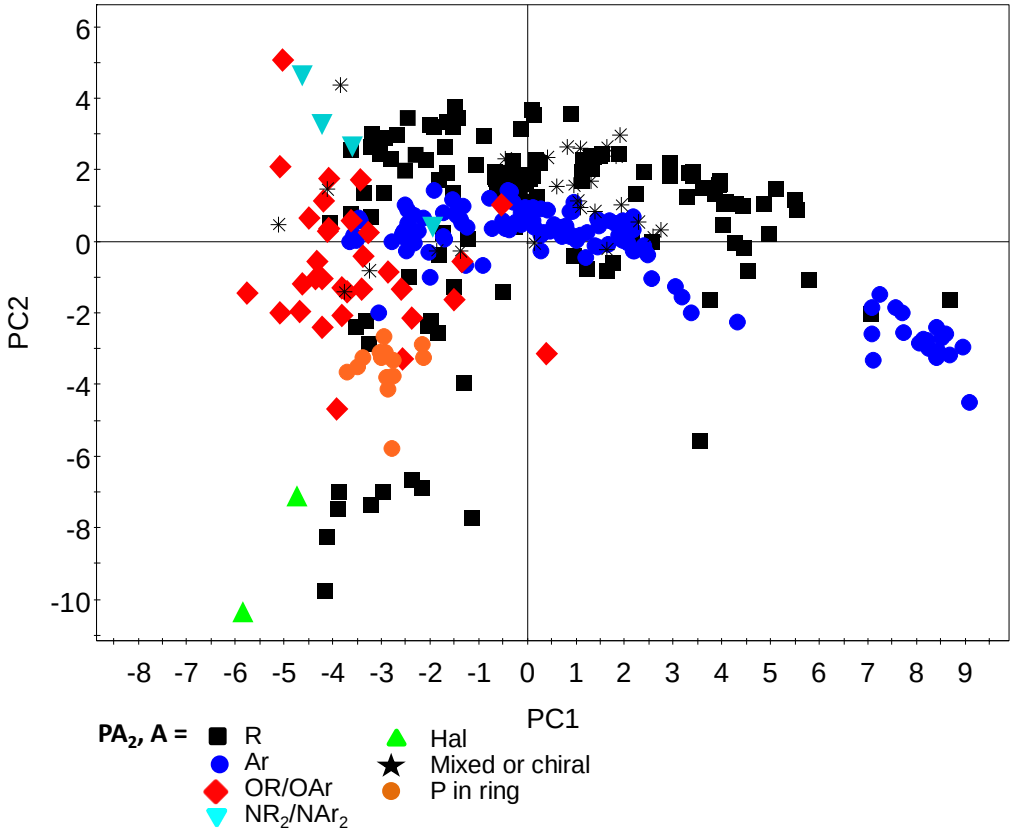

Figure 3-9. Map obtained from the P,P-donor LKB showing the comparison between 324 bidentate phosphorus ligands.[188]

Magnifying the phosphinine region (**Figure 3-10**, with symbols numbered according to the phosphinophosphinine ligands entered into the LKB) indicates that adjusting the substitution patterns on the ligands has a substantial effect on their properties. For example demethylated and desilylated phosphinophosphinine **N4** (2-diphenylphosphinophosphinine) is significantly different in terms of PC2, however, **N9** and **N13** containing the sterically bulky di(*tert*-butyl)phosphine (but with and without a trimethylsilyl substitutent respectively) are close in space to each other but are different along PC1 from the rest of the 2-phosphinophosphinines. The same grouping in the opposite direction along PC1 can also be observed for the dimethylphosphine ligands **N6** and **N10**. In terms of comparison between **2.1** and **2.5** (**N1** and **N2** respectively), there is a significant difference along PC2, however, removal of the methyl substituent on the ring (**N3**) would also have a significant impact, as is shown in

Figure 3-10. Importantly, **2.1** and **2.5** are close in space to PNP ligands **A** (24) and **B** (31) according to PC1, but with well-separated properties according to PC2.

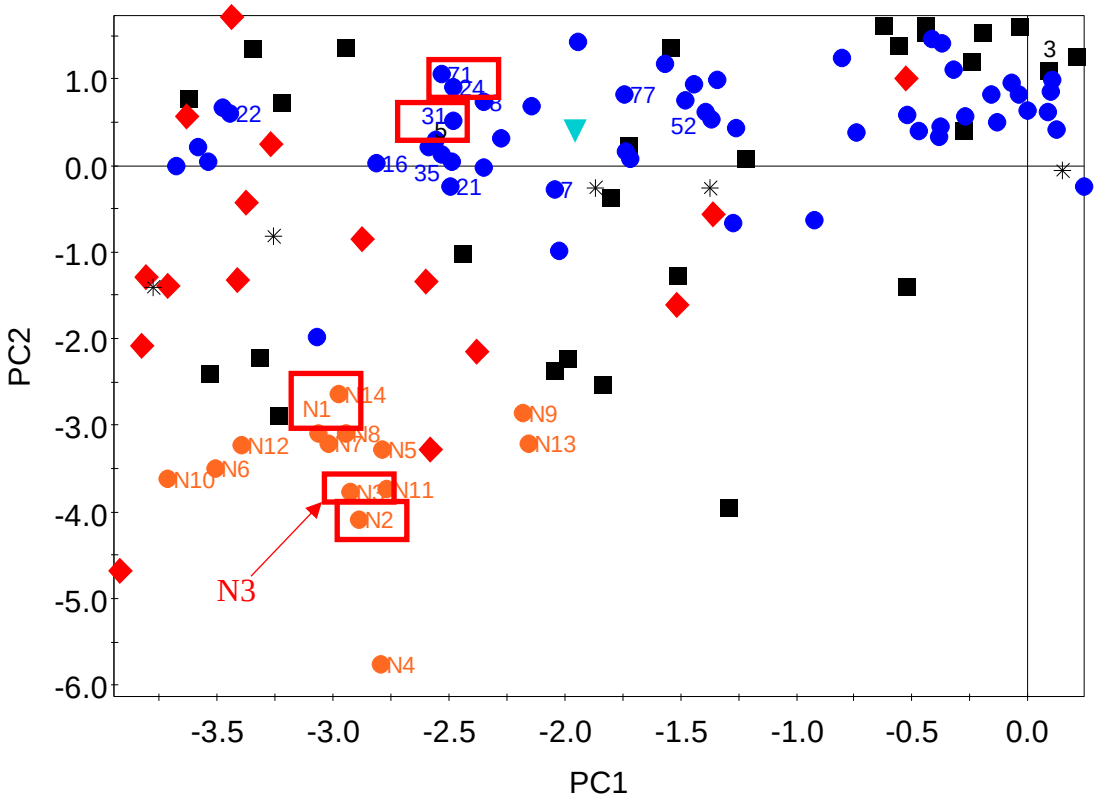

Figure 3-10.[188] Magnification of the phosphinine/phosphite/aryl phosphine region and numbered assignments of structures. **N1** (**2.1**), **N2** (**2.5**), **24** (**A**) and **31** (**B**) are highlighted

Looking at PC3, analysis of **Figure 3-11** shows a similar trend of that of **Figure 3-10**, however **2.1** and **2.5** (**N1** and **N2**) are closer in space to the optimal PNP ligands **A** and **B** (**24** and **31**). As a result, it was anticipated that the two 2-phosphinophosphinines might display some useful activity as ligands in the oligomerisation of ethylene. As the maps show a closer relationship between **2.1**, **2.5** and the less-sterically bulky PNP ligand **B** (**31**), which was expected due to the lack of any steric bulk on the two P-donors of the phosphinophosphinines, it was predicted that they would provide some measure of selectivity towards the production of 1-octene

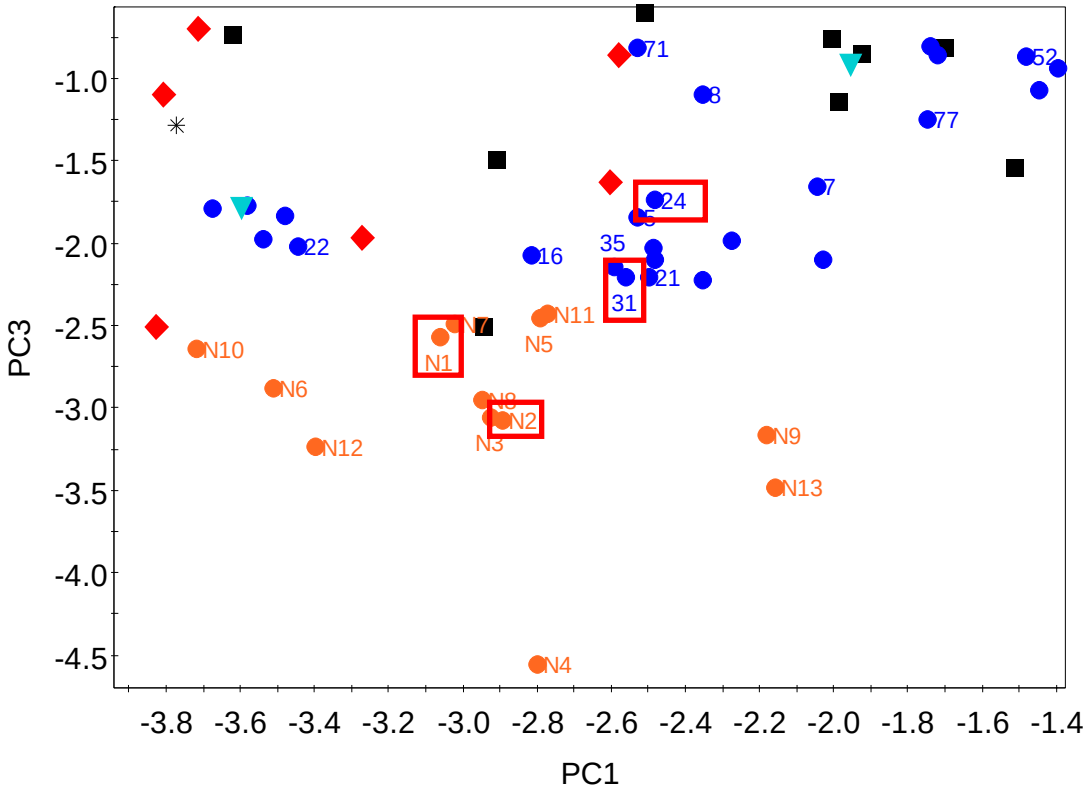

Figure 3-11.[188] Map showing the magnified phosphinine region in a comparison between PC1 and PC3. **N1** (**2.1**), **N2** (**2.5**), **24** (**A**) and **31** (**B**) are highlighted

3.3.3 Catalytic results

Dr David Smith and Dr Martin Hanton (of Sasol Technology U.K at the University of St Andrews) performed all the ethylene oligomerisation reactions using 2-phosphinophosphinines **2.1**, **2.5**, and PNP ligand **B** (for benchmarking) and undertook the subsequent GC data analysis. The majority of reactions (**Scheme 3-3**, **Table 3-7**) were investigated using **2.1** and the results shown for this ligand are averages over four runs, whilst results using **2.5** are an average of two runs.

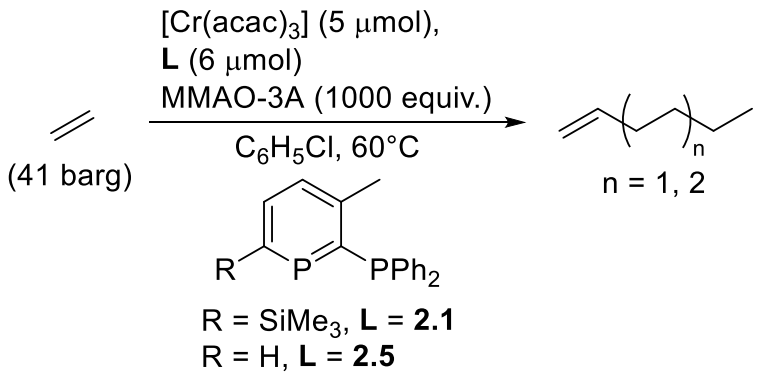

Scheme 3-3.[188] Experimental conditions for the oligomerisation of ethylene to C_6/C_8 LAO

Table 3-7.[188] Results relating to C_6 and C_8 LAO obtained from catalytic runs [a]

Run	Ligand [b]	Activity (g/gCr/h)	Weight % C_6 + C_8 LAO[c]	C_8/C_6 LAO Ratio	C_6 (C_6-LAO Weight%) [c]	C_8 (C_8-LAO Weight%) [c]	Polymer Weight% [d]
1[e]	None	176,671	25.9	0.78	36.5 (39.8)	12.6 (90.6)	98.0
2[f][g]	**B**	2,318,320	86.4	1.58	36.9 (90.6)	53.3 (99.4)	0.98
3[h]	**2.1**	31,200	37.1	2.83	18.4 (52.6)	29.5 (93.0)	15.1
4[h][i]	**2.1**	29,068	40.0	2.74	19.3 (55.4)	31.2 (93.9)	28.3
5[h][j]	**2.1**	55,387	34.2	2.32	18.3 (54.8)	25.9 (92.3)	19.0
6[h]	**2.5**	12,122	53.8	2.84	24.0 (58.6)	42.0 (94.7)	36.5

[a]: C_6 LAO = 1-hexene, C_8-LAO = 1-octene. [b]: 1.2 equiv. ligand per Cr. [c]: Weight % of liquid fraction. [d]: Polyethylene, weight % of total products. [e]: 8.0 minute run. [f]: 16.2 minute run. [g]: 1.25 μmol [$Cr(acac)_3$], **B** = $Ph_2P–N(^iPr)–PPh_2$. [h]: 30 minute run. [i]: Concentrated preactivation in a Schlenk flask. [j]: 2.5 μmol [$Cr(acac)_3$].

In comparison, **2.1** was more active than **2.5**, with activities of 31,200 and 12,122 g/gCr/h (combined liquid and solid fractions) respectively using the optimal reaction conditions. Although the activity of **2.1** was not the highest using these conditions (**Run 3**), a lower weight of polyethylene was obtained as well as a higher selectivity to 1-octene over 1-hexene. In comparison, **2.5** produced a higher weight percentage of the desired LAO in the liquid fraction, whilst maintaining the same ratio of 1-octene to 1-hexene as **2.1**. The biggest factor in governing selectivity to 1-hexene over 1-octene is the introduction of steric bulk,[227, 231] and as such these similar ratios imply that the trimethylsilyl substituent on **2.1** has little steric impact in this reaction. The differences in activity (31,200 versus 12,122 g/gCr/h) between **Run 3** and **6** and the differences in weight % of the polymer fraction (15.1 and 36.5%) could be due to electronic differences between the two ligands, or differences in stability.

To allow for benchmarking of results obtained from the two phosphinophosphinine ligands, the values were compared to those from runs using either no ligand (**Run 1**) or the PNP ligand **B** (**Run 2**). The ligand-free reaction did result in higher activity (176,671 g/gCr/h) and some measure of selectivity for C_6 alkenes over C_8, however, most of the product was polymer (98%) and the combined weight percentage of 1-hexene and 1-octene in the trace liquid fraction was very low (for example, only 39.8% of the C_6 fraction consisted of 1-hexene). The key finding is that without a suitable ligand, the majority (98%) of the ethylene was converted into polyethylene. In comparison, whilst the PNP ligand **B** produced a highly active (2,318,320 g/gCr/h)

catalyst that produced very little polyethylene (0.98%) and a larger weight percentage of the desired LAO, a lower selectivity for 1-octene (1.58 versus 2.83/2.84) was obtained. Whilst **Table 3-7** shows data relevant to the production of C_6 and C_8 alkenes/LAO, the actual product distribution obtained is more complex, because, for example, in **Run 3** to **Run 6** the weight percentage of C_6 and C_8 alkenes consists of between 44.7% (**Run 5**) and 66.0% (**Run 6**) of the total liquid fraction. Analysis of the gas-chromatographic traces[188] revealed that a large weight percentage of the liquid fraction consisted of C_{10-14} and C_{15+} alkenes/alkanes (including LAO, internal alkenes, branched alkenes/alkanes and cyclopentyl alkenes, **Figure 3-12**) as well as a small percentage (**Table 3-8**) of C_6 cyclopentyl alkenes/alkanes and C_4 alkenes. The breakdown of these additional components of the liquid fractions is shown in the **Figure 3-13**, (**Run 3**) and **Figure 3-14** (**Run 6**).

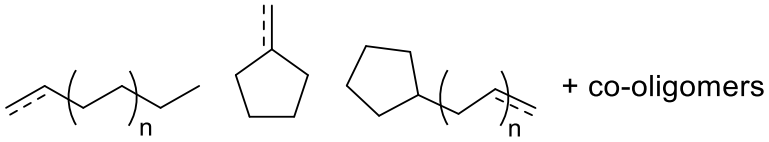

Figure 3-12. Examples of other products observed by GC

Table 3-8.[188] Weight percentages of other fractions[a]

Run	Ligand	C_4 (weight %)[b]	Cyclic C_6 (weight % of C_6)[c]	C_{10-14} (weight %)[d]	C_{15+} (weight %)[d]
1	None	5.5	6.0 (16.5)	26.7	18.8
2	**B**	0.2	3.3 (8.9)	7.4	2.3
3	**2.1**	2.3	6.5 (35.5)	17.5	32.3
4	**2.1**	2.6	6.2 (32.2)	16.6	30.3
5	**2.1**	1.8	6.7 (35.7)	18.2	35.4
6	**2.5**	3.8	5.5 (22.9)	14.2	16.2

[a]: Data is from same runs as **Table 3-7**. [b]: alkenes. [c]: methylcyclopentane and methylenecyclopentane. [d]: LAO, internal alkenes, linear and branched alkanes, cyclopentyl-substituted alkenes and alkanes.

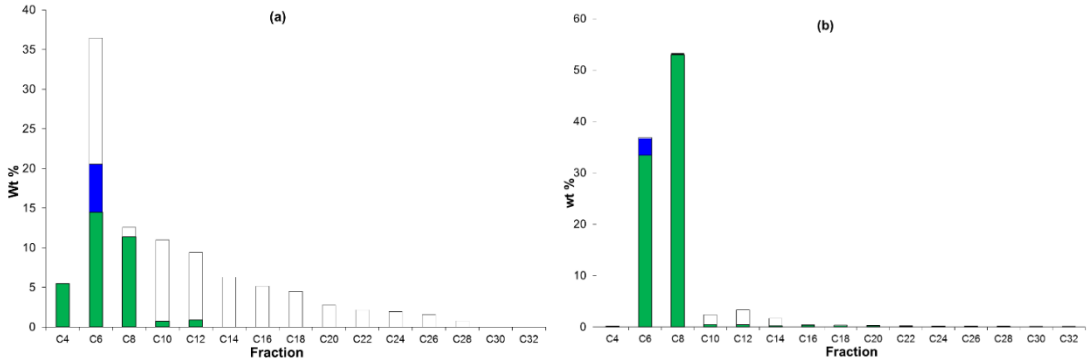

Figure 3-13. Graphs of the components of the liquid fraction for **Run 1** (left) and **Run 2** (right)‡

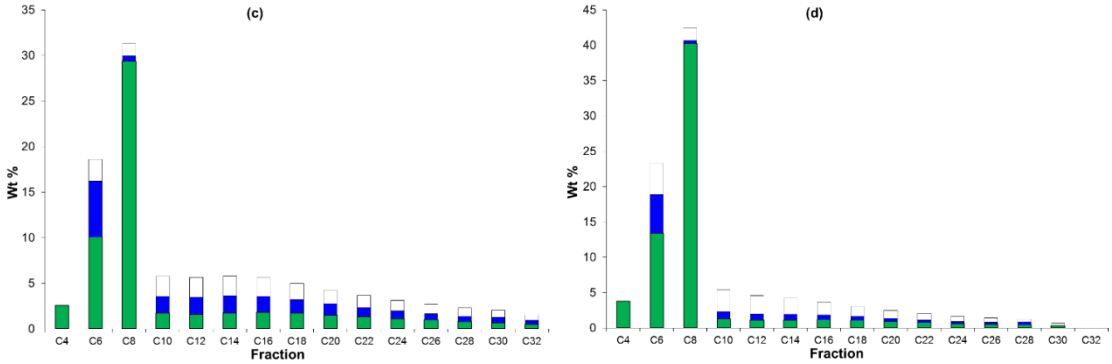

Figure 3-14. Graph of the components of the liquid fraction for **Run 3** (left) and **Run 6** (right)‡

‡: green bars correspond to alkenes, blue bars to cyclopentyl-substituted alkenes plus alkanes, and the white bars to alkanes as well as structural isomers.

Analysis of **Figure 3-13** and **Figure 3-14** allows for further breakdown of the higher molecular-weight components, and it can be seen that for **Run 3**, approximately one third of these consists of cyclopentyl compounds. The presence of these unusual products in **Run 6** (using the desilylated ligand **2.5**) was reduced, although increased formation of alkanes and isomeric materials was observed. The formation of cyclopentyl products in ethylene oligomerisation has been reported previously in the literature when S,S or S,P-donor bidentate ligands[240] and alkoxy/silyloxy-functionalised PNP ligands were used.[241] The mechanism behind their formation[188, 241] is believed to follow the steps in **Scheme 3-4**, where the intermediate chromacycloheptane (**1**) undergoes β-hydride elimination to form a terminal linear alkene and a chromium hydride (**2**). This species then rearranges to form complex (**3**), which can reductively eliminate to form methylcyclopentane, β-hydride eliminate to form methylenecyclopentane or continue chain growth by insertion of another equivalent of ethylene (**4**).

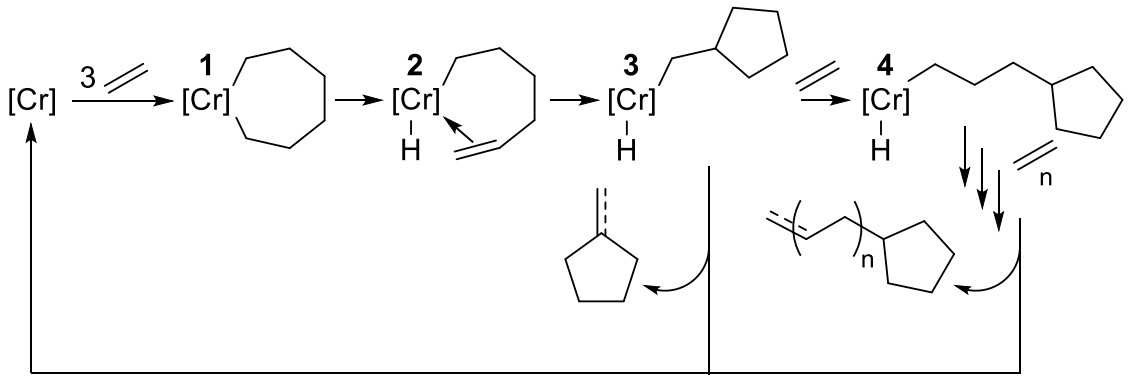

Scheme 3-4.[188, 241] Simplified catalytic cycle showing the formation of alkyl/alkenyl cyclopentanes and 1-hexene

3.4 Conclusions

By reacting the two phosphinophosphinine ligands **2.1** and **2.5** with a series of group 6 tetracarbonyl complexes containing labile diene ligands, five complexes of chromium, molybdenum and tungsten were successfully synthesised. They were isolated as analytically pure, crystalline solids in low to good yields, and their molecular structures were determined by X-ray diffraction, which confirmed that the group 6 series of **2.1** were isostructural, occupying a distorted octahedral geometry. Comparison of the A_1 ν(CO) stretching frequencies by infrared spectroscopy between the three complexes of **2.1** and two complexes of desilylated ligand **2.5** confirmed the validity of results obtained from DFT calculations by Ferro *et. al.*.[165] The recorded spectra indicated that addition of a trimethylsilyl substituent in the 6–position increased the π-accepting ability of the phosphinine, resulting in a higher value for ν(CO). The room-temperature reactivity of desilylated chromium complex **3.4** with water was observed by X-ray crystallography and demonstrated a dinuclear octacarbonyl complex resulting from successive [4+2] cyclisation and P=C double bond hydrolysis. After confirming that ligand **2.1** and chromium complex **3.1** did not react with MMAO, **2.1** and **2.5** were investigated in the chromium-catalysed oligomerisation of ethylene. The resulting (*in-situ* generated) catalysts gave good catalytic activity, with a preference for the formation of 1–octene over 1–hexene (formed in a ratio of 2.8:1, respectively, for both ligands) as well as a range of higher molecular weight oligomers, including unusual cyclopentyl–substituted products.

4 - Chemistry of ruthenium phosphinophosphinine complexes

4.1 Introduction

In the context of modern chemistry, ruthenium catalysts have an important role. It is the cheapest of the platinum group metals, and has also found great use in reactions such as olefin metathesis,[242, 243] C-H activation,[244] hydrogenation,[245] and transfer hydrogenation.[246] Whilst a number of λ^3 phosphinine complexes of ruthenium are known,[70, 75, 91-93, 99] none of these have been investigated in catalytic reactions. A ruthenium complex containing an anionic phosphacyclohexadienyl ligand was evaluated in the transfer-hydrogenation of ketones, but was found to require two and a half days at 80°C to reach acceptable levels of conversion.[247] This chapter has been published as a communication,[177] and a full paper is also in preparation.

4.2 Synthesis of precatalysts

4.2.1 An octahedral bis(phosphinophosphinine) complex

The initial starting point in investigating the ruthenium coordination chemistry of **2.1** was the preparation of *cis*-[Ru(**2.1**)$_2$(Cl)$_2$] (**4.1**, **Scheme 4-1**) by the reaction of the proligand with 0.5 equivalents of [Ru(dmso)$_4$(Cl)$_2$].

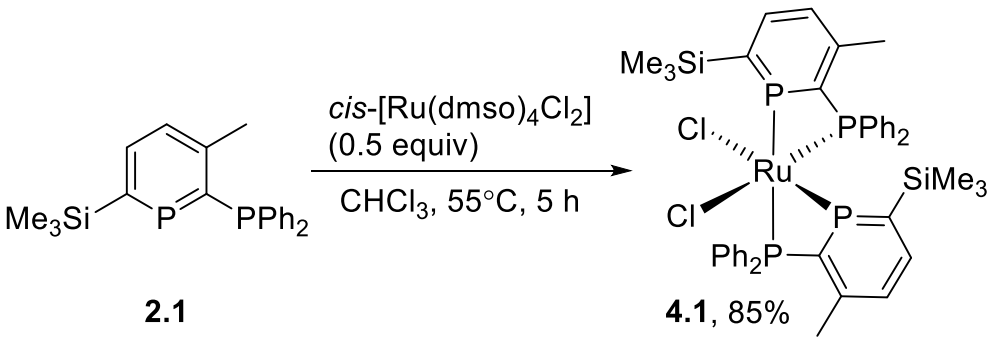

Scheme 4-1. Synthesis of octahedral complex **4.1**

Within minutes of heating the reaction mixture at 55°C, a colour change from the bright yellow of the ruthenium precursor to a deep red was observed. By following the reaction using $^{31}P\{^1H\}$ NMR spectroscopy, four new multiplets were observed (δ = 235.2 (m), 229.9 (ddd), 2.34 (m), -2.43 ppm (ddd)), and after working up the reaction to remove the liberated dmso, **4.1** was isolated as an air-sensitive bright orange powder in 85% yield. The presence of four distinct multiplets with a large, mutual *trans*-coupling ($^2J_{P\text{-}P}$ = 425 Hz) between one phosphinine and one phosphine suggested the selective formation of the C_1 isomer **4.1**, and this was confirmed by X-ray diffraction analysis of

single crystals grown by slow diffusion of petroleum ether into a C_6D_6 solution of **4.1** (**Figure 4-1**).

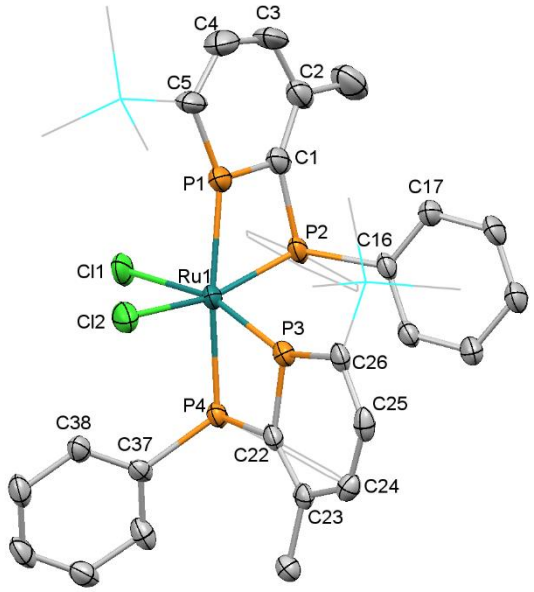

Figure 4-1. Molecular structure of **4.1** (thermal ellipsoids at 50% probability). All H-atoms have been omitted, and the trimethylsilyl groups as well as two phenyl rings have been displayed in wireframe for clarity.

Table 4-1. Key bond-lengths and angles for **4.1**

Bond Lengths (Å)		**Bond Angles (°)**	
P(1)-C(1)	1.710(7)	P(1)-C(1)-C(2)	125.2(5)
C(1)-C(2)	1.398(9)	C(1)-C(2)-C(3)	117.1(7)
C(2)-C(3)	1.384(11)	C(2)-C(3)-C(4)	125.9(8)
C(3)-C(4)	1.409(11)	C(3)-C(4)-C(5)	128.6(8)
C(4)-C(5)	1.405(8)	C(4)-C(5)-P(1)	115.4(5)
C(5)-P(1)	1.714(7)	C(5)-P(1)-C(1)	107.8(3)
C(1)-P(2)	1.826(7)	P(1)-C(1)-P(2)	97.7(3)
P(1)-Ru(1)	2.310(2)	P(3)-C(22)-C(23)	125.6(5)
P(2)-Ru(1)	2.342(2)	C(22)-C(23)-C(24)	117.9(5)
P(3)-C(22)	1.732(6)	C(23)-C(24)-C(25)	125.4(6)
C(22)-C(23)	1.391(8)	C(24)-C(25)-C(26)	128.9(6)
C(23)-C(24)	1.387(8)	C(25)-C(26)-P(3)	115.3(5)
C(24)-C(25)	1.397(8)	C(26)-P(3)-C(22)	107.0(3)
C(25)-C(26)	1.413(8)	P(3)-C(22)-P(4)	96.3(3)
C(26)-P(3)	1.718(8)	P(1)-Ru(1)-P(2)	69.93(7)
C(22)-P(4)	1.836(6)	P(3)-Ru(1)-P(4)	70.30(6)
P(3)-Ru(1)	2.241(2)		
P(4)-Ru(1)	2.369(2)		
Ru(1)-Cl(1)	2.430(2)		
Ru(1)-Cl(2)	2.477(2)		

The structure of **4.1** shows two bidentate phosphinophosphinine ligands coordinating to an octahedral ruthenium centre, which is significantly distorted due to the narrow bite-angles (P(1)-Ru(1)-P(2) = 69.93(7)°, P(3)-Ru(1)-P(4) = 70.30(6)°) enforced by the four-membered chelates. *cis*-[Ru(vdpp)$_2$(Cl)$_2$] (P(1)-Ru(1)-P(2) = 73.13(2)°, vdpp = 1,1-bis(diphenylphosphino)ethylene)[203] in comparison has a wider bite angle, emphasising the acute nature of the bite angles in this phosphinophosphinine. It is noteworthy that the phosphinine-ruthenium bond distances are shorter than the phosphine-ruthenium bond distances in both ligands (P(1)-Ru(1) = 2.310(2)Å, P(2)-Ru(1) = 2.342(2)Å) despite the fact that phosphinines are regarded as weaker donors than phosphines.[3] It is likely that this is an effect of the sp^2 hybridisation of the phosphinine lone pair resulting in shorter M-P bond lengths compared to conventional sp^3-hybridised phosphines.

4.2.2 Synthesis of half-sandwich phosphinophosphinine complexes

A common motif observed in many ruthenium catalysts reported in the literature is the inclusion of an η^6 *p*-cymene ligand,[248] with many such complexes derived from the addition of ligands to [{Ru(*p*-cymene)(μ-Cl)(Cl)}$_2$]. The reaction of **2.1** with this precursor was therefore attempted (**Scheme 4-2**). After heating the reaction mixture for five minutes, the reaction was analysed by $^{31}P\{^1H\}$ NMR spectroscopy and it was observed that all **2.1** had been consumed and that two products had been formed, with the characteristic signals of **4.1** allowing for it to be readily assigned. It was initially expected that the second product **4.2** (δ = 231.4 (d), 21.7 (d) ppm) would possess the desired half-sandwich geometry. Layering the reaction mixture with petroleum ether resulted in the production of two sets of crystals, the dark red crystals of **4.2** were manually separated from the crop of yellow crystals of **4.1** and analysed by X-ray diffraction. This revealed a dinuclear structure (**Figure 4-2**) resulting from the displacement of one *p*-cymene ligand instead of the separation of the dimer by breaking the two dative Cl→Ru bonds.

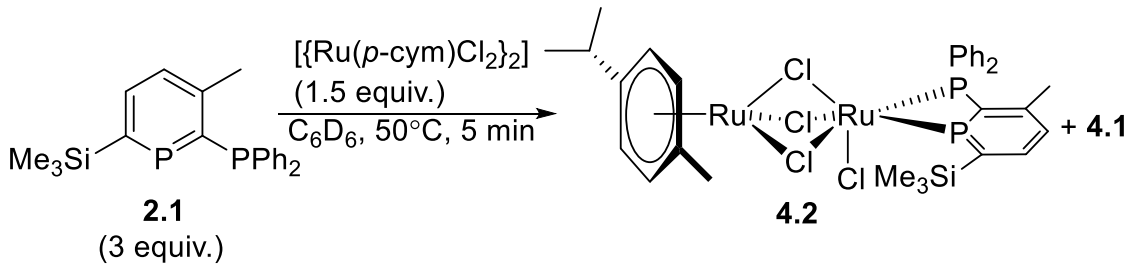

Scheme 4-2. Reaction of **2.1** with [{Ru(*p*-cymeme)(μ-Cl)(Cl)}$_2$]

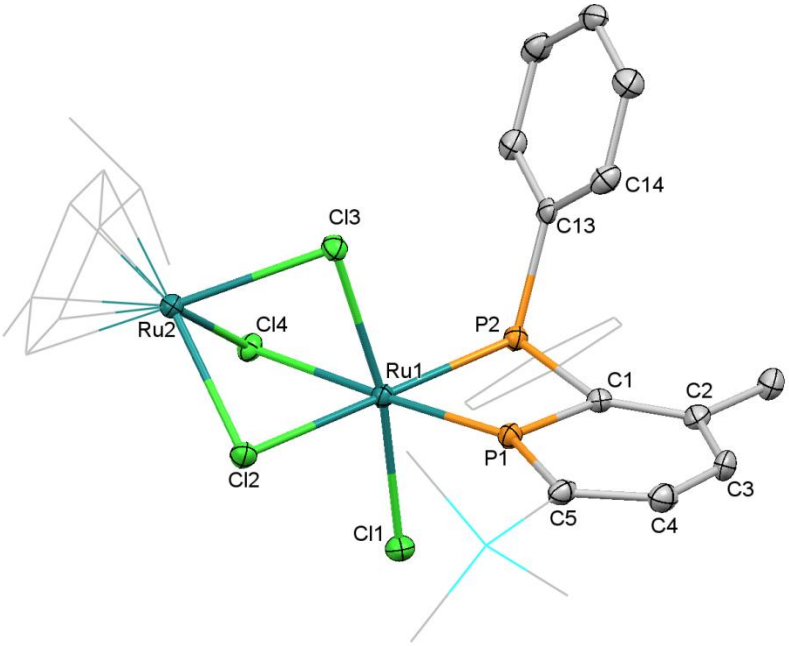

Figure 4-2. Molecular structure of **4.2** (thermal ellipsoids at 50% probability). All H-atoms have been omitted, and the trimethylsilyl group, the *p*-cymene ligand as well as one phenyl ring have been displayed in wireframe for clarity.

Table 4-2. Key bond lengths and angles for **4.2**

Bond Lengths (Å)		**Bond Angles (°)**	
P(1)-C(1)	1.717(3)	P(1)-C(1)-C(2)	125.1(2)
C(1)-C(2)	1.396(4)	C(1)-C(2)-C(3)	117.8(3)
C(2)-C(3)	1.405(4)	C(2)-C(3)-C(4)	125.2(3)
C(3)-C(4)	1.397(4)	C(3)-C(4)-C(5)	128.8(3)
C(4)-C(5)	1.409(4)	C(4)-C(5)-P(1)	114.9(2)
C(5)-P(1)	1.713(2)	C(5)-P(1)-C(1)	108.2(1)
C(1)-P(2)	1.837(2)	P(1)-C(1)-P(2)	93.1(1)
P(1)-Ru(1)	2.184(1)	P(1)-Ru(1)-P(2)	70.56(3)
P(2)-Ru(1)	2.283(1)	Cl(1)-Ru(1)-Cl(3)	169.60(3)
Ru(1)-Cl(1)	2.395(1)		
Ru(1)-Cl(2)	2.495(1)		
Ru(1)-Cl(3)	2.428(1)		
Ru(1)-Cl(4)	2.484(1)		
Ru(2)-Cl(2)	2.422(1)		
Ru(2)-Cl(3)	2.458(1)		
Ru(2)-Cl(4)	2.447(1)		

The structure of **4.2** showed one bidentate phosphinophosphinine ligand coordinating to a distorted octahedral Ru(II) centre with four chloride ligands, three of which are bridging to a second Ru(II) centre with an η^6 p-cymene ligand. Whilst the bond lengths in **4.2** changed very little from those in **2.1**, there are some significant changes in the bond angles around the ring such as the C(4)-C(5)-P(1) angle (114.9(1)° versus 121.0(2)° for **2.1**) and C(5)-P(1)-C(1) (108.2(1)° versus 103.6(1)° in **2.1**) angle. The

P(1)-C(1)-P(2) angle is also more acute than in **4.1** (93.1(1)° versus 97.7(3)° in **2.1**), although the P(1)-Ru(1)-P(2) bite-angle has not changed significantly.

Attempts were made to optimise the reaction conditions in order to favour the exclusive formation of **4.2**, however, varying the equivalents of **2.1** (including a 1:1 reaction) and the reaction temperature did not result in anything other than a mixture of two products. Therefore, insufficient material could be separated from the crystals of **4.1** to allow for complete characterisation of **4.2** or for it to be utilised in catalytic testing. Running a 4:1 reaction of **2.1**:[{Ru(*p*-cymene)(μ-Cl)(Cl)}$_2$] did result in the formation of **4.1** on an NMR scale, however, when scaled up to a practical scale for isolation of the product, the reaction was found to be inconsistent and did not always cleanly generate **4.1**.

In order to circumvent the issue of the lability of the *p*-cymene ligand, the reaction was repeated with the hexamethylbenzene dimer [{Ru(C_6Me_6)(μ-Cl)Cl}$_2$] using salts of non-coordinating anions in order to avoid the formation of an anionic phosphacyclohexadienyl ligand. Using $AgBF_4$, $AgSbF_6$ and $NaB(Ar^F)_4$ (Ar^F = 3,5-bis(trifluoromethyl)benzene) generated multiple products, however, NH_4PF_6 cleanly produced a single product by $^{31}P\{^1H\}$ NMR spectroscopy (**Figure 4-3**), although the observed shifts (δ = 11.6 (d), 8.8 (d) ppm) indicated that the phosphinine ligand was no longer aromatic.

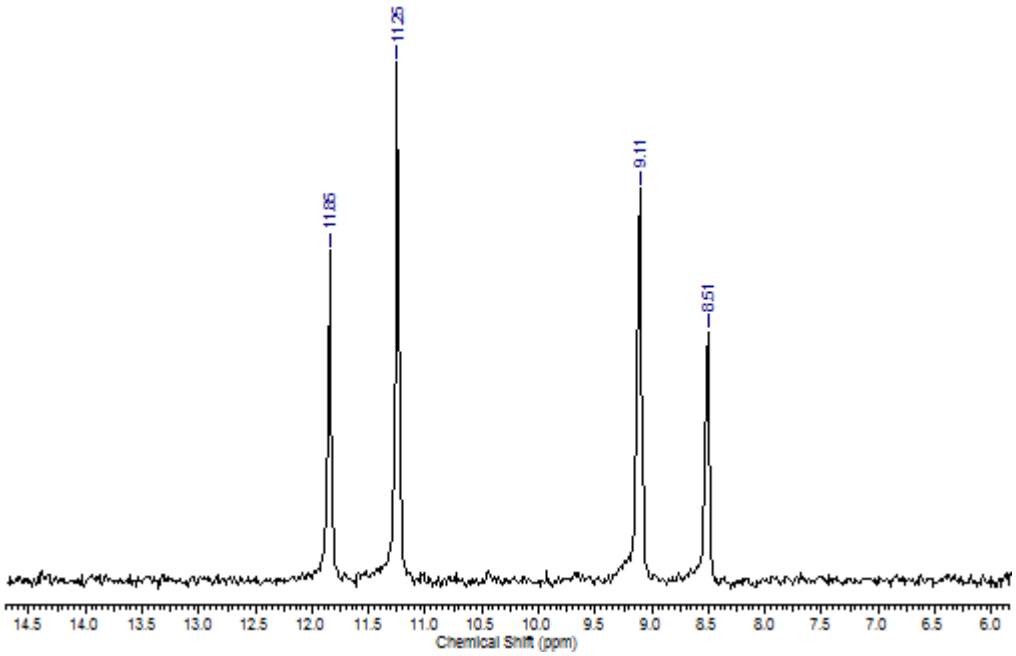

Figure 4-3. $^{31}P\{^1H\}$ NMR spectrum from the reaction of **2.1** with [{Ru(C_6Me_6)Cl_2}$_2$] and NH_4PF_6 ($[PF_6]^-$ resonance not shown)

Single crystals of the product were grown by slow diffusion of petroleum ether into a CH_2Cl_2 solution of the product, and the resulting orange needles were analysed by X-ray diffraction, revealing the product to be **4.3** (**Scheme 4-3**, **Figure 4-4**).

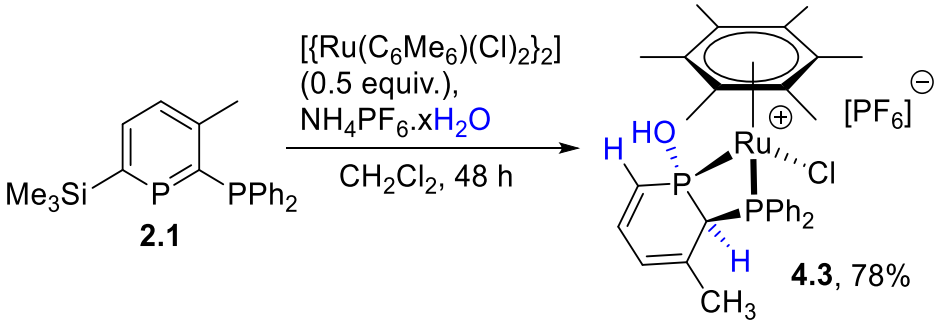

Scheme 4-3. Synthesis of complex **4.3**

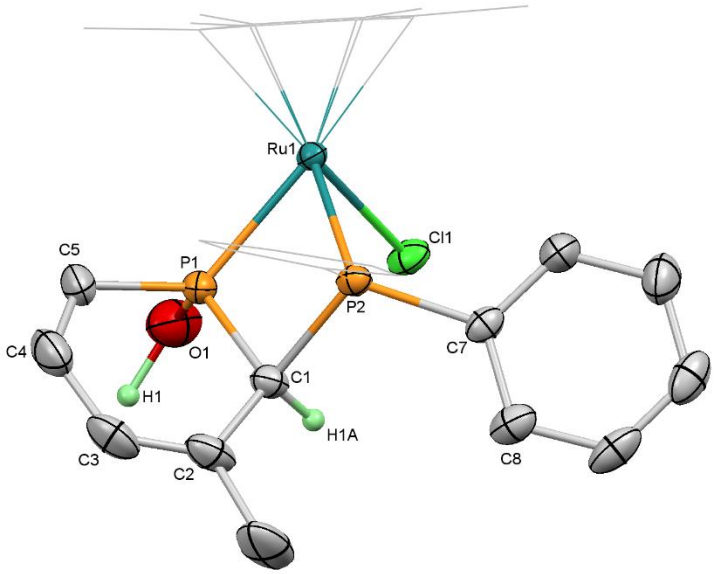

Figure 4-4. Molecular structure of **4.3** (thermal ellipsoids at 50% probability). The $[PF_6]^-$ anion and all H-atoms aside from H(1) and H(1A) have been omitted. The C_6Me_6 ligand as well as one phenyl ring have been displayed in wireframe for clarity. The crystallographic data obtained for **4.3** contains two molecules in the asymmetric unit (Z´ = 2), however only one is displayed here and in the table below for clarity

Table 4-3. Key bond lengths and angles for **4.3**

Bond Lengths (Å)		Bond Angles (°)	
P(1)-C(1)	1.861(3)	P(1)-C(1)-C(2)	118.9(2)
C(1)-C(2)	1.504(5)	C(1)-C(2)-C(3)	121.4(3)
C(2)-C(3)	1.328(6)	C(2)-C(3)-C(4)	126.2(4)
C(3)-C(4)	1.452(6)	C(3)-C(4)-C(5)	126.6(4)
C(4)-C(5)	1.336(5)	C(4)-C(5)-P(1)	121.7(3)
C(5)-P(1)	1.776(4)	C(5)-P(1)-C(1)	102.5(2)
C(1)-P(2)	1.880(3)	P(1)-C(1)-P(2)	92.2(1)
P(1)-O(1)	1.668(3)	P(1)-Ru(1)-P(2)	71.53(3)
P(1)-Ru(1)	2.286(1)		
P(2)-Ru(1)	2.326(1)		
Ru(1)-Cl(1)	2.401(1)		

Analysis of the structure revealed that water had added across the P(1)-C(1) double bond, forming a rare example of a hydroxyl-substituted P(III) centre. As ammonium salts are hygroscopic, it is likely that the NH_4PF_6 was the source of the water. It was also observed that the trimethylsilyl substituent had been cleaved; the mechanism behind this transformation is not known but could involve F^- dissociation from $[PF_6]^-$ or the possible involvement of OH^-. The structure shows P(1) now in a distorted tetrahedral geometry (C(3)-P(1)-Ru(1) = 129.96(8)°). As expected, the loss of aromaticity in the phosphacyclohexadiene ligand has a notable effect on the bond lengths and angles around the ring. As a C-C single bond, the C(1)-C(2) bond has lengthened significantly (1.504(5) Å) whilst the C(2)-C(3) and C(4)-C(5) alkene bonds (1.328(6) and 1.336(5) Å respectively) are shorter than they were in **2.1** (1.404(4) and 1.396(4) Å respectively). Whilst both the P(1)-C(1) and P(1)-C(5) bonds have lengthened (1.861(3) and 1.776(4) Å respectively compared to 1.754(3) and 1.749(3) respectively Å in **2.1**), only the P(1)-C(1), the reasons behind the difference in bond lengths between these P-C bonds is not known. The cleavage of $SiMe_3$ groups in the 6-position of phosphinines well established, with HCl in ether shown to cleanly desilylate several phosphinines,[187] including the free proligand **2.1** (see ligand chapter).

In order to prepare a half-sandwich complex with an aromatic phosphinine ligand, **2.1** was reacted with 0.25 equivalents of the chloro(pentamethylcyclopentadienyl)ruthenium (II) tetramer, $[\{Ru(Cp^*)(\mu_3\text{-}Cl)\}_4]$. The reaction proceeded rapidly in THF, with a colour change to deep red observed within seconds. The resulting complex proved to be very soluble, and exchange of the solvent for petroleum ether did not yield the desired precipitate. However, upon concentrating and storing the solution at 0°C for one hour,

the product was collected as an orange solid in 70% yield ($^{31}P\{^{1}H\}$ δ = 240.1 (d) and 18.2 ppm (d), **Figure 4-5**).

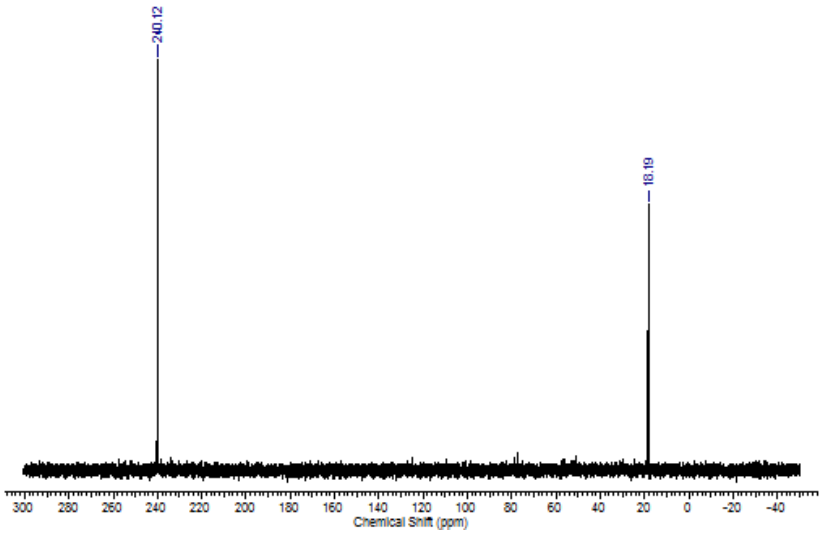

Figure 4-5. $^{31}P\{^{1}H\}$ NMR spectrum of **4.4**

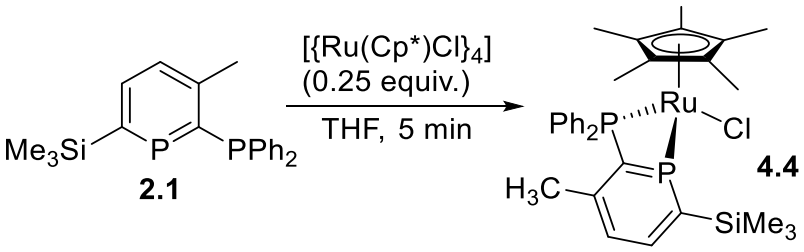

Scheme 4-4. Synthesis of **4.4**

The structure of the complex was confirmed by multinuclear ($^{1}H/^{13}C\{^{1}H\}/^{31}P\{^{1}H\}/^{29}Si\{^{1}H\}$) NMR spectroscopy (**Scheme 4-4**) and high-resolution mass spectrometry. Due to the high solubility of **4.4** single crystals were not obtained, even when poor solvents such as hexamethyldisiloxane were used; either the complex would remain in solution or an orange powder would be isolated. However, exposure of the solution to trace quantities of atmospheric water vapour allowed the crystallisation of small crystals upon storing a solution at 5°C for a period of several weeks. X-ray analysis proved that, similarly to the synthesis of **4.3**, **4.4** had reacted with water (**Scheme 4-5**, **Figure 4-6**), although this time the trimethylsilyl group had not been cleaved. As a result, **4.5** was obtained in a 12% yield,($^{31}P\{^{1}H\}$ δ = 78.3 (d), 18.0 (d) ppm). The complex was also characterised by $^{1}H/^{13}C\{^{1}H\}/^{29}Si\{^{1}H\}$ NMR spectroscopy, high-resolution mass spectrometry and CHN elemental analysis.

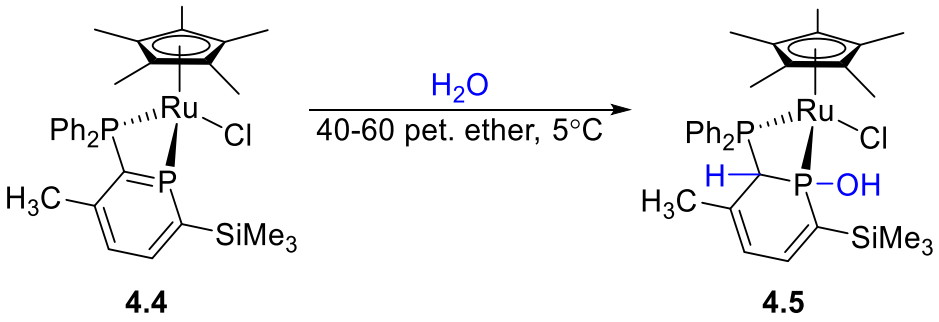

Scheme 4-5. Hydrolysis of **4.4**

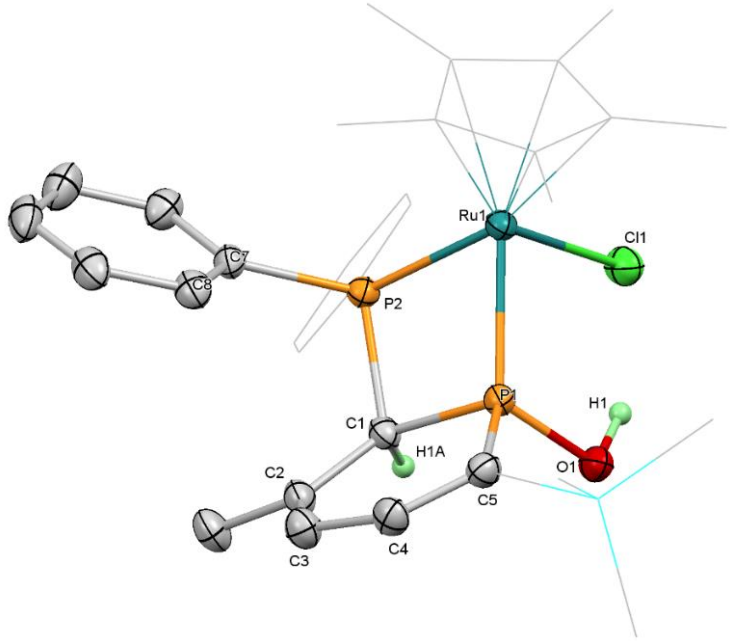

Figure 4-6. Molecular structure of **4.5** (thermal ellipsoids at 50% probability). All H-atoms aside from H(1) and H(1A) have been omitted. The Cp* ligand, the trimethylsilyl group and one phenyl ring have been displayed in wireframe for clarity

Table 4-4. Key bond lengths and angles for **4.5**

Bond Lengths (Å)		**Bond Angles (°)**	
P(1)-C(1)	1.860(5)	P(1)-C(1)-C(2)	118.5(3)
C(1)-C(2)	1.505(6)	C(1)-C(2)-C(3)	121.8(4)
C(2)-C(3)	1.345(6)	C(2)-C(3)-C(4)	126.3(4)
C(3)-C(4)	1.463(7)	C(3)-C(4)-C(5)	126.6(4)
C(4)-C(5)	1.359(6)	C(4)-C(5)-P(1)	127.7(4)
C(5)-P(1)	1.783(4)	C(5)-P(1)-C(1)	105.7(2)
C(1)-P(2)	1.883(4)	P(1)-C(1)-P(2)	91.1(2)
P(1)-O(1)	1.628(3)	P(1)-Ru(1)-P(2)	71.84(3)
P(1)-Ru(1)	2.280(1)		
P(2)-Ru(1)	2.276(1)		
Ru(1)-Cl(1)	2.449(1)		

As in **4.3**, the structure of **4.5** shows that P(1) occupies a distorted tetrahedral geometry ((C(3)-P(1)-Ru(1) = 124.59(9)°) and the –OH and –H substituents arising from reaction with water are oriented *syn* to each other. In terms of bond lengths and angles, **4.3** and **4.5** are very similar, as is expected due to their similar structures. There are few substantial changes in the bond lengths, although the P(2)-Ru(1) bond length has decreased slightly (2.276(1) Å compared to 2.326(1) Å in **4.3**). This was unexpected considering that the P(1)-Ru(1) bond lengths (2.280(1) Å compared to 2.286(1) Å for **4.3**) are identical within error despite the anticipated different donor properties of the phosphacyclohexadienyl lacking a $SiMe_3$ substituent in **4.3**.

4.3 Transfer Hydrogenation Catalysis

The reduction of carbonyl compounds is an industrially important reaction for the large-scale production of alcohols,[249] and many well-established reduction methods are known. This includes hydroalumination ($LiAlH_4$, $Al(i\text{-}Bu)_2H$ and others),[250] hydrogenation (with both homogeneous and heterogeneous catalysts)[251] and hydroboration.[252, 253] However, transfer hydrogenation has become increasingly popular, with catalysts based on ruthenium proving to be highly active.[248] This is advantageous because ruthenium is cheapest of the platinum group metals.[254] Using conditions (1 mol% catalyst, 10 mol% KO^{t}Bu in isopropanol at 82°C for one hour) reported by Willans and co-workers,[255] the prepared ruthenium phosphinine complexes were tested in the transfer hydrogenation of acetophenone, a common model substrate (**Scheme 4-6**). **4.1**, **4.3**, **4.4** and **4.5** were all tested but only the octahedral complex **4.1** acted as a precatalyst for this reaction (**Table 4-5**), with the half-sandwich complexes producing no 1-phenylethanol (**B**). For comparison, the classic small bite angle diphosphine ligand dppm was also examined by using *cis*-$[Ru(dppm)Cl_2]$, however, this also proved ineffective using the initial conditions.

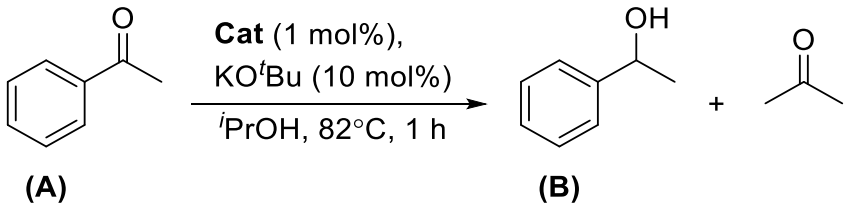

Scheme 4-6. Transfer hydrogenation of acetophenone

Table 4-5. Yields obtained from catalyst screen

Catalyst	Yield (%)[a]
4.1	89%
4.3	<1%
4.4	0
4.5	0
[Ru(dppm)$_2$Cl$_2$]	0

[a]: Yield measured against 1,3,5-trimethoxybenzene internal standard by ^{1}H NMR spectroscopy.

Whilst complete consumption of acetophenone was not observed for **4.1**, the obtained yield compared favourably against catalysts reported in the literature, with many requiring well over one hour to achieve an acceptable yield.[177] In order to further evaluate **4.1** to catalyse the transfer hydrogenation of acetophenone, the catalyst loading was lowered to 0.1 mol% and the amount of base reduced to 0.5 mol%. No reduction in yield was observed (95% in one hour), and in fact it was noticed that the reaction proceeded quickly in the first half hour and then slowed down, with a yield of 90% achieved in thirty minutes. This reduction in reaction rate is due to the formation of acetone as a side-product because the reaction is an equilibrium. A comparative yield (94%) was also obtained when the reaction was repeated at 20°C. In comparison to previously reported Ru catalysts for the transfer hydrogenation of acetophenones (**Figure 4-7**), and taking in to account the inactivity of *cis*-[Ru(dppm)$_2$Cl$_2$], these results points to the presence of a phosphinine donor in the precatalyst as being key to the high reactivity of **4.1**.

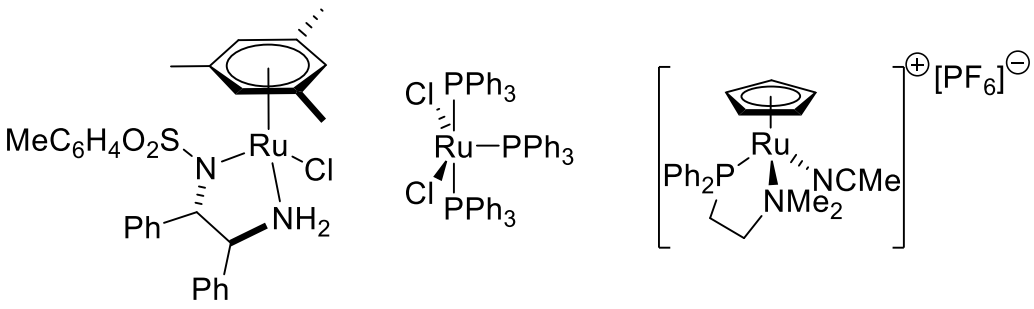

Figure 4-7. Previously reported Ru catalysts for the transfer hydrogenation of acetophenone[256-258]

To investigate this reaction further, a set of substituted acetophenones were reduced using the optimised conditions (**Scheme 4-7**, **Table 4-6**). It was noted that as well as acetophenone, electron-poor ketones (**Runs 2 & 3**) produced high yields of their respective 1-phenylethanol derivative, whereas electron-rich ketones (**Runs 6 – 11**) required heating to obtain the best possible yields. The results obtained for 4′-nitroacetophenone (**Runs 4** & **5**) are anomalous, as whilst it is an electron-poor ketone, it is also insoluble in ^{i}PrOH at 20°C and remains poorly soluble at 82°C. All the results in **Table 4-6** were obtained after one hour, unless indicated otherwise. No increase in yield was obtained if the reaction was left to proceed for any longer.

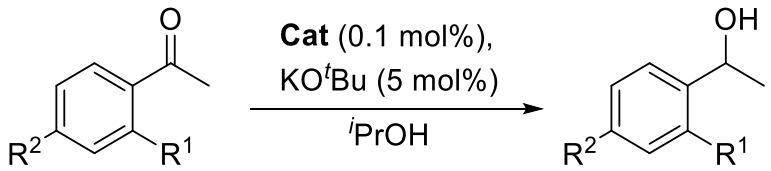

Scheme 4-7. Transfer hydrogenation of acetophenones using optimised conditions

Table 4-6. Results from transfer hydrogenation substrate scope

Run	R^1	R^2	Time (h)	Temp (°C)	Yield (%)[a]
1	H	H	1	20	94
2	H	Br	1	20	97
3	H	F	1	20	96
4	H	NO_2	24	20	5
5			1	82	72
6	H	Me	1	20	87
7			1	82	98
8	H	OMe	1	20	48
9			1	82	79
10	OMe	H	1	20	5
11			1	82	>99

[a]: Yield measured against 1,3,5-trimethoxybenzene internal standard by ^{1}H NMR spectroscopy.

The most notable difference between a reaction run at 20°C and at 82°C in **Table 4-6** is between runs **10** and **11**, with a ~99% yield observed upon heating the reaction compared to 5% at 20°C. It has been reported in the literature[259] that transfer-hydrogenation of ketones with a Lewis-basic β-substituent forms a more stable product due to hydrogen-bonding between the hydroxyl group of the product and the Lewis-basic substituent (**Figure 4-8**). The increased stability of the product results in the backwards reaction, re-oxidation to the ketone, being strongly disfavoured and drives

the equilibrium forward to the desired alcohol.[259] As 2′-methoxyacetophenone is a highly electron-rich substrate, the reaction did not proceed at 20°C, however, the reaction was kinetically favourable at higher temperature.

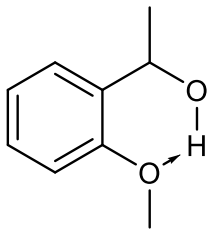

Figure 4-8. Hydrogen bonding in 1-(2-methoxyphenyl)ethanol

The activation of various precatalysts in transfer hydrogenation, as well as the active catalytic cycle, has been reported to proceed *via* multiple different mechanisms, and indeed this is a highly contested area of research.[260, 261] However, the common *inner sphere* mechanism is known to involve the formation of a metal hydride species. As these hydridic signals are observed in a distinct region, commonly below 0 ppm, the synthesis of the dihydride intermediate [Ru(**2.1**)$_2$(H)$_2$] (**4.6**) was investigated. Common reagents used to form metal hydride species did not react with **4.1** to form any appreciable amount of **4.6** ($LiAlH_4$ or $LiBEt_3H$) or formed multiple products ($NaBH_4$ in MeOH). As such, the more powerful reducing agent $NaBEt_3H$ was used (**Scheme 4-8**). Whilst four new multiplets were observed by $^{31}P\{^1H\}$ NMR spectroscopy, the spectrum also showed that the reaction did not proceed completely selectively to **4.6** (**Figure 4-9**). However, the ^1H NMR spectrum (**Figure 4-10**) revealed two ^1H multiplets (δ = -6.65, -7.15 ppm) that confirmed the likely formation of the desired product. Unfortunately, **4.6** proved to be highly soluble and could not be crystallised or precipitated out of common solvent systems, and was also unstable in the solid state, with rapid decomposition observed by a colour change from red to brown once the solvent had been removed. As such, further attempts at isolation were not fruitful, so far. Attempts were then made to observe **4.6** using ^1H and $^{31}P\{^1H\}$ NMR spectroscopy by reaction of **4.1** with varying equivalents of KO^tBu or NaOMe in isopropanol, however signals matching those in **Figure 4-9** and **Figure 4-10** were not observed amongst the multiple products present in solution.

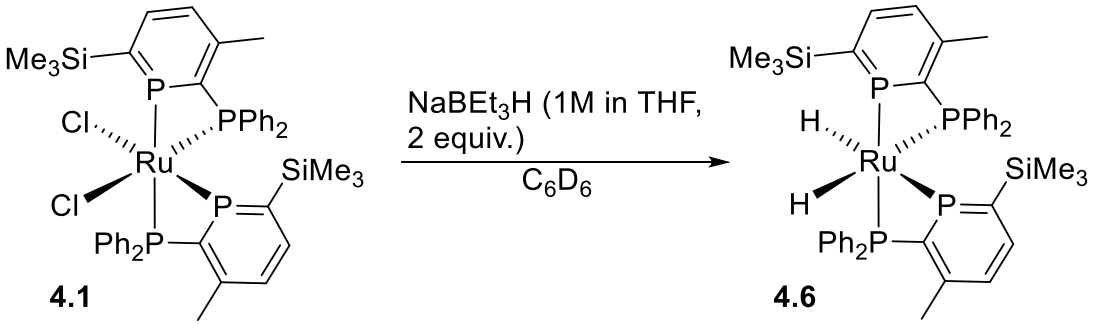

Scheme 4-8. NMR-scale synthesis of **4.6**

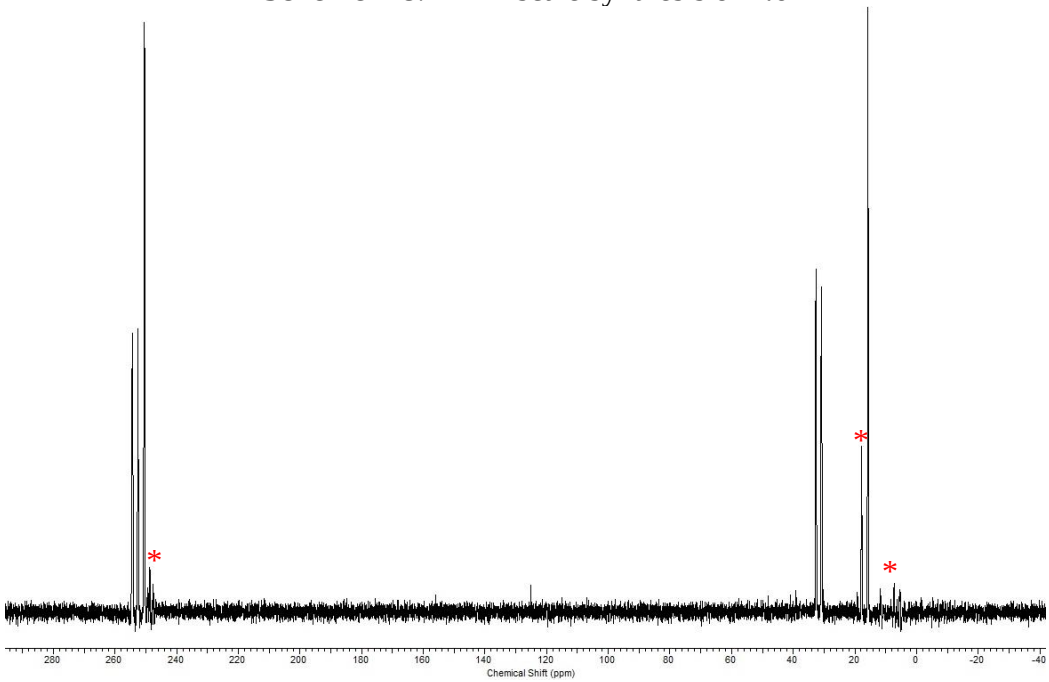

Figure 4-9. $^{31}P\{^{1}H\}$ NMR spectrum of crude **4.6** (* = impurities)

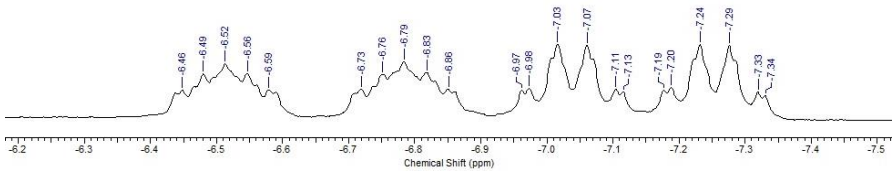

Figure 4-10. Ru-H signals in the ^{1}H NMR spectrum of **4.6**

As it has been indicated that $[Ru(PPh_3)_3(Cl)_2]$ is not the active catalyst for transfer hydrogenation, but that it is in fact reduced to Ru nanoparticles *in-situ*,[262] two common tests for nanoparticle catalysts were investigated. The first involved addition of increasing equivalents of 1,10-phenanthroline to the reaction mixture at the start, as this will bind strongly to the surface of nanoparticles, hindering any catalytic activity. Results using 0.025 mol% and 0.1 mol% phenanthroline resulted in an increased initial reaction rate (**Figure 4-11**), potentially due to ligand exchange, although comparable yields after one hour (94% and 95% respectively) were obtained. Addition of 0.2 mol%

phenanthroline (two equivalents with respect to **4.1**) was sufficient to poison the catalyst, however, to confirm the presence of nanoparticles, the yield would have had to have been notably reduced by the addition of a substoichiometric amount (in relation to the loading of **4.1**).[263] The second test involved addition of an excess of elemental mercury to the reaction, because this can amalgamate with nanoparticles.[262] No change in the yield of 1-phenylethanol was observed, confirming that **4.1** is likely to act as a suitable catalyst precursor for a true homogeneous catalyst for the transfer hydrogenation of ketones.

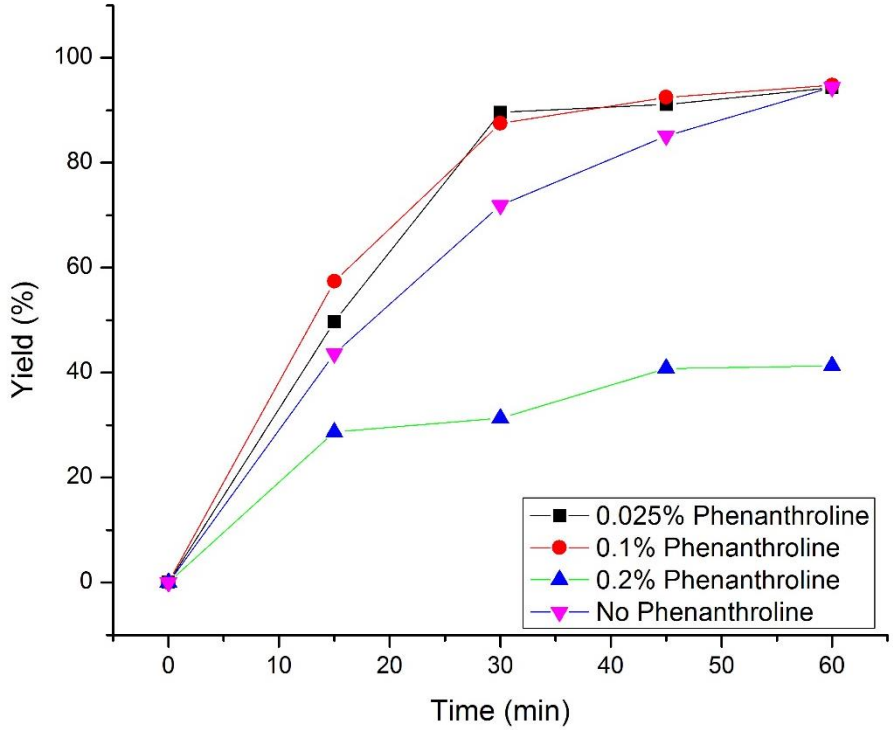

Figure 4-11. Yields obtained at 15 minute intervals after addition of varying percentages of 1,10-phenanthroline.

4.4 Catalytic upgrading of alcohols

The development of new "biofuels" is an important area of research that focuses on finding effective routes to environmentally-friendly alternatives to fuels derived from crude oil. Ethanol is a well-established biofuel, that is readily produced through fermentation.[264] However, it is corrosive to current engine technologies and has a lower energy density (the amount of energy stored per volume of fuel) than gasoline.[265] To counteract these issues, higher molecular weight alcohols have been investigated, namely *n*-butanol and isobutanol, because these have a higher energy density compared to EtOH (~90% that of gasoline) and can be either used on their own or blended with gasoline at higher percentages than ethanol.[265-267] While both alcohols are produced

industrially (isobutanol can be prepared from propylene by the petrochemical industry), they remain too expensive to be considered as fuels,[267] therefore, new routes are required. The Wass group at the University of Bristol has published a series of papers on the synthesis of both alcohols using the so-called "borrowed-hydrogen" method (**Scheme 4-9**),[265, 266, 268-270] based on the Guerbet reaction.[271] The synthesis proceeds *via* initial "borrowing" of hydrogen from the alcohol substrate(s) by the catalyst, forming the intermediate carbonyl compounds. These then undergo a base-mediated aldol reaction forming an α,β-unsaturated carbonyl compound. The hydrogen is then returned to this species, generating the upgraded alcohol. In the case of *n*-butanol, the reaction is complete after one cycle by homocoupling two equivalents of ethanol, whereas for isobutanol, the *n*-propanol intermediate resulting from the coupling of ethanol and methanol then completes a second cycle, reacting with another equivalent of methanol to form the product.

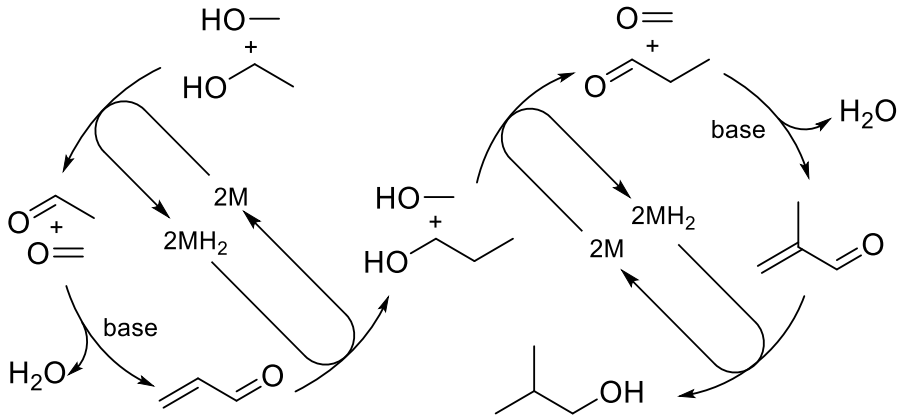

Scheme 4-9.[177] Synthesis of isobutanol by the catalytic upgrading of ethanol and methanol

The Wass group have shown that ligands with narrow bite-angles (such as dppm) are optimal for the Ru-catalysed upgrading of ethanol and methanol to isobutanol.[268] In collaboration with the Wass group, the complexes **4.1** and **4.3** were tested (**Scheme 4-10**, **Table 4-7**). Complexes **4.4** and **4.5** were not investigated due to lack of time and material.

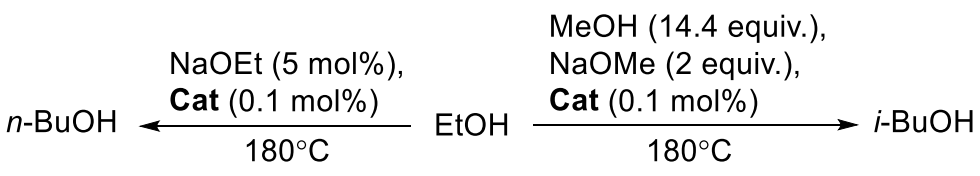

Scheme 4-10. Reaction conditions for upgrading of ethanol

Table 4-7. Results from the upgrading of ethanol to *n*-/*i*-butanol

Run	Cat	Time (h)	EtOH Conversion (%)	*n*-BuOH yield (%)	*i*-BuOH yield (%)	*n*-PrOH yield (%)	*n*-BuOH Selectivity (%)[e]	*i*-BuOH selectivity (%)[e]
1[a][b]	[d]	20	47.2	23.8			80.5	
2[a][b]	**4.1**	20	19.3	9.1			72.9	
3[a][c]	[d]	2	88.4	1.8	64.6	4.1		92.8
4[a][c]	**4.1**	2	51.4	0.0	38.1	5.3		87.7
5[a][c]	**4.1**	20	87.9	0.4	49.5	1.9		96.0
6[a][c]	**4.3**	2	40.8	0.0	11.1	4.1		73.1

[a]: Yields measured against hexadecane internal standard by GC. [b]: Upgrading of ethanol to *n*-butanol. [c]: Upgrading of ethanol and methanol to *i*-butanol. [d]: *trans*-[Ru(dppm)$_2$(Cl)$_2$] used as catalyst. [e]: Liquid fraction only.

As shown in **Table 4-7**, complex **4.1** performed poorly in the catalytic upgrading of ethanol to *n*-butanol (**Run 2**), with only a minor amount of the desired product formed. An unusually large amount of solid was formed during the reaction as well, of which 84% was NaOAc (3.3% overall yield). The results obtained using standard two-hour run to prepare isobutanol (**Run 3**) were considerably better, however, they were not competitive with *trans*-[Ru(dppm)$_2$(Cl)$_2$] as the catalyst. Lengthening the reaction time to twenty hours (**Run 5**) resulted in a significant improvement, with the yield of isobutanol comparable to that obtained by other complexes reported in the literature.[265] A low conversion of ethanol was obtained when **4.3** was used as the catalyst (**Run 6**); this was not unexpected as **4.3** was not an effective catalyst for the transfer hydrogen of ketones.

4.5 Investigating the stability/activation of **4.1**

As a final means of investigating the activation of **4.1** under transfer-hydrogenation conditions, mass spectrometric analysis of samples of the complex freshly mixed with KO^{t}Bu and dry isopropanol was carried out in collaboration with the EPSRC UK National Mass Spectrometry Facility (NMSF) at Swansea University. Unfortunately, as the NMSF does not have the facilities for air-sensitive chemistry, all mixing of compounds was carried out under air, and as **4.1** and the active catalytic species in transfer hydrogenation are likely to be air and moisture sensitive, this may explain the large distribution of products that was obtained (**Figure 4-12**). Using the available data, recorded 30, 60 and 120 seconds after mixing,[177] no species arising from attack of alkoxide ions, hydride formation, ligand displacement could be definitively identified.

However, it is clear that a number of reactions must be occurring. In order to obtain mass spectrometric data that more reliably correlates to that formed during a catalytic run, all handling and mixing of reagents and sample solutions would need to be performed under inert gas using a glove box equipped with an injection port.

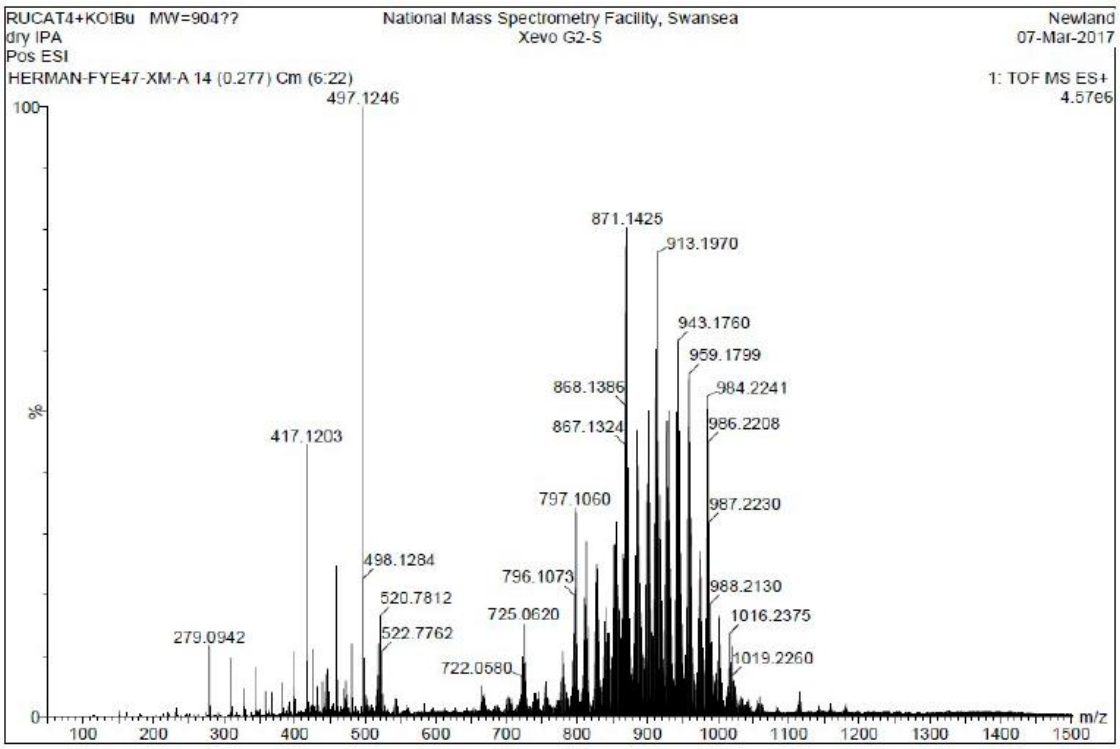

Figure 4-12.[177] Mass spectrum obtained 30 seconds after mixing **4.1** with five equivalents of KO^{t}Bu in isopropanol

4.6 Conclusions

By reaction of **2.1** with 0.5 equivalents of [Ru(dmso)$_4$(Cl)$_2$], bis(phosphinophosphinine) complex **4.1** was isolated. This complex was completely characetised by spectroscopic techniques and by X-ray diffraction and was the first reported structure for a chelating phosphinophosphinine complex. Attempts were made to synthesise a "half sandwich" ruthenium complex of **2.1** using [{Ru(*p*-cymene)(Cl)$_2$}$_2$] that instead afforded a mixture of dinuclear complex **4.2** (which was characterised by ^{31}P{^{1}H} NMR spectroscopy and X-ray diffraction) and octahedral complex **4.1** due to displacement of one and two *p*-cymene ligands respectively. To avoid displacement of the aryl ligand, the reaction was repeated using the hexamethylbenzene dimer [{Ru(C$_6$Me$_6$)(Cl)$_2$}$_2$] with various sources of weakly-coordinating anions, however, multiple products were obtained when silver salts (AgBF$_4$/AgSbF$_6$) or NaB(Ar^F)$_4$ were used. Addition of NH$_4$PF$_6$ yielded a single product, however, due to the hygroscopic nature of ammonium salts, the presence of water in the reaction resulted in the formation of the "hydrated" complex **4.3**, due to the

syn-addition of water across the P=C double bond. To avoid the need for weakly-coordinating anions, **2.1** was reacted with the highly reactive complex [{Ru(Cp*)Cl}$_4$]. The reaction proceeded cleanly and the complex was characterised spectroscopically, however, **4.4** proved to be highly soluble in any solvent tested, so the molecular structure was not obtained by X-ray diffraction. This complex also proved to be reactive towards water and **4.5**, that had undergone a *syn*-addition of water, was obtained.

All of the obtained Ru complexes (with the exception of **4.2**, which could not be obtained as a pure species) were then tested in the transfer hydrogenation of acetophenones. Only **4.1** was an active catalyst, and good to excellent yields were obtained for electron-poor ketones at room temperature (with the exception of 4′-nitroacetophenone, which is poorly soluble in isopropanol) at 0.1 mol% catalyst loading. The electron-rich acetophenones that were tested required heating, but gave good to excellent yields within one hour. Two common tests for nanoparticles indicated that **4.1** is also likely to be a true, homogeneous catalyst for transfer hydrogenation.

Complex **4.1** was tested in the catalytic "upgrading" of ethanol and methanol to *n*-butanol and isobutanol, in collaboration with the Wass group at the University of Bristol. In comparison to the leading catalyst for these reactions, [Ru(dppm)$_2$(Cl)$_2$], the yield of *n*-butanol obtained was poor, however, after extended reaction, isobutanol could be obtained in high selectivity and 49.5% yield. Complex **4.3** was also investigated in the production of isobutanol, however, it proved to be a very poor catalyst for this reaction.

5 - Chemistry of rhodium phosphinophosphinine complexes

5.1 Introduction

The use of rhodium phosphine catalysts is an important, multi-faceted area in chemistry (*e.g.* C-H activation,[272] hydrogenation[273] and hydroformylation[274]), with examples such as Wilkinson's catalyst ($[Rh(PPh_3)_3Cl]$)[275] still remaining popular since it was first synthesised over 50 years ago. However, whilst the chemistry of rhodium phosphine complexes has been thoroughly explored,[276] the use of λ^3 phosphinine rhodium complexes in catalysis has not been widely investigated despite several complexes being reported.[28, 111, 126, 152, 161, 277] The most significant example that we are aware of in the literature is a series of publications by Breit & co-workers on developing the regioselective hydroformylation of alkenes, leading to the branched isomer, using mainly monodentate phosphinine ligands.[28, 32, 160, 161] Their efforts showed that the use of tris(aryl)phosphinines (**Figure 5-1**, **A**) in place of classical ligands such as triphenylphosphine (PPh_3) and tris(2,4-di(*tert*-butyl)phenyl)phosphite (**Figure 5-1**, **B**) led to increased catalyst turnover frequencies (styrene TOF/h = 28.7 (**A**), 16.4 (**B**), 7.5 (PPh_3)).[278] Some contents of this chapter have recently been published in a communication.[279]

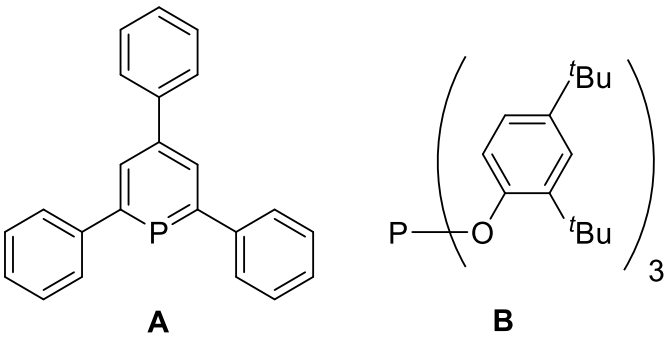

A B

Figure 5-1. Phosphorus ligands used in rhodium-catalysed hydroformylation

5.2 A rhodium carbonyl complex of **2.1**

As an initial reaction to begin the investigation of the coordination chemistry of 2-phosphinophosphinine **2.1** with rhodium, the proligand was added to half an equivalent of the rhodium carbonyl chloride dimer $[\{Rh(CO)_2(\mu\text{-}Cl)\}_2]$ (**Scheme 5-1**). As with the group 6 carbonyl complexes (see **Chapter 3**), **5.1** held utility as another means by which to compare the donor properties of **2.1** to diphosphines because geometrically similar diphosphine complexes have been reported by Mague and Mitchener,[280] with better IR spectroscopic data published by Sanger.[281]

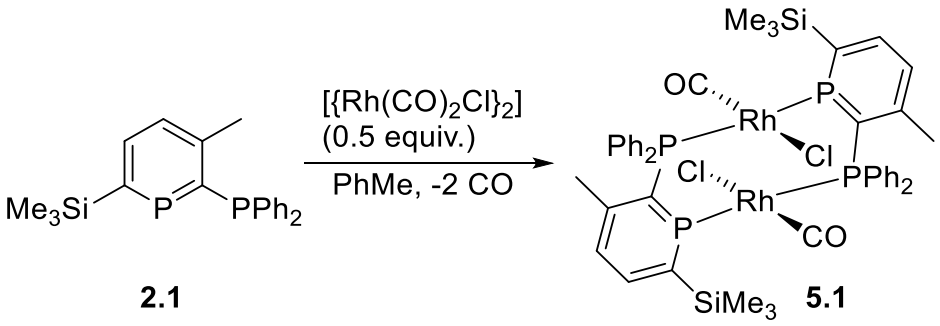

2.1 **5.1**

Scheme 5-1. Synthesis of dinuclear rhodium complex **5.1**

Upon addition of toluene to a mixture of the rhodium precursor and **2.1**, a rapid reaction took place with concomitant gas evolution observed, resulting in a deep purple solution from which the crystalline 1:1 toluene solvate of **5.1** deposited within minutes at 20°C. A yield of 63% was achieved after storage at -25°C for 24 h to obtain a second crop. Recrystallisation by layering a benzene-d_6 solution of **5.1** with petroleum ether yielded single crystals suitable for X-ray diffraction (**Figure 5-2**).

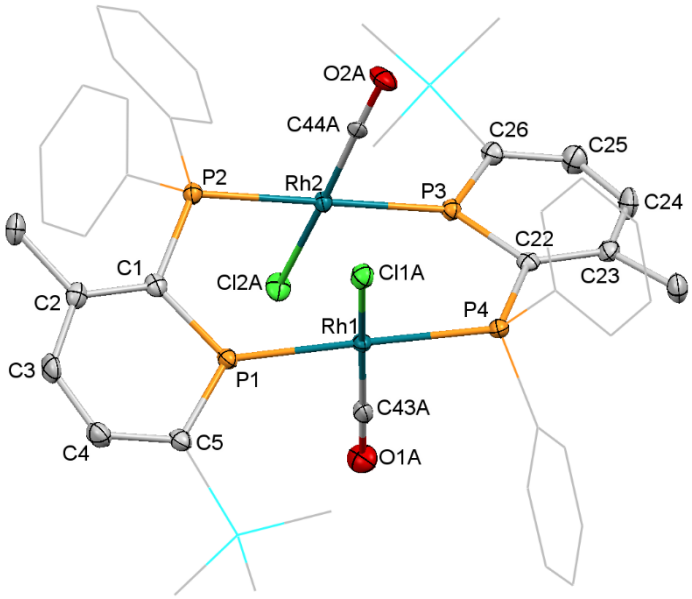

Figure 5-2. Molecular structure of **5.1** (thermal ellipsoids at 50% probability). All H-atoms have been omitted, and the phenyl rings and trimethylsilyl groups have been displayed in wireframe for clarity. One position each of the disordered carbonyl and chloride ligands has been removed. The ratio for the occupancies of the disordered sites was refined to 0.62:0.38

Table 5-1. Key bond lengths and angles for **5.1**

Bond Lengths (Å)		Bond Angles (°)	
P(1)-C(1)	1.734(4)	P(1)-C(1)-C(2)	121.4(2)
C(1)-C(2)	1.411(5)	C(1)-C(2)-C(3)	121.0(3)
C(2)-C(3)	1.402(5)	C(2)-C(3)-C(4)	125.6(3)
C(3)-C(4)	1.386(5)	C(3)-C(4)-C(5)	126.1(3)
C(4)-C(5)	1.394(5)	C(4)-C(5)-P(1)	118.0(3)
C(5)-P(1)	1.725(4)	C(5)-P(1)-C(1)	107.6(2)
C(1)-P(2)	1.844(3)	P(1)-C(1)-P(2)	114.9(2)
P(1)-Rh(1)	2.285(1)	P(3)-C(22)-C(23)	121.3(2)
P(2)-Rh(2)	2.323(1)	C(22)-C(23)-C(24)	121.6(3)
P(3)-C(22)	1.732(3)	C(23)-C(24)-C(25)	125.2(4)
C(22)-C(23)	1.414(5)	C(24)-C(25)-C(26)	125.8(3)
C(23)-C(24)	1.388(5)	C(25)-C(26)-P(3)	118.6(3)
C(24)-C(25)	1.390(5)	C(26)-P(3)-C(22)	107.2(2)
C(25)-C(26)	1.397(5)	P(3)-C(22)-P(4)	115.5(2)
C(26)-P(3)	1.721(3)		
C(22)-P(4)	1.837(3)		
P(3)-Rh(2)	2.293(1)		
P(4)-Rh(1)	2.312(1)		

Although the molecule does not reside on any crystallographic symmetry elements, only minor differences exist between the bond lengths and angles of the two halves of the molecule. Comparison of the bond lengths of **5.1** to those for the proligand **2.1** reveals few significant differences, however, there are notable changes in the angles P(1)-C(1)-C(2) (121.4(2) versus 124.0(2)° for **2.1**), C(5)-P(1)-C(1) (107.6(2) versus 103.6(1)° for **2.1**) and P(1)-C(1)-P(2) (114.9(2) versus 119.9(1)° for **2.1**). Due to the disorder of the carbonyl and chloride ligands on both Rh(1) and Rh(2), discussion of their bond lengths or angles would be potentially unreliable. Although these ligands are disordered over two positions, the relative orientation of the carbonyl and chloride ligands was assigned with comparison to the structures of similar $Rh_2(P\text{-}(CH_2)_n\text{-}P)_2(CO)_2Cl_2$ complexes that have been reported with *trans* geometries.[280, 281] The most important structural feature gained from the X-ray data is the overall twist in the structure (**Figure 5-3**); this is shown by the P(1)-Rh(1)-Rh(2)-P(2) and P(3)-Rh(2)-Rh(1)-P(4) dihedral angles (16.88(4)° and 16.93(4)°, respectively).

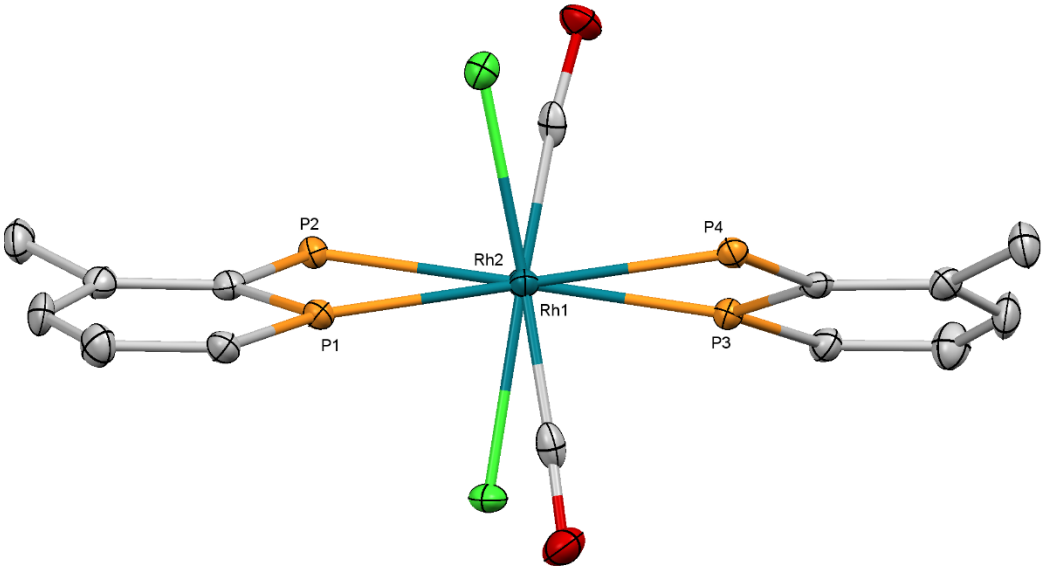

Figure 5-3. Side view of **5.1**. All H-atoms as well as phenyl rings and trimethylsilyl groups have been removed for clarity

The $^{31}P\{^{1}H\}$ NMR spectrum of **5.1** does not fit with what would be predicted for such a structure, where either a doublet of doublets or potentially a doublet of doublets of doublets (if there was a *trans*-coupling as well) was expected. However, due to coincidence of signals, the spectrum shows two sets of apparent doublets of triplets (δ = 250.6 (2P), 25.5 (2P) ppm, **Figure 5-4**). In collaboration with Dr Jason Lynam at the University of York, the individual coupling constants have been calculated using gNMR (**Table 5-2**). These calculated constants allowed for accurate interpretation of the multiplets observed in the $^{31}P\{^{1}H\}$ NMR spectrum. As expected, the largest coupling constants are the *trans* P(1)-P(4) and P(2)- P(3) couplings. The almost identical absolute magnitude of coupling constants of P(1) with Rh(2) and P(2) *etc.* are what then leads to the apparent triplets.

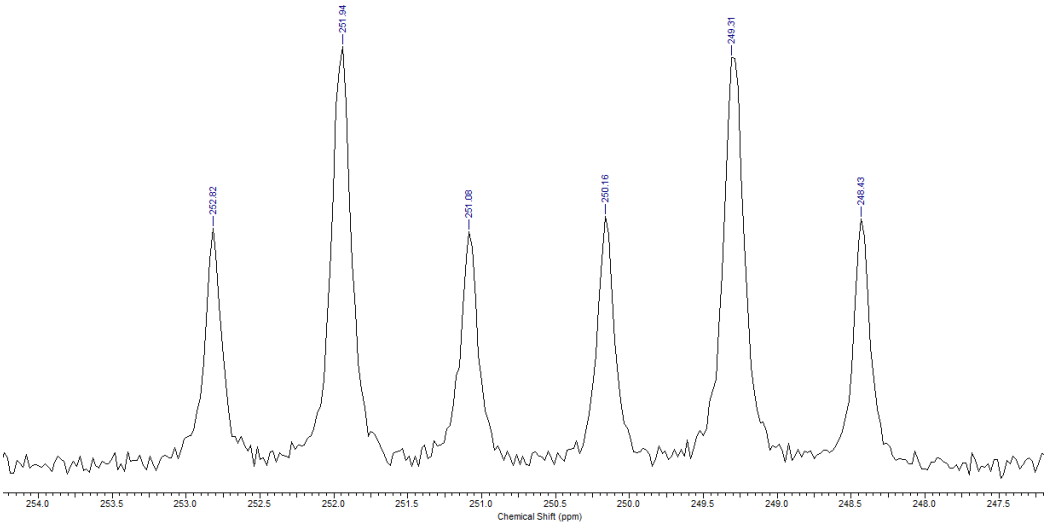

Figure 5-4. ^{31}P NMR spectrum (phosphinine region) of **5.1**
Table 5-2. Calculated chemical shifts, peak widths, and coupling constants for **5.1**

Atom	δ (ppm)	Width (Hz)	Coupling Constants (Hz) $J_{P(1)}$	$J_{P(2)}$	$J_{P(3)}$	$J_{P(4)}$	$J_{Rh(1)}$
P(1)	250.628	19.41					
P(2)	25.521	13.08	137.33				
P(3)	250.628	19.41	0.00	-430.25			
P(4)	25.521	13.08	-430.25	0.00			
Rh(1)	N/A	N/A	-143.57	3.00	3.28	-138.70	
Rh(2)	N/A	N/A	3.28	-138.70	-143.57	3.00	0.00

Analysis of the product by infrared spectroscopy revealed ν(CO) to be 1977 cm^{-1}; for the analogous dppm complex [{Rh(dppm)(CO)Cl}$_2$] ν(CO) is 1968 cm^{-1},[281] which agrees with our previous findings that **2.1** is a better π-acceptor than dppm (see **Chapter 3**).

5.3 Synthesis of a cationic rhodium cyclooctadiene complex

In order to prepare a chelating rhodium complex of **2.1** that could be catalytically useful, the synthesis of a cationic rhodium complex with a labile diene ligand was investigated because these are popular motifs in a wide variety of catalytic reactions, although these catalysts are commonly generated *in-situ*.[272, 282-284] The synthesis of rhodium cyclooctadiene complexes of dppm analogues typically requires large sterically bulky P-substituents ([Rh(dppm)(COD)][X] is not known) such as cyclohexyl or *tert*-butyl due to the Thorpe-Ingold effect – larger substituents on the P atoms results in a decrease in strain energy when coordinated.[82, 285] Initial research followed the methodology of Balakrishna and co-workers which involved *in-situ* generation of the complex (

Scheme 5-2 – **Route A**).[286] However, the formation of two dearomatised products was observed when $AgBF_4$ or $AgSbF_6$ were used as anion sources in this route because it is well known that these anions are potentially reactive.[287] This issue was successfully resolved by the use of a much less-coordinating anion, following the method of Weller, Willis and co-workers (

Scheme 5-2 – **Route B**).[283] Reacting **2.1** with [Rh(COD)$_2$][B(Ar^F)$_4$] (B(Ar^F)$_4$ = B{3,5-(CF$_3$)$_2$C$_6$H$_3$)$_4$} in dichloromethane resulted in the immediate formation of a dark red solution from which **5.2** was isolated in 80% yield, ($^{31}P\{^1H\}$ δ = 189.4 (ap dd), -6.8 (ap

dd) ppm) as an air-stable red powder. By slow diffusion of pentane into a $CDCl_3$ solution of **5.2** at -25°C, single crystals were obtained (**Figure 5-5**).

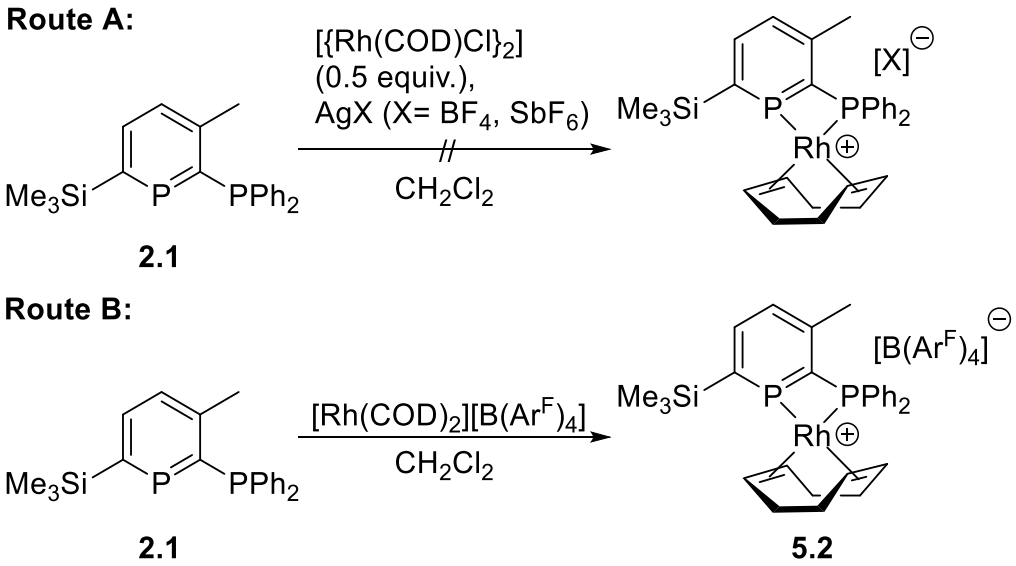

Scheme 5-2. Synthetic route to **5.2**

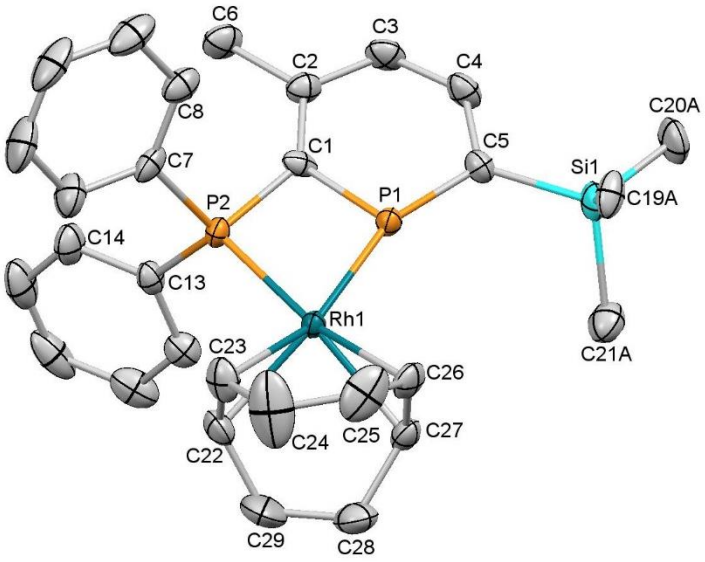

Figure 5-5. Molecular structure of **5.2** (thermal ellipsoids at 50% probability). All H-atoms and the $[B(Ar^F)_4]$ anion have been omitted for clarity. One position of the disordered trimethylsilyl group has been removed.

Table 5-3. Key bond lengths and angles for **5.2**

Bond Lengths (Å)		Bond Angles (°)	
P(1)-C(1)	1.732(3)	P(1)-C(1)-C(2)	125.1(2)
C(1)-C(2)	1.397(4)	C(1)-C(2)-C(3)	118.0(3)
C(2)-C(3)	1.397(5)	C(2)-C(3)-C(4)	125.7(3)
C(3)-C(4)	1.385(5)	C(3)-C(4)-C(5)	128.6(3)
C(4)-C(5)	1.409(4)	C(4)-C(5)-P(1)	115.7(2)
C(5)-P(1)	1.723(3)	C(5)-P(1)-C(1)	106.9(2)
C(1)-P(2)	1.801(3)	P(1)-C(1)-P(2)	97.3(1)
P(1)-Rh(1)	2.293(1)	P(1)-Rh(1)-P(2)	70.64(3)
P(2)-Rh(2)	2.294(1)		

The structure of **5.2** shows the diphosphorus ligand chelating to an approximately square planar cationic rhodium centre bearing a COD co-ligand. As this is the first example of a chelating rhodium phosphinophosphinine complex, there are no data available for direct comparison, however, the P(1)-Rh(1) bond length is similar to the distances reported for other rhodium COD complexes (**Figure 5-6**, **Table 5-4**) containing monodentate (**A**) or bidentate (**B**) phosphinine ligands.

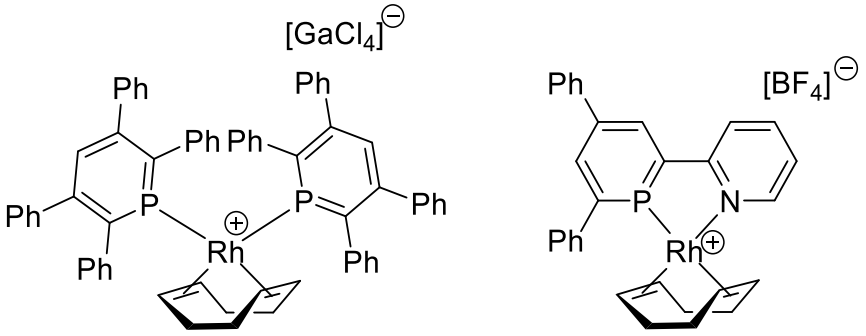

Figure 5-6. Cyclooctadienyl rhodium complexes containing phosphinine ligands

Table 5-4. P(1)-Rh(1) bond lengths (Å)

Complex	Bond Length (Å)	Ref.
A	2.301(1)	277
B	2.225(1)	152
5.2	2.293(1)	-

The most important metric for **5.2** is the P(1)-Rh(1)-P(2) bite angle (70.64(3)°), which is very acute for a Rh(κ_2-PCP)(COD) complex, especially due to the lack of any stabilising, bulky substituents on the P atoms. To put this value in context, cyclooctadienyl rhodium complexes of $H_2C(PCy_2)_2$[288] and (Me)(^{t}Bu)PCH_2P(^{t}Bu)$_2$[289]

have P-Rh-P bite angles of 72.64(2)° and 72.55(6)° respectively. This suggests that even without Thorpe-Ingold stabilisation,[82] the increased s-character (*ca.* 61%)[8] of the sp^2 cyclic phosphorus is presumably helping to stabilise the small bite-angle seen in **5.2** due to the decreased directional preference of the lone pair.

5.4 Hydroacylation

After synthesising complex **5.2**, hydroacylation was investigated because small bite-angle ligands (such as dppm derivatives with *tert*-butyl and cyclohexyl substituents on the P-atoms) have been reported to have high activity.[283] Hydroacylation involves the formal addition of an aldehyde C-H bond across an alkene or an alkyne forming a ketone. Whilst other transition metals have been used to catalyse this reaction, rhodium is most commonly used.[290] This reaction can be intermolecular (forming a linear ketone)[283] or intramolecular,[291] and is commonly used to form cyclopentanones, although recent advances have allowed for the synthesis of larger rings.[292] As intramolecular hydroacylation is less challenging (due to the potential decarbonylation pathway in the intermolecular variant),[290] the hydroacylation of 4-pentenal using **5.2** was attempted (**Scheme 5-3**).

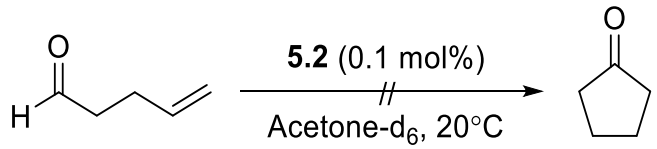

Scheme 5-3. Attempted hydroacylation of 4-pentenal

Unfortunately the formation of cyclopentanone was not observed by ^{1}H NMR spectroscopy. However, it was observed that **5.2** instead slowly catalysed the isomerisation of the alkene, forming a mixture of *cis* and *trans* 2- and 3-pentenal as well as at least two unknown products (**Figure 5-7**), although ultimately the reaction stopped before all 4-pentenal was consumed.

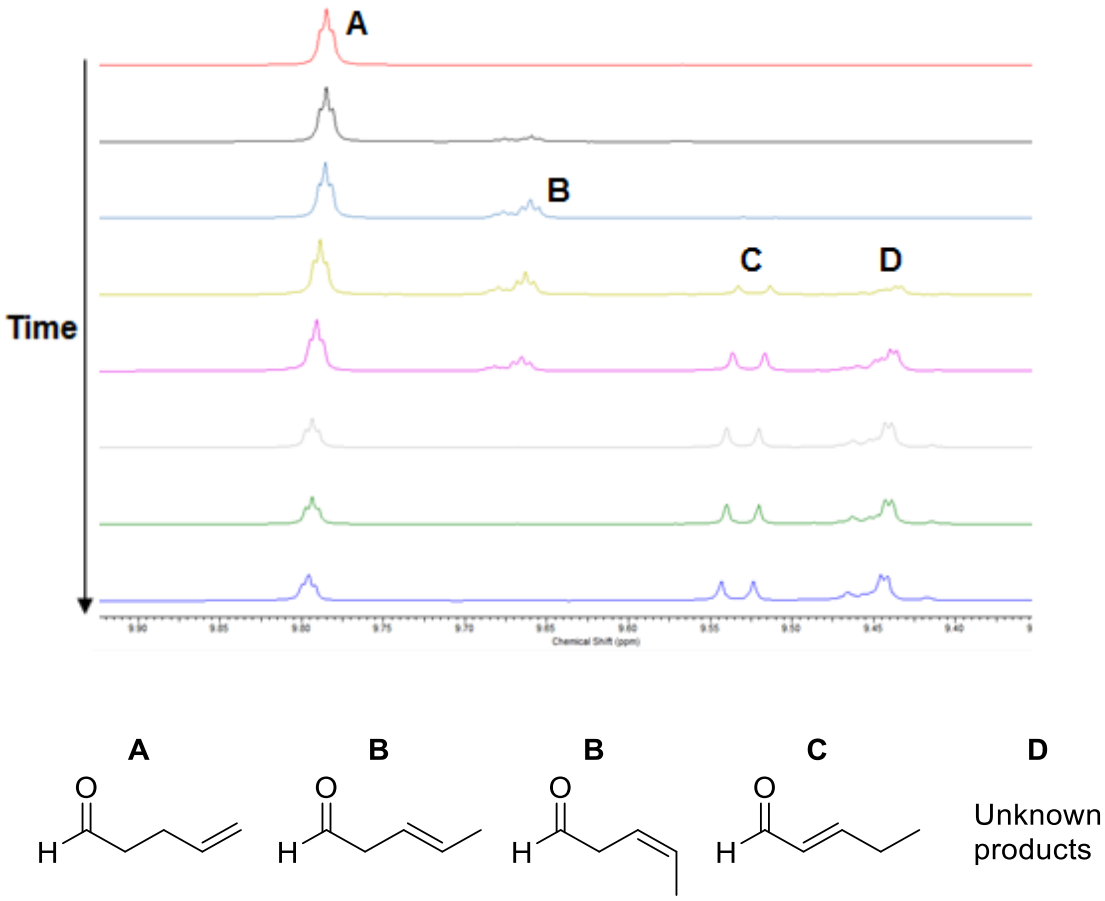

Figure 5-7. ^{1}H NMR spectrum (aldehyde region) showing the isomerisation of 4-pentenal over a period of 7 days at 20°C

Attempts to force the reaction to completion by heating to 70°C gave no improvement aside from an increased rate, and the reaction again stopped at approximately the mixture shown in **Figure 5-7**. The catalysis was also attempted in $CDCl_3$ at 85°C, however, the same reactivity was observed, only more slowly, possibly due to the lack of a coordinating solvent.

5.5 Hydroboration

5.5.1 Hydroboration of alkenes

The hydroboration of alkenes involves the reaction of a C=C double bond with a B-H bond, commonly derived from Lewis-base complexes of BH_3,[293] sodium borohydride,[294] or dioxaboroles such as catecholborane (**Scheme 5-4, A**).[295] The resulting alkyl boranes or borates can undergo a variety of transformations, however, they are most commonly converted to alcohols by basic peroxide oxidation.[294] The non-catalysed reaction is a classical organic chemistry reaction, however it requires a reactive B-H bond and can suffer from issues such as long reaction times, poor selectivity or the need for forcing conditions.[295] The first catalyst used for the

hydroboration of alkenes was [Rh(PPh$_3$)$_3$Cl], as discovered by Männig and Nöth, who reported yields of up to 83% in 25 minutes (although the branched:linear selectivity ratios were not reported) at room temperature, using catecholborane and 0.05 mol% catalyst loading.[296]

To assess the catalytic utility of **5.2** in the hydroboration of alkenes, styrene was chosen as the substrate (**Table 5-5**). No results are given for the use of [Rh(PPh$_3$)$_3$Cl] as there is a great deal of inconsistency between published results when this catalyst is used.[297] For example, [Rh(PPh$_3$)$_3$Cl] has been reported to give 10:90 **B**:**C**,[298] 100:0 **B**:**C**,[299] and other values in between, however, it is apparent that if the catalyst is stored under inert conditions or is stored under air then a different complex is obtained.[297]

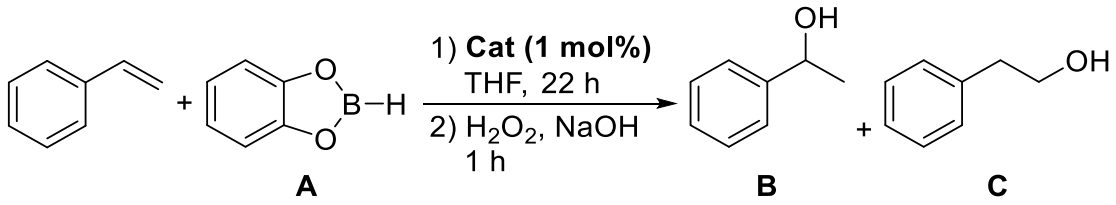

Scheme 5-4. Catalytic hydroboration of styrene

Table 5-5. Comparison between catalysts for the hydroboration of styrene

Catalyst	Yield (%)	B/C	Ref.
None[a]	16	0/100	300
[Rh(COD)$_2$][BF$_4$] + dppm[a]	95	77/23	300
5.2[b]	49[c]	66/34[c]	-

[a]: reaction at 25 °C. [b]: reaction at 20 °C. [c]: average of two runs.

In the literature, a 16% yield was reported for the non-catalysed reaction after 22 hours with 100% selectivity for the linear product, whereas when using an *in-situ* generated catalyst from dppm and [Rh(COD)$_2$][BF$_4$], a 95% yield with a 77:23 ratio of branched:linear products was obtained.[300] Following these conditions and using **5.2** as a catalyst, near-complete consumption of the styrene was achieved in 22 h, however, ^{1}H NMR spectroscopic analysis of the crude reaction mixture revealed the presence of multiple side-products (**Figure 5-8**), indicating that **5.2** is not a selective catalyst for alkene hydroboration. Due to the presence of these undesired products, after oxidative workup a mixture of **B** and **C** was isolated in only 49% yield, with ~2:1 selectivity for the branched product **B** (as an average of two runs). The yield and product mixture obtained did not compare favourably with values reported in the literature, with a poor

selectivity towards either of the desired products. As a result, the reaction was not investigated further.

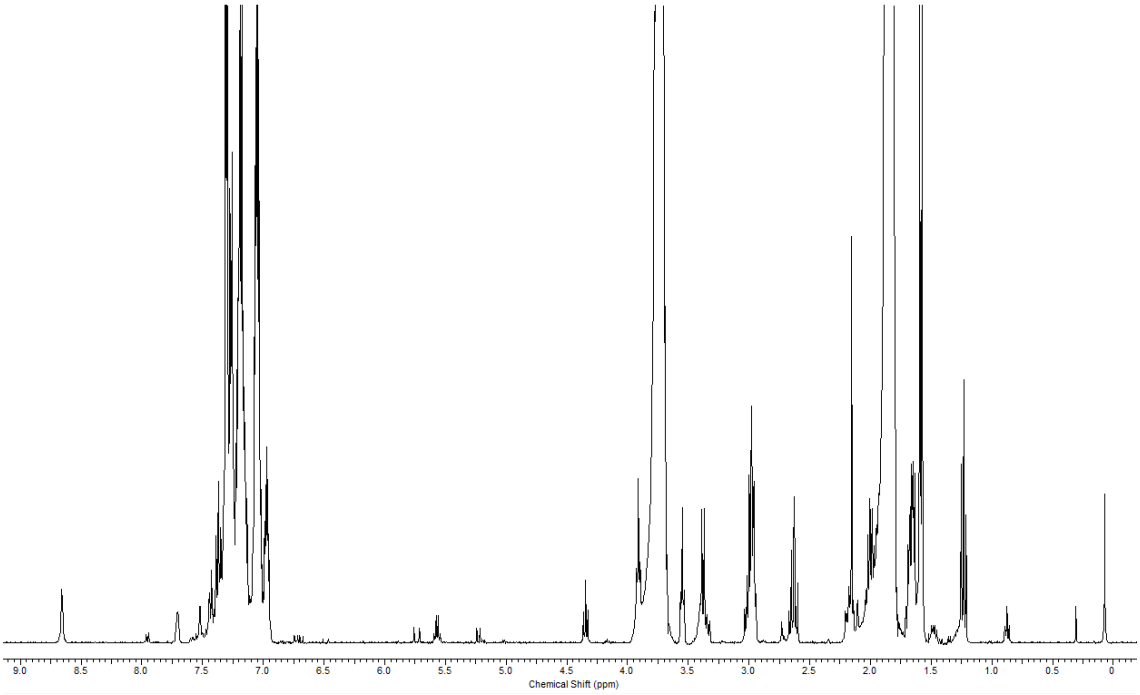

Figure 5-8. Crude ^{1}H NMR spectrum of the hydroboration of styrene with **5.2** after 22 hours.

5.5.2 Hydroboration of ketones and aldehydes

In their original paper on the hydroboration of alkenes using [$Rh(PPh_3)_3Cl$] and catecholborane, Männig and Nöth reported that 5-hexen-2-one and 5-norbornen-2-one reacted selectively at the ketone instead of the alkene if no catalyst was added.[296] Conversely, more challenging substrates such as acetophenones ($PhC(O)CH_3$) or benzophenones (Ph_2CO) react only very slowly (or not at all) with catecholborane/pinacolborane without the presence of a catalyst, and it wasn't until years later that initial results on the catalytic hydroboration of aryl ketones were reported.[253]

Recently there has been a wealth of catalysts reported for the hydroboration of carbonyl compounds, including s-block (e.g. Li,[68] Na,[301] Mg[302]) and p-block (e.g B,[9] Al,[303, 304] Ge, Sn[305]) elements, as well as first-row (e.g. Ti,[306] Mn,[307] Fe,[308] Ni[309]), early (Mo[310]) and late (Re,[311] Ru[312, 313]) transition metals, however, no rhodium catalysts were currently known for this reaction. After an exhaustive literature search, including several reviews,[59, 253, 314] a single example of rhodium participating in the hydroboration

of a carbonyl substrate was found for the reported stoichiometric reduction of benzaldehyde.[315] In addition, Evans and Hoveyda reported that the hydroboration of aliphatic β-hydroxy ketones in the presence of 5 mol% [$Rh(PPh_3)_3Cl$] provided a measure of increased diasterocontrol,[103] however, they observed no increase in reaction rate or yield. Due to the lack of any reports of a rhodium complex catalysing this reaction, it was decided to conduct a ligand and catalyst screen using 4′-bromoacetophenone (**Scheme 5-5**).

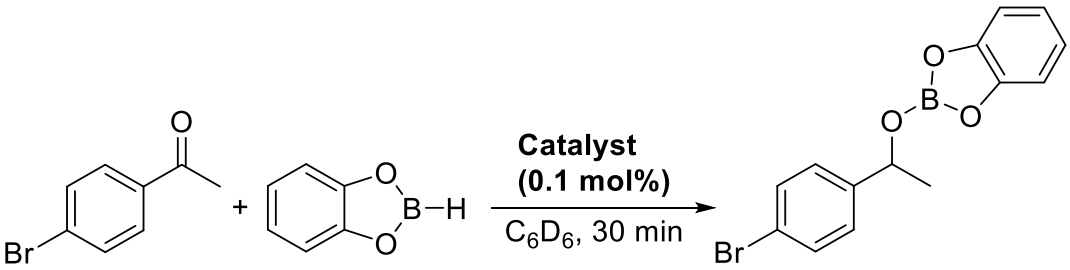

Scheme 5-5. Catalytic hydroboration of 4′ -bromoacetophenone

Table 5-6. Catalyst/ligand screen for the hydroboration of 4′-bromoacetophenone

Run	Catalyst	Yield (%)[c]
A	None	1
B	**2.1**	20
C	**5.1**	35
D	**5.2**	96
E	[Ru(**2.1**)$_2$Cl$_2$] (**4.1**)	12
F	[$Rh(PPh_3)_3Cl$]	3
G[a]	[$Rh(COD)_2$][$B(Ar^F)_4$] + 2 PCy_3	22
H[b]	0.5 [{$Rh(COD)Cl\}_2$] + 2 PCy_3	18
I[a]	[$Rh(COD)_2$][$B(Ar^F)_4$] + 2 PPh_3	7
J[a]	[$Rh(COD)_2$][$B(Ar^F)_4$] + dppm	7
K[a]	[$Rh(COD)_2$][$B(Ar^F)_4$] + 2 $P(OPh)_3$	6

[a]: Pre-mixed in THF (~0.1 cm^3) for 10 min before addition of substrate and catecholborane. [b]: Pre-mixed in C_6D_6 (~0.1 cm^3) for 10 min before addition of substrate and catecholborane. [c]: Yield measured against 1,3,5-trimethoxybenzene internal standard by ^{1}H NMR spectroscopy.

A dramatic difference in yield was observed between **5.2** and other the rhodium complexes tested, especially [$Rh(PPh_3)_3Cl$] which is the classical catalyst for alkene hydroboration. For the run with **5.2**, the reaction proceeded rapidly, with 94% conversion reached after ten minutes. Upon observing such a positive result, the substrate scope of the reaction was then investigated (**Table 5-7**). All reactions

proceeded cleanly, with the exception of 4′-methoxyacetophenone (not listed) which formed multiple products that could not be assigned. Upon testing **2.1** (0.1 mol%) as a catalyst, it was observed that 20% of the desired product formed within thirty minutes, making it the third-most active catalyst tested for this reaction. Repeating the reaction with 5 mol% **2.1** gave 95% conversion in three hours, indicating it has the potential to be investigated further as a catalyst for this reaction, although there was no time available to do so. Upon mixing **2.1** with HBCat in C_6D_6 no Lewis-adduct was created, so the observed catalytic activity could be due to the formation of a frustrated Lewis pair.[316]

Table 5-7. Acetophenone hydroboration substrate scope

Substrate	**Yield (%)[a]**
Acetophenone	97 [b]
4′-bromoacetophenone	96[b]
4′-fluoroacetophenone	>99[b]
4′-nitroacetophenone	98[b]
4′-methylacetophenone	92[c]
2′-methoxyacetophenone	99[b]

[a]: Yield measured against 1,3,5-trimethoxybenzene internal standard by ^{1}H NMR spectroscopy. [b]: After 30 minutes. [c]: After 60 minutes.

Almost complete conversion was observed for all substrates within 30 minutes, with the exception of the electron-rich 4′-methylacetophenone which required 60 minutes reaction time (**Table 5-7**, **Figure 5-9**). This was not surprising as it also proved to be a more challenging substrate for transfer hydrogenation as well (see **Chapter 4**). After the successful hydroboration of the acetophenones, benzophenone was then tested as a substrate. However, even after heating to 90°C for 18 hours, no conversion was observed by ^{1}H NMR spectroscopy. The reason for the lack of reactivity has not been confirmed, but is likely due to the increased steric bulk of the substrate. The hydroboration of aldehydes was also investigated, a catalytic reaction and the corresponding blank were run for benzaldehyde (**Scheme 5-6**, **Table 5-8**).

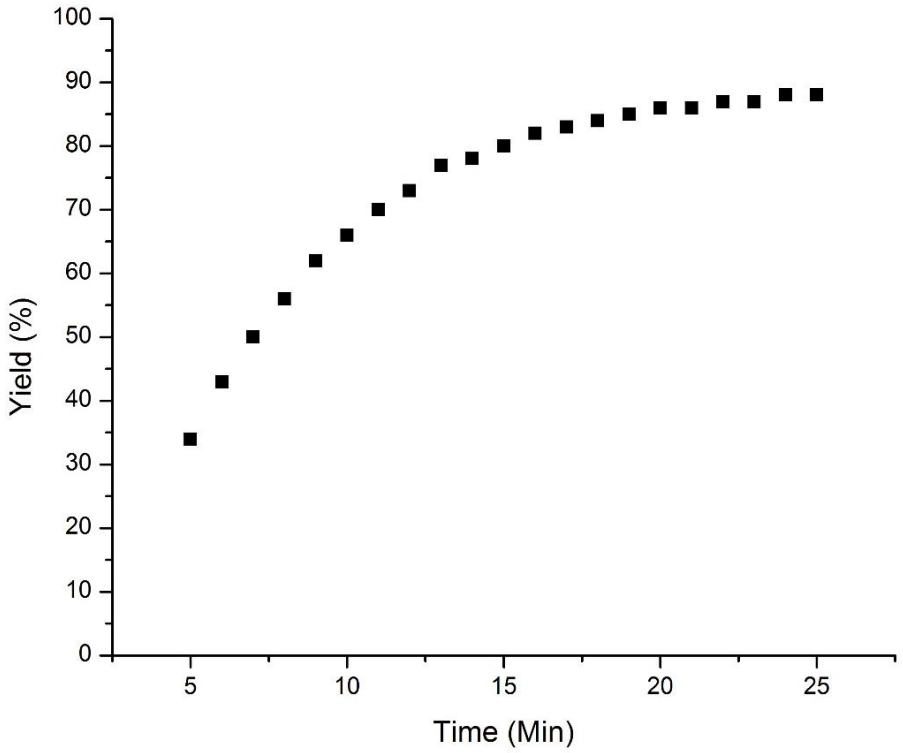

Figure 5-9. Reaction progress of 4′-methylacetophenone from 5 to 25 minutes

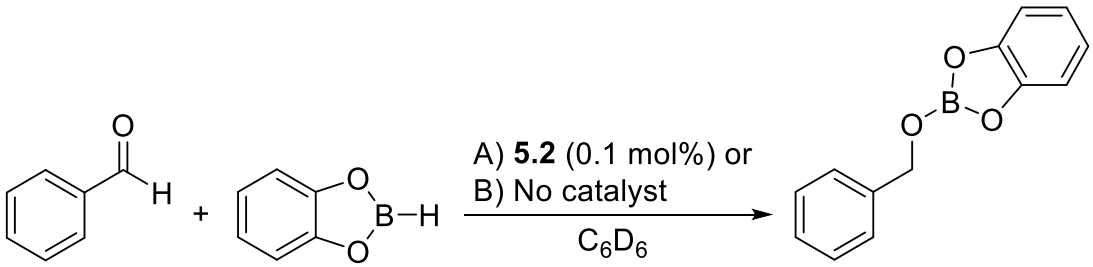

Scheme 5-6. Hydroboration of benzaldehyde

Table 5-8. Results for the hydroboration of benzaldehyde

		Yield (%)[a]		
Run	**Catalyst**	**10 min**	**30 min**	**60 min**
A	**5.2**	95	>99	
B	None	52	75	86

[a]: Yield measured against 1,3,5-trimethoxybenzene internal standard by ^{1}H NMR spectroscopy.

Whilst rapid conversion was obtained for the catalytic run, the background uncatalysed reaction rate was found to be substantial. Although the hydroboration of (aryl) aldehydes using pinacolborane has been reported by multiple groups,[302, 307-309, 317] it had not been previously demonstrated that benzaldehydes react readily with catecholborane without need for a catalyst.

To gauge the comparative hydroboration reactivity of catecholborane with ketones compared to alkenes using **5.2** as the catalyst, a set of competition reactions were performed (**Table 5-9**). First, the hydroboration of 1-octene with **5.2** was investigated (**Run 1**), then a 1:1 mixture of 1-octene and acetophenone with **5.2** (**Run 2**), then the same two-substrate mixture with [$Rh(PPh_3)_3Cl$] (**Run 3**). For comparison, Männig and Nöth reported that [$Rh(PPh_3)_3Cl$] (at 0.05 mol%) gave 77.7% conversion with 1-octene in 25 minutes.[296] Whilst this is notably higher than the result observed in **Run 3**, and at a lower catalyst loading, because acetophenone is a potential ligand, it may poison the catalyst and hinder coordination of the 1-octene.

Table 5-9. Results of competition reactions.

		1-Octene Conversion (%)[a][b]			**Acetophenone Conversion (%)[a]**		
Run	**Catalyst**	**10 min**	**30 min**	**60 min**	**10 min**	**30 min**	**60 min**
1[c]	**5.2**	5	12	19	-	-	-
2	**5.2**	7	22	37	22	45	60
3	[$Rh(PPh_3)_3Cl$]	3	33	55	2	6	9

[a]: Conversion measured against 1,3,5-trimethoxybenzene internal standard by ^1H NMR spectroscopy. [b]: For runs **2** and **3**, 1-octene consumption includes production of isomerised alkenes. [c]: After 19 hours: 73% conversion (23% isomerised to other alkene isomers).

As expected, **5.2** slowly catalysed the reaction of catecholborane with 1-octene, however, after being left for 19 hours, 73% of the alkene was consumed (23% of this was due to isomerisation to internal alkenes). Unexpectedly, **Run 2** gave a higher conversion of 1-octene after 1 hour, as well as a notably reduced conversion for acetophenone (compared to the results for only acetophenone). Minor amounts of alkene isomerisation were observed but the percentage couldn't be quantified due to the signals overlapping with the (benzylic) quartet formed by the hydroboration of acetophenone. It is suspected that the increased conversion of 1-octene was due to faster catalyst activation by acetophenone which, as a better nucleophile, can more readily displace the labile COD ligand. However, overall **5.2** is a faster catalyst for the hydroboration of ketones than for alkenes which is the opposite of known rhodium hydroboration catalysts.

5.5.3 Hydroboration of ketimines and N-heterocycles

Following the successful hydroboration of ketones with **5.2**, the hydroboration of imines was attempted as a more challenging set of substrates. Aldimine **A** (**Figure 5-10**) had previously been shown to react rapidly with catecholborane without the need for a catalyst by Westcott and co-workers,[104] so four ketimines were prepared by the method of Mou *et. al.*.[318]

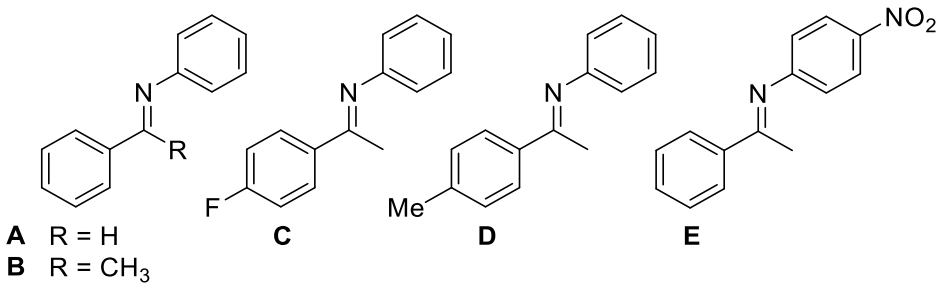

Figure 5-10. Ketimine substrates

After optimisation of the reaction conditions, the yields obtained for the hydroboration of substrates **B** to **E** (**Figure 5-11**) are displayed below (**Table 5-10**). A notable difference in yields between **B** to **D** was anticipated because the electronic properties of the phenyl rings in the acetophenone substrates had an impact on their reactivity, however, no significant differences were observed. Higher yields above those observed after one hour were not achieved, and heating for up to two more hours produced no further product. Changing the catalytic loading of **5.2** to 3 mol% also had no effect because it is poorly soluble in benzene, and above 2 mol% it started to oil out of solution.

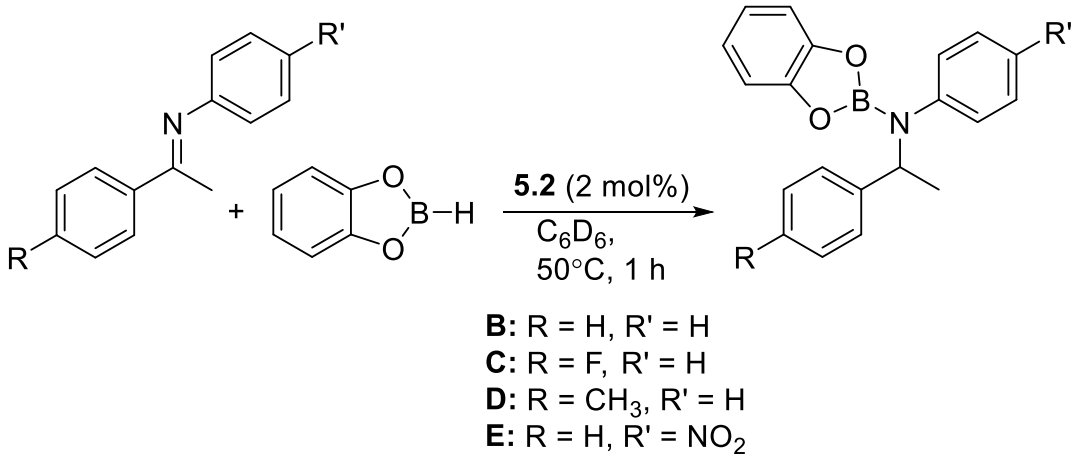

Figure 5-11. Hydroboration of ketimines

Table 5-10. Results for the hydroboration of ketimines

Substrate	Yield (%)[a]
B	86
C	86
D	85
E	16

[a]: Yield measured against 1,3,5-trimethoxybenzene internal standard by ^{1}H NMR spectroscopy.

After almost identical conversions were observed between substrates **B** to **D**, nitro-substituted ketimine **E** was investigated to compare how the electronics of the aniline ring affected the reactivity of the substrate. The presence of a strongly electron-withdrawing substituent on the aniline ring severely hindered the reaction, presumably because the electron-poor imine is less nucleophilic.

After investigating the reactivity of ketimines, the hydroboration of N-heterocyclic substrates was attempted. Initial reactions did not yield positive results; pyridazine (**Figure 5-12**, **A**) reacted rapidly with catecholborane without a catalyst, no reaction was observed with pyrazine (**Figure 5-12**, **B**) and pyridine only reacted slowly, with the formation of more than the two expected products.[319, 320] However, upon testing acridine (**Scheme 5-7**) and quinoline (**Scheme 5-8**), clean catalytic hydroboration was observed.

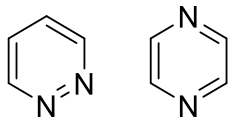

Figure 5-12. Pyridazine and pyrazine

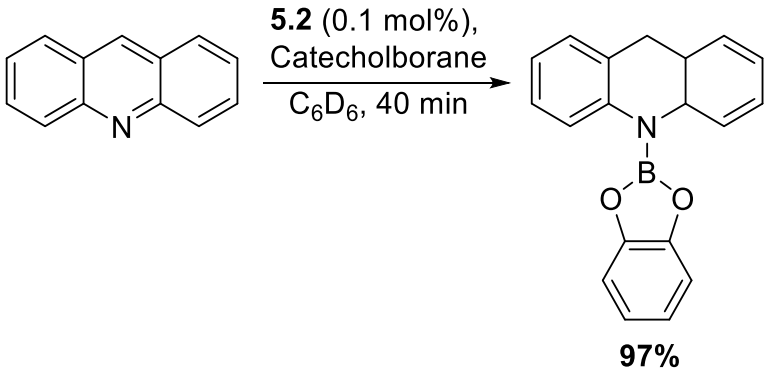

Scheme 5-7. Hydroboration of acridine at 25°C

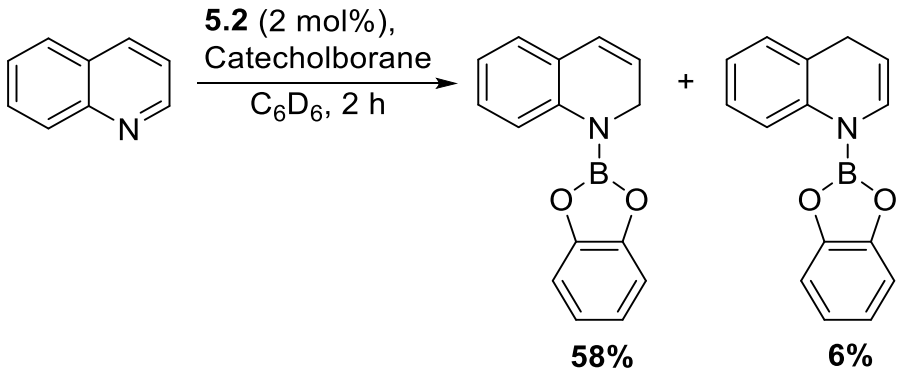

Scheme 5-8. Hydroboration of quinoline at 25°C

The hydroboration of acridine proceeded in near-quantitative yield in 40 minutes at a catalytic loading of 0.1 mol% **5.2**. Quinoline proved to be less successful, with the reaction stopping after two hours. The reaction did proceed with reasonable (~10:1) selectivity towards the 1,2 isomer, but Hill and co-workers reported 90% conversion in five hours with 100% selectivity to the 1,2 product using a magnesium catalyst, so the results are far from competitive.[319] Attempts to improve the conversion by heating the reaction to 50°C for two hours actually hindered the reaction, with ~3:1 selectivity and 55% conversion observed.

5.6 Hydrogenation of alkenes

One of the most industrially important rhodium-catalysed reactions is hydrogenation, with many valuable asymmetric variants reported in the literature.[321] Therefore, the ability of **5.2** to catalyse the hydrogenation of alkenes was investigated. The alkenes styrene and cyclohexene were reacted with 2 mol% **5.2** in fluorobenzene under an atmospheric pressure of hydrogen overnight. Due to limited time availability, the reaction times, solvent used and the catalyst loading (**Table 5-11**) were not optimised.

Table 5-11. Hydrogenation of alkenes

Substrate	Time (h)	Yield (%)[a]
Styrene	22	>99%
Cyclohexene	17	>99%

[a]: Yield measured against 1,3,5-trimethoxybenzene internal standard by ^{1}H NMR spectroscopy.

Despite not optimising the reaction times or catalyst loading, quantitative yields of the corresponding alkanes were observed without the need for high pressures of hydrogen

or dry/degassed solvent. Unfortunately, when more challenging substrates were tested (phenylacetylene and 4-nitroanisole) no conversion was observed.

5.7 Hydroformylation of 1-octene

Breit demonstrated that phosphinines are excellent ligands for hydroformylation,[28, 32, 160, 161] so the use of **2.1** in this reaction was tested. The hydroformylation of 1-octene was investigated in collaboration with Prof. Paul Kamer and Dr Rebecca How (University of St Andrews). Initially, activation of a 1:1 mixture of **2.1** and [Rh(acac)$(CO)_2$] under a 20 bar pressure of 1:1 CO/H_2 was investigated (**Scheme 5-9**). $^{31}P\{^1H\}$ NMR spectroscopic analysis of the reaction mixture showed that one major species was formed with two singlets observed (231 and 23 ppm, **Figure 5-13**), however, ^1H NMR spectroscopic analysis showed that no hydride-containing species were formed (**Figure 5-14**). In comparison, activation of a 1:1 mixture of Xantphos[322] and [Rh(acac)$(CO)_2$] under the same conditions gave clearly observable hydridic signals in the ^1H NMR spectrum (**Figure 5-15**).

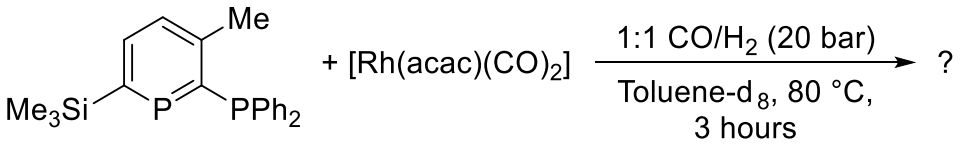

Scheme 5-9. Activation of **2.1** and [Rh(acac)$(CO)_2$] under standard hydroformylation conditions

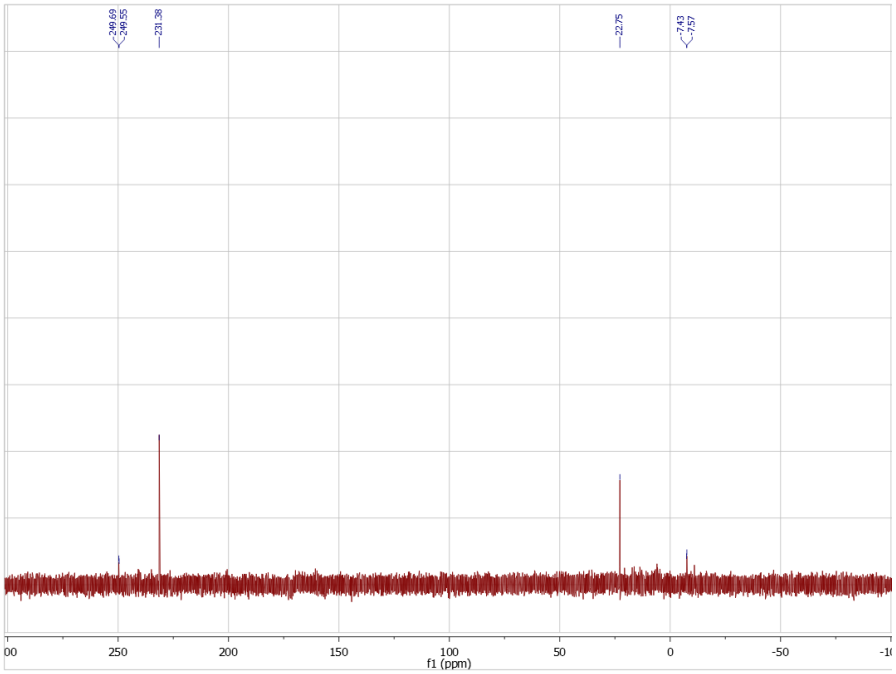

Figure 5-13. $^{31}P\{^{1}H\}$ NMR spectrum recorded after activation (**Scheme 5-9**)

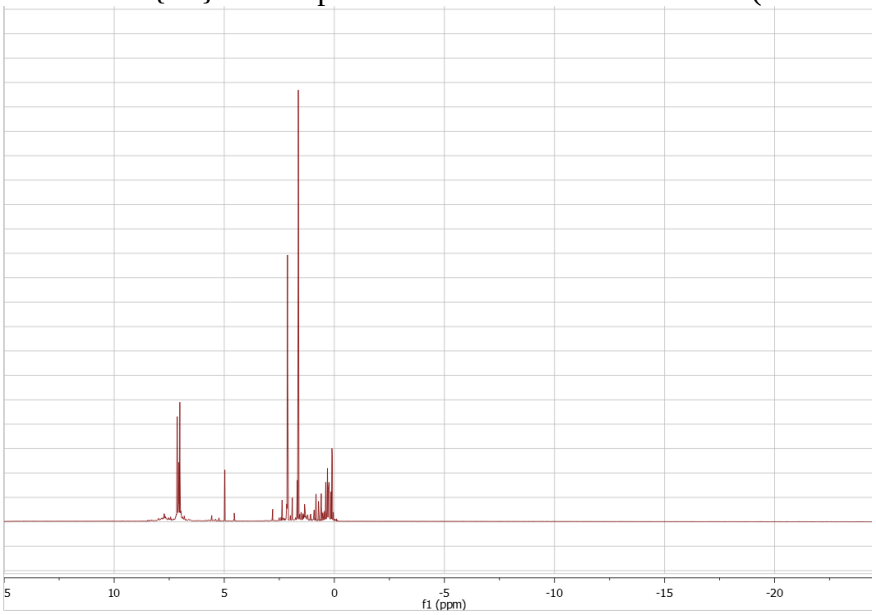

Figure 5-14. ^{1}H NMR spectrum recorded after activation (**Scheme 5-9**)

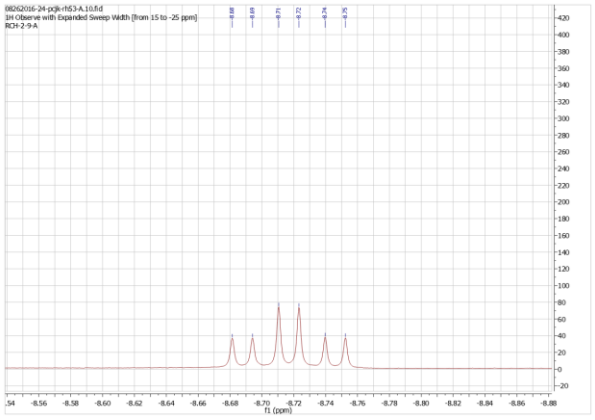

Figure 5-15. ^{1}H NMR spectrum showing a Rh-H formed by activation of Xantphos and $[Rh(acac)(CO)_2]$ under CO/H_2

To benchmark the performance of **2.1** as a ligand for the hydroformylation of 1-octene, three separate reactions were performed: $[Rh(acac)(CO)_2]$ without a ligand, with Xantphos, and with **2.1 (Scheme 5-10**, **Table 5-12**).

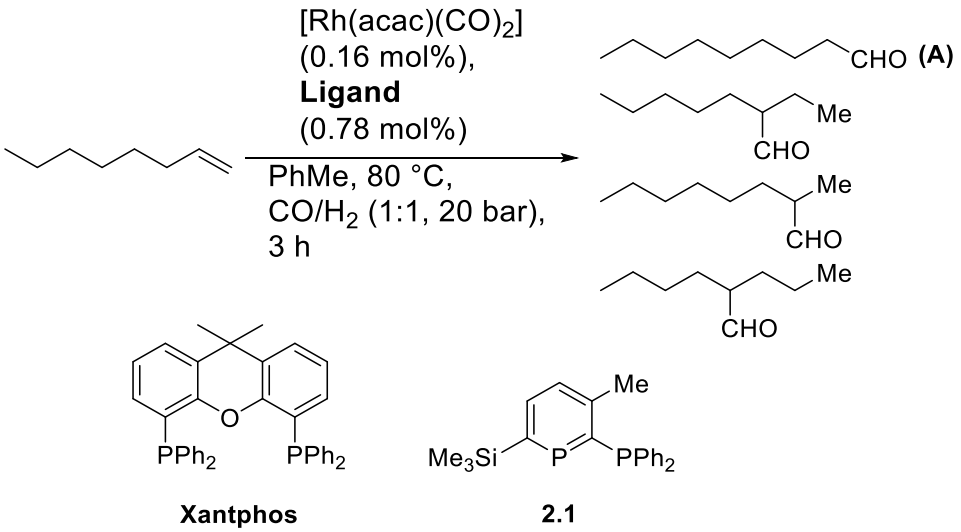

Scheme 5-10. Hydroformylation of 1-octene

Table 5-12. Results for the hydroformylation of 1-octene (averaged over the number of runs)

Ligand	# of runs	Consumption of 1-octene	Conversion to 1-octene isomers	Yield of aldehydes	Yield of A
none	3	97.9 %	27.1 %	68.7 %	27.8 %
Xantphos	4	46.3 %	3.8 %	40.0 %	39.2 %
2.1	2	7.2 %	2.3 %	4.3 %	3.3 %

The results in **Table 5-12** indicate that **2.1** is a poor ligand for hydroformylation, with only 4.3% of the substrate converted to a mixture of aldehydes. The runs where no ligand was used gave the highest conversion of 1-octene, however, ligands such as Xantphos are used because they provide a much greater selectivity to the industrially useful linear aldehyde. The poor results obtained from the use of **2.1** as a ligand in hydroformylation were not completely unexpected because whilst Breit demonstrated the effectiveness of phosphinines as ligands for this reaction, only monodentate or wide bite-angle ligands were used.[160] This is a common theme in hydroformylation catalysis because large bite-angle ligands often produce a higher ratio of linear to branched aldehyde, as well as more active catalysts.[88]

5.8 Conclusions

By reaction of **2.1** with 0.5 equivalents of [{$Rh(CO)_2Cl$}$_2$], the dinuclear complex **5.1** was isolated. The $^{31}P\{^1H\}$ NMR spectrum for **5.1** contained two second-order apparent

doublets-of-triplets instead of the expected doublets of doublets, and the coupling constants for these multiplets were obtained by calculations in collaboration with Dr Jason Lynam at the University of York. In addition to complete spectral characterisation, the molecular structure was obtained by X-ray diffraction.

In order to obtain a chelating complex that could be investigated in catalysis, the chelating COD co-ligand was used, and it was found that use of the weakly-coordinating anion $B(Ar^F)_4$ (tetrakis(3,5-bis{trifluoromethyl}phenyl)borate) was also necessary as $[BF_4]^-$ or $[SbF_6]^-$ salts afforded multiple products. Complex **5.2** was therefore obtained as an air stable solid and which was characterised completely.

Inspired by Weller, Willis and co-workers, who reported that rhodium complexes of small bite-angle diphosphines were highly active in hydroacylation,[283, 323] the use of **5.2** in the intramolecular hydroacylation of 4-pentenal was investigated, however, only alkene isomerisation was observed. The hydroboration of styrene was then attempted using catecholborane and **5.2**, however, whilst a mixture of the two (linear and branched) alcohols was obtained after oxidative workup, the obtained yields were poor and the regioselectivity (1.94 : 1, branched : linear) was not good.

The catalytic hydroboration of carbonyl substrates has been the focus of many recent papers,[253] and high activity was observed for **5.1** using 4′-bromoacetophenone as the substrate (96% in thirty minutes, 0.1 mol% **5.1**) whereas other catalysts performed poorly. A small substrate scope of acetophenones was studied, and high yields and clean reactivity was observed for all substrates with the exception of 4′-methoxyacetophenone, from which multiple (unknown) products were observed. After the success of ketone substrates, the hydroboration of benzaldehyde was investigated, however, it was observed that the rate of the background, non-catalysed reaction meant that the use of a catalyst was unnecessary. For more challenging substrates, the hydroboration of four ketimines was also attempted, and with the exception of an imine derived from *p*-nitroaniline, good yields (85-86%) were obtained within one hour at 50°C after increasing the catalyst loading to 1 mol%, although the reaction did not proceed further. Rapid hydroboration of acridine was possible using the optimised conditions of ketones, however, quinoline proved to be challenging, and high conversion to the 1,2- and 1,4- isomers could not be obtained. It was also observed that **5.2** was an active catalyst for the hydrogenation of styrene and cyclohexene, although the reaction conditions were not optimised.

In collaboration with Prof. Paul Kamer and Dr Rebecca How (of the Kamer group), the use of **2.1** in the Rh-catalysed hydroformylation of 1-octene was investigated, with

comparison to Xantphos. However, the results indicated that **2.1** was not a useful ligand for this reaction, with only 7.2% conversion of 1-octene, and a yield of 3.3% to 1-nonanal.

6 - Conclusions

6.1 Synthesis of phosphinophosphinines

Three new (phosphino)phosphinines have been prepared and fully characterised. Although addition of the first equivalent of phosphinoalkyne to diazaphosphinine went selectively, it was observed that the reaction of the second equivalent of diphenyl(prop-1-ynyl)phosphine was not regioselective during the second cycloaddition-cycloreversion step, resulting in the formation of two regioisomeric products, although their differing solubilities allowed for facile, chromatography-free separation. This reactivity differs markedly from the synthesis of 2,6-bis(diphenylphosphino)-3,5-diphenylphosphinine by Le Floch, Mathey and coworkers using 2-(diphenylphosphino)phenylacetylene, as they only observed a single product that required thirty-two hours for full conversion, compared to two weeks for the synthesis of **2.6** and **2.7**. The previously reported 2-(diphenylphosphino)-3-methylphosphinine was also prepared cleanly in good yield by desilylation of **2.1** using a method described previously for hydrocarbyl-substituted phosphinines. This synthetic route avoids the need for an expensive diene (piperylene, £74 for 1g) as well as a Pd(0) catalysed cross-coupling to install the phosphine. 2,6-bis(phosphino)phosphinine **2.6** was reacted with two equivalents of mesityl azide, affording a bis(iminophosphorane), however, it did not coordinate cleanly to any of the transition metal complexes that were examined.

6.2 Phosphinophosphinine coordination chemistry with group 6 metals

An optimised route to five phosphinophosphinine tetracarbonyl complexes of the group 6 metals was developed by reaction of **2.1** and **2.5** with $[M(diene)(CO)_4]$ precursors instead of the volatile homoleptic carbonyls. Infrared spectroscopic analysis of the carbonyl stretching frequencies facilitated the first experimental confirmation of a theory based on DFT calculations that *ortho*-$SiMe_3$ substitution of phosphinines increases their π-accepting properties. Comparison of the spectral data to that of analogous complexes containing phosphorus ligands placed the donor properties of **2.1** between PPh_3 and $P(OMe)_3$.

Calculations by Dr Natalie Fey allowed for evaluation of the properties of **2.1**, **2.5** and a range of other possible, similar phosphinophosphinines in comparison to known ligands through use of the P,P ligand knowledge base. The “maps” obtained indicated that the choice of substituent placement on the phosphinine ring could have a substantial effect

on the donor properties of the phosphinine. A degree of similarity to known PNP ligands used for selective ethylene oligomerisation was also observed, although they are more readily differentiated in the second principal component.

In collaboration with Sasol UK, **2.1** and **2.5** were tested as ligands for this ethylene oligomerisation. Whilst reduced activity and increased polymer formation was observed in comparison to the commerical PNP ligand, the obtained results demonstrated high selectivity to 1-octene over 1-hexene, although increased amounts of higher MW oligomers were produced as well.

6.3 Ruthenium phosphinophosphinine complexes

The first structurally characterised example of a complex (**4.1**) containing a chelating phosphinophosphinine ligand was prepared by reaction of **2.1** with *cis*-$[Ru(dmso)_4(Cl)_2]$. Attempts to prepare "half-sandwich" complexes from $[\{Ru(\eta^6\text{-arene})Cl_2\}_2]$ precursors were generally unsuccessful, as reaction with the *p*-cymene dimer proceeded by displacement of the arene, affording a mixture of a dinuclear complex as well as **4.1**. Reactions with the hexamethylbenzene dimer in the presence of various halide-abstracting reagents resulted in the formation of multiple, inseparable products with the exception of NH_4PF_6. However, due to the hygroscopic nature of ammonium salts, the water present in the salt resulted in the formation of a complexes containing a P-hydroxy phosphacyclohexadiene ligand, as well as cleavage of the $SiMe_3$ group. The reaction of **2.1** with $[\{Ru(Cp^*)Cl\}_4]$ yielded a single, spectroscopically characterised complex, however, the only crystal structure obtained also contained a phosphacyclohexadienyl ligand after *syn* addition of water to a P=C bond.

The obtained Ru complexes were tested in the catalytic transfer hydrogenation of acetophenones, and it was found that only octahedral complex **4.1** was active in this reaction. However, it demonstrated high reactivity with good to excellent yields obtained within one hour at 0.1 mol% loading. **4.1** was also a competent catalyst for the upgrading of ethanol and methanol to isobutanol in the Guerbet reaction, producing the desired alcohol in a 50% yield, although extended reaction times were required compared to the leading catalyst.

6.4 Rhodium phosphinophosphinine complexes

Upon reaction of **2.1** with $[\{Rh(CO)_2Cl\}_2]$, a dinuclear chlorocarbonyl complex with bridging ligands was observed. In an attempt to prepare a chelating complex, COD was used as a co-ligand by reaction of **2.1** with $[\{Rh(COD)Cl\}_2]$ in the presence of $AgBF_4$

or $AgSbF_6$, however, multiple products were observed by $^{31}P\{^1H\}$ NMR. By switching precursors to $[Rh(COD)_2][B(Ar^F)_4]$, which contains a very bulky and poorly coordinating anion, the air-stable complex **5.2** was obtained. After complete characterisation of both complexes, their use in the hydroboration of carbonyl compounds was investigated. Complex **5.2** proved to be a highly active catalyst, and is the first reported rhodium catalyst for this reaction. Whilst **5.1** was considerably less reactive, it was still a more efficient catalyst than any other combination of rhodium precursor and phosphorus ligand tested.

7 - Future Work

7.1 Ligand Design

The computational ligand mapping done in collaboration with Dr Natalie Fey revealed that substituent modification on *ortho*-(phosphino)phosphinine ligands can have a substantial effect on their properties.[188] As there is wide commercial availability or synthetic accessibility of alkynes, Grignard reagents, chlorosilanes and dialkyl/diarylchlorophosphines or phosphites, a thorough experimental investigation of the effects of substituent variation in (phosphino)phosphinine ligands is vital for the further development of the field and to aid ligand optimisation. **Scheme 7-1** details a brief overview of how these substituent variations could be incorporated to facilitate changes both electronically and sterically. Whilst this is not an entirely generic methodology, as reagents such as $ClPMe_2$ are not readily available, it allows for a substantial range of modification. There is also the potential for installing chiral centres, for example, using binapthyl fragments, or synthesis of chiral-at-phosphorus ligands using common chiral-auxiliaries such as (-)-menthol. Conveniently, Imamoto *et. al.* have published the synthesis of P-stereogenic phosphinoalkynes[324] derived from the widely used and easily resolved secondary phosphine (*tert*-butyl)methylphosphine.[325-328]

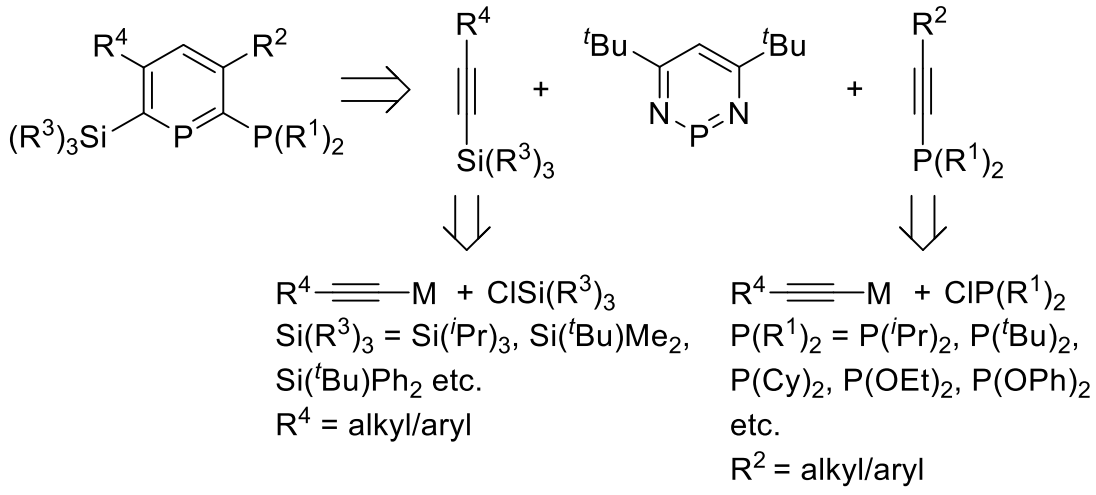

Scheme 7-1. Synthetic route to modified (phosphino)phosphinine ligands based on the structure of **2.1**. M = alkali metal or MgX

To expand the bite-angle of the ligands, a silyl methyl "bridge" could also be incorporated (**Scheme 7-2**, **A**). Whilst a silylphosphine (**B)** could theoretically be used directly, the phosphorus-silicon bond is known to be highly sensitive.

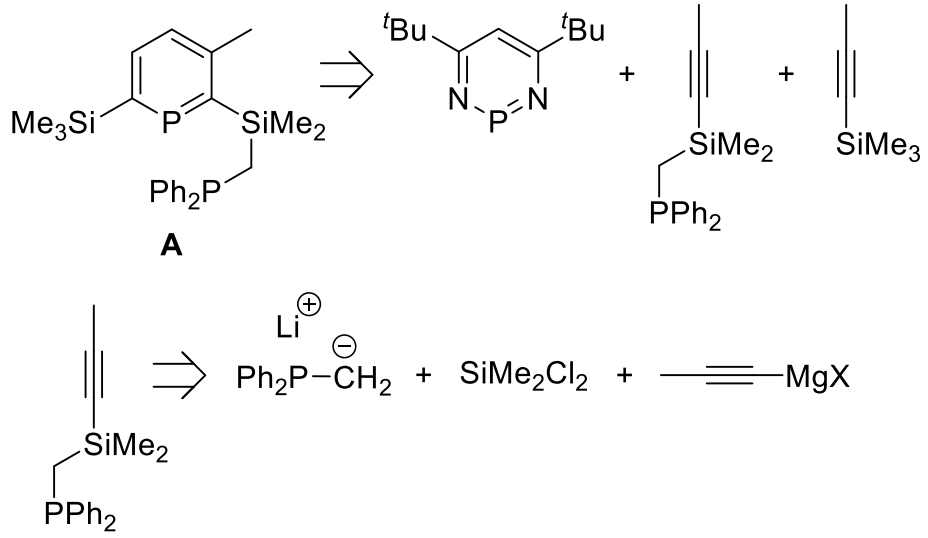

Scheme 7-2. Potential synthetic route to **A**

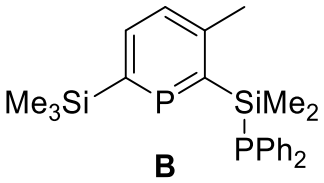

Figure 7-1. Hypothetical (silylphosphino)phosphinine **B**

When a library of appropriate size has been prepared, efficient comparisons can be made by investigating their use in a catalytic reaction.

7.2 Catalytic Reactions

This thesis covers only a limited range of catalytic reactions due to available time and limitations on the coordination of **2.1** to many metal fragments, however, it is important to investigate both the activation mechanisms of the reported catalysts (*e.g.* **4.1** and **5.1**) as well as discover new (phosphino)phosphinine catalysts to expand upon the foundations laid by this work.

Brief attempts at synthesis of an η^6-fluorobenzene complex from **5.1** by hydrogenation of the labile cyclooctadiene ligand, based on work by Weller and Willis,[283] resulted in the formation of a major product by $^{31}P\{^1H\}$ NMR spectroscopy, although no fluorine incorporation was observed. The suspected, but unconfirmed, product is **C** (**Figure 7-2**), based on the analogous product obtained by hydrogenation of [Rh(dppe)(COD)][BF_4].[329, 330] However, this issue could be circumvented by the use of

a non-aryl phosphine donor. The scope of utility for both **5.1** and future Rh complexes is large, and could include such reactions as alkyne trimerisation[331] and the conjugate addition of boronic acids to enones.[332]

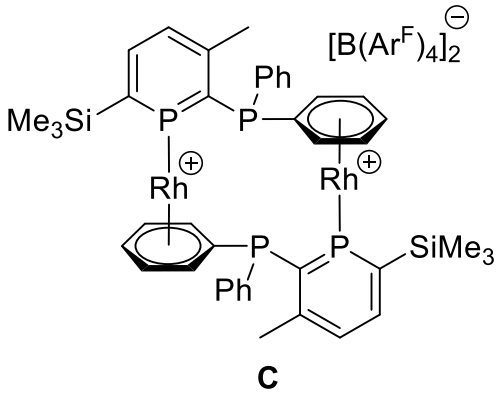

C

Figure 7-2. Suspected dinuclear product **C**

Initial tests implied that Ru complex **4.1** is a true homogeneous catalyst for the transfer hydrogenation of acetophenones. However, studies including monitoring NMR reactions in isopropanol-d_8 by $^{31}P\{^1H\}$ NMR spectroscopy, isolation of the dihydride complex **4.6** and DFT calculations are all necessary. These will enable a greater understanding to why **4.1** displays high activity (at room temperature), when *cis*-$[Ru(dppm)_2(Cl)_2]$ is inactive and initial studies into *cis*-$[Ru\{PPh_2(2\text{-}Pyr)\}_2(Cl)_2]$ also suggest reduced activity for this species.

Further work is also necessary to understand the activity of **5.1** in the hydroboration of carbonyl substrates, when other ligands tested produced poorly active catalysts. It was also noted that free (phosphino)phosphinine **2.1** displayed increased catalytic activity versus other Rh catalysts in the same reaction, although a yield of 95% was observed only after 14 hours at 0.1 mol%. Whilst not a highly efficient catalyst, it is worth investigating whether the **2.1**-catalysed hydroboration of other substrates such as alkenes/alkynes would be possible.

8 - Experimental

8.1 Experimental methods

All reactions were performed under an oxygen-free nitrogen atmosphere using standard Schlenk line techniques or by using an MBRAUN UNIlab Plus glovebox unless otherwise noted. Anhydrous toluene, dichloromethane, acetonitrile and THF were obtained from an MBRAUN SPS-800 solvent purification system. 40-60 petroleum ether was distilled from sodium wire under nitrogen. Chloroform, $CDCl_3$, HMDSO, pivalonitrile, and triethylamine were distilled from calcium hydride. Isopropanol and CD_2Cl_2 were dried over 4Å molecular sieves. Benzene-d_6 was dried over molten potassium, distilled under a static vacuum and stored in the glovebox. Anhydrous ethanol and methanol were purchased from Sigma-Aldrich. All anhydrous solvents were degassed before use and stored over activated molecular sieves. Non-dry solvents were used as received from Fisher Scientific. Borane-dimethylsulfide complex, 1,4-diazabicyclo[2.2.2]octane (DABCO), diphenyl(prop-1-ynyl)phosphine, 1M HCl in ether, **2.4** , **2.5**, **2.8**, [Cr(NBD)$(CO)_4$], [Mo(NBD)$(CO)_4$], [W(COD)$(CO)_4$], **3.1**, **3.2**, **3.3**, **3.4**, **3.5**, **4.1**, [Ru(Cp*)$Cl_2]_n$, [{Ru(Cp*)Cl}$_4$], **4.3**, **4.4**, **4.5** [{Rh$(CO)_2$Cl}$_2$], **5.1**, [{Rh(COD)Cl}$_2$], Na[B$(Ar^F)_4$] and catecholborane were stored under a nitrogen atmosphere. 4,6-di(tert-butyl)-1,3,2-diazaphosphinine was used immediately after preparation. Catecholborane was distilled under a static vacuum and stored at -25°C, all other commercial reagents were used as received. NMR spectra were recorded at 25°C, unless otherwise stated, on a Bruker AVIII300, AVI400, AV500, AV600 or a Jeol ECS400 spectrometer using the internal residual protio resonance from the deuterated solvent as a reference (^{1}H and ^{13}C{^{1}H} NMR spectra). ^{11}B, ^{29}Si, ^{19}F and ^{31}P were referenced to external samples of $BF_3.OEt_2$, $SiMe_4$, $CFCl_3$ and 85% H_3PO_4 in H_2O respectively as 0 ppm. 4,6-di(tert-butyl)-1,3,2-diazaphosphinine,[57] diphenyl(1-prop-1-ynyl)phosphine,[166] mesityl azide,[333] [Cr(NBD)$(CO)_4$],[334] [Mo(NBD)$(CO)_4$],[334] [W(COD)$(CO)_4$],[335] [Ru$(DMSO)_4Cl_2$],[336] [Ru(Cp*)$Cl_2]_n$,[337] [{Ru(Cp*)Cl}$_4$],[338] [{Ru(*p*-cymene)Cl_2}$_2$],[339] [{Ru$(C_6Me_6)Cl_2$}$_2$],[340] [{Rh$(CO)_2$Cl}$_2$],[341] [{Rh(COD)Cl}$_2$],[342] Na[B$(Ar^F)_4$],[343] and [Rh$(COD)_2$][B$(Ar^F)_4$][344] were prepared according to literature procedures. Mass spectrometry analysis was performed at the EPSRC UK National Mass Spectrometry Facility at Swansea University using an Atmospheric Solids Analysis Probe interfaced to a Waters Xevo G2-S (**2.2**, **2.3**, **2.8**, **3.1**, **3.3**, **3.4**, **3.5**, **4.1**, **4.2**, **4.3**, **4.4**, **4.5**, **5.1**, **5.2**), using EI on a MAT95 instrument (**2.5**), or at the University of Edinburgh using EI on a ThermoElectron MAT 900 (**2.6**, **3.2**) or on a Finnigan

(Thermo) LCQ Classic ion trap mass spectrometer (**2.1**). FTIR was performed on a Thermo Scientific Nicolet iS5/iD5 ATR spectrometer. Elemental analyses were conducted by Dr Brian Hutton using an Exeter CE-440 elemental analyser at Heriot-Watt University or by Mr Stephen Boyer at London Metropolitan University.

8.2 Chapter 2 – Ligand synthesis

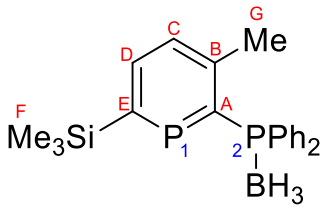

2.2 - 2-diphenylphosphino-borane-3-methyl-6-trimethylsilylphosphinine

To a solution of diazaphosphinine (2.73g, 13.8 mmol) in 100 cm^3 toluene was added a dry and degassed solution of diphenyl(prop-1-ynyl)phosphine (3.09g, 13.8 mmol, 1 equiv.) in toluene (10 cm^3) and the reaction was stirred at 125°C for 2 hours. After confirming consumption of the diazaphosphinine by $^{31}P\{^1H\}$ NMR spectroscopy, trimethylsilylacetylene (2.0 cm^3, 14.4 mmol, 1.04 equiv.) was added and the reaction stirred at 85°C for 20 hours. Once the reaction was confirmed to be complete by ^{31}P NMR spectroscopy, the contents of the flask were transferred to a round-bottomed flask and all volatiles removed on a rotary evaporator. With vigorous stirring, the contents of the flask were extracted with 400 cm^3 of ether and the solution filtered through a sintered-glass funnel; this process was repeated two more times before all solvent was removed on a rotary evaporator. The resulting oil was eluted through a 5cm plug of silica with toluene until the eluent was colourless. All solvent was then removed on a rotary evaporator and the oil transferred to a Schlenk flask fitted with a magnetic stir-bar. 30 cm^3 of pentane was added to the Schlenk flask and the RBF was washed with a further 20 cm^3. With vigorous stirring, borane-dimethylsulfide (1.4 cm^3, 14.8 mmol, 1.1 equiv.) was added via syringe. After a few seconds a white precipitate formed and heterogeneous mixture was stirred for 15 minutes. The stirrer-bar was then removed and the suspension left to stand for 24 hours. After cannula filtration and two subsequent (30 cm^3) pentane washes, the precipitate was dried under high-vacuum to give **2.2** (3.64g, 9.57 mmol, 69%) as a colourless, foul-smelling solid. Crystals suitable for X-ray diffraction were grown from the pentane filtrate upon standing at room temperature overnight.

^{1}H NMR (400 MHz, $CDCl_3$): δ = 7.98 (m, 1H, H_D), 7.75-7.41 (m, 10H, PPh_2), 7.36 (m, 1H, H_C), 2.48 (s, 3H, H_G), 2.08-0.74 (bm, 3H, BH_3), 0.27 (s, 9H, H_F); **^{31}P{^{1}H} NMR (162 MHz, $CDCl_3$):** δ = 255.4 (d, P_1, $^{2}J_{P1\text{-}P2}$ = 72.8 Hz), 22.7 (bs, P_2); **^{13}C{^{1}H} NMR (100 MHz, $CDCl_3$):** δ = 167.3 (dd, C_E, $^{2}J_{CE\text{-}P1}$ = 80.3 Hz, $^{2}J_{CE\text{-}P2}$ = 5.9 Hz), 156.8 (dd, C_A, $^{1}J_{CA\text{-}P1}$ = 84.7 Hz, $^{1}J_{CA\text{-}P2}$ = 41.6 Hz), 150.4 (dd, C_B, $^{2}J_{CB\text{-}P1}$ = 12.2 Hz, $^{2}J_{CB\text{-}P2}$ = 12.0 Hz), 136.6 (dd, PPh_2), 132.7 (dd, C_C, $^{3}J_{CC\text{-}P1}$ = 19.3 Hz, $^{3}J_{CC\text{-}P2}$ = 8.9 Hz), 131.5 (s, PPh_2), 129.8 (dd, C_D, $^{2}J_{CD\text{-}P1}$ = 57.4 Hz, $^{4}J_{CD\text{-}P2}$ = 6.0 Hz) 128.9 (d, PPh_2), 26.3 (d, C_G, $^{3}J_{CG\text{-}P1}$ = 7.0 Hz), 0.1 (d, C_F, $^{3}J_{CF\text{-}P1}$ = 7.0 Hz); **^{11}B{^{1}H} NMR (96 MHz, $CDCl_3$):** δ = -35.8 (bs, BH$_3$); **^{29}Si{^{1}H} NMR (79 MHz, $CDCl_3$):** δ = -0.8 (dd, SiMe$_3$, $^{2}J_{Si\text{-}P1}$ = 37.3 Hz, $^{4}J_{Si\text{-}P2}$ = 1.6 Hz); **HRMS (ASAP/QTof):** *m/z*: ([M-H]$^{+}$) Calcd. for $C_{21}H_{27}BP_2Si$: 379.1376; Found: 379.1370; **Elemental Analysis:** Anal. Calcd. for $C_{21}H_{24}P_2Si$: C 66.33, H 7.16; Found: C 66.41, H 7.17

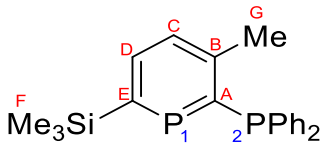

<u>2.1</u> - 2-diphenylphosphino-3-methyl-6-trimethylsilylphosphinine

Method A: To a Schlenk flask containing **2.2** (597 mg, 1.57 mmol, 1 equiv.) and 1,4-diazabicyclo[2.2.2]octane (88.1 mg, 0.79 mmol, 0.5 equiv.) was added dry toluene (10 cm^3), and the pale yellow solution was allowed to stir for 18 hours. All volatiles were then removed under high vacuum. The residue was then extracted with pentane (3 x 20 cm^3), concentrated to ~20 cm^3 and stored at -25°C for 1 hour. Cannula filtration of the cold mixture removed the majority of residual [DABCO(BH$_3$)$_2$] before all volatiles were then removed under high vacuum leaving a viscous oil which solidified over several hours. Under air, the resulting solid was transferred to a fritted filter funnel and extracted with 3 x 20 cm^3 portions of hexane. All solvent was then removed under vacuum leaving **2.1** (558 mg, 1.52 mmol, 97%) as a pale yellow solid.

Method B: The crude reaction mixture from the above phosphinine synthesis was concentrated to a thick oil on a rotovap. This oil was adsorbed onto silica gel by dissolution in dichloromethane, addition of silica gel and careful concentration on a rotovap. This process was repeated until a dry, free-flowing powder was obtained. This powder was then loaded onto a silica gel column (5 cm x 20 cm) and eluted initially with 40-60 petrol to remove impurities. The product was then eluted with 5:95 ethyl acetate:40-60 petrol. Fractions containing the product were combined and concentrated on a rotovap, yielding a thick yellow oil that slowly solidified. The crude product was

dissolved in a minimum of pentane and stored at -25°C for 24h. The precipitated product was collected on a frit and dried *in vacuo*. The filtrate was concentrated to ½ volume on a rotovap and stored at -25°C to collect a second crop, with a total yield of 60-70%.

Crystals of the product suitable for X-ray diffraction were grown from degassed hexane solution at -25°C.

^{1}H NMR (400 MHz, $CDCl_3$): δ = 7.92 (m, 1H, H_D), 7.44-7.28 (m, 11H, PPh_2 & H_C), 2.53 (s, 3H, H_G), 0.29 (s, 9H, H_F); **^{31}P{^{1}H} NMR (162 MHz, $CDCl_3$):** δ = 249.8 (d, P_1, $^{2}J_{P1\text{-}P2}$ = 31.6 Hz), -7.5 (d, P_2, $^{2}J_{P2\text{-}P1}$ = 31.6 Hz); **^{13}C{^{1}H} NMR (100 MHz, $CDCl_3$):** δ = 167.9 (d, C_E, $^{1}J_{CE\text{-}P1}$ = 80.7 Hz), 166.4 (dd, C_A, $^{1}J_{CA\text{-}P1}$ = 87.1 Hz, $^{1}J_{CA\text{-}P2}$ = 24.0 Hz), 148.1 (dd, C_B, $^{2}J_{CB\text{-}P1}$ = 23.2 Hz, $^{2}J_{CB\text{-}P2}$ = 12.0 Hz), 137.5 (d, PPh_2), 136.2 (m, C_C), 134.3 (dd, PPh_2), 130.5 (dd, C_D, $^{2}J_{CD\text{-}P1}$ = 20.8 Hz, $^{4}J_{CD\text{-}P2}$ = 4.0 Hz), 128.8 (s, PPh_2), 128.4 (d, PPh_2), 24.1 (d, C_G, $^{3}J_{CG\text{-}P1}$ = 24.8 Hz), -0.1 (d, C_F, $^{3}J_{CF\text{-}P1}$ = 6.4 Hz); **^{29}Si{^{1}H} NMR (79 MHz, $CDCl_3$):** δ = -1.6 (d, $SiMe_3$, $^{2}J_{Si\text{-}P1}$ = 36.6 Hz); **EI** *m/z*: ([M]$^{+}$) 366.1; **Elemental Analysis:** Anal. Calcd. for $C_{21}H_{24}P_2Si$: C 68.83, H 6.60; Found: C 68.74, H 6.69.

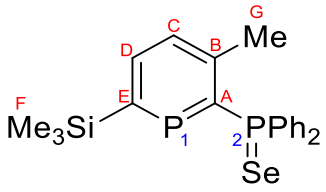

<u>2.3</u> - 2-seleno-diphenylphosphino-3-methyl-6-trimethylsilylphosphinine

An ampoule was charged with **2.1** (100 mg, 0.27 mmol), selenium powder (50 mg, 0.63 mmol, 2.3 equiv.) and toluene (2 cm^3) then sealed with a Youngs tap. The reaction was heated to 120°C for 18 hours, then filtered to remove excess selenium. The filtrate was concentrated to ½ volume and stored at -25°C for one week. Filtration, followed by drying under high-vacuum yielded **2.3** (80 mg, 66%) as pale yellow crystalline powder.

^{1}H NMR (400 MHz, $CDCl_3$): δ = 8.09-8.03 (m, 4H, *ortho*-PPh_2), 7.68-7.63 (m, 1H, H_D), 7.01-6.94 (m, 7H, PPh_2 & H_C), 2.69 (s, 3H, H_G), 0.15 (s, 9H, H_F); **^{31}P{^{1}H} NMR (162 MHz, $CDCl_3$):** δ = 249.0 (d, P_1, $^{2}J_{P1\text{-}P2}$ = 100.6 Hz), 34.4 (d, P_2, $^{2}J_{P1\text{-}P2}$ = 97.1 Hz, ^{77}Se satellites (7.63% abundant): dd, $^{1}J_{Se\text{-}P2}$ ≈ 749.1 Hz); **HRMS (ASAP/QTof):** *m/z*: ([M+H]$^{+}$) Calcd. for $C_{21}H_{24}P_2SeSi$: 447.0367; Found: 447.0369; **Elemental Analysis:** Anal. Calcd. for $C_{21}H_{24}P_2SeSi$: C 56.63, H 5.43; Found: C 56.89, H 5.37.

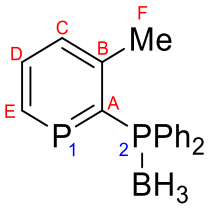

2.4 - 2-diphenylphosphino-borane-3-methylphosphinine

To a Schlenk flask containing a solution of **2.2** (1.006 g, 2.65 mmol) in dry CH_2Cl_2 (15 cm^3) was added a 1M solution of HCl in ether (2.65 cm^3, 2.65 mmol). The resulting solution was stirred for 24 h before an aliquot was analysed by ^{31}P NMR spectroscopy. Once the reaction was confirmed to be complete, all volatiles were removed *in vacuo* and the resulting solid dried under high vacuum. The product was recrystallized from toluene at -25°C, producing a crop of analytically pure, colourless single crystals suitable for X-ray diffraction (432 mg, 1.40 mmol, 53 %).

^{1}H NMR (400 MHz, $CDCl_3$): δ = 8.59 (m, 1H, H_E), 7.85 (m, 1H, H_D), 7.73 (m, 4H, *o*-PPh_2), 7.59-7.44 (m, 7H, *m,p*-PPh_2, H_C), 2.55 (s, 3H, H_F), 2.12-0.87 (bm, 3H, BH_3); **^{31}P{^{1}H} NMR (162 MHz, $CDCl_3$):** δ = 229.7 (d, P_1, $^2J_{P1\text{-}P2}$ = 79.8 Hz), 23.0 (bs, P_2); **^{13}C{^{1}H}-NMR (100 MHz, $CDCl_3$):** δ = 156.6 (dd, phosphinine C, *J* = 40.2 Hz, 70.4 Hz), 151.37 (dd, phosphinine CH, *J* = 10.1 Hz, 57.3 Hz), 150.4 (m, 2 overlapping phosphinine CH, *J* = 8.0 Hz, 13.1 Hz), 135.2 (dd, PPh_2, *J* = 3.0 Hz, 11.1 Hz), 133.8-133.5 (m, PPh_2, *J* = 2.0 Hz, 9.1 Hz), 131.4 (d, PPh_2, *J* = 2.0 Hz), 129.8-129.1 (dd, phosphinine CH, *J* = 7.0 Hz, 58.3 Hz), 128.8 (d, PPh_2, *J* = 11.1 Hz), 26.1 (d, C_F, $^3J_{C\text{-}P1}$ = 7.4 Hz); **^{11}B{^{1}H} NMR (128 MHz, $CDCl_3$):** δ = -36.1 (bs, BH_3); **Elemental Analysis:** Anal. Calcd. for $C_{18}H_{19}BP_2$: C 70.17, H 6.22; Found: C 70.11, H 6.14.

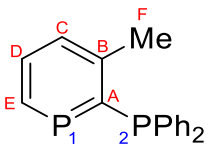

2.5 - 2-diphenylphosphino-3-methylphosphinine

To a Schlenk flask containing a solution of **2.1** (512.3 mg, 1.40 mmol) in dry CH_2Cl_2 (10 cm^3) was added a 1M solution of HCl in ether (1.4 cm^3, 1.4 mmol, 1 equiv.). The resulting solution was stirred for 24 h before an aliquot was analysed by ^{31}P NMR spectroscopy. Once the reaction was confirmed to be complete, all volatiles were removed *in vacuo* and the resulting solid dried under high vacuum. The product was recrystallized from 40-60 petrol at -25°C, producing a colourless microcrystalline solid (319 mg, 1.08 mmol, 77%). Data match literature values.[50]

^{1}H NMR (300 MHz, C_6D_6): δ = 8.37 (dd, 1H, H_E, $^{2}J_{HE-P1}$ = 40.7 Hz, $^{3}J_{HE-H5}$ = 9.9 Hz), 7.46-7.40 (m, 4H, *o*-PPh_2), 7.30 (m, 1H, H_D), 7.06-7.04 (m, 6H, *m,p*-PPh_2), 6.94-6.89 (m, 1H, H_C) 2.42 (s, 3H, H_F); **^{31}P{^{1}H} NMR (121 MHz, C_6D_6):** δ = 224.9 (d, P_1, $^{2}J_{P1-P2}$ = 31.2 Hz), -7.6 (d, P_2, $^{2}J_{P2-P1}$ = 31.2 Hz); **HRMS** (EI/MS) *m/z* ([M]$^{+}$) Calc. for $C_{18}H_{16}P_2$ 294.0722; Found 294.0715; **Elemental Analysis:** Anal. Calcd. for $C_{18}H_{16}P_2$: C 73.45, H 5.48; Found: C 73.39, H 5.45.

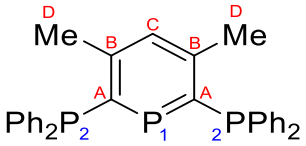

2.6 – 2,6-bis(diphenylphosphino)-3,5-dimethylphosphinine

To a solution of diazaphosphinine (374 mg, 1.78 mmol) in 20 cm^3 toluene was added a solution of diphenyl(prop-1-ynyl)phosphine (798 mg, 3.56 mmol, 2 equiv.) in toluene (5 cm^3). The solution was heated at 120°C in a sealed Youngs ampoule until ^{31}P NMR spectroscopy showed complete conversion of diazaphosphinine to two isomeric products in a 60:40 ratio (~2 weeks). All volatiles were removed under reduced pressure and the resulting oil was extracted with 150 cm^3 of 40-60 petrol and filtered through a frit. The workup must be completed as quickly as possible to avoid decomposition of product under air. The residual solid was then returned to the flask and extracted until ^{31}P NMR spectroscopy of the solid showed no triplet at 244 ppm (~5 times). Once all of **2.6** had been extracted, the petrol extract was concentrated on a rotovap. The resulting oil was dissolved in CH_2Cl_2 and concentrated in volume under reduced pressure to leave a thick, reddish-black oil. Pentane (10 cm^3) was slowly added by pipette down the side of the flask, forming a layer on top of the oil. The flask was left for a maximum of an hour (to avoid decomposition) to allow for slow precipitation of a brown crystalline solid. If precipitation did not occur to a satisfactory level, 50 ml more pentane was added and the contents shaken well then filtered through a sinter. The brown precipitate was washed with 3 x 10 ml portions of pentane then dried thoroughly under vacuum. Recrystallisation from toluene at -25°C produced the pure product as a colourless solid (0.45g, 0.91 mmol, 51%). Crystals suitable for X-ray diffraction were grown from a 10:1 solution of anhydrous THF and 40-60 petroleum ether at -25°C.

^{1}H NMR (400 MHz, , $CDCl_3$): δ = 7.32-7.20 (m, 20H, 2 x PPh_2), 7.18-7.14 (m, 1H, H_C), 2.35 (s, 6H, H_D); **^{31}P{^{1}H} NMR (162 MHz, $CDCl_3$):** δ = 244.8 (t, P_1, $^{2}J_{P-P}$ = 38.9 Hz), -8.1 (d, 2P, P_2,, $^{2}J_{P-P}$ = 38.9 Hz); **^{13}C{^{1}H} NMR (100 MHz, $CDCl_3$):** δ = 164.22 (dd, 2C, C_A, $^{1}J_{CA-P1}$ = 84.5 Hz, $^{1}J_{CA-P2}$ = 24.1 Hz), 147.38 (dd, 2C, C_B, $^{2}J_{CB-P1}$ = 23.1 Hz,

$^{2}J_{CB\text{-}P2}$ = 11.1 Hz), 136.1 (t, C_C, $^{3}J_{CC\text{-}P2}$ = 9.8 Hz) 134.5-128.0 (m, 2 x P*Ph*$_2$), 23.5 (d, 2C, C_D, $^{3}J_{CD\text{-}P}$ = 23.1 Hz); **EI:** *m/z*: ([M]$^+$) 492.1; **Elemental Analysis:** Anal. Calcd. for $C_{31}H_{27}P_3$: C 75.61, H 5.53. Found: C 75.50, H 5.49.

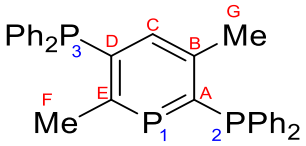

<u>2.7</u> – 2,5-bis(diphenylphosphino)-3,6-dimethylphosphinine

The petrol insoluble crude solid from the previous procedure was mixed with sand and transferred to a Soxhlet thimble. The Soxhlet apparatus was then connected to a round-bottom flask containing 300 cm^3 of hexane and a condenser. The solid was then extracted for one week under air, ensuring the volume of hexane in the apparatus didn't decrease significantly. Over the course of one week a white precipitate formed in the flask. Once the extraction was finished the precipitate was collected on a sintered funnel, washed with 3 x 10 cm^3 portions of hexane and dried *in vacuo*. The product was then dissolved in a minimum amount of boiling toluene and the solution stored at -25°C, yielding a pure, colourless solid (0.19 g, 0.39 mmol, 22%). Single crystals suitable for X-ray diffraction were grown by slow diffusion of ether into a THF solution (obtained by boiling the solvent and allowing to cool) of the recrystallized product.

^{1}H-NMR (300 MHz, CDCl$_3$): δ = 7.45-7.31 (m, 20H, 2 x P*Ph*$_2$) 6.74 (bs, 1H, H_C), 2.49 (d, 3H, H_F, $^{3}J_{HF\text{-}P1}$ = 16.0 Hz), 2.17 (s, 3H, H_G); **^{31}P{^{1}H}-NMR (162 MHz, CDCl$_3$):** δ = 220.8 (dd, P_1, $^{2}J_{P1\text{-}P2}$ = 29.2 Hz, $^{3}J_{P1\text{-}P3}$ = 4.9 Hz), -9.1 (dd, P_2, $^{2}J_{P2\text{-}P1}$ = 29.4 Hz, $^{5}J_{P2\text{-}P3}$ = 2.5 Hz), -10.4 (d, P_3, $^{3}J_{P3\text{-}P1}$ = 4.9 Hz); **^{13}C{^{1}H}-NMR (100 MHz, CDCl$_3$):** δ = 169.6 (dd, C_E, $^{1}J_{CE\text{-}P1}$ = 59.9 Hz, $^{2}J_{CE\text{-}P3}$ = 19.2 Hz), 167.1 (dd, C_A, $^{1}J_{CA\text{-}P1}$ = 75.1 Hz, $^{2}J_{CA\text{-}P2}$ = 24.0 Hz), 145.3 (dd, C_B, $^{2}J_{CB\text{-}P1}$ = 22.4 Hz, $^{2}J_{CB\text{-}P2}$ = 12.8 Hz), 142.6 (dd, C_D, $^{1}J_{CD\text{-}P1}$ = 22.4 Hz, $^{2}J_{CD\text{-}P3}$ = 12.8 Hz), 136.5 (m, C_C, $^{3}J_{CC\text{-}P1}$ = 15.2 Hz), 136.0 (t, PPh$_2$, *J* = 8.8 Hz), 135.7 (d, PPh$_2$, *J* = 11.2 Hz), 134.3(t, PPh$_2$, *J* = 20.0 Hz), 129.1-128.5 (m, PPh$_2$), 23.8 (d, C_G, $^{3}J_{CG\text{-}P1}$ = 24.1 Hz), 23.5 (dd, C_F, $^{2}J_{CF\text{-}P1}$ = 43.3 Hz, $^{3}J_{CF\text{-}P3}$ = 24.1 Hz); **EI:** *m/z:* ([M]$^+$) 492.1; **Elemental Analysis:** Anal. Calcd. for $C_{31}H_{27}P_3$: C 75.61, H 5.53. Found: C 75.47, H 5.71.

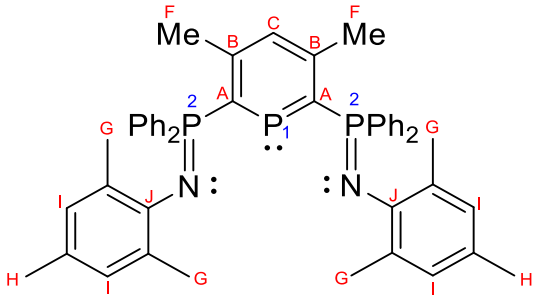

2.8 - 2,6-bis{diphenyl(N-mesityl)iminophosphorano}-3,5-dimethylphosphinine

To a Schlenk flask containing freshly recrystallized **2.6** (432 mg, 0.88 mmol) was added sequentially anhydrous HMDSO (15 cm^3) and mesityl azide (311 mg, 1.93 mmol, 2.2 equiv.). The heterogeneous mixture was heated under reflux for 24h, affording a bright yellow precipitate. Once cool, the precipitate was collected *via* cannula filtration and washed with a further 10 cm^3 of anhydrous HMDSO. The product was dried overnight under high vacuum, yielding a yellow solid (564 mg, 0.74 mmol, 85%). An analytically pure sample was obtained by recrystallization from toluene at -25°C.

^{1}H-NMR (400 MHz, $CDCl_3$): δ = 7.75-7.70 (m, 8H, 2 x *o*-P*Ph*$_2$) 7.05-6.83 (m, 16H, 2 x *m,p*-P*Ph*$_2$, H_I), 6.71 (s, 1H, H_C), 2.49 (s, 6H, H_F), 2.32 (s, 6H, H_H), 2.24 (s, 12H, H_G); **^{31}P{^{1}H}-NMR (162 MHz, $CDCl_3$):** δ = 246.9 (t, P_1, $^2J_{P1\text{-}P2}$ = 99.7 Hz), -9.4 (d, 2P, P_2, $^2J_{P2\text{-}P1}$ = 99.7 Hz); **^{13}C{^{1}H}-NMR (100 MHz, $CDCl_3$):** δ = 160.0-158.4 (m, 2C, C_A), 151.5-151.2 (m, 2C, C_B), 145.1 (s, 2C, C_J), 139.3-138.9 (m, C_C), 134.0-129.0 (m, C_I & 2 x PPh_2), 24.3 (m, 2C, C_F), 21.1 (s, 4C, C_G), 20.6 (s, 2C, C_H); **HRMS (ASAP/QTof):** *m/z*: ([M-H]$^+$) Calcd. for $C_{49}H_{49}N_2P_3$: 759.3187; Found: 759.3196; **Elemental Analysis:** Anal. Calcd. for $C_{49}H_{49}N_2P_3$: C 77.54, H 6.51. Found: C 77.55, H 6.42.

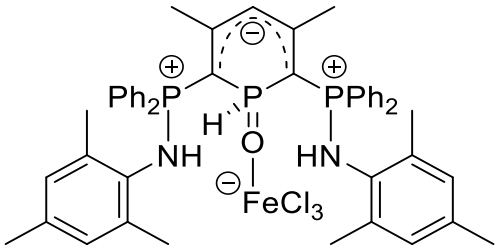

2.9

An ampoule was charged with **7** (100 mg, 0.13 mmol, 1 equiv.), anhydrous $FeCl_2$ (17 mg, 0.13 mmol, 1 equiv.) and dry THF (10 cm^3), sealed with a Teflon tap and heated to 70°C for 18 hours. All volatiles were removed under high vacuum and the resulting residue dissolved in dry dichloromethane (1 cm^3). The solution was cannula filtered and layered with 40-60 petroleum ether (4 cm^3), with yellow needles of the product produced over one week.

$^{31}P\{^{1}H\}$-NMR (162 MHz, $CDCl_3$): δ = 18.4 (bs)

8.3 Chapter 3 – Metal carbonyls

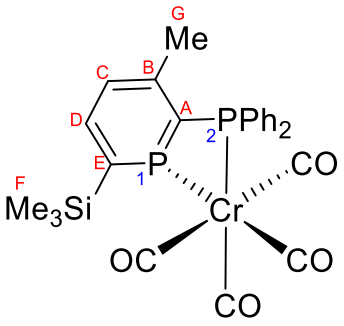

<u>3.1</u> - 2-diphenylphosphino-3-methyl-6-trimethylsilylphosphinine chromium(0) tetracarbonyl

$[Cr(NBD)(CO)_4]$ (72 mg, 0.273 mmol) and one equivalent of **2.1** (101 mg, 0.273 mmol) were dissolved in toluene (20 cm^3) and stirred at 60°C for 24 h, during which time the solution turned from yellow-orange to red-orange. Volatiles were then removed under reduced pressure forming an orange oil, which was washed with petroleum ether forming a solid. This solid was dissolved in toluene, and orange crystals formed when the solution was cooled to-25°C for 24 h. These were isolated by filtration and dried under vacuum (109 mg, 0.204 mmol, 75%).

^{1}H NMR ($CDCl_3$, 400 MHz): δ = 7.88 (ddd, 1H, H_D, $^{3}J_{HD\text{-}P1}$ = 23.2 Hz, $^{3}J_{HD\text{-}HC}$ = 8.5 Hz, $^{5}J_{HC\text{-}P2}$ = 1.5 Hz), 7.60 (m, 4H, PPh_2), 7.47 (m, 6H, PPh_2), 7.00 (app. dt, 1H, H_C, $^{3}J_{HC\text{-}HD}$ = 8.8 Hz, $^{4}J_{HC\text{-}P1}$ = 3 Hz), 1.94 (s, 3H, H_G), 0.42 (s, 9H, H_F); **$^{31}P\{^{1}H\}$-NMR ($CDCl_3$, 162 MHz):** δ = 273.6 (d, P_1, $^{2}J_{P1\text{-}P2}$ = 38.2 Hz), 40.5 (d, P_2, $^{2}J_{P2\text{-}P1}$ = 38.2 Hz); **$^{13}C\{^{1}H\}$-NMR ($CDCl_3$, 100 MHz):** δ = 229.3 (dd, CO, J = 13.6, 1.6 Hz), 227.5 (dd, CO, $J \approx$ 11, 3 Hz), 221. 9 (dd, CO, J = 17.8, 11.9 Hz), 166.5 (dd, phosphinine C, J = 13.4, 4.5 Hz), 164.0 (dd, phosphinine C, J = 52.0, 20.8 Hz), 146.1 (app. d, phosphinine C, $J \approx$ 11, 5 Hz,), 144.6 (dd, phosphinine CH, J = 14.9, 3.0 Hz), 133.1 (dd, *ipso*-Ph C, J = 28.2, 10.4 Hz), 131.6 (d, *o*-Ph CH, J = 11. 9 Hz), 130.3 (s, *p*-Ph CH), 128.9 (d, *m*-Ph CH, J = 8.9 Hz, 5.94 Hz), 127.0 (dd, phosphinine CH, J = 34.2, 6.0 Hz), 21.7 (app. t, C_G, $^{3}J_{CG\text{-}P1}$ = 5.9 Hz), -0.3 (d, C_F, $^{4}J_{CF\text{-}P1}$ = 3.0 Hz); **$^{29}Si\{^{1}H\}$-NMR ($CDCl_3$, 79 MHz):** δ = -1.1 (dd, $SiMe_3$ $^{2}J_{Si\text{-}P1}$ = 21.6 Hz, $^{4}J_{Si\text{-}P2}$ = 2.6 Hz,); **HRMS (ASAP/QTof):** *m/z:* ($[M+H]^+$) Calcd. for $C_{25}H_{25}CrO_4P_2Si$: 531.0403; Found 531.0404; **FTIR (ATR):** ν(cm^{-1}) 1895 (CO), 1906 (CO), 2013 (CO); **Elemental Analysis**: Anal. Calcd. for $C_{25}H_{24}O_4P_2SiCr$: C 56.60, H 4.56; Found: C 56.50, H 4.63.

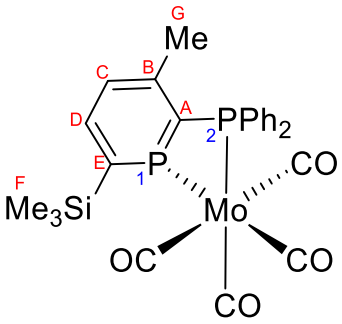

3.2 - 2-diphenylphosphino-3-methyl-6-trimethylsilylphosphinine molybdenum(0) tetracarbonyl

[Mo(NBD)(CO)$_4$] (85 mg, 0.280 mmol) and one equivalent of **2.1** (103 mg, 0.280 mmol) were reacted as for **3.1** at 20°C for 2 h yielding the product as pale yellow crystals (48 mg, 0.09 mmol, 30%).

^{1}H NMR (CDCl$_3$, 400 MHz): δ 7.93 (ddd, 1H, H_D, $^3J_{HD\text{-}P1}$ = 22.6 Hz, $^3J_{HD\text{-}HC}$ = 8.5 Hz, $^5J_{HC\text{-}P2}$ = 2.1 Hz), 7.58 (m, 4H. PPh$_2$), 7.47 (m, 6H, PPh$_2$), 7.06 (m, 1H, H_C), 1.93 (s, 3H, H_G), 0.44 (s, 9H, H_F); **^{31}P{^{1}H}-NMR (CDCl$_3$, 162 MHz):** δ 244.8 (d, P_1, $^2J_{PP}$ = 72.8 Hz), 18.9 (d, $^2J_{PP}$ = 72.8 Hz, 2-*P*); **^{13}C{^{1}H}-NMR (CDCl$_3$, 100 MHz):** δ = 219.1 (dd, CO, *J* = 31.2, 8.9 Hz), 217.8 (dd, CO, *J* = 26.8, 8.9 Hz), 210.3 (dd, CO, *J* ≈ 11, 8 Hz), 168.5 (d, phosphinine C, *J* = 14.9 Hz), 161.1 (dd, phosphinine C, *J* = 52.0, 19.3 Hz,), 148.0 (dd, phosphinine C, *J* = 11.9, 6.0 Hz), 143.8 (d, phosphinine CH, *J* = 17.8 Hz), 133.0 (dd, *ipso*-Ph C, *J* = 28.2, 10.4 Hz), 131.7 (d, *o*-Ph C, *J* = 11.9 Hz), 130.2 (s, *p*-Ph CH), 128.9 (d, *m*-Ph CH, *J* = 8.9 Hz), 127.7 (dd, phosphinine CH, *J* = 34.2, 4.5 Hz), 21.9 (app. t, C_G, $^3J_{CG\text{-}P1}$ = 6.0 Hz), -0.3 (d, C_F, $^3J_{CF\text{-}P1}$ = 3.0 Hz); **^{29}Si{^{1}H}-NMR (CDCl$_3$, 79 MHz):** δ -0.8 (dd, $^2J_{Si\text{-}P1}$ = 22.1 Hz, $^4J_{Si\text{-}P2}$ =2.7 Hz); **MS (EI/MS):** m/z: 576.0 ([M]$^+$, 6.3%); **FTIR (ATR):** ν(cm^{-1}) 1888 (CO), 1926 (CO), 2026 (CO); **Elemental Analysis:** Anal. Calcd. for $C_{25}H_{24}O_4P_2SiMo$: C 52.27, H 4.21; Found: C 52.14, H 4.36.

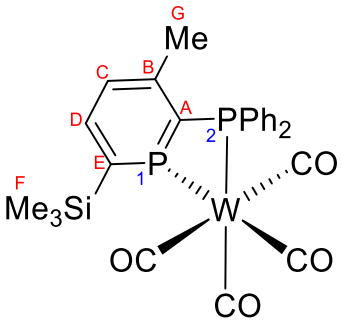

3.3 - 2-diphenylphosphino-3-methyl-6-trimethylsilylphosphinine tungsten(0) tetracarbonyl

$[W(COD)(CO)_4]$ (110 mg, 0.273 mmol) and one equivalent of **2.1** (101 mg, 0.273 mmol) were reacted as for **3.1** at 75°C for 4 days yielding the product as red crystals (125 mg, 0.188 mmol, 69%).

^{1}H NMR ($CDCl_3$, 300 MHz): δ = 7.95 (ddd, 1H, H_D, $^{3}J_{HD-P1}$ = 24.6 Hz, $^{3}J_{HD-HC}$ = 8.4 Hz, $^{5}J_{HD-P2}$ = 2.6 Hz), 7.58 (m, 4H, PPh_2), 7.47 (m, 6H, PPh_2), 7.06 (m, 1H, H_C), 1.93 (s, 3H, H_G), 0.44 (s, 9H, H_F); **^{31}P{^{1}H}-NMR ($CDCl_3$, 121 MHz):** δ 209.6 (d, P_1, $^{2}J_{P1-P2}$ = 78.0 Hz, ^{183}W satellites (14.3% abundant): dd, $^{1}J_{W-P1} \approx 212$ Hz), -0.1 (d, P_2, $^{2}J_{P2-P1}$ = 78.0 Hz, ^{183}W satellites (14.3% abundant): dd, $^{1}J_{W-P2}$ = 200.3 Hz); **^{13}C{^{1}H}-NMR ($CDCl_3$, 75 MHz):** δ = 210.0 (dd, CO, *J* = 31.0, 6.6 Hz), 209.0 (dd, CO, *J* = 24.3, 7.7 Hz), 203.7 (dd, CO, *J* = 10.0, 6.6 Hz), 172.0 (d, phosphinine C, *J* = 21.0 Hz), 155.8 (dd, phosphinine C, *J* = 44.2, 21.0 Hz), 149.7 (dd, phosphinine C, *J* = 12.2, 5.5 Hz), 143.8 (dd, phosphinine CH, *J* = 17.7, 3 Hz), 131.9 (dd, *ipso*-Ph C, *J* = 34.3, 11.1 Hz), 131.8 (d, *o*-Ph CH, *J* = 13.3 Hz), 130.5 (s, *p*-Ph CH), 128.9 (d, *m*-Ph CH, *J* = 10.0 Hz), 126.5 (dd, phosphinine CH, *J* = 35.4, 5.5 Hz), 21.7 (app. t, C_G, *J* = 6.6 Hz), -0.4 (d, C_F, *J* = 3.0 Hz); **^{29}Si{^{1}H}-NMR ($CDCl_3$, 79 MHz):** δ -0.7 (dd, $SiMe_3$, $^{2}J_{Si-P1}$ = 20.9 Hz, $^{4}J_{Si-P2}$ =2.3 Hz); **HRMS (ASAP/QTof):** *m/z:* ($[M+H]^+$) Calcd. for $C_{25}H_{25}O_4P_2SiW$: 663.0509; Found 663.0508; **FTIR (ATR):** ν(cm^{-1}) 1883(CO), 1914 (CO), 2021 (CO); **Elemental Analysis:** Anal. Calcd. for $C_{25}H_{24}O_4P_2SiW$: C 45.34, H 3.65; Found: C 45.49, H 3.55

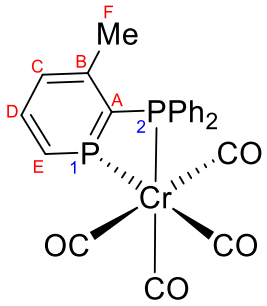

3.4 - 2-diphenylphosphino-3-methylphosphinine chromium(0) tetracarbonyl

$[Cr(NBD)(CO)_4]$ (109 mg, 0.427 mmol) and one equivalent of **2.5** (126 mg, 0.427 mmol) were reacted as for **3.1** at 65°C for 24 h yielding the product as red crystals (62 mg, 0.135 mmol, 32%).

^{1}H NMR (C_6D_6, 400 MHz): δ = 7.71-7.61 (m, 1H, H_E), 7.55-7.51 (m, 4H, *o*-PPh_2), 7.13-6.99 (m, 7H, H_D & *m,p*-PPh_2), 6.37 (bs, 1H, H_C), 1.52 (s, 3H, H_F); **^{31}P{^{1}H}-NMR (C_6D_6, 162 MHz):** δ = 250.3 (d, P_1, $^2J_{P1\text{-}P2}$ = 33.8 Hz), 41.8 (d, P_2, $^2J_{P2\text{-}P1}$ = 33.8 Hz); **^{13}C{^{1}H}-NMR (C_6D_6, 100 MHz):** δ = 230.3 (d, CO, *J* = 13.6 Hz), 228.4 (dd, CO, *J* = 11.2, 3.2 Hz), 223.0 (dd, CO, *J* = 17.6, 11.2 Hz), 166.9 (dd, phosphinine C, *J* = 15.2, 1.6 Hz) 149.6 (dd, phosphinine CH, *J* = 28.0, 20.0 Hz), 146.9 (dd, phosphinine C, *J* = 12.8, 7.2 Hz), 140.6 (dd, phosphinine CH, *J* = 16.0, 3.2 Hz), 133.5 (dd, *ipso*-Ph C *J* = 28.8, 10.4 Hz), 132.1 (d, PPh_2, *J* = 12.0 Hz), 130.8 (d, PPh_2, *J* = 2.4 Hz), 129.5 (d, PPh_2, *J* = 9.6 Hz), 128.6-128.2 (m, phosphinine CH and C_6D_6 overlapping), 21.9 (t, C_F, $^3J_{CF\text{-}P1}$ = 7.2 Hz); **HRMS (ASAP/QTof):** *m/z:* ($[M+H]^+$) Calcd. for $C_{22}H_{17}MoO_4P_2$: 459.0007; Found 459.0001; **FTIR (ATR)**: ν(cm^{-1}) 1864 (CO), 1898 (CO), 2003 (CO); **Elemental Analysis:** Anal. Calcd. for $C_{22}H_{16}CrO_4P_2$: C 57.66, H 3.52; Found: C 58.08, H 3.44.

Crystals of complex **3.6** were obtained by following the same synthetic route, for **3.4**, however the crude reaction mixture was dissolved in a minimum amount of DCM and layered with 40-60 petroleum ether. After approximately two weeks, amongst a large amount of amorphous precipitate, a small crop of orange crystals of **3.6** were observed. No analytical data was obtained due to the trace amount of material.

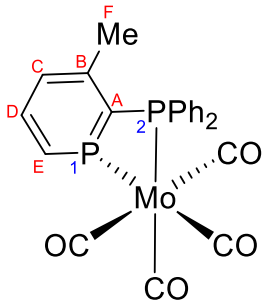

3.5 - 2-diphenylphosphino-3-methylphosphinine molybdenum(0) tetracarbonyl

[Mo(NBD)(CO)$_4$] (20 mg, 0.068 mmol) and one equivalent of **2.5** (20 mg, 0.068 mmol) were dissolved in toluene (2 cm^3) and stirred at 20°C for 2 h, during which time a yellow precipitate was observed. All volatiles were removed under reduced pressure and the resulting solid was dried under high vacuum, yielding the product as an analytically pure pale yellow microcrystalline powder (20 mg, 0.041 mmol, 60%).

^{1}H NMR (C$_6$D$_6$, 400 MHz): δ = 7.70-7.60 (m, 1H, *H$_E$*), 7.49 (bs, 4H, *o*-PPh$_2$), 7.09-6.97 (m, 7H, *H$_D$* & *m,p*-PPh$_2$), 6.37 (bs, 1H, *H$_C$*), 1.52 (s, 3H, *H$_F$*); **^{31}P{^{1}H}-(NMRC$_6$D$_6$, 162 MHz):** δ = 222.7 (d, *P$_1$* $^2J_{P1\text{-}P2}$ = 71.1 Hz), 20.0 (d, *P$_2$*, $^2J_{P2\text{-}P1}$ = 71.1 Hz); **^{13}C{^{1}H}-(NMR (C$_6$D$_6$, 100 MHz):** δ = 218.8 (dd, CO, *J* = 32.0, 9.6 Hz), 217.5 (dd, CO, *J* = 26.4, 8.8 Hz), 210.3 (dd, CO, *J* ≈ 11, 8 Hz), 168.4 (dd, phosphinine C, *J* = 16.8, 1.6 Hz) 148.0 (dd, phosphinine CH, *J* = 12.0, 5.6 Hz), 146.4 (dd, phosphinine C, *J* = 25.6, 19.2 Hz), 139.1 (dd, phosphinine CH, *J* = 16.0, 2.4 Hz), 132.8 (dd, *ipso*-Ph C, *J* = 28.8, 10.4 Hz), 131.5 (d, PPh$_2$, *J* = 12.8 Hz), 130.0 (d, PPh$_2$, *J* = 1.6 Hz), 128.8 (d, PPh$_2$, *J* = 9.6 Hz), 128.3-127.5 (m, phosphinine CH and C$_6$D$_6$ overlapping), 21.4 (s, *C$_F$*); **HRMS (ASAP/ QTof):** *m/z:* ([M+H]$^+$) Calcd. for C$_{22}$H$_{17}$MoO$_4$P$_2$: 504.9661; Found 504.9666; **FTIR (ATR):** ν(cm^{-1}) 1867 (CO), 1910 (CO), 2017 (CO); **Elemental Analysis:** Anal. Calcd. for C$_{22}$H$_{16}$MoO$_4$P$_2$: C 52.59, H 3.21; Found: C 52.46, H 3.17.

8.4 Chapter 4 – Ruthenium complexes

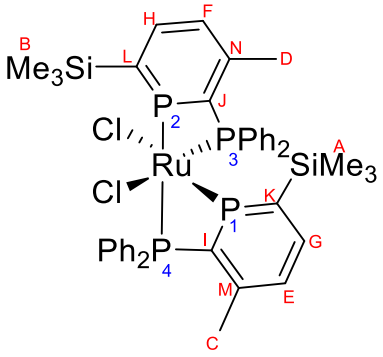

4.1 - Dichlorobis(2-diphenylphosphino-3-methyl-6-trimethylsilylphosphinine) ruthenium(II)

Method A: To a Schlenk flask containing **2.1** (558 mg, 1.52 mmol, 2 equiv.) and *cis*-[$RuCl_2(dmso)_4$] (361 mg, 0.75 mmol, 1 equiv) was added 10 cm^3 of anhydrous $CHCl_3$. The reaction mixture was heated to 55°C for 5 hours, before the solvent was removed under reduced pressure. The contents of the flask were then heated to 70°C under high vacuum for 8 hours before being washed with 3 x 20 cm^3 portions of 40-60 pet. ether. The precipitate was dried under high vacuum, yielding the complex (583 mg, 0.64 mmol, 85%) as an air-sensitive bright orange powder. Crystals suitable for X-ray diffraction were grown from slow diffusion of 40-60 pet. ether into a C_6D_6 solution of the complex. Further purification (if dmso remains) was achieved by recrystallisation from hot THF or slow diffusion of 40-60 pet. ether into a CH_2Cl_2 solution, which yields the 1:1 DCM solvate.

Method B: To a Schlenk flask containing **2.1** (942 mg, 2.7 mmol, 2 equiv.) and *cis*-[$RuCl_2(dmso)_4$] (654 mg, 1.35 mmol, 1 equiv) was added 5 cm^3 of anhydrous toluene. The reaction mixture was heated to 75°C for 18 hours, with the formation of a bright orange precipitate observed. The reaction mixture was then cooled in an ice bath before the precipitate was separated by cannula filtration and washed with 3 x 10 cm^3 portions of 40-60 pet. ether. The product was dried thoroughly under high vacuum, yielding the complex (652 mg, 0.72 mmol, 53%) as a bright orange powder. Concentration of the filtrate and storage at -25°C for 2 days provided a second crop that wasn't pure enough to use. Despite the lower yield, this route is recommended due to the facile work-up and that no further purification is needed to remove residual DMSO.

Method C: An NMR tube was charged with **2.1** (20 mg, 0.05 mmol, 1 equiv), [{Ru(p-Cym)Cl_2}$_2$] (16 mg, 0.03 mmol, 0.5 equiv) and C_6D_6. The tube was sealed with a Youngs tap and heated to 50°C for 5 minutes. Analysis of the resulting red solution by ^{31}P NMR spectroscopy showed a mixture of **4.1** and **4.2**. Layering the C_6D_6 solution

with 40-60 pet ether produced a mixture of yellow (**4.1**) and red (**4.2**) single crystals suitable for X-ray diffraction. Varying the equivalents of **2.1** did not enable clean isolation of **4.2**, the reaction always formed **4.1**. Despite the rapid reaction of **2.1** with [{Ru(*p*-Cym)Cl_2}$_2$], attempts to scale up to preparative scale did not consistently produce pure **4.1**.

^{1}H-NMR (500 MHz, 25 °C, $CDCl_3$): δ = 7.98 (ddd, 1H, H_H, $^3J_{HH-P2}$ = 22.4 Hz, $^3J_{HH-HF}$ = 8.5 Hz, $^5J_{HH-P3}$ = 5.4 Hz), 7.83 (dd, 2H, PPh_2), 7.67 (dd, 2H, PPh_2), 7.56-7.49 (m, 3H, PPh_2 & H_G), 7.34 (m, 1H, PPh_2), 7.29-7.21 (m, 3H, PPh_2), 7.19-7.11 (m, 4H, PPh_2), 7.07-7.04 (m, 3H, H_F & PPh_2), 6.92-6.86 (m, 5H, H_E & PPh_2), 2.16 (s, 3H, H_C), 1.62 (s, 3H, H_D), 0.50 (s, 9H, H_B), -0.01 (s, 9H, H_A); **^{31}P{^{1}H}-NMR (202 MHz, 25 °C, $CDCl_3$):** δ = 235.2 (ddd, P_1, $^2J_{P1-P2}$ = 10.1 Hz, $^2J_{P1-P3}$ = 12.1 Hz, $^2J_{P1-P4}$ = 28.3 Hz), 229.9 (ddd, P_2, $^2J_{P2-P1}$ = 10.1 Hz, $^2J_{P2-P3}$ = 30.4 Hz, $^2J_{P2-P4}$ = 424.8 Hz), 2.3 (ddd, P_3, $^2J_{P3-P1}$ = 12.1 Hz, $^2J_{P3-P2}$ = 30.4 Hz, $^2J_{P3-P4}$ = 20.2 Hz), -2.4 (ddd, P_4, $^2J_{P4-P1}$ = 28.3 Hz, $^2J_{P4-P2}$ = 425.7 Hz, $^2J_{P4-P3}$ = 20.2 Hz); **^{13}C{^{1}H}-NMR (126 MHz, 25 °C, $CDCl_3$):** δ = 166.75 (d, C_L, $^1J_{CL-P2}$ = 27.0 Hz), 160.86 (dd, C_K, $^1J_{CK-P1}$ = 24.7 Hz, $^3J_{CK-P4}$ = 5.4 Hz), 156.95 (ddd, C_J, $^1J_{CJ-P2}$ = 67.1 Hz, $^1J_{CJ-P3}$ = 20.0 Hz, $^3J_{CJ-P4}$ = 10.8 Hz), 149.91-148.85 (m, C_I & C_M, $^1J_{CI-P1}$ = 42.39 Hz, $^1J_{CI-P4}$ = 10.0 Hz), 147.18 (dd, C_N, $^2J_{CN-P2}$ = 11.6 Hz, $^2J_{CN-P3}$ = 6.9 Hz), 144.62 (d, C_G, $^2J_{CG-P1}$ = 18.5 Hz), 144.20 (dd, C_H, $^2J_{CH-P2}$ = 20.0 Hz, $^4J_{CH-P3}$ = 3.1 Hz), 134.13-127.62 (m, PPh_2), 126.78 (dd, C_F, $^3J_{CF-P2}$ = 35.5 Hz, $^3J_{CF-P3}$ = 6.9 Hz), 124.55 (dd, C_E, $^3J_{CE-P1}$ = 37.8 Hz, $^3J_{CE-P4}$ = 6.9 Hz), 23.31 (t, C_C, $^3J_{CC-P1}$ = 6.9 Hz), 21.53 (t, C_D, $^3J_{CD-P2}$ = 6.2 Hz), 0.59 (d, C_A, $^3J_{CA-P1}$ = 1.5 Hz), 0.1 (t, C_B, $^3J_{CB-P2}$ = 2.3 Hz); **^{29}Si{^{1}H}-NMR (99 MHz, 25 °C, $CDCl_3$):** δ = -0.13 (dd, $SiMe_3$, $^2J_{Si-P}$ = 21.8 Hz, $^4J_{Si-P}$ = 2.4 Hz), -0.95 (dd, $SiMe_3$, $^2J_{Si-P}$ = 19.4 Hz, $^4J_{Si-P}$ = 3.0 Hz); **HRMS (ASAP/ QTof):** *m/z*: ([M-Cl]$^+$) Calcd. for $C_{42}H_{48}ClP_4RuSi_2$: 869.0985; Found: 869.0995; **Elemental Analysis:** Anal. Calcd. for $C_{42}H_{48}Cl_2P_4RuSi_2$: C 55.75, H 5.35; Found: C 55.91, H 5.40.

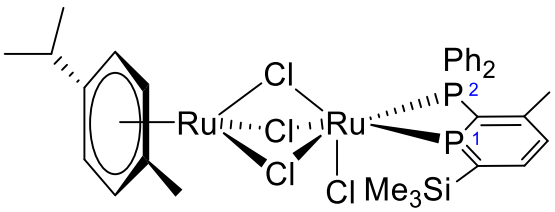

4.2

Prepared using **4.1 Method C**.

^{31}P{^{1}H}-NMR (162 MHz, C_6D_6): δ = 231.4 (d, P_1, $^2J_{P1-P2}$ = 55.5 Hz), 21.7 (d, P_2, $^2J_{P2-P1}$ = 55.5 Hz).

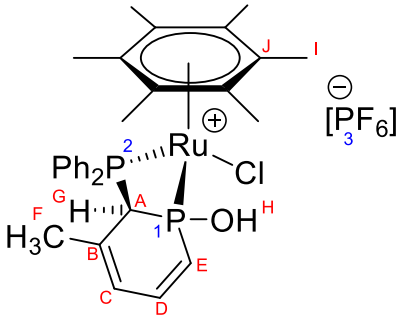

4.3 - Chloro(hexamethylbenzene)(1-hydroxy-2-diphenylphosphino-3-methylphosphacyclohexa-3,5-diene)ruthenium (II) hexafluorophosphate

To a Schlenk flask containing **2.1** (71 mg, 0.19 mmol, 1 equiv), [{Ru(C_6Me_6)Cl_2}$_2$] (65 mg, 0.1 mmol, 0.5 equiv), and NH_4PF_6 (32 mg, 0.19 mmol, 1 equiv) was added 15 cm^3 of anhydrous dichloromethane. The resulting heterogeneous mixture was stirred at high speed for 64 hours. The precipitated NH_4Cl was removed by cannula filtration and the reaction mixture concentrated to ~1 cm^3 before being layered with 10 cm^3 40-60 petrol. Once crystallisation was complete, the solvent was removed by cannula filtration and the orange needles of product (113 mg, 0.15 mmol, 78%) were separated manually from a white powder. ^{1}H-NMR spectrum showed notable sample contamination by silicone oil (from crystallography) as well as minor side-products.

^{1}H-NMR (400 MHz, CD_2Cl_2): δ = 7.79-7.60 (m, 7H, PPh_2 & H_E), 7.54-7.50 (m, 2H, PPh_2), 7.24-7.19 (m, 2H, PPh_2), 6.96 (ddd, 1H, H_D, $^3J_{HD-P1}$ = 33.75 Hz, $^3J_{HD-HE}$ = 12.32 Hz, $^3J_{HD-HC}$ = 7.04 Hz), 6.59 (dd, 1H, H_H, $^2J_{HH-P1}$ = 24.06 Hz, $^2J_{HH-HE}$ = 12.32 Hz), 5.89 (bs, 1H, H_C), 5.32 (t, 1H, H_G, $^2J_{HG-P1}$ = 15.55 Hz), 2.20 (s, 18H, H_I), 1.65 (s, 3H, H_F); **^{31}P{^{1}H}-NMR (162 MHz, CD_2Cl_2):** δ = 11.6 (d, P_1, $^2J_{P1-P2}$ = 97.1 Hz), 8.8 (d, P_2, $^2J_{P2-P1}$ = 97.1 Hz), -144.49 (sept, P_3, $^1J_{P3-F}$ = 711.4 Hz); **^{19}F{^{1}H}-NMR (79 MHz, 25 °C, CD_2Cl_2):** δ = -73.3 (d, 6F, PF_6, $^2J_{F-P3}$ = 709.5 Hz); **HRMS (ASAP/ QTof):** *m/z*: ([M-PF_6]$^+$) Calcd. for $C_{30}H_{36}ClOP_2Ru$: 611.0978; Found: 611.0983; **Elemental Analysis:** Anal. Calcd. for $C_{30}H_{36}ClF_6OP_3Ru$: C 47.66, H 4.80; Found: C 47.89, H 5.17.

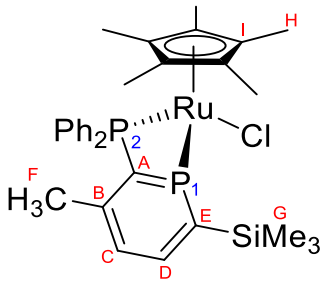

4.4 - Chloro(pentamethylcyclopentadienyl)(2-diphenylphosphino-3-methyl-6-trimethylsilylphosphinine)ruthenium (II)

To a Schlenk flask containing **2.1** (30 mg, 0.08 mmol, 1 equiv.) and [{Ru(Cp*)Cl}$_4$] (22 mg, 0.02 mmol, 0.25 equiv) was added 2 cm^3 of anhydrous THF. The deep red solution was stirred for 5 minutes before the solvent was removed under reduced pressure. The resulting oily solid was then dissolved in 5 cm^3 of 40-60 pet. ether and the solution cooled in an ice bath until an orange precipitate was observed. The precipitate was separated by cannula filtration and dried for at least 18 hours under high vacuum, yielding the complex (36 mg, 0.06 mmol, 70%) as a highly air-sensitive orange powder. **^{1}H-NMR (400 MHz, C$_6$D$_6$):** δ = 8.24-8.19 (m, 2H, PPh$_2$), 7.63 (dd, 1H, *H$_D$*, $^3J_{HD-P1}$ = 22.51 Hz, $^3J_{HD-HC}$ = 8.48 Hz), 7.41-7.36 (m, 2H, PPh$_2$), 7.22-6.93 (m, 6H, PPh$_2$), 6.46 (ap dt, 1H, *H$_C$*, $^3J_{HC-HD}$ = 8.48 Hz, $^4J_{HC-P1}$ = 2.92 Hz, $^4J_{HC-P2}$ = 2.63 Hz), 1.74 (s, 3H, *H$_F$*), 1.62 (t, 15H, *H$_H$*, $^3J_{HH-P1}$ = 2.05 Hz), 0.47 (s, 9H, *H$_F$*); **^{31}P{^{1}H}-NMR (162 MHz, C$_6$D$_6$):** δ = 240.1 (d, *P$_1$*, $^2J_{P1-P2}$ = 6.9 Hz), 18.2 (d, *P$_2$*, $^2J_{P2-P1}$ = 6.9 Hz); **^{13}C{^{1}H}-NMR (126 MHz, 25 °C, CDCl$_3$):** δ = 168.8 (d, *C$_E$*, $^1J_{CE-P1}$ = 18.0 Hz), 151.3 (dd, *C$_A$*, $^1J_{CA-P1}$ = 61.4 Hz, $^1J_{CA-P2}$ = 19.1 Hz), 146.6 (dd, *C$_B$*, $^2J_{CB-P1}$ = 11.1 Hz, $^2J_{CB-P2}$ = 7.9 Hz), 144.1 (dd, *C$_D$*, $^2J_{CD-P1}$ = 17.1 Hz, $^4J_{CD-P2}$ = 3.4 Hz), 135.5 (d, PPh$_2$, *J* = 12.0 Hz), 134.2 (dd, PPh$_2$, *J* = 37.9, 6.5 Hz), 132.0 (d, PPh$_2$, *J* = 9.9 Hz), 130.3 (dd, PPh$_2$, *J* = 23.4 Hz, 14.6 Hz), 129.9 (d, PPh$_2$, *J* = 2.4 Hz), 129.1 (d, PPh$_2$, *J* = 2.1 Hz), 123.6 (dd, *C$_C$*, $^3J_{CC-P1}$ = 32.7 Hz, $^3J_{CC-P2}$ = 6.1 Hz), 89.1 (ap. t, 5C, *C$_I$*, $^2J_{CI-P1}$ = 2.6 Hz, $^2J_{CI-P2}$ = 2.5 Hz), 21.6 (ap. t, *C$_F$*, $^3J_{CF-P1}$ = 6.7 Hz, $^3J_{CF-P2}$ = 6.7 Hz) 10.4 (s, 5C, *C$_H$*), 0.0 (d, 3C, *C$_G$*, $^3J_{CG-P1}$ = 3.5 Hz); **^{29}Si{^{1}H}-NMR (79 MHz, 25 °C, CDCl$_3$):** δ = -2.4 (dd, SiMe$_3$, $^2J_{Si-P1}$ = 22.0 Hz, $^4J_{Si-P2}$ = 3.0 Hz); **HRMS (ASAP/ QTof):** *m/z*: ([M-Cl]$^+$) Calcd. for C$_{31}$H$_{39}$P$_2$RuSi: 603.1348; Found: 603.1347.

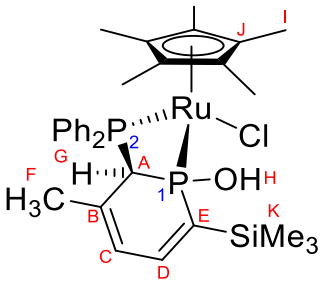

4.5 - Chloro(pentamethylcyclopentadienyl)(1-hydroxy-2-diphenylphosphino-3-methyl-6-trimethylsilylphosphacyclohexa-3,5-diene) ruthenium (II)

4.4 was prepared using **2.1** (76 mg, 0.2 mmol, 1 equiv) and [{Ru(Cp*)Cl}$_4$] (56 mg, 0.05 mmol, 0.25 equiv). After removal of the solvent, the residue was dissolved in 5 cm^3 40-60 pet. ether and stored at 5°C until small crystals were observed. After the structure was recorded, the crystals were separated by cannula filtration and dried under high vacuum, leaving the hydrated complex (16 mg, 0.02 mmol, 12%) as a red crystalline powder. ^{1}H-NMR spectrum showed minor contamination by silicone oil (from crystallography) as well as minor side-products.

^{1}H-NMR (400 MHz, CD_2Cl_2): δ = 7.76-7.14 (m, 10H, PPh_2), 6.67 (dd, 1H, H_D, $^3J_{HD-P1}$ = 36.68 Hz, $^3J_{HD-HC}$ = 6.75 Hz), 6.48 (bs, 1H, H_H), 5.81 (d, 1H, H_C, $^3J_{HC-HD}$ = 6.46 Hz), 5.08 (ap t, 1H, H_G, $^2J_{HG-P1}$ = 12.32 Hz, $^2J_{HG-P2}$ = 12.03 Hz), 1.59 (t, 15H, H_I, $^3J_{HI-P1}$ = 2.05 Hz), 1.39 (s, 3H, H_F), 0.37 (s, 9H, H_K); **^{31}P{^{1}H}-NMR (162 MHz, CD_2Cl_2):** δ = 78.3 (d, P_1, $^2J_{P1-P2}$ = 59.5 Hz), 18.0 (d, P_2, $^2J_{P2-P1}$ = 59.5 Hz); **^{29}Si{^{1}H}-NMR (79 MHz, 25 °C, CD_2Cl_2):** δ = -2.7 (d, $SiMe_3$, $^2J_{Si-P1}$ = 15.6 Hz); **HRMS (ASAP/ QTof):** *m/z*: ([M-Cl-H_2O]$^+$) Calcd. for $C_{31}H_{39}P_2RuSi$: 603.1348; Found: 603.1360; **Elemental Analysis:** Anal. Calcd. for $C_{31}H_{41}ClOP_2RuSi$: C 56.73, H 6.30; Found: C 56.73, H 6.52.

8.5 Chapter 5 – Rhodium chemistry

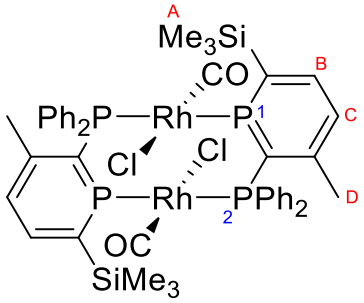

<u>5.1</u> - trans-dichlorobis(μ-{2-diphenylphosphino-3 methyl 6-trimethylsilylphosphinine}) dirhodium(I) carbonyl

A Schlenk flask was charged with **2.1** (186 mg, 0.5 mmol) and [{$Rh(CO)_2Cl$}$_2$] (99 mg, 0.25 mmol, 0.5 equiv). With efficient stirring, toluene (5 cm^3) was added, affording a deep purple solution with concomitant evolution of carbon monoxide. The reaction was stirred for 5 minutes at room temperature before concentration of the heterogeneous mixture to ~1 cm^3. The reaction mixture was stored at -25°C for 48h before the product was separated by cold cannula filtration and dried under high vacuum, yielding analytically pure **2.PhMe** as an air-sensitive deep purple crystalline powder (181 mg 0.16 mmol, 63%). The filtrate still held a purple colour, however no further pure material could be obtained (the material is somewhat unstable in solution). Crystals suitable for X-ray diffraction were grown from slow diffusion of 40-60 petrol into a C_6D_6 solution (~5:1) of the complex.

^{1}H-NMR (400 MHz, 25 °C, $CDCl_3$): δ = 8.10-7.19 (m, 29H, 2x (*H$_B$*, *H$_C$*, P*Ph*$_2$), *Ph*Me), 2.40 (s, 3H, Ph*Me*), 2.00 (s, 6H, *H$_D$*), 0.57 (s, 18H, *H$_A$*); **^{31}P{^{1}H}-NMR (162 MHz, 25 °C, $CDCl_3$):** δ = 250.6 (app. dt, 2x *P$_1$* $^2J_{P1\text{-}P2}$ = 137.3 Hz, $^1J_{P1\text{-}Rh}$ = 143.6 Hz, $^2J_{P1\text{-}P4}$ = 430.3 Hz), 25.5 (app. dt, 2x *P$_2$*, $^2J_{P2\text{-}P1}$ = 137.3 Hz, $^1J_{P2\text{-}Rh}$ = 138.7 Hz, $^2J_{P1\text{-}P4}$ = 430.3 Hz); **^{13}C{^{1}H}-NMR (100 MHz, 25 °C, $CDCl_3$):** δ = 187.2-186.2 (m, *C*O), 181.9 (d, *C*O, $^1J_{C\text{-}Rh}$ = 72.6 Hz), 159.3-158.6 (m, 2x phosphinine *C*, *J* = 14.7 Hz), 154.3 (d, 2x phosphinine *C*), 148.4-147.6 (m, 2x phosphinine *C*), 144.0 (d, 2x *C$_B$*, $^2J_{CB\text{-}P1}$ = 18.4 Hz), 137.9 (s, *Ph*Me), 133.8-132.0 (m, 2x P*Ph*$_2$), 130.3 (dd, 2x *C$_C$*, $^3J_{CC\text{-}P1}$ = 32.2 Hz, $^3J_{CC\text{-}P2}$ = 4.6 Hz), 129.7-127.7 (m, *Ph*Me, 2x P*Ph*$_2$), 125.4 (s, *Ph*Me), 27.1 (s, 2x *C$_D$*), 21.5 (s, Ph*Me*) 1.1 (d, 2x *C$_A$*, $^3J_{CA\text{-}P1}$ = 2.8 Hz); **^{29}Si{^{1}H}-NMR (79 MHz, 25 °C, $CDCl_3$):** δ = 1.5 (d, $^2J_{Si\text{-}P1}$ = 25.0 Hz); **HRMS (ASAP/QTof)** *m/z*: ([M-Cl-2CO]$^+$) Calcd. for $C_{42}H_{49}P_4Rh_2Si_2$: 973.0043; Found: 973.0040; **FTIR (ATR):** ν(cm^{-1}) 1977 (CO); **Elemental Analysis:** Anal. Calcd. for $C_{44}H_{48}Cl_2O_2P_4Rh_2Si_2$: C 49.58, H 4.54; Found: C 49.04, H 4.57.

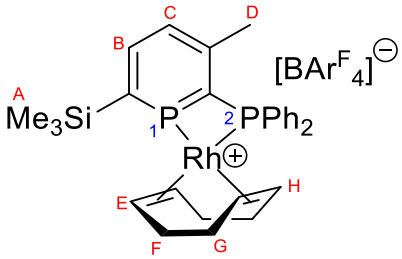

5.2 – (2-diphenylphosphino-3-methyl-6-trimethylsilylphosphininyl) cyclooctadienyl rhodium(I) tetrakis(3,5-bis{trifluoromethyl}phenyl)borate

A 25 cm^3 Schlenk flask was charged with pro-ligand **2.1** (149 mg, 0.41 mmol) and [Rh(COD)$_2$][B(Ar^F)$_4$] (482 mg, 0.41 mmol, 1 equiv) . CH_2Cl_2 (5 cm^3) was added and the resulting dark red solution stirred for 10 minutes before being concentrated to ~1 cm^3. 40-60 petrol ether (20 cm^3) was added and the resulting biphasic system stirred at high speed overnight. The pale red top layer was then removed by cannulation and discarded, leaving a sticky red oil. The contents of the flask were slowly subjected to high vacuum (to avoid rapid foaming), and the resulting solid dried thoroughly under high vacuum to leave analytically pure **3** (473 mg, 0.33 mmol, 80%) as an air-stable orange crystalline powder. Crystals suitable for X-ray diffraction were grown from slow diffusion of pentane into a concentrated $CDCl_3$ solution (~10:1) of the complex under air at -25°C.

^{1}H-NMR (400 MHz, 25 °C, $CDCl_3$): δ = 8.15 (ddd, 1H, *H$_B$*, $^4J_{HC\text{-}P1}$ = 24.94 Hz, $^3J_{HC\text{-}HB}$ = 8.51 Hz, $^4J_{HB\text{-}P2}$ = 0.88 Hz), 7.76-7.55 (m, 22H, B*Ar*^{F} & P*Ph*$_2$), 7.45-7.41 (m, 1H, *H$_B$*), 5.90 (bs, 2H, *H$_E$*), 5.02 (bs, 2H, *H$_H$*), 2.56-2.28 (m, 8H, *H$_F$* & *H$_G$*), 2.10 (s, 3H, *H$_D$*), 0.40 (s, 9H, *H$_A$*); **^{31}P{^{1}H}-NMR (162 MHz, 25 °C, $CDCl_3$):** δ = 189.4 (app. dd, *P$_1$*, $^2J_{P1\text{-}P2}$ = 16.0 Hz, $^1J_{P1\text{-}Rh}$ = 122.9 Hz), -6.8 (app. dd, *P$_2$*, $^2J_{P2\text{-}P1}$ = 16.0 Hz, $^1J_{P2\text{-}Rh}$ = 148.2 Hz); **^{13}C{^{1}H}-NMR (100 MHz, 25 °C, $CDCl_3$):** δ = 167.2 (d, phosphinine C, *J* = 24.8 Hz), 161.7 (q, 4x *C*-B, $^1J_{C\text{-}B}$ = 49.5 Hz), 153.6-152.7 (m, phosphinine *C*), 151.5-151.2 (m, phosphinine *C*), 145.0 (d,*C$_B$*, $^2J_{CB\text{-}P1}$ = 18.4 Hz), 134.8 (s, BAr^F), 132.9-132.5 (m, P*Ph*$_2$), 131.9 (dd, *C$_C$*, $^3J_{CC\text{-}P1}$ = 38.4 Hz, $^3J_{CC\text{-}P2}$ = 8.0 Hz), 129.9 (d, P*Ph*$_2$, *J* = 11.2 Hz), 128.9 (qq, BAr^F, $^2J_{F\text{-}C}$ = 32.0 Hz, $^3J_{C\text{-}B}$ = 3.2 Hz), 126.4 (dd, P*Ph*$_2$, J = 43.1 Hz, 5.6 Hz), 117.5 (t, BAr^F), $^3J_{C\text{-}F}$ = 3.2 Hz), 100.8 (dd, *C$_E$*, J = 9.6, 6.4 Hz), 95.4 (t, *C$_H$*, J = 9.6 Hz), 30.9 (s, *C$_E$*), 29.7 (s, *C$_H$*), 21.4 (t, *C$_D$*, $^3J_{CD\text{-}P1}$ = 6.4 Hz), 124.5 (q, BAr^F, $^1J_{C\text{-}F}$ =273.2 Hz), 134.33 (dd, P*Ph*$_2$), 130.48 (dd, *C$_D$*, $^2J_{CD\text{-}P1}$ = 20.8 Hz, $^4J_{CD\text{-}P2}$ = 4.0 Hz), -0.7 (d, *C$_A$*, $^3J_{C\text{-}P1}$ = 3.2 Hz); **^{19}F{^{1}H}-NMR (376 MHz, 25°C, $CDCl_3$):** -62.4 (s, 24F, BAr^F); **^{11}B{^{1}H}-NMR (128 MHz, 25°C, $CDCl_3$):** -6.6 (s, 1B, BAr^F); **^{29}Si{^{1}H}-NMR (79 MHz, 25 °C, $CDCl_3$):** δ = 0.2 (dd, $^2J_{Si\text{-}P1}$ = 20.5 Hz, $^4J_{Si\text{-}P2}$ = 2.6 Hz); **HRMS (ASAP/Qtof)** *m/z*: ([M-BAr^F]$^+$) Calcd. for $C_{29}H_{36}P_2RhSi$: 577.1116; Found: 577.1127; **Elemental**

Analysis: Anal. Calcd. for $C_{61}H_{48}BF_{24}P_2RhSi$: C 50.85, H 3.36; Found: C 50.94, H 3.24.

8.6 Catalytic methods

8.6.1 Ethylene oligomerisation

All operations were conducted at Sasol Technology UK by David Smith and Martin Hanton under dry argon using standard Schlenk and cannula techniques, or in an argon-filled glove box. Solvents were procured from Aldrich, purified and dried using a Solvent Purification System (passage over alumina), and de-oxygenated prior to use. $Cr(acac)_3$ was procured from Strem and MMAO-3A was sourced from Akzo Nobel. The ethylene (grade 4.5) and Ar (grade 4.8) were sourced from BOC and passed through alumina and oxygen scrubbing columns before use. $Cr(acac)_3$, the phosphinine ligands **2.1** & **2.5** and MMAO-3A were all used as dilute stock solutions in chlorobenzene, (2.0, 2.0 and 1960 mM, respectively), stored in glass ampoules fitted with Young's taps and connected to a standard Ar-filled Schlenk line.

GC-FID analysis was performed on an Agilent Technologies 6890N GC system equipped with a PONA (50 m × 0.20 mm × 0.50 µm) column. GC-MS analysis was performed on an Agilent Technologies 6890N GC system equipped with PONA (50 m × 0.20 mm × 0.50 µm) column, coupled to an Agilent Technologies 5973N MSD Mass Spectrometric instrument equipped with EI source. Hydrogenative GC-FID analysis was performed using an Agilent Technologies 6890N GC System equipped an inlet liner packed with hydrogenating catalyst (Pt on Chromosorb W at 200 o C) and PONA column (50 m × 0.20 mm × 0.50 µm). 12

Catalysis was performed in stainless steel 250 mL specified working volume (280 mL total volume) Büchi autoclaves with Viton-ETP seals, equipped with a mechanical stirrer, internal cooling coil (tap water), fluidised jacket (connected to a Haake A28 refrigerated thermostatic bath with Haake SC 150 controller) and temperature and pressure monitoring. Dry, deoxygenated solvent was added via HPLC pump. Ethylene was entrained with ~1 ppm O 2 and was added to the reaction under pressure control using a regulator and supplied on demand to maintain reaction pressure via a Siemens MASSFLO MASS 2100 Coriolis mass flow meter, with a lower flow detection threshold of 0.1 g/min^{-1}.

The rigorously cleaned autoclave was heated (100 °C) under vacuum for 30 mins, then cooled to reaction temperature and back-filled with ethylene (10 barg). Solvent was added via HPLC pump, and then the vessel was vented to 0 barg via a septa to purge the inlet valve. From an ampule attached to a Schlenk line, aliquots of $Cr(acac)_3$ and ligand

stock solution, followed by an aliquot of MMAO-3A were added to the autoclave via syringe. After addition of the catalyst solutions the autoclave was rapidly pressurised and the pressure kept constant throughout the reaction by the continuous addition of ethylene, which was monitored via a flow-meter. Heating and cooling were controlled to maintain a stable reaction temperature. Once the desired reaction time was reached, the gas supply was closed, 5 mL of EtOH was added via burette using an overpressure of Ar, and the reactor cooled to -5 °C. The reactor was then carefully vented. The reactor contents were treated with 1000 µL of nonane (GC internal standard), 50 mL of toluene and stirred vigorously for 5 minutes. The reactor contents (all liquid and solid) were then transferred to a Schott bottle containing 50 mL of distilled water and vigorously shaken. A sample of the organic phase was taken for liquid phase sample GC-FID analysis. Any solid was collected by filtration, washed with acetone, and dried overnight and weighed. The analysis from the liquid phase GC-FID analysis was then reconciled with the mass of solid to create an overall analysis of the product slate.

8.6.2 Transfer hydrogenation

To a dry Schlenk flask, under N_2, fitted with a stirrer bar containing 1,3,5-trimethoxybenzene (55.5 mg, 0.33 mmol), ^{i}PrOH and substrate (1 mmol) were added stock solutions of catalyst (0.1 mol%) and KO^{t}Bu (0.5 mol%) in ^{i}PrOH, to a total solvent volume of 2.3 cm^3. After 1 hour, 0.1 cm^3 was removed by syringe and the ^{1}H-NMR spectrum ($CDCl_3$) recorded. Reactions run at 82°C were run in a 50 cm^3 Schlenk flask fitted with a Teflon tap, NMR tubes were chilled in an ice bath to quench sample.

8.6.3 Ethanol/methanol co-condensation

All operations were conducted at The University of Bristol by Richard Wingad. Samples obtained from methanol/ethanol co-condensation experiments were analysed by GC-FID, using an Agilent 7820A GC, fitted with a DB-WX capillary column, 30 m x 0.32 mm, I.D. 0.25 µm. Method: starting oven temp 50°C, hold at 50°C for 5 min, heat to 250°C at 50°C min^{-1}, hold at 250°C for 5 min

Catalyst (0.017 mmol, 0.1 mol%), and sodium methoxide (1.85 g, 34.26 mmol, 200 mol%) were added to a clean oven-dried fitted PTFE insert inside a glove box. The insert was sealed within a 100 cm^3 Parr stainless steel autoclave which was then transferred to a N_2/vacuum manifold. Methanol (10 cm^3) was injected into the autoclave through an inlet against a flow of nitrogen followed by ethanol (1 cm^3, 17.13 mmol).

The autoclave was sealed and placed into a pre-heated (180 °C) aluminium heating mantle. After the reaction run time (2 or 20h), the autoclave was cooled to room temperature in an ice-water bath. The autoclave was vented to remove any gas generated during the reaction. A liquid sample was removed, filtered through a short plug of alumina (acidic) and analysed by GC (100 µL of sample, 25 µL of hexadecane standard, 1.7 cm^3 Et_2O – sample refiltered through a glass filter paper to remove insoluble salts).

8.6.4 Carbonyl/imine/heterocycle hydroboration

A dry NMR tube was charged with substrate (0.43 mmol, 1 equiv), **5.2** (0.1-3 mol%), freshly distilled catecholborane (56.7 mg, 0.47 mmol, 1.1 equiv), 1,3,5-trimethoxybenzene (~15 mg, 0.09 mmol, internal standard) and C_6D_6 (0.6 cm^3) before being sealed under nitrogen with a Youngs tap and shaken thoroughly. For the majority of substrates, the reaction was followed by running the required number (30-150) of 60 second NMR experiments (4 scans, d1 > 10 seconds, RG = 32) consecutively using multizg and integrating product signals against the 3H or 9H singlets of trimethoxybenzene. For substrates that required heating, after mixing the NMR tube was clamped in a pre-heated oil bath until the desired time period had passed. At which point, the tube was rapidly cooled in an ice bath before being analysed using the same ^{1}H-NMR parameters listed above.

8.6.5 Alkene hydroboration

A Schlenk flask was charged with **5.2** (1 mol%), THF (2 cm^3) and catecholborane (1 mmol). The resulting brown solution was stirred for five minutes before the substrate was added. Once complete, the reaction was cooled in an ice bath and ethanol (2 cm^3), 1M NaOH (6 cm^3) and H_2O_2 (6 cm^3) were added sequentially. The flask was then removed from the ice bath and stirred for one hour before being transferred to a separatory funnel. The aqueous solution was extracted with ether (3 x 10 cm^3) and the combined organic extracts washed once with NaOH (10 cm^3) and a saturated NaCl solution (10 cm^3). The organic layer was then dried over magnesium sulphate and filtered. 1,3,5-trimethoxybenzene (50 mg, 0.3 mmol) was then added as an internal standard and the solution concentrated under reduced pressure before analysis by ^{1}H NMR spectroscopy.

8.6.6 Alkene hydrogenation

Under air, a 250 cm^3 Schlenk flask was charged with substrate (1 mmol), **5.2** (29 mg, 2 mol%) and fluorobenzene (2 cm^3). The flask was then subjected to three freeze-pump-thaw cycles. On the third cycle, the flask was sealed under high-vacuum and hydrogen admitted *via* a balloon. The solution was allowed to thaw and stirred vigorously under a hydrogen atmosphere for the length of the reaction. The flask was then opened to air and a known amount of 1,3,5-trimethoxybenzene (as an internal standard) added. An aliquot of the solution was then analysed by ^{1}H-NMR spectroscopy to determine conversion.

8.6.7 Hydroformylation of 1-octene

All operations were conducted by Rebecca How and Paul Kamer at St. Andrew's University. A GC vial was charged with [Rh(acac)$(CO)_2$] (0.3 mg, 0.001 mmol), **2.1** (0.005 mmol), toluene (0.85 cm^3), 1-octene (0.1 cm^3) and decane (0.05 cm^3). The reaction was stirred at 80°C under a 1:1 CO/H_2 (20 bar) atmosphere for 3 hours before analysis by GC (method not given).

8.7 X-ray diffraction

8.7.1 General methods

Single crystals of the samples were covered in inert oil and placed under the cold stream of the diffractometer. Exposures were collected and indexing, data collection and absorption correction were performed using either the APEXII suite of programs or CrysalisPro. Structures were solved using direct methods (SHELXT) and refined by full-matrix least-squares (SHELXL) interfaced with the programme OLEX2.

Diffractometers: Bruker X8 APEXII four-circle diffractometer, Mo-Kα radiation (λ = 0.71073) (Heriot-Watt), Bruker APEXII four-circle diffractometer, Mo-Kα radiation (λ = 0.71073) (University of Edinburgh), EPSRC National Crystallography Service XtaLAB AFC12 (RCD3) Kappa single diffractometer, Mo-Kα radiation (University of Southampton), Oxford Diffraction four-circle Supernova diffractometer, Mo-Kα or Cu-Kα radiation (University of Edinburgh).

Additional details

2.7 showed the central phosphinine ring and Me substituents to be disordered, and this was successfully modelled over two positions.

4.1 had a partially occupied benzene solvate molecule that refined to 80.5 % occupancy, and AFIX 66 was used to force the six carbon atoms to form a regular hexagon.

There was a disordered CH_2Cl_2 solvate molecule in **3.6** that was successfully modelled over two positions.

Compound **5.1** co-crystallised with a benzene solvate molecule and the Cl / CO ligands were disordered over two positions that refined to occupancy factors of 0.62/0.38 (Cl1A, O1A and C43A /Cl1B, O1B and C43B) and 0.58/0.42 (Cl2A, O2A and C44A/Cl2B, O2B and C44B). Compound **5.2** had a disordered $SiMe_3$ group and CF_3 group that were both modelled over two positions.

8.7.2 Chapter 2

	2.1	**2.2**
Empirical formula	$C_{21}H_{24}P_2Si$	$C_{21}H_{27}BP_2Si$
Formula weight	366.43	380.26
Temperature/K	100.0	100.0
Crystal system	monoclinic	monoclinic
Space group	$P2_1/c$	$P2_1/n$
a/Å	16.815(4)	10.1934(5)
b/Å	5.8402(15)	9.3080(4)
c/Å	21.487(5)	22.7635(9)
α/°	90	90
β/°	104.221(10)	102.195(2)
γ/°	90	90
Volume/Å^3	2045.5(9)	2111.07(16)
Z	4	4
ρ_{calc}g/cm^3	1.190	1.196
μ/mm^{-1}	0.271	0.264
F(000)	776.0	808.0
Crystal size/mm^3	0.37 × 0.1 × 0.04	0.45 × 0.20 × 0.20
Radiation	Mo-Kα (λ = 0.71073)	Mo-Kα (λ = 0.71073)
2Θ range for data collection/°	4.998 to 54.814	4.744 to 61.188
Index ranges	-21 ≤ h ≤ 19 -7 ≤ k ≤ 7 -21 ≤ l ≤ 27	-14 ≤ h ≤ 14 -13 ≤ k ≤ 13 -32 ≤ l ≤ 32
Reflections collected	15927	59456
Independent reflections	4534 [R_{int} = 0.0525, R_{sigma} = 0.0596]	6461 [R_{int} = 0.0548, R_{sigma} = 0.0357]
Data/restraints/ parameters	4534/0/221	6461/0/239
Goodness-of-fit on F^2	1.080	1.035
Final R indexes [I>=2σ (I)]	R_1 = 0.0622 wR_2 = 0.1623	R_1 = 0.0361 wR_2 = 0.0821
Final R indexes [all data]	R_1 = 0.0850 wR_2 = 0.1779	R_1 = 0.0505 wR_2 = 0.0886
Largest diff. peak/hole / e Å^{-3}	0.85/-0.52	0.41/-0.31
Diffractometer	APEXII	APEXII

	2.4	**2.6**
Empirical formula	$C_{18}H_{19}BP_2$	$C_{31}H_{27}P_3$
Formula weight	308.08	492.43
Temperature/K	100.0	100.0
Crystal system	orthorhombic	triclinic
Space group	$P2_12_12_1$	P-1
a/Å	7.6784(3)	7.5692(9)
b/Å	13.3365(5)	12.6145(16)
c/Å	16.2366(5)	15.2354(17)
α/°	90	69.228(5)
β/°	90	76.539(5)
γ/°	90	73.790(5)
Volume/Å^3	1662.68(10)	1291.5(3)
Z	4	2
ρ_{calc}g/cm^3	1.231	1.266
μ/mm^{-1}	0.252	0.248
F(000)	648.0	516.0
Crystal size/mm^3	0.40 × 0.20 × 0.10	0.4 × 0.4 × 0.15
Radiation	Mo-Kα (λ = 0.71073)	Mo-Kα (λ = 0.71073)
2Θ range for data collection/°	3.952 to 55.052	3.536 to 60.984
Index ranges	$-9 \le h \le 9$ $-17 \le k \le 17$ $-21 \le l \le 21$	$-10 \le h \le 10$ $-17 \le k \le 17$ $-21 \le l \le 20$
Reflections collected	28893	34832
Independent reflections	3811 [R_{int} = 0.0434, R_{sigma} = 0.0296]	7806 [R_{int} = 0.0276, R_{sigma} = 0.0291]
Data/restraints/ parameters	3811/0/200	7806/0/309
Goodness-of-fit on F^2	1.041	1.044
Final R indexes [I>=2σ (I)]	R_1 = 0.0277 wR_2 = 0.0655	R_1 = 0.0331 wR_2 = 0.0823
Final R indexes [all data]	R_1 = 0.0323 wR_2 = 0.0674	R_1 = 0.0424 wR_2 = 0.0873
Largest diff. peak/hole / e Å^{-3}	0.25/-0.20	0.37/-0.24
Flack Parameter	0.01(3)	
Diffractometer	APEXII	APEXII

	2.7	**2.8**
Empirical formula	$C_{31}H_{28}P_3$	$C_{53}H_{60}Cl_{11}FeN_2OP_3$
Formula weight	493.44	1279.74
Temperature/K	100.0	100.0
Crystal system	monoclinic	triclinic
Space group	$P2_1/n$	P-1
a/Å	9.9671(13)	12.3741(5)
b/Å	8.0650(11)	14.0430(5)
c/Å	15.9450(18)	19.6151(7)
α/°	90	104.833(2)
β/°	99.576(9)	93.541(2)
γ/°	90	114.316(2)
Volume/Å^3	1263.9(3)	2948.1(2)
Z	2	2
ρ_{calc}g/cm^3	1.297	1.442
μ/mm^{-1}	0.254	0.875
F(000)	518.0	1316.0
Crystal size/mm^3	0.17 × 0.1 × 0.1	0.38 × 0.22 × 0.1
Radiation	Mo-Kα (λ = 0.71073)	Mo-Kα (λ = 0.71073)
2Θ range for data collection/°	5.24 to 55.118	3.678 to 55.62
Index ranges	$-12 \leq h \leq 11$ $-10 \leq k \leq 8$ $-20 \leq l \leq 20$	$-16 \leq h \leq 15$ $-18 \leq k \leq 18$ $-25 \leq l \leq 25$
Reflections collected	9164	51076
Independent reflections	2854 [R_{int} = 0.0756, R_{sigma} = 0.1155]	13575 [R_{int} = 0.0345, R_{sigma} = 0.0395]
Data/restraints/parameters	2854/54/192	13575/2/657
Goodness-of-fit on F^2	1.059	1.158
Final R indexes [I>=2σ (I)]	R_1 = 0.0782 wR_2 = 0.1379	R_1 = 0.0525 wR_2 = 0.1045
Final R indexes [all data]	R_1 = 0.1458 wR_2 = 0.1621	R_1 = 0.0605 wR_2 = 0.1081
Largest diff. peak/hole / e Å^{-3}	0.82/-0.57	0.62/-0.84
Diffractometer	APEXII	APEXII

8.7.3 Chapter 3

	3.1	**3.2**
Empirical formula	$C_{25}H_{24}O_4SiP_2Cr$	$C_{25}H_{24}O_4SiP_2Mo$
Formula weight	530.47	574.41
Temperature/K	100(2)	99.9(2)
Crystal system	triclinic	triclinic
Space group	*P*-1	*P*-1
a/Å	9.6172(5)	9.66244(18)
b/Å	11.1208(7)	11.2567(3)
c/Å	12.9795(7)	12.7533(3)
α/°	108.632(3)	108.568(2)
β/°	96.671(4)	97.2722(17)
γ/°	96.811(3)	97.5682(18)
Volume/Å^3	1288.51(13)	1282.35(5)
Z	2	2
ρ_{calc}g/cm^3	1.367	1.488
μ/mm^{-1}	0.643	0.712
F(000)	548.0	584.0
Crystal size/mm^3	0.65 × 0.18 × 0.10	0.20 × 0.06 × 0.03
Radiation	Mo-Kα (λ = 0.71073)	Mo-Kα (λ = 0.71073)
2Θ range for data collection/°	5.02 to 61.78	5.96 to 54.96
Index ranges	-13 ≤ h ≤ 13 -16 ≤ k ≤ 15 -18 ≤ l ≤ 18	-12 ≤ h ≤ 12 -14 ≤ k ≤ 13 -16 ≤ l ≤ 16
Reflections collected	23711	18889
Independent reflections	7939 [R_{int} = 0.0403, R_{sigma} = 0.0479]	5815 [R_{int} = 0.0223, R_{sigma} = 0.0205]
Data/restraints/parameters	7939/0/302	5815/0/302
Goodness-of-fit on F^2	1.012	1.074
Final R indexes [I>=2σ (I)]	R_1 = 0.0370, wR_2 = 0.0857	R_1 = 0.0217, wR_2 = 0.0533
Final R indexes [all data]	R_1 = 0.0543, wR_2 = 0.0947	R_1 = 0.0227, wR_2 = 0.0538
Largest diff. peak/hole / e Å^{-3}	0.48/-0.77	0.49/-0.24
Diffractometer	APEXII	XtaLAB AFC12

	3.3
Empirical formula	$C_{25}H_{24}O_4P_2SiW$
Formula weight	662.32
Temperature/K	150
Crystal system	triclinic
Space group	*P*-1
a/Å	9.6318(5)
b/Å	11.2188(7)
c/Å	12.8268(7)
α/°	108.550(3)
β/°	97.060(3)
γ/°	97.253(3)
Volume/Å^3	1283.76(13)
Z	2
ρ_{calc}g/cm^3	1.713
μ/mm^{-1}	4.699
F(000)	648.0
Crystal size/mm^3	0.30 × 0.08 × 0.02
Radiation	Mo-Kα (λ = 0.71073)
2Θ range for data collection/°	5.02 to 61.554
Index ranges	-13 ≤ h ≤ 13 -15 ≤ k ≤ 16 -18 ≤ l ≤ 18
Reflections collected	42703
Independent reflections	7885 [R_{int} = 0.0388, R_{sigma} = 0.0386]
Data/restraints/parameters	7885/0/302
Goodness-of-fit on F^2	1.054
Final R indexes [I>=2σ (I)]	R_1 = 0.0241 wR_2 = 0.0435
Final R indexes [all data]	R_1 = 0.0309 wR_2 = 0.0452
Largest diff. peak/hole / e Å^{-3}	0.75/-0.67
Diffractometer	APEXII

	3.4	**3.6**
Empirical formula	$C_{22}H_{16}CrO_4P_2$	$C_{45}H_{36}Cl_2Cr_2O_9P_4$
Formula weight	458.29	1019.52
Temperature/K	100.0	100.0
Crystal system	monoclinic	monoclinic
Space group	$P2_1$	$P2_1/n$
a/Å	9.6235(17)	9.5617(10)
b/Å	10.906(2)	18.983(2)
c/Å	10.8800(18)	24.980(3)
α/°	90	90
β/°	113.499(5)	92.328(6)
γ/°	90	90
Volume/Å^3	1047.2(3)	4530.5(9)
Z	2	4
ρ_{calc}g/cm^3	1.453	1.495
μ/mm^{-1}	0.724	0.794
F(000)	468.0	2080.0
Crystal size/mm^3	0.20 × 0.10 × 0.04	0.20 × 0.16 × 0.16
Radiation	Mo-Kα (λ = 0.71073)	Mo-Kα (λ = 0.71073)
2Θ range for data collection/°	5.534 to 54.81	4.592 to 55.046
Index ranges	-12 ≤ h ≤ 12 -14 ≤ k ≤ 13 -13 ≤ l ≤ 14	-12 ≤ h ≤ 11 -24 ≤ k ≤ 24 -32 ≤ l ≤ 32
Reflections collected	9638	47155
Independent reflections	4725 [R_{int} = 0.0415, R_{sigma} = 0.0767]	10348 [R_{int} = 0.0835, R_{sigma} = 0.0931]
Data/restraints/parameters	4725/1/263	10348/22/589
Goodness-of-fit on F^2	0.967	0.987
Final R indexes [I>=2σ (I)]	R_1 = 0.0406 wR_2 = 0.0718	R_1 = 0.0627 wR_2 = 0.1641
Final R indexes [all data]	R_1 = 0.0527 wR_2 = 0.0761	R_1 = 0.1198 wR_2 = 0.1944
Largest diff. peak/hole / e Å^{-3}	0.30/-0.40	1.15/-0.61
Flack parameter	0.01(2)	
Diffractometer	APEXII	APEXII

8.7.4 Chapter 4

	4.1	**4.2**
Empirical formula	$C_{46.83}H_{52.83}Cl_2P_4RuSi_2$	$C_{31}H_{38}Cl_4P_2Ru_2Si$
Formula weight	967.71	844.58
Temperature/K	100.0	100.0
Crystal system	monoclinic	triclinic
Space group	$P2_1/c$	P-1
a/Å	19.2383(11)	9.8194(5)
b/Å	25.4095(17)	10.9184(6)
c/Å	10.8916(6)	16.7816(9)
α/°	90	99.502(3)
β/°	105.042(3)	94.824(3)
γ/°	90	105.119(3)
Volume/Å^3	5141.8(5)	1697.74(16)
Z	4	2
ρ_{calc}g/cm^3	1.250	1.652
μ/mm^{-1}	0.609	1.355
F(000)	1999.0	848.0
Crystal size/mm^3	0.6 × 0.3 × 0.02	0.2 × 0.2 × 0.2
Radiation	Mo-Kα (λ = 0.71073)	Mo-Kα (λ = 0.71073)
2Θ range for data collection /°	3.884 to 49.554	5.276 to 55.356
Index ranges	-22 ≤ h ≤ 22 -29 ≤ k ≤ 26 -12 ≤ l ≤ 12	-12 ≤ h ≤ 12 -14 ≤ k ≤ 14 -21 ≤ l ≤ 21
Reflections collected	46318	50022
Independent reflections	8777 [R_{int} = 0.1045, R_{sigma} = 0.1060]	7730 [R_{int} = 0.0489, R_{sigma} = 0.0403]
Data/restraints/parameters	8777/36/518	7730/0/368
Goodness-of-fit on F^2	1.039	1.062
Final R indexes [I>=2σ (I)]	R_1 = 0.0644 wR_2 = 0.1373	R_1 = 0.0308 wR_2 = 0.0618
Final R indexes [all data]	R_1 = 0.1240 wR_2 = 0.1593	R_1 = 0.0445 wR_2 = 0.0659
Largest diff. peak/hole / e Å^{-3}	0.88/-0.63	0.56/-0.76
Diffractometer	APEXII	APEXII

	4.3	**4.5**
Empirical formula	$C_{30.5}H_{37}Cl_2F_6OP_3Ru$	$C_{31}H_{41}ClOP_2RuSi$
Formula weight	798.48	656.19
Temperature/K	150.01	120.01(10)
Crystal system	monoclinic	triclinic
Space group	$P2_1/n$	P-1
a/Å	8.8172(4)	14.6758(5)
b/Å	37.4359(16)	14.7658(4)
c/Å	19.6657(9)	15.2176(3)
α/°	90	92.281(2)
β/°	90.340(2)	105.461(2)
γ/°	90	101.298(2)
Volume/Å^3	6491.1(5)	3101.93(15)
Z	8	4
ρ_{calc}g/cm^3	1.634	1.405
μ/mm^{-1}	0.855	6.394
F(000)	3240.0	1360.0
Crystal size/mm^3	0.274 × 0.269 × 0.188	0.202 × 0.054 × 0.02
Radiation	Mo-Kα (λ = 0.71073)	Cu-Kα (λ = 1.54184)
2Θ range for data collection/°	4.68 to 56.784	7.478 to 152.286
Index ranges	$-11 \leq h \leq 11$ $-50 \leq k \leq 49$ $-26 \leq l \leq 26$	$-18 \leq h \leq 17$ $-18 \leq k \leq 17$ $-18 \leq l \leq 19$
Reflections collected	222582	49418
Independent reflections	16043 [R_{int} = 0.0388, R_{sigma} = 0.0188]	12852 [R_{int} = 0.0820, R_{sigma} = 0.0664]
Data/restraints/parameters	16043/2/810	12852/1/697
Goodness-of-fit on F^2	1.127	1.045
Final R indexes [I>=2σ (I)]	R_1 = 0.0422 wR_2 = 0.0973	R_1 = 0.0516 wR_2 = 0.1277
Final R indexes [all data]	R_1 = 0.0493 wR_2 = 0.1009	R_1 = 0.0635 wR_2 = 0.1358
Largest diff. peak/hole / e Å^{-3}	1.25/-0.94	1.04/-1.39
Diffractometer	APEXII (UoE)	Supernova

8.7.5 Chapter 5

Identification code	**5.1**	**5.2**
Empirical formula	$C_{50}H_{54}Cl_2O_2P_4Rh_2Si_2$	$C_{61}H_{48}BF_{24}P_2RhSi$
Formula weight	1143.71	1440.74
Temperature/K	100(1)	120(1)
Crystal system	orthorhombic	triclinic
Space group	$P2_12_12_1$	P-1
a/Å	13.6107(5)	13.2396(4)
b/Å	19.3024(5)	14.6179(4)
c/Å	19.5658(7)	18.0412(5)
α/°	90	98.298(2)
β/°	90	102.651(2)
γ/°	90	110.657(3)
Volume/Å^3	5140.3(3)	3092.50(16)
Z	4	2
ρ_{calc}g/cm^3	1.478	1.547
μ/mm^{-1}	0.955	0.459
F(000)	2328.0	1448.0
Crystal size/mm^3	0.20 × 0.10 × 0.02	0.29 × 0.22 × 0.17
Radiation	Mo-Kα (λ = 0.71073)	Mo-Kα (λ = 0.71073)
2Θ range for data collection/°	5.128 to 56.64	5.758 to 59.498
Index ranges	-18 ≤ h ≤ 17 -25 ≤ k ≤ 25 -25 ≤ l ≤ 25	-17 ≤ h ≤ 18 -19 ≤ k ≤ 18 -24 ≤ l ≤ 24
Reflections collected	62167	69611
Independent reflections	12732 [R_{int} = 0.0496, R_{sigma} = 0.0464]	15721 [R_{int} = 0.0487, R_{sigma} = 0.0479]
Data/restraints/parameters	12732/18/623	15721/78/896
Goodness-of-fit on F^2	1.024	1.024
Final R indexes [I>=2σ (I)]	R_1 = 0.0280 wR_2 = 0.0504	R_1 = 0.0550 wR_2 = 0.1258
Final R indexes [all data]	R_1 = 0.0350 wR_2 = 0.0523	R_1 = 0.0695 wR_2 = 0.1340
Largest diff. peak/hole / e Å^{-3}	0.43/-0.38	1.46/-0.96
Flack parameter	-0.015(10)	
Diffractometer	APEXII	Supernova

9 -References

1. G. Jones, in *Comprehensive Heterocyclic Chemistry II*, eds. C. W. Rees and E. F. V. Scriven, Pergamon, Oxford, 1996, pp. 167-243.
2. D. L. Comins and S. P. Joseph, in *Comprehensive Heterocyclic Chemistry II*, eds. C. W. Rees and E. F. V. Scriven, Pergamon, Oxford, 1996, pp. 37-89.
3. C. Müller, L. E. E. Broeckx, I. de Krom and J. J. M. Weemers, *Eur. J. Inorg. Chem.*, 2013, 187-202.
4. G. Märkl, *Angew. Chem. Int. Ed.*, 1966, **5**, 846-847.
5. H. Albers, *Angew. Chem.*, 1950, **62**, 451.
6. T. E. Gier, *J. Am. Chem. Soc.*, 1961, **83**, 1769-1770.
7. A. J. Ashe, *Eur. J. Inorg. Chem.*, 2016, **2016**, 572-574.
8. P. Le Floch, *Coord. Chem. Rev.*, 2006, **250**, 627-681.
9. J. R. Lawson, L. C. Wilkins and R. L. Melen, *Chem.-Eur. J.*, 2017, **23**, 10997-11000.
10. A. J. Ashe, *J. Am. Chem. Soc.*, 1971, **93**, 3293-3295.
11. M. H. Habicht, F. Wossidlo, T. Bens, E. A. Pidko and C. Müller, *Chem.-Eur. J.*, 2018, **24**, 944-952.
12. C. Müller and D. Vogt, *C. R. Chim.*, 2010, **13**, 1127-1143.
13. A. J. Ashe, W.-T. Chan and E. Perozzi, *Tetrahedron Lett.*, 1975, **16**, 1083-1086.
14. C. Müller and D. Vogt, *Dalton Trans.*, 2007, 5505-5523.
15. C. Müller and D. Vogt, in *Phosphorus Compounds: Advanced Tools in Catalysis and Material Sciences*, eds. M. Peruzzini and L. Gonsalvi, Springer, Netherlands, 2011, ch. 6, pp. 151-181.
16. C. Müller, in *Phosphorus(III) Ligands in Homogeneous Catalysis: Design and Synthesis*, John Wiley & Sons, Ltd, 2012, pp. 287-307.
17. P. Tokarz and P. M. Zagórski, *Chem. Heterocycl. Compd. (N. Y., NY, U. S.)*, 2017, **53**, 858-860.
18. N. Mézailles, F. Mathey and P. Le Floch, in *Prog. Inorg. Chem.*, ed. K. D. Karlin, 2007, vol. 49, ch. 4, pp. 455-550.
19. A. Loibl, I. de Krom, E. A. Pidko, M. Weber, J. Wiecko and C. Müller, *Chem. Commun.*, 2014, **50**, 8842-8844.
20. C. Müller, D. Wasserberg, J. J. M. Weemers, E. A. Pidko, S. Hoffmann, M. Lutz, A. L. Spek, S. C. J. Meskers, R. A. J. Janssen, R. A. v. Santen and D. Vogt, *Chem.-Eur. J.*, 2007, **13**, 4548-4559.
21. J. R. Bell, A. Franken and C. M. Garner, *Tetrahedron*, 2009, **65**, 9368-9372.
22. N. A. van der Velde, H. T. Korbitz and C. M. Garner, *Tetrahedron Lett.*, 2012, **53**, 5742-5744.
23. C. Müller, E. A. Pidko, D. Totev, M. Lutz, A. L. Spek, R. A. van Santen and D. Vogt, *Dalton Trans.*, 2007, 5372-5375.
24. J. J. M. Weemers, W. N. P. v. d. Graaff, E. A. Pidko, M. Lutz and C. Müller, *Chem.-Eur. J.*, 2013, **19**, 8991-9004.
25. C. Müller, E. A. Pidko, A. J. P. M. Staring, M. Lutz, A. L. Spek, R. A. van Santen and D. Vogt, *Chem.-Eur. J.*, 2008, **14**, 4899-4905.
26. C. Müller, L. G. López, H. Kooijman, A. L. Spek and D. Vogt, *Tetrahedron Lett.*, 2006, **47**, 2017-2020.
27. M. Rigo, J. A. W. Sklorz, N. Hatje, F. Noack, M. Weber, J. Wiecko and C. Müller, *Dalton Trans.*, 2016, **45**, 2218-2226.
28. B. Breit, R. Winde, T. Mackewitz, R. Paciello and K. Harms, *Chem.-Eur. J.*, 2001, **7**, 3106-3121.
29. J. J. Lee and E. J. Corey, in *Name Reactions in Heterocyclic Chemistry* Wiley, 2011, vol. 2, ch. 8, pp. 401-419.

30. M. H. Habicht, F. Wossidlo, M. Weber and C. Müller, *Chem.-Eur. J.*, 2016, **22**, 12877-12883.
31. W. Rösch and M. Regitz, *Z. Naturforsch*, 1986, **41b**, 931-933.
32. B. Breit, *J. Mol. Catal. A: Chem.*, 1999, **143**, 143-154.
33. M. Z. Bani-Fwaz, A. E. Fazary and G. Becker, *J. Coord. Chem.*, 2017, **70**, 2224-2248.
34. N. Trathen, V. K. Greenacre, I. R. Crossley and S. M. Roe, *Organometallics*, 2013, **32**, 2501-2504.
35. N. Kazunari, T. Shohei, S. Ken and N. Yoshiaki, *Angew. Chem. Int. Ed.*, 2015, **54**, 7597-7601.
36. B. Wrackmeyer and U. Klaus, *J. Organomet. Chem.*, 1996, **520**, 211-226.
37. F. Mathey, *Tetrahedron*, 1973, **29**, 707-714.
38. F. Mathey, *Tetrahedron Lett.*, 1979, **20**, 1753-1756.
39. J.-M. Alcaraz, A. Breque and F. Mathey, *Tetrahedron Lett.*, 1982, **23**, 1565-1568.
40. Y. Mao and F. Mathey, *Org. Lett.*, 2012, **14**, 1162-1163.
41. W. Huaiqiu, L. Chuan, G. Dingjin, C. Hui, D. Zheng and M. François, *Chem.-Eur. J.*, 2010, **16**, 10659-10661.
42. N. S. Isaacs and G. N. El-Din, *Synthesis*, 1989, **1989**, 967-967.
43. F. Mathey, F. Mercier, C. Charrier, J. Fischer and A. Mitschler, *J. Am. Chem. Soc.*, 1981, **103**, 4595-4597.
44. C. Charrier, H. Bonnard and F. Mathey, *J. Org. Chem.*, 1982, **47**, 2376-2379.
45. C. Hui, L. Jin, W. Huaiqiu, L. Hui, D. Zheng and M. François, *Eur. J. Inorg. Chem.*, 2011, **2011**, 1540-1543.
46. S. Holand, L. Ricard and F. Mathey, *J. Org. Chem.*, 1991, **56**, 4031-4035.
47. P. Le Floch and F. Mathey, *Tetrahedron Lett.*, 1989, **30**, 817-818.
48. P. Le Floch, L. Ricard and F. Mathey, *Polyhedron*, 1990, **9**, 991-997.
49. P. Le Floch, D. Carmichael and F. Mathey, *Organometallics*, 1991, **10**, 2432-2436.
50. P. Le Floch, D. Carmichael, L. Ricard and F. Mathey, *J. Am. Chem. Soc.*, 1993, **115**, 10665-10670.
51. P. Le Floch, L. Ricard and F. Mathey, *J. Chem. Soc., Chem. Commun.*, 1993, 789-791.
52. H. Trauner, P. Le Floch, J.-M. Lefour, L. Ricard and F. Mathey, *Synthesis*, 1995, **1995**, 717-726.
53. K. Nataliya, E. Cecilia, E. Magnus, G. S. Villa and B. Annette, *Eur. J. Org. Chem.*, 2013, **2013**, 4756-4759.
54. G. Märkl and G. Dorfmeister, *Tetrahedron Lett.*, 1987, **28**, 1093-1096.
55. G. Märkl, C. Dörges, T. Riedl, F. G. Klärner and C. Lodwig, *Tetrahedron Lett.*, 1990, **31**, 4589-4592.
56. M. M. Hansmann has recently reported the synthesis of 1,3-azaphosphinines from triazines, however they were formed as a mixture with the analogous 1,4-azaphosphinine. M.M. Hansmann, Chem. Eur. J, 2018, Accepted Author Manuscript, DOI: 10.1002/chem.201802173
57. N. Avarvari, P. Le Floch and F. Mathey, *J. Am. Chem. Soc.*, 1996, **118**, 11978-11979.
58. N. Avarvari, P. Le Floch, L. Ricard and F. Mathey, *Organometallics*, 1997, **16**, 4089-4098.
59. I. Beletskaya and A. Pelter, *Tetrahedron*, 1997, **53**, 4957-5026.
60. S. A. Orr, A. R. Kennedy, J. J. Liggat, R. McLellan, R. E. Mulvey and S. D. Robertson, *Dalton Trans.*, 2016, **45**, 6234-6240.
61. K. Dimroth, *Acc. Chem. Res.*, 1982, **15**, 58-64.

62. M. Doux, P. Thuéry, M. Blug, L. Ricard, P. Le Floch, T. Arliguie and N. Mézailles, *Organometallics*, 2007, **26**, 5643-5653.
63. A. Moores, L. Ricard and P. Le Floch, *Angew. Chem. Int. Ed.*, 2003, **42**, 4940-4944.
64. D. G. Gilheany, in *Organophosphorus Compounds* ed. F. R. Hartley, Wiley, 1993, ch. 1, pp. 2-44.
65. C. Müller and D. Vogt, in *Phosphorus Compounds: Advanced Tools in Catalysis and Material Sciences*, eds. M. Peruzzini and L. Gonsalvi, Springer Netherlands, Dordrecht, 2011, pp. 151-181.
66. C. A. Tolman, *Chem. Rev.*, 1977, **77**, 313-348.
67. M. Rigo, M. Weber and C. Müller, *Chem. Commun.*, 2016, **52**, 7090-7093.
68. R. McLellan, A. R. Kennedy, R. E. Mulvey, S. A. Orr and S. D. Robertson, *Chem.-Eur. J.*, 2017, **23**, 16853-16861.
69. C. Elschenbroich, M. Nowotny, A. Behrendt, K. Harms, S. Wocadlo and J. Pebler, *J. Am. Chem. Soc.*, 1994, **116**, 6217-6219.
70. C. Elschenbroich, J. Six, K. Harms, G. Frenking and G. Heydenrych, *Eur. J. Inorg. Chem.*, 2008, **2008**, 3303-3309.
71. P. Le Floch and F. Mathey, *J. Chem. Soc., Chem. Commun.*, 1993, 1295-1296.
72. C. Elschenbroich, M. Nowotny, J. Kroker, A. Behrendt, W. Massa and S. Wocadlo, *J. Organomet. Chem.*, 1993, **459**, 157-167.
73. L. Canoira and R. J. Gonzalo, *J. Chem. Res., Synop.*, 1988, 68-69.
74. The synthesis of this complex was not confirmed by any characterisation, see Ref. 3 in Angew. Chem. Int. Ed. Engl., 1992, 31, 1343-1345
75. N. Mézailles, L. Ricard, F. Mathey and P. Le Floch, *Organometallics*, 2001, **20**, 3304-3307.
76. D. Jürgen and N. Heinrich, *Chem. Ber.*, 1970, **103**, 2541-2547.
77. D. Jürgen and N. Heinrich, *Chem. Ber.*, 1973, **106**, 2222-2226.
78. J. Deberitz and H. Nöth, *J. Organomet. Chem.*, 1973, **49**, 453-468.
79. V. C. Gibson, C. Redshaw and G. A. Solan, *Chem. Rev.*, 2007, **107**, 1745-1776.
80. X.-M. Gan, E. N. Duesler and R. T. Paine, *Inorg. Chem.*, 2001, **40**, 4420-4427.
81. C. Gunanathan and D. Milstein, *Acc. Chem. Res.*, 2011, **44**, 588-602.
82. S. M. Mansell, *Dalton Trans.*, 2017, **46**, 15157-15174.
83. E. P. Goudriaan, P. W. N. M. van Leeuwen, M. N. Birkholz and J. N. H. Reek, *Eur. J. Inorg. Chem.*, 2008, **2008**, 2939-2958.
84. M. G. Gardiner and C. C. Ho, *Coord. Chem. Rev.*, 2018.
85. S. Schick, T. Pape and F. E. Hahn, *Organometallics*, 2014, **33**, 4035-4041.
86. L. Chun-Chin, K. Wei-Chi, C. Kai-Ting, L. Chun-Liang, H. Ching-Han and L. H. Man, *Chem.-Eur. J.*, 2007, **13**, 582-591.
87. S. G., *Helv. Chim. Acta*, 1952, **35**, 2344-2359.
88. R. P. J. Bronger, P. C. J. Kamer and P. W. N. M. van Leeuwen, *Organometallics*, 2003, **22**, 5358-5369.
89. D. S. McGuinness, *Chem. Rev.*, 2011, **111**, 2321-2341.
90. F. Mathey and P. Le Floch, *Chem. Ber.*, 1996, **129**, 263-268.
91. P. Le Floch, S. Mansuy, L. Ricard, F. Mathey, A. Jutand and C. Amatore, *Organometallics*, 1996, **15**, 3267-3274.
92. P. Rosa, L. Ricard, F. Mathey and P. Le Floch, *Organometallics*, 1999, **18**, 3348-3352.
93. P. Rosa, L. Ricard, F. Mathey and P. Le Floch, *Organometallics*, 2000, **19**, 5247-5250.
94. P. Rosa, N. Mézailles, F. Mathey and P. Le Floch, *J. Org. Chem.*, 1998, **63**, 4826-4828.

95. N. Mézailles, P. Rosa, L. Ricard, F. Mathey and P. Le Floch, *Organometallics*, 2000, **19**, 2941-2943.
96. P. Rosa, N. Mézailles, L. Ricard, F. Mathey, P. Le Floch and Y. Jean, *Angew. Chem. Int. Ed.*, 2001, **40**, 1251-1253.
97. P. Le Floch, D. Carmichael, L. Ricard and F. Mathey, *J. Am. Chem. Soc.*, 1991, **113**, 667-669.
98. P. Le Floch, L. Ricard and F. Mathey, *Bull. Soc. Chim. Fr.*, 1994, **131**, 330-334.
99. D. Carmichael, P. Le Floch, L. Ricard and F. Mathey, *Inorg. Chim. Acta*, 1992, **198-200**, 437-441.
100. M. J. Bakker, F. W. Vergeer, F. Hartl, K. Goubitz, J. Fraanje, P. Rosa and P. Le Floch, *Eur. J. Inorg. Chem.*, 2000, **2000**, 843-845.
101. P. Le Floch, L. Ricard, F. Mathey, A. Jutand and C. Amatore, *Inorg. Chem.*, 1995, **34**, 11-12.
102. T. Kruck and A. Prasch, *Z. Anorg. Allg. Chem.*, 1969, **371**, 1-22.
103. D. A. Evans and A. H. Hoveyda, *J. Org. Chem.*, 1990, **55**, 5190-5192.
104. R. T. Baker, J. C. Calabrese and S. A. Westcott, *J. Organomet. Chem.*, 1995, **498**, 109-117.
105. Y. Matsusaka, S. Shitaya, K. Nomura and A. Inagaki, *Inorg. Chem.*, 2017, **56**, 1027-1030.
106. As well as other elements more electropositive than carbon
107. A dimethyltin-bridge diphosphinine was also prepared by Teunissen and Bickelhaupt from an organozinc derivative, however it was only obtained in low yield due to a high rate of decomposition. (H. T. Teunissen, F. Bickelhaupt, Organometallics, 1996, 15 (2), 802-808
108. S. Choua, C. Dutan, L. Cataldo, T. Berclaz, M. Geoffroy, N. Mézailles, A. Moores, L. Ricard and P. Le Floch, *Chem.-Eur. J.*, 2004, **10**, 4080-4090.
109. A. Winter, G. R. Newkome and U. S. Schubert, *ChemCatChem*, 2011, **3**, 1384-1406.
110. There is no digital access to this journal, however the abstract states that "With 2,6-dibromophosphinines, the same coupling reaction is not observed and a functional phosphinine resulting from the nucleophilic attack of a phosphacyclohexadienide anion onto the C2-Br bond has been obtained..."
111. N. Mézailles, N. Avarvari, L. Ricard, F. Mathey and P. Le Floch, *Inorg. Chem.*, 1998, **37**, 5313-5316.
112. A. K.-W. Chan, D. Wu, K. M.-C. Wong and V. W.-W. Yam, *Inorg. Chem.*, 2016, **55**, 3685-3691.
113. U. Rhörig, N. Mézailles, N. Mézailles, L. Mézailles, F. Mathey and P. Le Floch, *Eur. J. Inorg. Chem.*, 2000, **2000**, 2565-2571.
114. A. R. Jupp and J. M. Goicoechea, *Angew. Chem. Int. Ed.*, 2013, **52**, 10064-10067.
115. X. D. Chen, S. Alidori, F. F. Puschmann, G. Santiso-Quinones, Z. Benko, Z. S. Li, G. Becker, H. F. Grutzmacher and H. Grutzmacher, *Angew. Chem. Int. Ed.*, 2014, **53**, 1641-1645.
116. C. M. Vogels, P. E. O'Connor, T. E. Phillips, K. J. Watson, M. P. Shaver, P. G. Hayes and S. A. Westcott, *Canadian Journal of Chemistry-Revue Canadienne De Chimie*, 2001, **79**, 1898-1905.
117. C. Xiaodan, L. Zhongshu, Y. Fan and G. Hansjörg, *Eur. J. Inorg. Chem.*, 2016, **2016**, 633-638.
118. D. M. Homden and C. Redshaw, *Chem. Rev.*, 2008, **108**, 5086-5130.
119. S.-Y. Li, Y.-W. Xu, J.-M. Liu and C.-Y. Su, *Int. J. Mol. Sci.*, 2011, **12**, 429.
120. O. L. Kaliya, E. A. Lukyanets and G. N. Vorozhtsov, *J. Porphyrins Phthalocyanines*, 1999, **03**, 592-610.

121. A. B. Sorokin, *Chem. Rev.*, 2013, **113**, 8152-8191.
122. B. Meunier, *Chem. Rev.*, 1992, **92**, 1411-1456.
123. J. Barona-Castaño, C. Carmona-Vargas, T. Brocksom and K. de Oliveira, *Molecules*, 2016, **21**, 310.
124. G. S. Ananthnag and V. S. Shetti, *Dalton Trans.*, 2017, **46**, 14062-14082.
125. W. Zhang, W. Lai and R. Cao, *Chem. Rev.*, 2017, **117**, 3717-3797.
126. N. Avarvari, N. Mézailles, L. Ricard, P. Le Floch and F. Mathey, *Science*, 1998, **280**, 1587-1589.
127. N. Mézailles, N. Maigrot, S. Hamon, L. Ricard, F. Mathey and P. Le Floch, *J. Org. Chem.*, 2001, **66**, 1054-1056.
128. N. Avarvari, N. Maigrot, L. Ricard, F. Mathey and P. Le Floch, *Chem.-Eur. J.*, 1999, **5**, 2109-2118.
129. A. Moores, N. Mézailles, N. Maigrot, L. Ricard, F. Mathey and P. Le Floch, *Eur. J. Inorg. Chem.*, 2002, **2002**, 2034-2039.
130. N. Mézailles, N. Avarvari, N. Maigrot, L. Ricard, F. Mathey, P. Le Floch, L. Cataldo, T. Berclaz and M. Geoffroy, *Angew. Chem. Int. Ed.*, 1999, **38**, 3194-3197.
131. D. McIntosh and G. A. Ozin, *Inorg. Chem.*, 1977, **16**, 51-59.
132. L. Cataldo, S. Choua, T. Berclaz, M. Geoffroy, N. Mézailles, L. Ricard, F. Mathey and P. Le Floch, *J. Am. Chem. Soc.*, 2001, **123**, 6654-6661.
133. D. G. Holah, A. N. Hughes, K. L. Knudsen and R. Perrier, *J. Heterocycl. Chem.*, 1988, **25**, 155-160.
134. I. G. M. Campbell, R. C. Cookson, M. B. Hocking and A. N. Hughes, *J. Chem. Soc.*, 1965, 2184-2193.
135. R. R. Schmidt, D. Schwille and U. Sommer, *Justus Liebigs Ann. Chem.*, 1969, **723**, 111-118.
136. K. Waschbüsch, P. Le Floch and F. Mathey, *Organometallics*, 1996, **15**, 1597-1603.
137. N. Mézailles, P. Le Floch, K. Waschbüsch, L. Ricard, F. Mathey and C. P. Kubiak, *J. Organomet. Chem.*, 1997, **541**, 277-283.
138. K. Waschbüch, P. Le Floch, L. Ricard and F. Mathey, *Chem. Ber.*, 1997, **130**, 843-849.
139. C. Xiaodan, L. Zhongshu and G. Hansjörg, *Chem.-Eur. J.*, **0**.
140. Structure obtained from the CSD. Code: YUYPIT
141. B. Schmid, L. M. Venanzi, A. Albinati and F. Mathey, *Inorg. Chem.*, 1991, **30**, 4693-4699.
142. I. de Krom, E. A. Pidko, M. Lutz and C. Müller, *Chem.-Eur. J.*, 2013, **19**, 7523-7531.
143. I. de Krom, L. E. E. Broeckx, M. Lutz and C. Müller, *Chem.-Eur. J.*, 2013, **19**, 3676-3684.
144. L. E. E. Broeckx, A. Bucci, C. Zuccaccia, M. Lutz, A. Macchioni and C. Müller, *Organometallics*, 2015, **34**, 2943-2952.
145. M. Doux, C. Bouet, N. Mézailles, L. Ricard and P. Le Floch, *Organometallics*, 2002, **21**, 2785-2788.
146. M. Doux, N. Mezailles, M. Melaimi, L. Ricard and P. Le Floch, *Chem. Commun.*, 2002, 1566-1567.
147. M. Trincado and H. Grützmacher, in *Cooperative Catalysis*, ed. R. Peters, Wiley, 2015, pp. 67-110.
148. C. Müller, E. A. Pidko, M. Lutz, A. L. Spek and D. Vogt, *Chem.-Eur. J.*, 2008, **14**, 8803-8807.
149. A. Breque, C. C. Santini, F. Mathey, J. Fischer and A. Mitschler, *Inorg. Chem.*, 1984, **23**, 3463-3467.

150. B. Schmid, L. M. Venanzi, T. Gerfin, V. Gramlich and F. Mathey, *Inorg. Chem.*, 1992, **31**, 5117-5122.
151. I. de Krom, M. Lutz and C. Müller, *Dalton Trans.*, 2015, **44**, 10304-10314.
152. A. C. Carrasco, E. A. Pidko, A. M. Masdeu-Bulto, M. Lutz, A. L. Spek, D. Vogt and C. Müller, *New J. Chem.*, 2010, **34**, 1547-1550.
153. A. Campos-Carrasco, L. E. E. Broeckx, J. J. M. Weemers, E. A. Pidko, M. Lutz, A. M. Masdeu-Bultó, D. Vogt and C. Müller, *Chem.-Eur. J.*, 2011, **17**, 2510-2517.
154. N. Mezailles and P. Le Floch, *Curr. Org. Chem.*, 2006, **10**, 3-25.
155. F. Knoch, F. Kremer, U. Schmidt, U. Zenneck, P. Le Floch and F. Mathey, *Organometallics*, 1996, **15**, 2713-2719.
156. P. Le Floch, F. Knoch, F. Kremer, F. Mathey, J. Scholz, W. Scholz, K. H. Thiele and U. Zenneck, *Eur. J. Inorg. Chem.*, 1998, **1998**, 119-126.
157. E. F. DiMauro and M. C. Kozlowski, *J. Chem. Soc., Perkin Trans. 1*, 2002, 439-444.
158. M. Rigo, L. Hettmanczyk, F. J. L. Heutz, S. Hohloch, M. Lutz, B. Sarkar and C. Müller, *Dalton Trans.*, 2017, **46**, 86-95.
159. P. W. N. M. van Leeuwen and C. Claver, *Rhodium Catalyzed Hydroformylation*, Springer Netherlands, 2002.
160. B. Breit, *Chem. Commun.*, 1996, 2071-2072.
161. B. Breit, R. Winde and K. Harms, *J. Chem. Soc., Perkin Trans. 1*, 1997, 2681-2682.
162. E. Neumann, PhD Thesis, University of Basel, 2006, chapter 3, 51-79, https://edoc.unibas.ch/374/1/DissB_7467.pdf
163. M. T. Reetz and X. Li, *Angew. Chem. Int. Ed.*, 2005, **44**, 2962-2964.
164. S. Aguado-Ullate, J. A. Baker, V. Gonzalez-Gonzalez, C. Müller, J. D. Hirst and J. J. Carbo, *Catal. Sci. Tech.*, 2014, **4**, 979-987.
165. V. R. Ferro, S. Omar, R. H. González-Jonte and J. M. García de la Vega, *Heteroat. Chem.*, 2003, **14**, 160-169.
166. W. Hewertson, I. C. Taylor and S. Trippett, *J. Chem. Soc. C*, 1970, 1835-1839.
167. P. Spies, R. Fröhlich, G. Kehr, G. Erker and S. Grimme, *Chem.-Eur. J.*, 2008, **14**, 333-343.
168. J. Trotter, *Tetrahedron*, 1960, **8**, 13-22.
169. J. Gauss and J. F. Stanton, *J. Phys. Chem. A*, 2000, **104**, 2865-2868.
170. L. Pauling and L. O. Brockway, *J. Am. Chem. Soc.*, 1937, **59**, 1223-1236.
171. L. Nyulaszi, T. Veszpremi and J. Reffy, *J. Phys. Chem.*, 1995, **99**, 10142-10146.
172. T. Fanjul, G. Eastham, J. Floure, S. J. K. Forrest, M. F. Haddow, A. Hamilton, P. G. Pringle, A. G. Orpen and M. Waugh, *Dalton Trans.*, 2013, **42**, 100-115.
173. M. Bruce, G. Meissner, M. Weber, J. Wiecko and C. Müller, *Eur. J. Inorg. Chem.*, 2014, **2014**, 1719-1726.
174. H. Brisset, Y. Gourdel, P. Pellon and M. Le Corre, *Tetrahedron Lett.*, 1993, **34**, 4523-4526.
175. U. V. Mallavadhani and N. Fleury-Bregeot, in *Encyclopedia of Reagents for Organic Synthesis*, John Wiley & Sons, Ltd, 2001.
176. G. C. Lloyd-Jones and N. P. Taylor, *Chem.-Eur. J.*, 2015, **21**, 5423-5428.
177. R. J. Newland, M. F. Wyatt, R. L. Wingad and S. M. Mansell, *Dalton Trans.*, 2017, **46**, 6172-6176.
178. H. Schmidbaur, R. Herr and J. Riede, *Chem. Ber.*, 1984, **117**, 2322-2327.
179. D. W. Allen and B. F. Taylor, *J. Chem. Soc., Dalton Trans.*, 1982, 51-54.
180. S. Holand, J.-M. Alcaraz, L. Ricard and F. Mathey, *Heteroat. Chem.*, 1990, **1**, 37-42.

181. D. G. Holah, A. N. Hughes and K. L. Knudsen, *J. Chem. Soc., Chem. Commun.*, 1988, 493-495.
182. A. Moores, T. Cantat, L. Ricard, N. Mezailles and P. Le Floch, *New J. Chem.*, 2007, **31**, 1493-1498.
183. M. N. Chevykalova, L. F. Manzhukova, N. V. Artemova, Y. N. Luzikov, I. E. Nifant"ev and E. E. Nifant"ev, *Russ. Chem. Bull.*, 2003, **52**, 78-84.
184. U. Beckmann, D. Süslüyan and P. C. Kunz, *Phosphorus, Sulfur Silicon Relat. Elem*, 2011, **186**, 2061-2070.
185. C. Glidewell and E. J. Leslie, *J. Chem. Soc., Dalton Trans.*, 1977, 527-531.
186. At the time of writing, trans-piperylene is only available from Sigma-Aldrich at the price of £74.70 for 1 gram
187. M. Blug, O. Piechaczyk, M. Fustier, N. Mézailles and P. Le Floch, *J. Org. Chem.*, 2008, **73**, 3258-3261.
188. R. J. Newland, A. Smith, D. M. Smith, N. Fey, M. J. Hanton and S. M. Mansell, *Organometallics*, 2018, **37**, 1062-1073.
189. J. M. M. B. Smith, *March's Advanced Organic Chemistry (6th edition)*, Wiley, 2007.
190. C. Gunanathan and D. Milstein, *Science*, 2013, **341**.
191. N. Maigrot, M. Melaimi, L. Ricard and P. Le Floch, *Heteroat. Chem.*, 2003, **14**, 326-333.
192. M. Doux, N. Mézailles, L. Ricard, P. Le Floch, P. Adkine, T. Berclaz and M. Geoffroy, *Inorg. Chem.*, 2005, **44**, 1147-1152.
193. M. Doux, N. Mézailles, L. Ricard, P. Le Floch, P. D. Vaz, M. J. Calhorda, T. Mahabiersing and F. Hartl, *Inorg. Chem.*, 2005, **44**, 9213-9224.
194. M. Doux, N. Mézailles, L. Ricard and P. Le Floch, *Eur. J. Inorg. Chem.*, 2003, **2003**, 3878-3894.
195. M. Doux, L. Ricard, P. Le Floch and N. Mezailles, *Dalton Trans.*, 2004, 2593-2600.
196. T. Arliguie, M. Blug, P. Le Floch, N. Mézailles, P. Thuéry and M. Ephritikhine, *Organometallics*, 2008, **27**, 4158-4165.
197. J. García-Álvarez, S. E. García-Garrido and V. Cadierno, *J. Organomet. Chem.*, 2014, **751**, 792-808.
198. J. M. Hoyt, V. A. Schmidt, A. M. Tondreau and P. J. Chirik, *Science*, 2015, **349**, 960-963.
199. L. Boubekeur, L. Ricard, N. Mézailles and P. Le Floch, *Organometallics*, 2005, **24**, 1065-1074.
200. H. Staudinger and J. Meyer, *Helv. Chim. Acta*, 1919, **2**, 635-646.
201. T. Keicher and S. Löbbecke, in *Organic Azides*, John Wiley & Sons, Ltd, 2010, pp. 1-27.
202. W. Zhang and T. S. A. Hor, *Dalton Trans.*, 2011, **40**, 10725-10730.
203. F. A. Cotton, M. P. Diebold and M. Matusz, *Polyhedron*, 1987, **6**, 1131-1134.
204. T. Mayer, E. Parsa and H.-C. Böttcher, *J. Organomet. Chem.*, 2011, **696**, 3415-3420.
205. J. A. Clucas, R. H. Dawson, P. A. Dolby, M. M. Harding, K. Pearson and A. K. Smith, *J. Organomet. Chem.*, 1986, **311**, 153-162.
206. H. Schmidbaur, R. Herr, G. Mueller and J. Riede, *Organometallics*, 1985, **4**, 1208-1213.
207. J. Blanco-Urgoiti, L. Anorbe, L. Perez-Serrano, G. Dominguez and J. Perez-Castells, *Chem. Soc. Rev.*, 2004, **33**, 32-42.
208. M. van Boven, N. H. Alemdaroglu and J. M. L. Penninger, *Product R&D*, 1975, **14**, 259-264.
209. S. E. Gibson and A. Stevenazzi, *Angew. Chem. Int. Ed.*, 2003, **42**, 1800-1810.

210. S. C. van der Slot, J. Duran, J. Luten, P. C. J. Kamer and P. W. N. M. van Leeuwen, *Organometallics*, 2002, **21**, 3873-3883.
211. D. R. Anton and R. H. Crabtree, *Organometallics*, 1983, **2**, 621-627.
212. Z. Özer and S. Özkar, *Turk. J. Chem.*, 1999, **23**, 9-14.
213. C. Decker, W. Henderson and B. K. Nicholson, *J. Chem. Soc., Dalton Trans.*, 1999, 3507-3513.
214. D. T. Dixon, J. C. Kola and J. A. S. Howell, *J. Chem. Soc., Dalton Trans.*, 1984, 1307-1315.
215. F. A. Cotton, *Helv. Chim. Acta*, 1967, **50**, 117-130.
216. J. Chatt and L. A. Duncanson, *J. Chem. Soc.*, 1953, 2939-2947.
217. Data submitted to CSD by F. R. Fronczek in 2014, DOI: 10.5517/cc13njw5
218. G. Märkl, F. Lieb and A. Merz, *Angew. Chem.*, 1967, **79**, 59-59.
219. A. J. Ashe and T. W. Smith, *Tetrahedron Lett.*, 1977, **18**, 407-410.
220. H. Lehmkuhl, R. Paul, C. Krüger, Y. H. Tsay, R. Benn and R. Mynott, *Liebigs Ann. Chem.*, 1981, **1981**, 1147-1161.
221. M. Yang, X. Tian and F. You, *Ind. Eng. Chem. Res.*, 2018, **57**, 5980-5998.
222. C. W. Fernelius, H. Wittcoff and R. E. Varnerin, *J. Chem. Educ.*, 1979, **56**, 385.
223. A. Forestière, H. Olivier-Bourbigou and L. Saussine, *Oil & Gas Science and Technology - Rev. IFP*, 2009, **64**, 649-667.
224. D. F. Wass, *Dalton Trans.*, 2007, 816-819.
225. P. W. N. M. van Leeuwen, N. D. Clément and M. J. L. Tschan, *Coord. Chem. Rev.*, 2011, **255**, 1499-1517.
226. W. Keim, *Angew. Chem. Int. Ed.*, 2013, **52**, 12492-12496.
227. G. J. P. Britovsek, D. S. McGuinness, T. S. Wierenga and C. T. Young, *ACS Catal.*, 2015, **5**, 4152-4166.
228. A. J. Rucklidge, D. S. McGuinness, R. P. Tooze, A. M. Z. Slawin, J. D. A. Pelletier, M. J. Hanton and P. B. Webb, *Organometallics*, 2007, **26**, 2782-2787.
229. A. Carter, S. A. Cohen, N. A. Cooley, A. Murphy, J. Scutt and D. F. Wass, *Chem. Commun.*, 2002, 858-859.
230. A. Bollmann, K. Blann, J. T. Dixon, F. M. Hess, E. Killian, H. Maumela, D. S. McGuinness, D. H. Morgan, A. Neveling, S. Otto, M. Overett, A. M. Z. Slawin, P. Wasserscheid and S. Kuhlmann, *J. Am. Chem. Soc.*, 2004, **126**, 14712-14713.
231. K. Blann, A. Bollmann, J. T. Dixon, F. M. Hess, E. Killian, H. Maumela, D. H. Morgan, A. Neveling, S. Otto and M. J. Overett, *Chem. Commun.*, 2005, 620-621.
232. T. Agapie, *Coord. Chem. Rev.*, 2011, **255**, 861-880.
233. J. T. Dixon, M. J. Green, F. M. Hess and D. H. Morgan, *J. Organomet. Chem.*, 2004, **689**, 3641-3668.
234. M. J. Overett, K. Blann, A. Bollmann, R. de Villiers, J. T. Dixon, E. Killian, M. C. Maumela, H. Maumela, D. S. McGuinness, D. H. Morgan, A. Rucklidge and A. M. Z. Slawin, *J. Mol. Catal. A: Chem.*, 2008, **283**, 114-119.
235. A. Dulai, H. Bod, M. J. Hanton, D. M. Smith, S. Downing, S. M. Mansell and D. F. Wass, *Organometallics*, 2009, **28**, 4613-4616.
236. J. Jover, N. Fey, J. N. Harvey, G. C. Lloyd-Jones, A. G. Orpen, G. J. J. Owen-Smith, P. Murray, D. R. J. Hose, R. Osborne and M. Purdie, *Organometallics*, 2012, **31**, 5302-5306.
237. L. E. Bowen, M. F. Haddow, A. G. Orpen and D. F. Wass, *Dalton Trans.*, 2007, 1160-1168.
238. J. Jover, N. Fey, J. N. Harvey, G. C. Lloyd-Jones, A. G. Orpen, G. J. J. Owen-Smith, P. Murray, D. R. J. Hose, R. Osborne and M. Purdie, *Organometallics*, 2010, **29**, 6245-6258.
239. J. Jover and N. Fey, *Chemistry – An Asian Journal*, 2014, **9**, 1714-1723.

240. Q. Yin, Y. Soltani, R. L. Melen and M. Oestreich, *Organometallics*, 2017, **36**, 2381-2384.
241. J. A. Suttil, P. Wasserscheid, D. S. McGuinness, M. G. Gardiner and S. J. Evans, *Catal. Sci. Tech.*, 2014, **4**, 2574-2588.
242. M. Scholl, S. Ding, C. W. Lee and R. H. Grubbs, *Org. Lett.*, 1999, **1**, 953-956.
243. G. C. Vougioukalakis and R. H. Grubbs, *Chem. Rev.*, 2010, **110**, 1746-1787.
244. P. B. Arockiam, C. Bruneau and P. H. Dixneuf, *Chem. Rev.*, 2012, **112**, 5879-5918.
245. R. Noyori, T. Ohkuma, M. Kitamura, H. Takaya, N. Sayo, H. Kumobayashi and S. Akutagawa, *J. Am. Chem. Soc.*, 1987, **109**, 5856-5858.
246. R. Noyori and S. Hashiguchi, *Acc. Chem. Res.*, 1997, **30**, 97-102.
247. M. Dochnahl, M. Doux, E. Faillard, L. Ricard and P. Le Floch, *Eur. J. Inorg. Chem.*, 2005, **2005**, 125-134.
248. D. Wang and D. Astruc, *Chem. Rev.*, 2015, **115**, 6621-6686.
249. J. Magano and J. R. Dunetz, *Org. Process Res. Dev.*, 2012, **16**, 1156-1184.
250. A. Mitra and D. A. Atwood, in *Comprehensive Organometallic Chemistry III*, ed. R. H. Crabtree, Elsevier, Oxford, 2007, pp. 265-285.
251. M. Yoshimura, S. Tanaka and M. Kitamura, *Tetrahedron Lett.*, 2014, **55**, 3635-3640.
252. E. J. Corey and C. J. Helal, *Angew. Chem. Int. Ed.*, 1998, **37**, 1986-2012.
253. C. C. Chong and R. Kinjo, *ACS Catal.*, 2015, **5**, 3238-3259.
254. According to Johnson Matthey on 28/02/2018, one troy ounce of Ru is $200. The next cheapest, Ir, is $980.
255. J. Holmes, C. M. Pask and C. E. Willans, *Dalton Trans.*, 2016, **45**, 15818-15827.
256. S. Hashiguchi, A. Fujii, J. Takehara, T. Ikariya and R. Noyori, *J. Am. Chem. Soc.*, 1995, **117**, 7562-7563.
257. R. L. Chowdhury and J.-E. Backvall, *J. Chem. Soc., Chem. Commun.*, 1991, 1063-1064.
258. C. Standfest-Hauser, C. Slugovc, K. Mereiter, R. Schmid, K. Kirchner, L. Xiao and W. Weissensteiner, *J. Chem. Soc., Dalton Trans.*, 2001, 2989-2995.
259. I. Lavandera, A. Kern, V. Resch, B. Ferreira-Silva, A. Glieder, W. M. F. Fabian, S. de Wildeman and W. Kroutil, *Org. Lett.*, 2008, **10**, 2155-2158.
260. S. E. Clapham, A. Hadzovic and R. H. Morris, *Coord. Chem. Rev.*, 2004, **248**, 2201-2237.
261. J. S. M. Samec, J.-E. Backvall, P. G. Andersson and P. Brandt, *Chem. Soc. Rev.*, 2006, **35**, 237-248.
262. J. Toubiana and Y. Sasson, *Catal. Sci. Tech.*, 2012, **2**, 1644-1653.
263. K.-N. T. Tseng, J. W. Kampf and N. K. Szymczak, *Organometallics*, 2013, **32**, 2046-2049.
264. M. Yang, X. Tian and F. You, *Ind. Eng. Chem. Res.*, 2018, **ASAP Article**, DOI: 10.1021/acs.iecr.1027b03731.
265. R. L. Wingad, E. J. E. Bergstrom, M. Everett, K. J. Pellow and D. F. Wass, *Chem. Commun.*, 2016, **52**, 5202-5204.
266. R. L. Wingad, P. J. Gates, S. T. G. Street and D. F. Wass, *ACS Catal.*, 2015, **5**, 5822-5826.
267. A. M. Brownstein, in *Renewable Motor Fuels*, Butterworth-Heinemann, Boston, 2015, pp. 47-56.
268. G. R. M. Dowson, M. F. Haddow, J. Lee, R. L. Wingad and D. F. Wass, *Angew. Chem. Int. Ed.*, 2013, **52**, 9005-9008.
269. H. Aitchison, R. L. Wingad and D. F. Wass, *ACS Catal.*, 2016, **6**, 7125-7132.

270. K. J. Pellow, R. L. Wingad and D. F. Wass, *Catal. Sci. Tech.*, 2017, **7**, 5128-5134.
271. S. Veibel and J. I. Nielsen, *Tetrahedron*, 1967, **23**, 1723-1733.
272. R. S. Manan and P. Zhao, *Nat. Commun.*, 2016, **7**, 11506.
273. T. Imamoto, K. Tamura, Z. Zhang, Y. Horiuchi, M. Sugiya, K. Yoshida, A. Yanagisawa and I. D. Gridnev, *J. Am. Chem. Soc.*, 2012, **134**, 1754-1769.
274. R. Franke, D. Selent and A. Börner, *Chem. Rev.*, 2012, **112**, 5675-5732.
275. J. A. Osborn, F. H. Jardine, J. F. Young and G. Wilkinson, *J. Chem. Soc. A*, 1966, 1711-1732.
276. P. W. N. M. van Leeuwen, *Homogeneous Catalysis: Understanding the Art*, Springer, 1st edn., 2004.
277. M. Doux, L. Ricard, F. Mathey, Pascal L. Floch and N. Mézailles, *Eur. J. Inorg. Chem.*, 2003, **2003**, 687-698.
278. C. Müller and D. Vogt, *Phosphinine-Based Ligands in Homogeneous Catalysis: State of the Art and Future Perspectives*, 2011.
279. R. J. Newland, J. M. Lynam and S. M. Mansell, *Chem. Commun.*, 2018, **54**, 5482-5485.
280. J. T. Mague and J. P. Mitchener, *Inorg. Chem.*, 1969, **8**, 119-125.
281. A. R. Sanger, *J. Chem. Soc., Chem. Commun.*, 1975, 893-894.
282. R. R. Schrock and J. A. Osborn, *J. Am. Chem. Soc.*, 1976, **98**, 2134-2143.
283. A. B. Chaplin, J. F. Hooper, A. S. Weller and M. C. Willis, *J. Am. Chem. Soc.*, 2012, **134**, 4885-4897.
284. R. E. Kinder and R. A. Widenhoefer, *Org. Lett.*, 2006, **8**, 1967-1969.
285. F. Eisentrager, A. Gothlich, I. Gruber, H. Heiss, C. A. Kiener, C. Kruger, J. Ulrich Notheis, F. Rominger, G. Scherhag, M. Schultz, B. F. Straub, M. A. O. Volland and P. Hofmann, *New J. Chem.*, 2003, **27**, 540-550.
286. S. A. Bhat, M. K. Pandey, J. T. Mague and M. S. Balakrishna, *Dalton Trans.*, 2017, **46**, 227-241.
287. R. V. Honeychuck and W. H. Hersh, *Inorg. Chem.*, 1989, **28**, 2869-2886.
288. A. L. Colebatch, A. I. McKay, N. A. Beattie, S. A. Macgregor and A. S. Weller, *Eur. J. Inorg. Chem.*, 2017, **2017**, 4533-4540.
289. G. Hoge, H.-P. Wu, W. S. Kissel, D. A. Pflum, D. J. Greene and J. Bao, *J. Am. Chem. Soc.*, 2004, **126**, 5966-5967.
290. M. C. Willis, *Chem. Rev.*, 2010, **110**, 725-748.
291. K. F. Johnson, E. A. Schneider, B. P. Schumacher, A. Ellern, J. D. Scanlon and L. M. Stanley, *Chem.-Eur. J.*, 2016, **22**, 15619-15623.
292. M. M. Coulter, P. K. Dornan and V. M. Dong, *J. Am. Chem. Soc.*, 2009, **131**, 6932-6933.
293. H. C. Brown, A. K. Mandal and S. U. Kulkarni, *J. Org. Chem.*, 1977, **42**, 1392-1398.
294. H. C. Brown and B. C. S. Rao, *J. Am. Chem. Soc.*, 1956, **78**, 5694-5695.
295. H. C. Brown and S. K. Gupta, *J. Am. Chem. Soc.*, 1975, **97**, 5249-5255.
296. D. Männig and H. Nöth, *Angew. Chem. Int. Ed.*, 1985, **24**, 878-879.
297. K. Burgess, W. A. Van der Donk, S. A. Westcott, T. B. Marder, R. T. Baker and J. C. Calabrese, *J. Am. Chem. Soc.*, 1992, **114**, 9350-9359.
298. T. Hayashi, Y. Matsumoto and Y. lto, *Tetrahedron: Asymmetry*, 1991, **2**, 601-612.
299. D. A. Evans and G. C. Fu, *J. Org. Chem.*, 1990, **55**, 2280-2282.
300. D. H. Nguyen, J. Bayardon, C. Salomon-Bertrand, S. Jugé, P. Kalck, J.-C. Daran, M. Urrutigoity and M. Gouygou, *Organometallics*, 2012, **31**, 857-869.
301. Y. Wu, C. Shan, J. Ying, J. Su, J. Zhu, L. L. Liu and Y. Zhao, *Green Chem.*, 2017, **19**, 4169-4175.

302. M. Arrowsmith, T. J. Hadlington, M. S. Hill and G. Kociok-Kohn, *Chem. Commun.*, 2012, **48**, 4567-4569.
303. V. K. Jakhar, M. K. Barman and S. Nembenna, *Org. Lett.*, 2016, **18**, 4710-4713.
304. V. A. Pollard, S. A. Orr, R. McLellan, A. R. Kennedy, E. Hevia and R. E. Mulvey, *Chem. Commun.*, 2018, **54**, 1233-1236.
305. T. J. Hadlington, M. Hermann, G. Frenking and C. Jones, *J. Am. Chem. Soc.*, 2014, **136**, 3028-3031.
306. A. A. Oluyadi, S. Ma and C. N. Muhoro, *Organometallics*, 2013, **32**, 70-78.
307. G. Zhang, H. Zeng, J. Wu, Z. Yin, S. Zheng and J. C. Fettinger, *Angew. Chem. Int. Ed.*, 2016, **55**, 14369-14372.
308. S. R. Tamang and M. Findlater, *J. Org. Chem.*, 2017.
309. A. E. King, S. C. E. Stieber, N. J. Henson, S. A. Kozimor, B. L. Scott, N. C. Smythe, A. D. Sutton and J. C. Gordon, *Eur. J. Inorg. Chem.*, 2016, **2016**, 1635-1640.
310. A. Y. Khalimon, P. Farha, L. G. Kuzmina and G. I. Nikonov, *Chem. Commun.*, 2012, **48**, 455-457.
311. R. Arevalo, C. M. Vogels, G. A. MacNeil, L. Riera, J. Perez and S. A. Westcott, *Dalton Trans.*, 2017, **46**, 7750-7757.
312. L. Koren-Selfridge, H. N. Londino, J. K. Vellucci, B. J. Simmons, C. P. Casey and T. B. Clark, *Organometallics*, 2009, **28**, 2085-2090.
313. A. Kaithal, B. Chatterjee and C. Gunanathan, *Org. Lett.*, 2015, **17**, 4790-4793.
314. J. M. Brown, in *Modern Rhodium-Catalyzed Organic Reactions*, Wiley-VCH Verlag GmbH & Co. KGaA, 2005, pp. 33-53.
315. M. W. Drover, L. L. Schafer and J. A. Love, *Angew. Chem. Int. Ed.*, 2016, **55**, 3181-3186.
316. D. W. Stephan and G. Erker, *Angew. Chem. Int. Ed.*, 2015, **54**, 6400-6441.
317. S. Chen, D. Yan, M. Xue, Y. Hong, Y. Yao and Q. Shen, *Org. Lett.*, 2017, **19**, 3382-3385.
318. Z.-d. Mou, N. Deng, F. Zhang, J. Zhang, J. Cen and X. Zhang, *Eur. J. Med. Chem.*, 2017, **138**, 72-82.
319. M. Arrowsmith, M. S. Hill, T. Hadlington, G. Kociok-Köhn and C. Weetman, *Organometallics*, 2011, **30**, 5556-5559.
320. S. Park and S. Chang, *Angew. Chem. Int. Ed.*, 2017, **56**, 7720-7738.
321. P. Etayo and A. Vidal-Ferran, *Chem. Soc. Rev.*, 2013, **42**, 728-754.
322. P. C. J. Kamer, P. W. N. M. van Leeuwen and J. N. H. Reek, *Acc. Chem. Res.*, 2001, **34**, 895-904.
323. J. F. Hooper, S. Seo, F. R. Truscott, J. D. Neuhaus and M. C. Willis, *J. Am. Chem. Soc.*, 2016, **138**, 1630-1634.
324. I. Tsuneo, S. Youichi, K. Aya, O. Tomokazu and Y. Kazuhiro, *Angew. Chem. Int. Ed.*, 2007, **46**, 8636-8639.
325. K. G. M. Kou, L. E. Longobardi and V. M. Dong, *Adv. Synth. Catal.*, 2015, **357**, 2233-2237.
326. K. Nagata, S. Matsukawa and T. Imamoto, *J. Org. Chem.*, 2000, **65**, 4185-4188.
327. T. Imamoto, Y. Horiuchi, E. Hamanishi, S. Takeshita, K. Tamura, M. Sugiya and K. Yoshida, *Tetrahedron*, 2015, **71**, 6471-6480.
328. T. Imamoto, K. Sugita and K. Yoshida, *J. Am. Chem. Soc.*, 2005, **127**, 11934-11935.
329. J. Halpern, D. P. Riley, A. S. C. Chan and J. J. Pluth, *J. Am. Chem. Soc.*, 1977, **99**, 8055-8057.
330. J. Halpern, A. S. C. Chan, D. P. Riley and J. J. Pluth, in *Inorganic Compounds with Unusual Properties—II*, American Chemical Society, 1979, vol. 173, ch. 2, pp. 16-25.

331. M. P. Lamata, E. San José, D. Carmona, F. J. Lahoz, R. Atencio and L. A. Oro, *Organometallics*, 1996, **15**, 4852-4856.
332. T. Hayashi and K. Yamasaki, *Chem. Rev.*, 2003, **103**, 2829-2844.
333. S. W. Kwok, J. R. Fotsing, R. J. Fraser, V. O. Rodionov and V. V. Fokin, *Org. Lett.*, 2010, **12**, 4217-4219.
334. M. A. Bennett, L. Pratt and G. Wilkinson, *J. Chem. Soc.*, 1961, 2037-2044.
335. J. P. Shupp, A. S. Kinne, H. D. Arman and Z. J. Tonzetich, *Organometallics*, 2014, **33**, 5238-5245.
336. E. A. I. Bratsos, M. E. Ringenberg and T. B. Rauchfuss, in *Inorg. Synth.*, John Wiley & Sons, Inc., 2010, vol. 35, pp. 148-152.
337. B. C. Boren, S. Narayan, L. K. Rasmussen, L. Zhang, H. Zhao, Z. Lin, G. Jia and V. V. Fokin, *J. Am. Chem. Soc.*, 2008, **130**, 8923-8930.
338. P. J. Fagan, M. D. Ward and J. C. Calabrese, *J. Am. Chem. Soc.*, 1989, **111**, 1698-1719.
339. M. A. Bennett, T. N. Huang, T. W. Matheson, A. K. Smith, S. Ittel and W. Nickerson, in *Inorg. Synth.*, John Wiley & Sons, Inc., 2007, pp. 74-78.
340. R. Lalrempuia and M. Rao Kollipara, *Polyhedron*, 2003, **22**, 3155-3160.
341. R. Cramer, J. A. McCleverty and J. Bray, in *Inorg. Synth.*, John Wiley & Sons, Inc., 2007, pp. 14-18.
342. G. Giordano, R. H. Crabtree, R. M. Heintz, D. Forster and D. E. Morris, in *Inorg. Synth.*, John Wiley & Sons, Inc., 2007, pp. 88-90.
343. D. L. Reger, T. D. Wright, C. A. Little, J. J. S. Lamba and M. D. Smith, *Inorg. Chem.*, 2001, **40**, 3810-3814.
344. S. C. Ensign, E. P. Vanable, G. D. Kortman, L. J. Weir and K. L. Hull, *J. Am. Chem. Soc.*, 2015, **137**, 13748-13751.